UNIVERSIDAD REY JUAN CARLOS

FACULTAD DE CIENCIAS DE LA SALUD

TESIS DOCTORAL

ROLE OF TOLL-LIKE RECEPTOR 4 (TLR4) IN TWO MODELS OF PAIN IN RAT

MIGUEL ÁNGEL MARTÍNEZ GARCÍA

MADRID, 2017

Universidad Rey Juan Carlos

Facultad de Ciencias de la Salud
Departamento de Ciencias Básicas de la Salud

D. CARLOS GOICOECHEA GARCÍA, CATEDRÁTICO DE FARMACOLOGÍA Y NUTRICIÓN DE LA UNIVERSIDAD REY JUAN CARLOS, Y **D. DAVID PASCUAL SERRANO**, PROFESOR CONTRATADO DOCTOR DE LA UNIVERSIDAD REY JUAN CARLOS

CERTIFICAN:

Que el trabajo de investigación titulado "Role of toll-like receptor 4 (TLR4) in two models of pain in rat" ha sido realizado por **D. Miguel Ángel Martínez García** en el Departamento de Ciencias Básicas de la Salud de la Universidad Rey Juan Carlos, bajo nuestra supervisión y dirección, cumpliendo con los requisitos necesarios para optar al grado de Doctor, y así autorizamos su defensa.

Y para que así conste donde proceda se firma este certificado en Alcorcón, a 17 de marzo de 2017.

Fdo. Carlos Goicoechea García

Fdo. David Pascual Serrano

Dedicated to my Family and to my Love.

Miracles occur single-handedly when in motion.

M. McMardigan.

AKNOWLEDGEMENTS / AGRADECIMIENTOS

Quisiera aprovechar las primeras palabras de esta Tesis para dirigirme a mis dos directores de tesis:

En primer lugar, quisiera agradecer al **Dr. Carlos Goicoechea** que apostara por mi y, sobretodo, que no desistiera en sus intentos por enseñarme. Carlos, has sido mi tutor, mi director y mi referente para todo desde que puse el pie en el Departamento. Entrar en el laboratorio no habría sido posible sin tu aprobación. Siempre has tenido la puerta abierta para lo que necesitase y me has permitido aprender mucho de ti. Aún recuerdo preguntarte si aprendería técnicas histológicas y moleculares o me quedaría con las ratas. Al final hemos tocado muchos palos: farmacología, etiología, biología molecular, histología, neurociencia, cirugías, bioinformática… Gracias por todo ese tiempo, por llevarme a congresos internacionales, por permitirme conocer cómo trabajan en otros sitios, por tus consejos y por tu ayuda. Por tu manera de ser, por motivarme a aprender y por defenderme a capa y espada. Estaré siempre en deuda contigo.
En segundo lugar, al **Dr. David Pascual**, no solo codirector de mi tesis sino también un verdadero cómplice dentro de un laboratorio con tantas mujeres. Me llevo muy buenos consejos, tanto desde el punto de vista académico como filosofía de vida. Porque "si te enfadas tienes dos problemas: enfadarte y desenfadarte". Gracias por el tiempo que me has dedicado, por asistir y aconsejarme en mis clases y por hacer todo momento más distendido. Dicen que los primeros doctorandos son los que más pesan en el recuerdo, espero que así sea yo para ti.

A la **Dra. María Isabel Martín Fontelles**. Maribel, me permitiste formar parte de tu "gran familia", tu laboratorio. Llegué un mes de septiembre cuando tenía ya pensado pasar un año en blanco y me acogisteis dándome la posibilidad de realizar un Máster Oficial y un doctorado. Siempre serán una referencia para mi tu actitud y templancia en la vida. Porque un verdadero líder no debe solo preocuparse en ser la cabeza pensante del grupo, sino también, y quizás más importante, ocuparse de ser el termómetro que cuida de la estabilidad del mismo. Gracias por tantas enseñanzas y por mucho más.

A la **Dra. Visitación López-Miranda** y el **Dr. Ernesto Quesada**, gracias por brindarme vuestro apoyo y amistad. Visi, fuiste junto a Maribel y Carlos mi primer contacto y creo que no te he conocido ningún día sin una sonrisa en la cara. Gracias por ayudarme con mis inicios en el Máster y gracias por estar siempre de alguna manera ahí. Ernesto, sin ti esta tesis tampoco podría haberse llevado a cabo. Te debo también mucho y no se trata solo de fármacos. Creo que hay un tema de conejos pendiente. Gracias por todo.

A la **Dra. Raquel Abalo**, por ser un ejemplo de dedicación y superación, en búsqueda constante de nuevos conocimientos. Gracias por esas pequeñas charlas y por mostrarme el apasionante mundo de la motilidad gastrointestinal.

A la **Dra. Eva Sánchez**, por tu sencillez y humildad, por interesarte siempre en lo que hago y porque durante una tesis no se realizan solo experimentos sino que se comparten clases, prácticas

y vivencias, gracias también a ti por ensañarme tanto. Y a las **Dras. Rocío Girón** y **Esperanza Herradón**, a las que he tenido como maestras bien durante el máster o durante la enseñanza en grado. Gracias por poder contar con vosotras cuando lo he necesitado.

A las **Dras. Gema Vera**, **Ana Bagüés** y **Cristina González**, mis tres hadas. Porque el buen funcionamiento de un laboratorio depende y mucho de la calidad humana de las personas con las que trabajas. Me habéis servido de ejemplo como personas y como trabajadoras. Gracias por vuestro apoyo y por todos los buenos momentos compartidos.

A **Nancy**, mi mejor amiga dentro del laboratorio. El mejor ejemplo de persona en el que pueda pensar. Por tu bondad, tu lucha y tu eterna paciencia. Gracias por tu confianza y apoyo durante todos estos años. Recuerda Nancy, el mejor perfume se guarda en frascos pequeños.

A **Maica Merino** y **Guadalupe Pablo**, por escucharme y hacerme reír en los días más duros y por vuestra ayuda desinteresada para cualquier cosa que he necesitado. Gracias por vuestra complicidad y por todos los ratos compartidos. A **Iván Álvarez**, por sus enseñanzas y por los buenos momentos dentro y fuera de la Facultad.

A **Cristina Rivas**, gracias por haber estado pendiente siempre de cuanto he necesitado. Siempre que recuerdo el cumpleaños de alguien no puedo evitar pensar en ti. Muchas gracias por todos tus cuidados y tu atención.

A las **Dras. Marta Miguel** y **Marta Garcés,** al **Dr. Pablo Cabezos**, la **Dra. Patricia Caldas**, **Gabriela Firpo**, **María Martínez** y **Ana Rodríguez**, por los ratos compartidos.

Al Dr. **José Antonio Uranga**, quien me abrió las puertas de su laboratorio. Gran parte de esta tesis se asienta en técnicas histológicas e inmunológicas y he sentido el laboratorio de Histología en todo momento como una continuación del laboratorio de Farmacología. Muchas gracias por ponérmelo tan fácil. Y a **Antonio**, **Julio** y **Raquel**, la prolongación del Dr. Uranga dentro del laboratorio. Habéis realizado y me habéis enseñado a realizar multitud de técnicas histológicas. Sabéis que os guardo un cariño especial.

Al Dr. **José Castro**, las **Dras. Fani Neto**, **Joana Gomes** y **Sara Adães** de la Facultad de Medicina de la Universidad de Oporto (FMUP). Quienes han hecho las veces de directores, profesores y colaboradores y que son conocedores del gran peso que tienen en mi formación y en esta Tesis. Muchas gracias por todo. Y a las **Dras. María Luisa Guardão** y **Zita Ferreira** y su equipo de la Unidad Veterinaria de la FMUP, quienes me dieron todas las facilidades para aprovechar al máximo mi estancia en Portugal. Con vosotras ha sido imposible no llevar una sonrisa cada día al trabajo. Hicisteis muy llevadera la estancia, muchas gracias.

Al Dr. **Julian S. Taylor** y a sus discípulos **Gerardo Ávila** e **Iriana Galán**. Por su ayuda desinteresada, por su enseñanza y su amistad. Espero mantener el contacto durante mucho tiempo.

Al **Dr. Sergio Ferreiro**, **Alejandro Gómez** y **Davinia Hernández** de la Unidad Veterinaria por todo el apoyo durante el desarrollo de esta tesis.

Al **Dr. José Antonio Mas** y **María Conejero**, y a los doctores y doctorandos del **Área de Bioquímica**, por vuestra simpatía y por ofrecerme vuestro apoyo siempre que lo he necesitado.

A **Andrea,** con quien a pesar de haber coincidido brevemente, ha tenido un gran significado para mi al haber sido mi predecesora en la investigación de los TLR4 en el campo del dolor. También tú formas parte de alguna manera de esto.

Y porque cuando he estado abajo me han ayudado siempre a levantarme, porque cuando no he estado de humor me han aguantado y por todos los momentos robados, esta tesis también tiene un gran pedacito de todos vosotros: a mi **FAMILIA** y a **Chiyo**, por todo lo que habéis soportado conmigo. Os lo debo todo. Sabéis que sin vosotros esto difícilmente habría sido posible.

Por último quisiera agredecer a la **Universidad Rey Juan Carlos** el haberme brindado la oportunidad de trabajar con una beca durante estos años; sin ella, la realización de este trabajo no hubiera sido posible.

La investigación de esta Tesis Doctoral ha sido financiada por los proyectos: SAF2009-12422-C02-01 y SAF2012-40075-C02-01 del Ministerio de Educación, Cultura y Deporte.

TABLE OF CONTENTS

INDEX OF ABBREVIATIONS

AMPA	α-amino-3-hydroxy-5-methyl-4-isoxazolepropionic acid
AP-1	activating protein-1
APC	antigen presenting cell
AQP4	aquaporin-4
ATP	adenosine triphosphate
cAMP	cyclic adenosine monophosphate
CCL2	chemokine (C-C motif) ligand 2
CCR2	chemokine (C-C motif) receptor 2
CD11b	cluster of differentiation molecule 11b
CD14	Cluster of differentiation 14
CGRP	Calcitonin gene-related peptide
CNS	Central Nervous System
Cox-2	cyclooxygenase-2
CRH	Corticotropin-releasing hormone
CytR	Cytokine receptor
CXC3L1	chemokine (C-X3-C motif) ligand 1
CXC3R1	chemokine (C-X3-C motif) receptor 1
DAMP	damage-associated molecular pattern
DOR	δ-opioid receptor
DRG	Dorsal Root Ganglia
EAAC1	Excitatory amino acid carrier 1
ECM	Extracellular matrix
EFIC	The European Federation of IASP Chapters

ELISA	Enzyme-linked Immunosorbent Assay
EPHAR	The Federation of European Pharmacological Societies
EPISER	estudio sobre la prevalencia e impacto de las enfermedades reumáticas realizado por la Sociedad Española de Reumatología
ERK	extracellular signal-regulated kinase
eVAS	electronic visual analogic scale
FNIII EDA	fibronectin type III variant containing the extra domain A
GA3P	glyceraldehyde-3-phosphate
GAPDH	glyceraldehyde-3-phosphate dehydrogenase
GLAST	glutamate-aspartate transporter
GFAP	Glial fibrillary acidic protein
GLT-1	glutamate transporter-1
GlyT1	glycine transporter 1
GPCR	G protein-coupled receptor
GSH	glutation
i.p.	intraperitoneal
i.t.	intrathecal
IκB	inhibitor of κ-light-polypeptide-gene-enhancer in B cells
Ικκε	inhibitor of κ-light-polypeptide-gene-enhancer in B cells kinase subunit ε
IASP	International Association for the Study of Pain
Iba-1	ionized calcium-binding adapter molecule 1
IFN	interferon
IL	interleukin
IP-10	IFN-γ-inducible protein-10
IRAK	interleukin-1 receptor-associated kinase

IRF-3	interferon-regulatory factor-3
JNK	c-jun N-terminal kinase
KOR	κ-opioid receptor
LGC	Ligand-gated channel
LOS	lipoolygosaccharide
LPS	lipopolysaccharide
M3G	morphine-3-glucuronide
M6G	morphine-6-glucuronide
Mal	MyD88-adapter-like (protein)
MAPK	mitogen activated protein kinase
MD-2	Myeloid differentiation factor-2
MIA	monosodic iodoacetate
MMP	matrix metalloproteinase
MOR	μ-opioid receptor
MyD88	myeloid differentiation primary response gene 88
NFκB	nuclear factor κ-light-chain-enhancer of activated B cells
NMDAR	N-methyl-D-aspartate receptor
nNOS	neuronal nitric oxide synthase
NO	nitric oxide
NSAID	Nonsteroidal anti-inflammatory drugs
OA	osteoarthritis
OARSI	Osteoarthritis Research Society International
OIH	Opioid-Induced Hyperalgesia / Opioid-Induced Hypersensitivity
ORL-1	opioid receptor-like-1
$P2X_4R$	purinergic $2X_4$ receptor

p38	protein 38
p50	protein 50
p65	protein 65
PAMP	pathogen-associated molecular pattern
PKC	protein kinase C
PNS	Peripheral Nervous System
PO	postoperative
RANTES	regulated on activation, normal T cell expressed and secreted (chemokine)
RVM	rostral ventromedial (medulla)
SEF	Sociedad Española de Farmacología
SER	Sociedad Española de Reumatología
SP	substance P
SYSADOA	symptomatic slow action rrugs for osteoarthritis
TAK1	Transforming growth factor β-activated kinase 1
TBK-1	TANK-binding kinase-1
TICAM	TIR domain-containing adapter molecule
TIR	toll/interleunkin-1 receptor
TIRAP	TIR domain-containing adapter protein
TLR4	Toll-like Receptor 4
TNF-α	tumor necrosis factor-alpha
TPA	12-O-tetradecanoylphorbol-13-acetate
TRAF	TNF receptor-associated factor
TRAM	TRIF-related adaptor molecule
TRIF	Toll/IL-1 receptor domain-containing adaptor inducing IFN-β
TrkA	tropomyosin receptor kinase A

TSAR	thermal stimulation and response processing system
VIP	vasoactive intestinal peptide
WDR	wide dynamic range
WHO	World Health Organisation

I. INTRODUCTION

1. Introduction to pain.

According to the definition given by the International Association for the Study of Pain (IASP), pain is "an unpleasant sensory and emotional experience that is primarily associated with tissue damage or described in such terms" (Merskey, 1986). As inferred from the previous line, an unpleasant sensation confined to a definite anatomical area of the sufferer is not enough to categorize pain, but coexists with cognitive and emotional components that escape to the external observer's eye. That is, pain is a personal and subjective experience (Melzack and Katz, 2001).

The significance and vocabulary related to pain varied among societies and ages alike throughout world history. In Europe, mentions to pain lexicon and its meaning can yet be found in texts so distant in the past such as those of the Ancient Greece (Rey *et al*., 1998). Thereafter, influx of new medical practices and knowledge by the hand of the Islamic expansion during Middle Ages, followed by the advances in anatomy and war surgery during the Modern Age, prepared the land for the upcoming medical schools and treatises in the study of pain, hence contributing to globalise the concept, study and treatment of pain. To this respect, Descartes' *Traité de l'homme* (1664) signifies the first incursion into pain transmission as we know it today (see **Fig.1**).

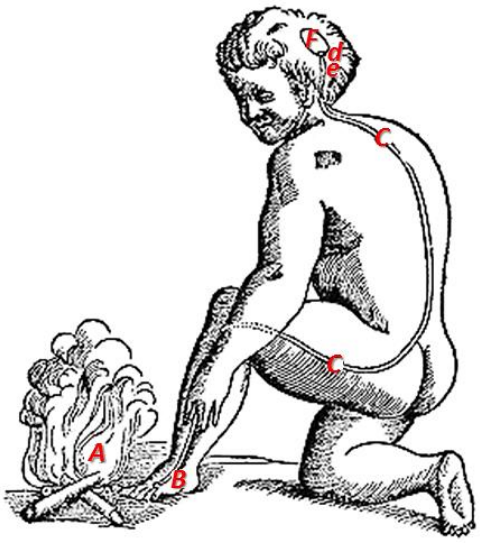

Figure 1. Illustration of the pain pathway in René Descartes' *Traité de l'homme* (Treatise of Man) 1664. According to Descartes, if a fire (A) comes near a foot (B), the minute particles residing in it, which move with great velocity, have the power to make the area of skin they touch to rustle, thus pulling upon an internal thread (C-C) it is attached to and causing a pore (d e) at the opposite end of the thread to open up. This causes the spirits to leave the compartment where they were confined in (F) towards the muscles. Consequently, the foot is withdrawn from the fire and therefore kept out of danger. Descartes approached herein the concept of pain for the first time as an alarm system, which he explained with a metaphor: "pulling on one end of a cord one makes to strike at the same instant a bell which hangs at the opposite end".

The concept of nociceptor was introduced by English neurophysiologist Charles Scott Sherrington (1857-1952), who developed Descartes' ideas in *The integrative action of the nerve system* (1906) and *The reflex activity in the spinal cord* (1932). Additionally, the multifaceted figure of English naturalist Herbert Spencer (1820-1903) has been related to the integration of

pain and emotions during its time course, whence physiology and psychology led in the 20th century to definitions of pain in terms of innate and conditioned reflex responses to noxious stimulation.

American physiologists Walter Bradford Cannon (1871-1945) and his disciple Philip Bard (1898-1977) timidly started flirting with the role of emotions and the autonomous system in pain, opening the new field of biopsychology of emotions. Also American neuropsychiatrist Eric Kandel (1929) with his works on *Aplysia californica* established the physiological bases of memory introducing the modern terms of habituation, sensitisation and conditioning. Later on, in 1965, Canadian psychologist Ronald Melzack (1929) together with his English colleague, the neuroscientist Patrick Wall (1925-2001) broke into the history of pain research with a revolutionary theory on its whole concept: *the gate control theory of pain*.

The gate control theory unified the trends seen for the 19th and 20th century and added the concept of central control giving a dominant role to the brain: psychological processes in the brain such as past experience, suggestion, and attention (subjective perceptions) modulate pain-signalling transmission down on the spinal cord by the relative activity of incoming large and small fibres and by descending messages from the brain (see **Fig.2**). In addition to that, Melzack contributed to the neural plasticity and chronic pathological pain theories as well (Wall *et al*., 1994), discussed in the next sections.

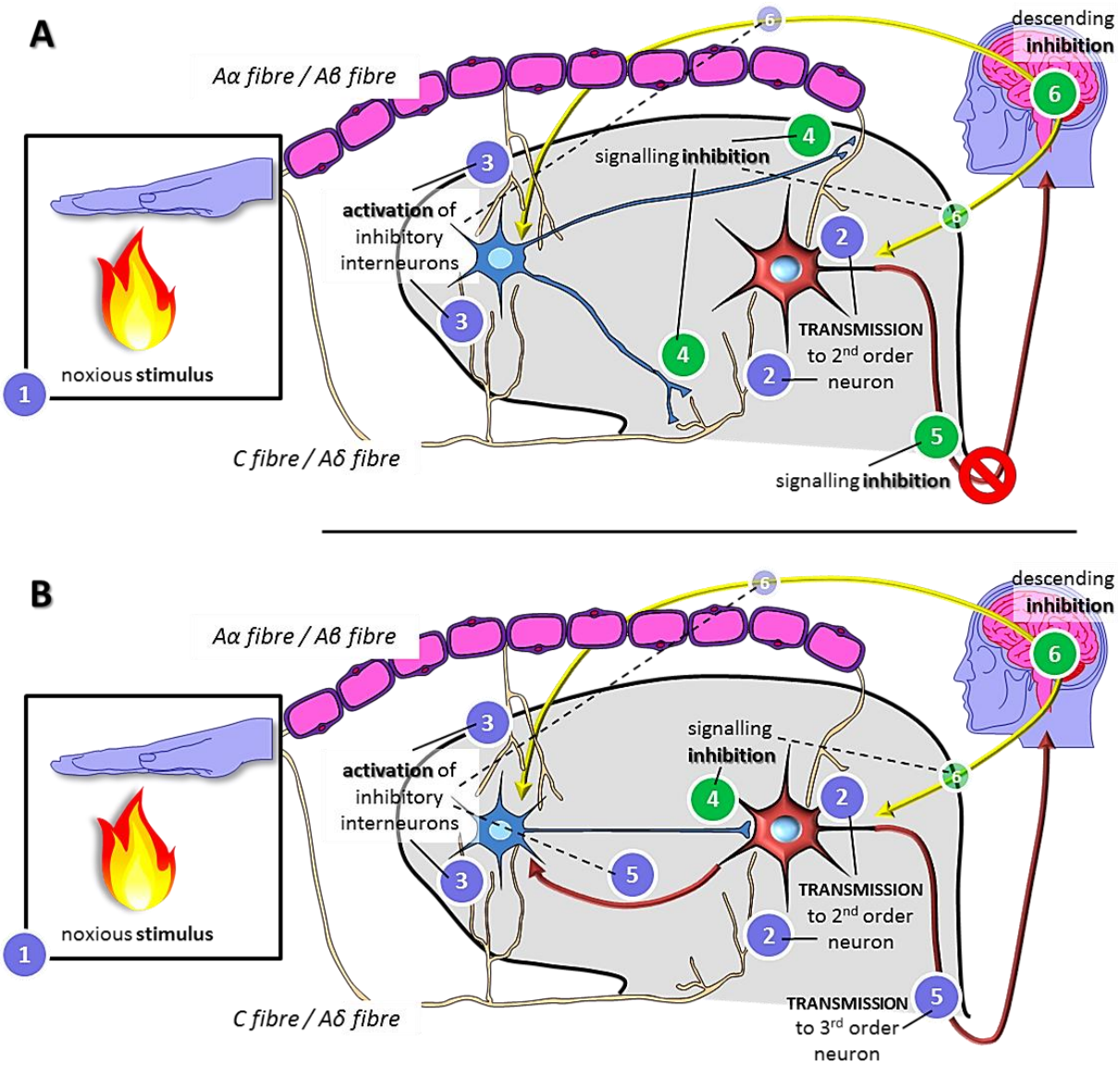

Figure 2. Gate control theory. Upper pannel (A). When a hand is thrust into a fire (**1**), the stimulus energy transformed into action potentials is transmitted through afferent large (Aα and Aβ) and small fibres (Aδ and C) to secondary neurons in the dorsal horn of the spinal cord (**2**). On the way, incoming action potentials can also activate inhibitory interneurons (**3**) which may hinder in turn these primary afferent fibres from further signalling (**4**). As result no more messages are released by 2nd order neurons to the brain (**5**). However if a considerable amount of action potentials reaches the upper centres in the brain, a central control mechanism activates and a descending modulatory pathway may either activate additional inhibitory interneurons or inhibit 2nd order neurons at the dorsal horn (**6**). That is, the central nervous system modulates the incoming signals before the threat a noxious stimulus can suppose. **Lower panel (B).** Activated inhibitory interneurons may also make contact and inhibit secondary neurons (**4**) and activated 2nd order neurons themselves can stimulate inhibitory interneurons by a process known as lateral inhibition too (**5**), or on the contrary send action potentials to the next neuron located at higher centres in the brain (**5**).

1.1. Pain physiology.

In general terms, pain is a natural mechanism that works on behalf of the individual avoiding the stimuli that could represent a potential damage to the integrity of themselves. This protective mechanism is known as acute or physiological pain and its goal is to drive the behaviours that remove or minimize the threat (IASP Scientific Program Committee, 2014).

Briefly, a noxious stimulus –high intensity thermal, mechanical or chemical– activates a system that starts at the peripheral terminals of primary afferent sensory neurons: the so-called nociceptors. The stimulus is then codified into action potentials that travel inwards as nerve electric impulses, with relays through spinal and supraspinal nuclei (brain stem, thalamus) in the central nervous system (CNS), and ultimately activates a matrix of cortical areas associated with the multiple conscious dimensions of pain. This is actually a complex process modulated by diverse targets and actors at different points all over the sensory tracts (Kitahata, 1993) (**Fig. 3**). Physiological pain is therefore a defence system with the neural process itself as its major component. That is, the detection of the external insult by the nervous system. This alert perception commonly disappears as the originating noxious source moves off (Cervero and Laird, 1996).

Until the 1960s (the gate control theory was published in 1965) emphasis was given to signal transmission. However, these days it is worldwide accepted that pain has both sensory and emotional features that modulate its final perception as a whole, transferring the stress onto signal modulation (Chapman and Nakamura, 1999).

In terms of sensory neurophysiology, four names are generally given to the different mechanisms depicted in the previous paragraphs (Kitahata, 1993):

- TRANSDUCTION, which refers to the conversion of the stimulus energy into electrical activity.
- TRANSMISSION, which exclusively regards the journey of such nerve impulse from the peripheral site to the different relay stations in the CNS.
- PERCEPTION, that is the subjective appreciation of the incoming signals integrated as a whole[1] and represented at the somatosensory cortex.
- And MODULATION, which considers dumping and spurring actions on the noxious signal along its transmission.

[1] Affective perception and emotional/cognitive reactions play a significant role in the perception of pain; the so-called *experience of knowing* (located at the limbic system), in comparison to the *experience of feeling* or detection of the noxious source by the nervous system itself (at the primary somatosensory cortex). Information from both experiences is combined and integrated in the thalamus.

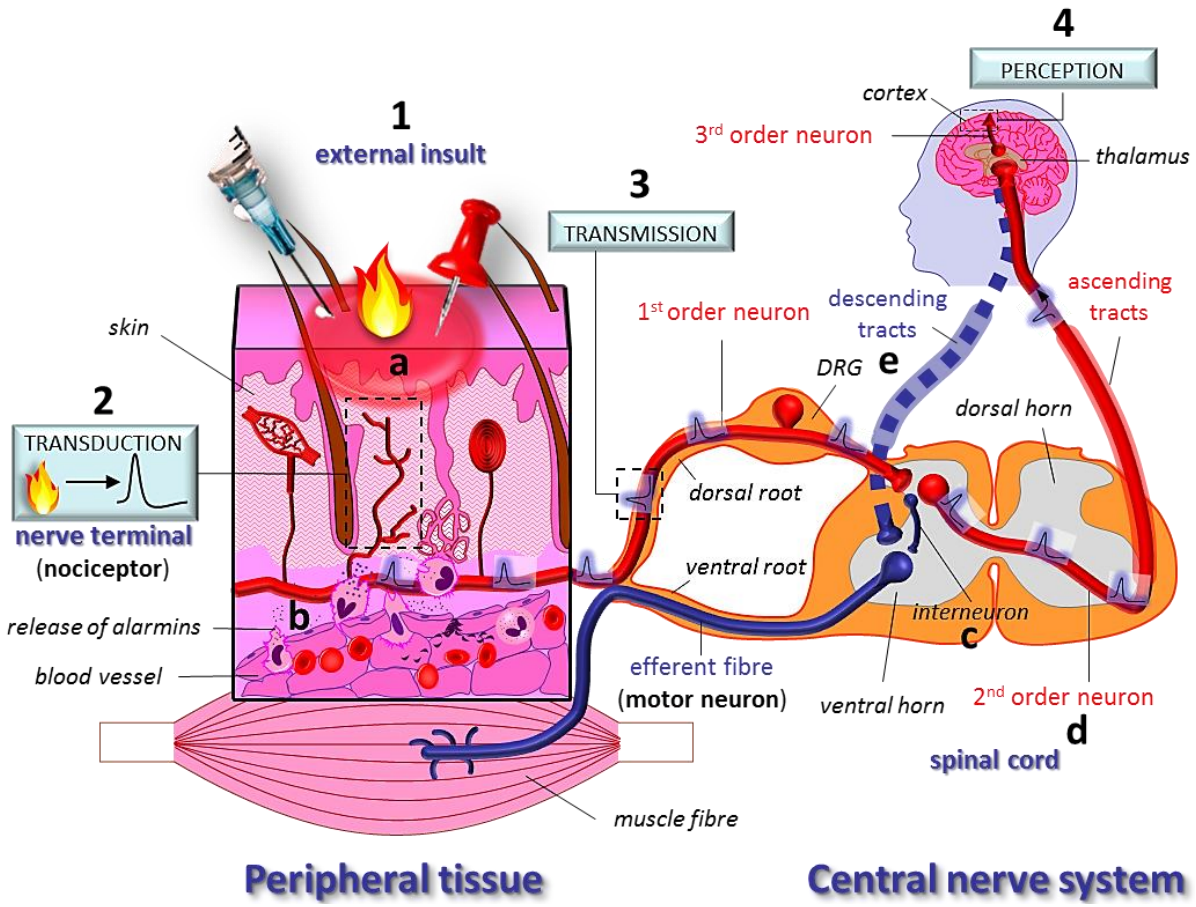

Figure 3. Physiological pain. Activation of nociceptive sensory fibres (**1**) leads to a chain of events that culminates in the perception of a painful stimulus within the brain. Nociceptors respond to acute or threaten tissue-damaging stimuli directly (**a**), through transduction of the stimulus energy by receptors on nerve terminals, or indirectly (**b**), through activation of channels and/or the release of molecules (alarmins), which, in turn, act on sensory neuron receptors (**2**). The yet codified stimuli travel now along these primary neurons as nerve impulses (**3**) and cause the release of neurotransmitter vesicles on the opposite edge, at the synapsis with a secondary neuron at the dorsal horn of the spinal cord. At this point, there are two possibilities: the incoming nerve fibre contacts an interneuron which consequently activates an efferent motor neuron for withdrawal from the external source of damage (**c**), or it interacts with a second order neuron and information then ascends through the sensory tracts and is transmitted to the thalamus (**d**), where a third neuron will ultimately stimulate specific areas of the somatosensory cortex for conscious perception (**4**). A descending pathway (**e**) activates then the efferent motor neurons for escaping from the noxious source. The nociceptive signal may be modified all along the sensory tract: at the nociceptor milieu, at the spinal cord by bypassing interneurons or descending inhibitory systems, or at the supraspinal cognitive and emotional centres (signal MODULATION).

1.2. Pathologic pain.

Chronic pain is a group of mechanistically separable nervous system disorders produced by one or more abnormal cellular signalling mechanisms, as quoted by M. Salter (Salter, 2014). Electrolyte and immunological-derived changes occurring in the periphery following trauma may lead to peripheral sensitisation and primary hyperalgesia. In addition, inflammation at peripheral nerve endings can also cause originally mechano-insensitive nerve fibres to become mechano-sensitive. This recruitment of silent nociceptors significantly increases the nociceptive input to the spinal cord and may partly explain the phenomena of central sensitisation and allodynia, that is, why even normally non-noxious stimuli may be felt as painful (Schaible, 2006). In this section we will focus on the process of peripheral and central sensitisation (**Fig.4**).

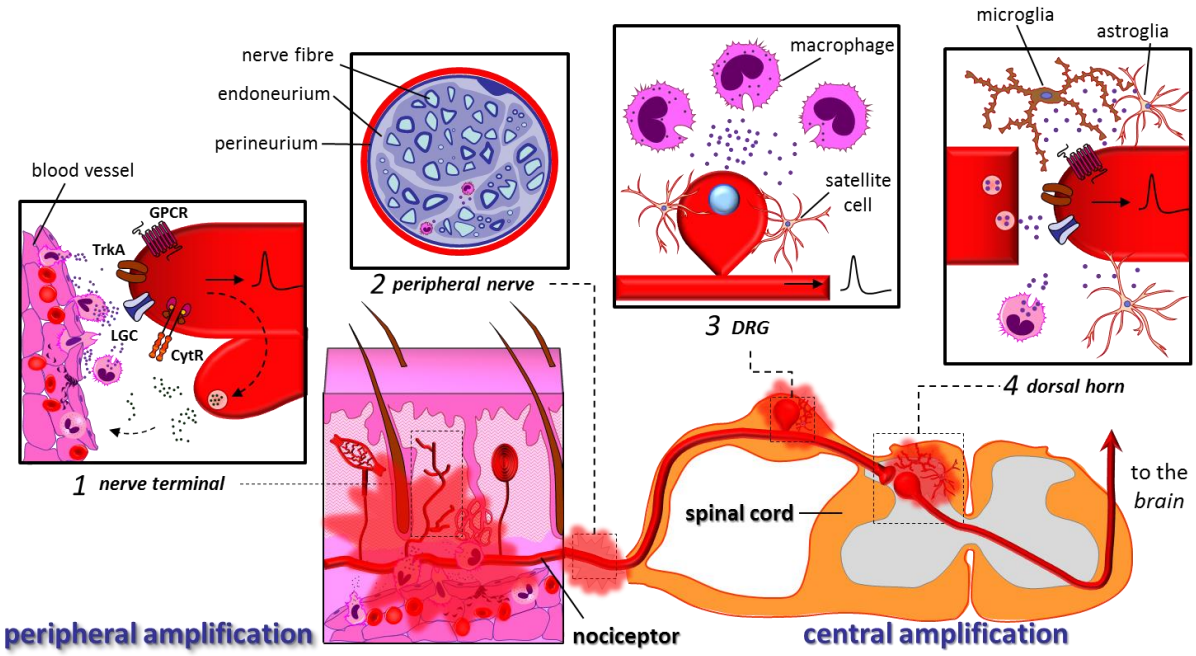

Figure 4. Chronic pain. Peripheral and central amplification may be mediated by injury-induced altered expression of receptors, ion channels and neurotransmitters, which might cause increased neuronal excitability and generation of action potentials, but also changes in synaptic connectivity and reorganisation of central nociceptive circuitry. Neuronal cell death can occur too. Peripheral nerve injury provokes a reaction from the immune system which has been observed at various anatomical locations: (**1**,**2**) injured nerve, (**3**) DRG, (**4**) spinal cord and supraspinal sites associated with pain pathways. Interaction between neurons, inflammatory immune and immune-like glial cells, as well as a raft of immune cell-derived inflammatory cytokines and chemokines may be involved in chronic pain pathogenesis. (GPCR = G protein-coupled receptor; TrkA = tropomyosin receptor kinase A; LGC = ligand-gated channel; CytR = cytokine receptor).

PERIPHERAL SENSITISATION. Nociceptors are likely to be sensitised by intense or prolonged stimulation. Reduction in threshold and outlasting excitation of sensory fibres can result in the alteration of neuronal function by the action of transmitters released from surveying immune cells. These molecules can equally act as neurotransmitters or inflammatory

mediators inducing neurogenic inflammation and further recruitment of immune cells[2]. Accumulation of inflammatory products has much to do with the sensitisation or direct activation of neuronal fibres, what can be originated at different anatomical levels on the periphery: axonal endings within target tissues or peripheral nerves (Austin and Moalem-Taylor, 2010). Peripheral sensitisation is considered to be evidence of increased heat sensitivity (Woolf *et al*., 2012).

CENTRAL SENSITISATION. Afferent fibres of different types (Aα, Aβ, Aδ or C) and of different origins (visceral: organ; or somatic: muscle, skin, tissue) interact presynaptically, under normal conditions, in the spinal cord. Prolonged inputs can cause altered excitability and synaptic efficacy of neurons at the dorsal horn. These plastic changes can in fact make original not nociception-transmitter neurons and nociceptors to interact at the dorsal horn of the spinal cord (Cervero and Laird, 1996). However, plastic changes are not restricted to the dorsal horn but can occur also at higher levels. Central sensitisation is considered to manifest particularly as dynamic tactile allodynia, but also as secondary punctate or pressure hyperalgesia, aftersensations, and enhanced temporal summation (Woolf, 2011).

In sum, damage to peripheral nervous system may result from traumatic injury, surgical intervention, disease or infection and leads to an acute phase response, which is characterised by nociceptive pain, inflammation, and restriction of normal function. Usually, following this acute phase, there is a recovery period of diminishing inflammation, reduced pain, healing of the injury and return to normal function. However, in 7-18% of the general population pain persists despite injury healing, resulting in a state of chronic neuropathic pain (Echeverry *et al*., 2012). This refers to a variety of chronic pain conditions with different underlying pathophysiologic mechanisms originated from severe neuronal tissue damage. To this respect, both damaged and undamaged axons have highly abnormal properties as a consequence of this nerve impairment. Neuropathic pain however can also originate from a dysfunction in the nervous system such as dysregulated gene expression or generation of ectopic discharges (Latremoliere and Woolf, 2009).

[2] Both *neurogenic inflammation* (neuroinflammation) and *recruitment of immune cells* (inflammatory response) are terms that will be retrieved when itemising the results obtained for the two animal models of pain herein employed (section IV.2.1-2.3).

Recently, activation of the immune system seems to have a crucial role in both peripheral and central abnormal sensory processing, and chronic neuropathic pain may now be considered a neuro-immune disorder (Nguyen *et al*., 2002; Raghavendra and DeLeo, 2003). Endoneural vessels surrounding nerve fascicles can supply damaged nerves with circulating immune cells (mast cells, macrophages and T cells), which release factors that initiate and maintain sensory abnormalities after injury. However other immune-like elements can also proliferate at the site of injury (e.g.: Schwann cells). Immune-derived factors might either induce activity in the axons they act on or be transported retrogradely to cellbodies in the dorsal root ganglion (DRG), where they alter the gene expression of neurons. Extravasation or proliferation of resident immune (or immune-like) cells may also happen in the spinal cord after peripheral nerve damage. That is, peripheral nerve injuries that lead to neuropathic pain states can cause immune-mediated changes not only in the damaged peripheral nerve and DRG, but also in the CNS. Hence, activation of immune and immune-like glial cells in the injured nerve, dorsal root ganglia and spinal cord results in the release of pro- and anti-inflammatory cytokines, as well as algesic and analgesic mediators, the balance of which determines whether pain chronicity is established (Marchand *et al*., 2005; Vallejo *et al*., 2010).

As a final remark, distinction between acute and chronic pain should comply the different physiopathological mechanisms by which they originate rather than the duration pain relief takes. Consequently, management of pain would depend on the kind of pain and efforts in basic health science should be addressed on understanding the physiological and molecular mechanisms underlying the different evoked pains. For which purpose, animal models are of great help.

2. Pathophysiology of pain.

2.1. Modulation of the nociceptive stimuli.

NERVE INPUT. All primary afferent neurons are pseudounipolar, formed by a cell body (perikarya) located within the DRG and a single axon with two branches: one going towards the periphery, and one traveling to the spinal grey matter. The former bifurcates at the end to innervate the peripheral tissue, while the latter ends in dendrites that synapse with

second order neurons at the dorsal horn. Information is transferred to higher centres of the brain through two different nociceptive pathways: the spinothalamic tract that receives signal inputs from primary Aδ and C nerve fibres and conveys temperature and nociception, and the lemniscal tract that receives input from primary Aα, Aβ and Aδ nerve fibres and is responsible for touch and proprioception feelings (Dubuc *et al*., 2013) (**Fig.5**).

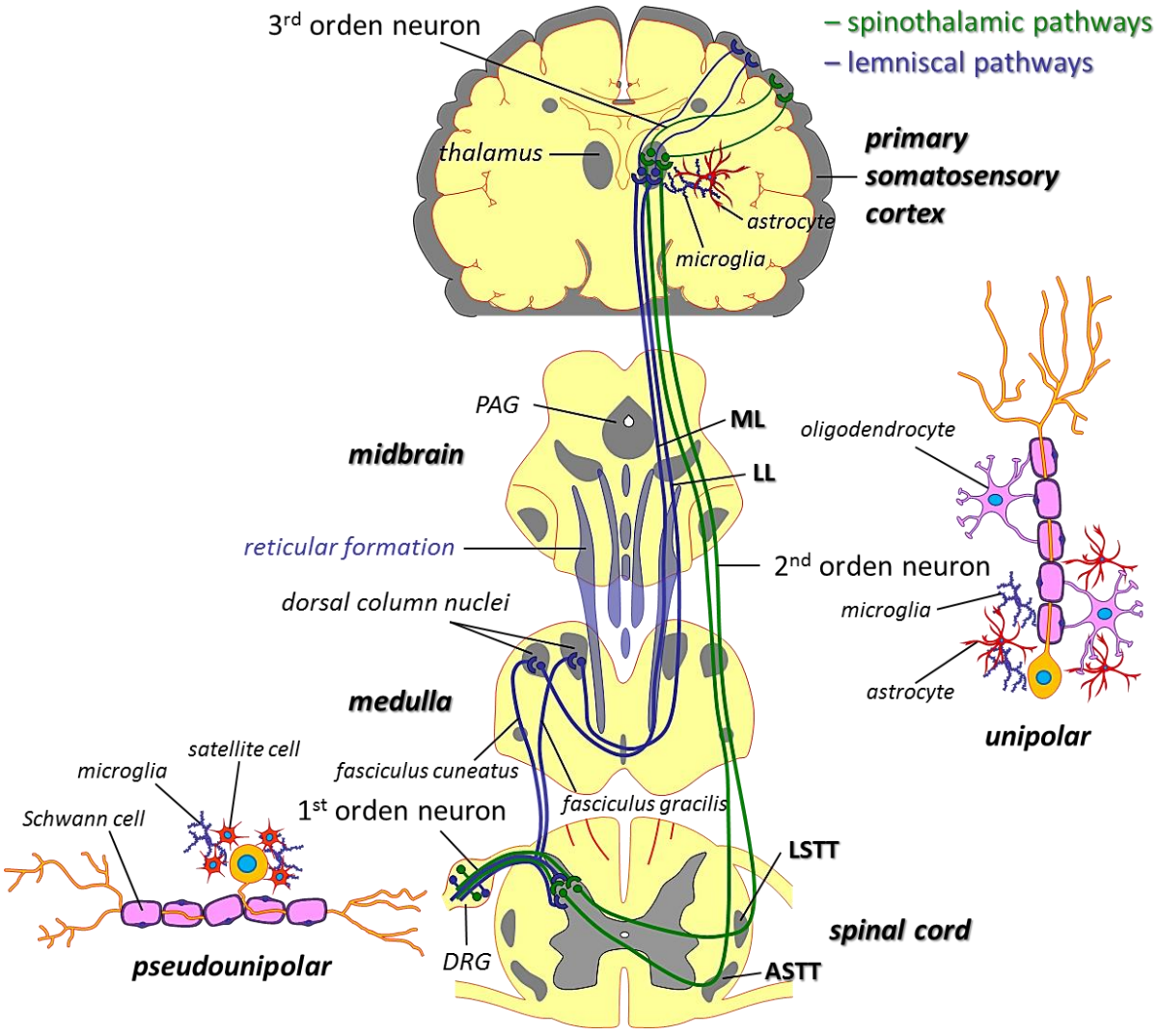

Figure 5. Ascending pain pathways: spinothalamic and lemniscal systems. Nociceptive pathways consist of a chain of three neurons that pass the nerve impulses from one to the next. Spinothalamic pathways are represented in green, whereas lemniscal pathways show up in blue. (Other alternative spino-reticular and spino-mesencephalic subpathways not shown). Labels are merely illustrative. DRG = dorsal root ganglion, ASTT = anterior spinotalamic tract, LSTT = lateral spinotalamic tract, LL = lateral lemniscus, ML = medial lemniscus, PAG = periaqueductal grey matter. Note the different level of the **decussation** between spinothalamic and lemniscal pathways; at the spinal cord the former and at the medulla the latter.

Considering the participants cited above:

- Peripheral nerves display several Schwann cells along their axons. These cells form a myelin segment for one axon only (myelinated) or can include several axons

(unmyelinated) in order to facilitate sending appropriate electrical signals throughout the nervous system. Schwann cells are essential for survival and regeneration of the axons and influence axonal thickness[3] (Brodal, 2010a; Dubovy *et al*., 2014). Expression of pattern recognition receptors (PRR) on the surface of their cell membrane allow Schwann cells to recognize exogenous (PAMP) as well as endogenous (DAMP) danger signals[4]. Upon activation, they start upregulating and secreting inflammatory mediators, what can lead to inflammatory neuropathies (Ydens *et al*., 2013).

- DRG not only contain soma, but also satellite glial cells and resident or invading macrophages that watch over the correct functioning of the neurons. In 2010, a work based on the existence of resident microglial cells in the DRG together with the aforementioned elements came to light, suggesting they could act as neuroprotective cells following peripheral injury (Patro *et al*., 2010). This is in contradiction with the role described by a different group (Romero-Sandoval *et al.*, 2008a). A conciliatory solution suggests they may contribute both to destruction of myelin and axons and to regenerative processes depending on the local situation (Brodal, 2010a).
- In the same line as stipulated for the other two elements, spinal dorsal horn contains nerve cells (dendrites of primary neurons, soma of second order neurons, interneurons) and immune-like cells (astrocytes, microglial cells and oligodendrocytes). Neuroglial cells are of especial relevance to our interest since they can modulate the nociceptive stimulus in a different way to what seen in the previous section (I.1) for interneurons. As it will further be discussed in this section, glial activation and subsequent mediator release are implicated in the creation and maintenance of persistent pain states (Raghavendra and DeLeo, 2003).

NERVE OUTPUT. CNS has facilitatory and inhibitory descending pain pathways that are different in their anatomy and pharmacological reactivity, and which presumably become

[3] A nerve fibre consists of an axon and surrounding Schwann cells. These can therefore influence the thickness of nerve fibres but interestingly, they can also affect axonal thickness. This fact will be of great importance at the discussion section.

[4] PAMP = pathogen-associated molecular pattern; DAMP = damage-associated molecular pattern.

activated simultaneously when acute nociception occurs (**Fig.6**). Descending facilitatory pathways are confined to the *ventral/ventrolateral funiculi* whereas descending inhibitory pathways descend in the *dorsolateral funiculi* (Mulak *et al*., 2012), both expressing different receptors for specific chemical activation (**table 1**). Unbalanced activation between these modulatory pathways might occur under persistent nociceptive input. Such sustained activation may result in neuroplastic changes at medullary sites, leading to both anatomical and biochemical changes in favour of the descending facilitatory pathway, thus increasing pain sensation. This is thought to underlie some states of chronic pain.

	receptors
facilitatory pathways	5-HT3–R (serotonin), AMPA–R, KAR, NMDA–R
inhibitory pathways	5-HT3–R (serotonin), β-adrenergic–R, dopamine–R, opioid-R

Table 1. Descending facilitatory and inhibitory pathways in the spinal cord and their corresponding molecular targets. 5-HT3-R = 5-hydroxy-tryptamine3 receptor; AMPA-R = α-amino-3-hydroxy-5-methyl-4-isoxazolepropionic acid receptor; KAR = kainate receptor; NMDAR = N-methyl-D-aspartate receptor

The rostral ventromedial medulla (RVM) constitutes a group of neurons that modulates nociceptive signals delivering electrical output to the spinal dorsal horn. RVM neurons are functionally heterogeneous. Three different classes of neurons have been described so far: ON, OFF and neutral cells (Fields *et al*., 1995). ON-cells promote nociception and OFF-cells suppress it, whereas the role of neutral cells, which could represent a subtype of ON- or OFF-cells, is not yet well understood. As described in the previous paragraph, nociceptive facilitating outflow from the RVM is dominant after nerve injury. This may be explained by the fact that immediately before an external noxious stimulus occurs, OFF-cells, which are tonically active, pause in firing at the same time that ON-cells accelerate outburst (Porreca *et al*., 2002).

As reviewed in section I.1.2., mechanical allodynia and hyperalgesia correspond to clinical manifestations of significant central sensitisation in chronic pain states (e.g. neuropathic pain). However, increased excitability of primary afferent fibres and sensitisation of dorsal horn neurons does not explain maintenance of neuropathic pain behaviour itself. On the

contrary, strong evidence suggests that active participation of supraspinal RVM of medulla is required for chronic pain state[5] (Carlson *et al*., 2007).

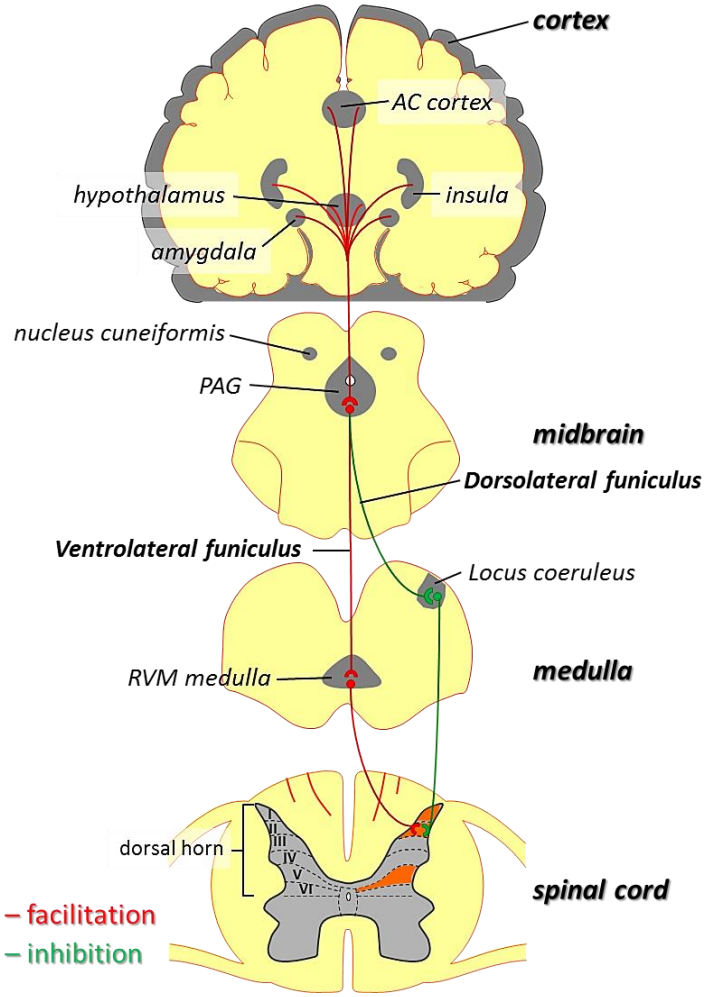

Figure 6. Descending pain modulatory system: ventrolateral and dorsolateral funiculi. According to electrophysiological, anatomical and pharmacological studies the final relay for common descending pain pathways from the brain corresponds to the rostroventral medulla (RVM). RVM neurons project efferent signals downward to various levels of the spinal cord making contact with inhibitory or activatory interneurons. However, from a strict point of view, facilitatory pathways are confined to the ventral/ventrolateral funiculi whereas descending inhibitory pathways descend in the dorsolateral funiculi. **Facilitatory pathways.** Glutamate is the main excitatory transmitter, acting on AMPA, kainite and NMDA receptors. **Inhibitory pathways.** *Dorsolateral funiculus* joins together descending axons of serotonergic, noradrenergic and dopaminergic neurons, and terminates on the inhibitory interneurons in the dorsal horn of the spinal cord. As regards opioid transmission, cortical areas communicate through endorphins-mediated synaptic connections with the anterior cingulate cortex (AC cortex). Endogenous opioids are also present in synapsis between interneurons and primary nociceptive afferent fibres in the dorsal horn. Facilitatory pathways are represented in red, whereas inhibiting pathways show up in green. Labels are merely illustrative. AC cortex = anterior cingulate cortex, PAG = periaqueductal grey matter, RVM medulla = rostral ventromedial medulla. (Other structures such as dorsolateral pontine tegmentum, tectospinal tract, dorsal reticulospinal tract not shown).

2.2. Dorsal horn plasticity.

The dorsal root fibres vary in thickness, what represents a direct function of conduction velocity. Although functionally equivalent, terms differ for classification of muscle and

[5] Primary hyperalgesia, a phenomenon defined by increased sensitivity to stimulation at the local site of the tissular injury and increased input at the spinal dorsal horn, is a mechanism dependent on the excitability of nociceptors. Contrary to this, when there is also increased sensitivity to stimuli from uninjured tissue adjacent to or at some distance from the site of injury, a mechanism dependent on the excitability of neurons in the CNS underlies. That is secondary hyperalgesia. Changes in excitability of neurons that contribute to maintenance of secondary hyperalgesia are not restricted to one unique area, but reside in the spinal cord and also in RVM. Peripheral tissue insult and persistent input engage double-sense spinal-brain stem mechanisms that maintain central sensitization and contribute to development of secondary hyperalgesia (Gebhart, 2004).

cutaneous fibres. Group I muscle afferents typically correspond to Aα cutaneous fibres, group II to Aβ, group III to Aδ and group IV to C (**table 2**).

Afferent fibre diameter	*Conduction velocity (m/s)*	*Class*	*Function*	*Electrical threshold*
Myelinated				
10 – 18 µm	60 – 100	I (Aα)	Proprioceptive	lowest
5 – 12 µm	20 – 70	II (Aβ)	Proprioceptive	
1 – 5 µm	2.5 – 20	III (Aδ)	Nociceptive	
Unmyelinated				
< 1 µm	< 1	IV (C)	Nociceptive	highest

Table 2. Diameters of nerve fibres and their classification.

Weak electrical stimulation of peripheral nerves evokes activity only in the thickest myelinated fibres (Aα), and with increasing intensity, the thinner fibres are recruited progressively (Aβ, Aδ and C, in this order). The primary fibres transporting temperature and nociceptive signals in normal conditions can be thinly myelinated (Aδ fibres, which conduct signals from cold receptors) or unmyelinated fibres (C fibres, which conduct signals from heat receptors), while signals from low-threshold mechanoreceptors are conducted in thick myelinated fibres (Aα and Aβ) (Brodal, 2010b). It can be therefore easily deduced that under normal conditions nociceptors remain silent. However, after nerve or tissue injury, nociceptors become active and even Aβ fibres can cross-talk with Aδ or C fibres, which will convert innocuous sensory signals into noxious signals.

In brief, small- and medium-size neurons, that is, C and Aδ nerve fibres, make synaptic contacts in lamina I and II of spinal dorsal horn (referred as temperature and nociception inputs). On the contrary, larger size neurons send their projections into lamina III and IV (related to as touch and proprioception information). Therefore, when the nature of large-size neurons is altered, these neurons could interpret innocuous signals as noxious signals, in which a light touch stimulus could be interpreted as a nociceptive signal (Cui and Fu, 2014).

a) Laminae of the dorsal horn in the spinal cord.

   The central terminals of primary sensory neurons in mammals are highly organized in horizontal (dorsoventral) planes in the grey matter of the spinal cord. Yet during embryogenesis, the dorsoventral axis is arranged so each lamina in the spinal cord topographically codifies a specific surface area of the body (Doubell *et al*., 1997). Rexed

classified the grey matter of the spinal cord in ten different laminae according to the heterogeneous arrangement of soma in it (Rexed, 1952) (**Fig.7**).

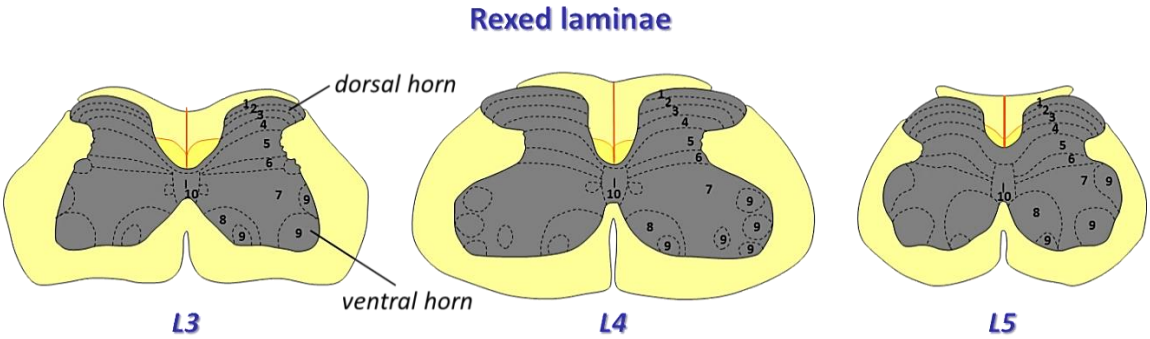

Figure 7. Anatomy of the spinal cord: Rexed laminae in dorsal and ventral horns. For our purpose only lumbar segments 3, 4 and 5 are represented. Note the different contour of the butterfly-shaped grey matter for every lumbar section.

Somatosensory afferent neurons conducting –or potentially able to transmit– nociceptive information terminate in the dorsal horn of the spinal grey matter (Brown, 1982), which is typically organised in six laminae:

- Lamina I and V contain mainly nociceptive neurons that receive mainly high threshold mechano- and thermoceptive primary afferent Aδ fibre inputs.
- Noci- and thermoceptive C-fibres mainly synapse in lamina II.
- Low threshold cutaneous Aβ mechanoceptors sprout in laminae III and IV.
- Lamina VI receives input from thick myelinated fibres responding to joint movement and cutaneous stimulation.

b) Synaptic plasticity.

Synaptic plasticity refers to a progressive increase in the responsiveness of an input at the synaptic structure, may be due to the amount of neurotransmitters released or to the amount or sensibility of the receptors on the postsynaptic neuron. A tissue injury causes an initial imbalance in environmental homeostasis at the site of lesion. Immediate cells to the wound release their inflammatory cytoplasmic content (bradykinin, serotonin, histamine and protons) into the environ causing the disruption of normal tissue pH and a switch on the transmembrane potential of nearby nerve endings by binding and therefore activating the receptors on their surface. Activated nociceptors send electrical signals in the direction of the spinal cord but also count on an efferent function, the so-called axon reflex, which consists on the peripheral release of neuropeptides and excitatory aminoacids (e.g. substance P, glutamate) promoting

neurogenic inflammation and affecting the nearby vasculature (causing increased capillary permeability and oedema). Infiltrating mast cells, in last term, release histamine, what additionally activates nociceptors (Mapp, 1995)[6] (**Fig.8**).

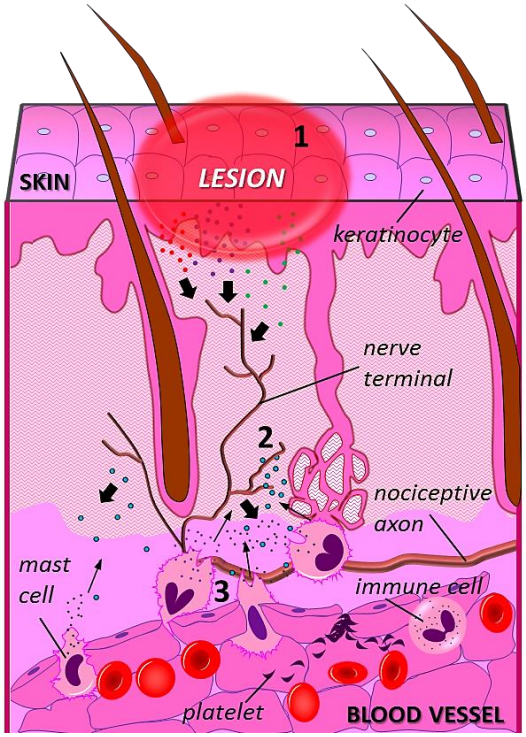

Figure 8. Activation of peripheral sensory fibres.
(1) Tissular damage results in the environmental increase of K^+, prostaglandin, serotonin and bradykinin levels, thus activating adjacent nociceptors.
(2) As a consequence, excitatory aminoacids are released from nerve endings and bind to receptors on cutaneous, endothelial and mast cells, thus increasing vasodilation and contributing to inflammation.
(3) Eventually, mast cells start releasing histamine, which activates nociceptor endings, triggering an ouroboros process.
The end result of this local neuroinflammation confined to the nerve terminal is the increased amount of electric signals delivered at the dorsal horn of the spinal cord.

If peripheral nerve terminals are damaged by this inflammatory response, other mechanisms may be operative. In fact, persisting insults to peripheral nerves or directly peripheral nerve injury cause a sterile inflammation to develop in sympathetic and dorsal root ganglia (DRG)[7], and it may ultimately affect central terminals (McLachlan and Hu, 2014). As previously reported (Coggeshall, CJ Woolf P Shortland RE, 1992; Mapp, 1995), the area responsible for pain sensation at the spinal dorsal horn (laminae I and II) may become occupied by nerve fibres which sprout in from the adjacent area responsible for proprioception (laminae III and IV). Thus, proprioceptive nerve fibres have now an input into a nociceptive area of the spinal cord. The result of this may be pain on normal touch or movement, that is, pain mediated by A-fibres.

Demonstration that cholera toxin b subunit (CTb), with target on myelinated neurons, could also label not myelinated neurons after peripheral nerve injury (Tong *et al*., 1999;

[6] For further detailed reading see (Mifflin and Kerr, 2014).
[7] Immune cells patrolling the organism are chemically attracted to the ganglia, releasing further proinflammatory cytokines that lead to hyperexcitability and ectopic discharge, what may contribute to neuropathic pain.

Ma and Tian, 2001; Shehab *et al.*, 2003), seemed to pull the theory of neuronal arrangement to pieces[8]. However several works employing different techniques (electrophysiological, biochemical or different labelling protocols) reopened the debate (Shortland and Molander, 1998; Bao *et al*., 2002; Kohno *et al*., 2003; Wang *et al*., 2004). Nowadays, synaptic plasticity is fully accepted but how it occurs is yet a subject of controversy[9]. Three forms of synaptic plasticity have been described so far to our knowledge (Ikeda *et al*., 2009):

- **Classical central sensitisation** consists on an immediate activity-dependent increase in the excitability of nociceptive neurons in the spinal dorsal horn. These increased synaptic efficacy is not restricted to nociceptor synapses (that is to C and Aδ fibres), but also to synapses formed by Aβ fibres, which are not activated by the nociceptive conditioning stimuli.
- **Windup**, another type of synaptic plasticity, consists on a progressive increase of action potential in dorsal horn neurons during a series of repeated C-fibre nociceptor stimuli. Repeated long-lasting depolarization of the postsynaptic membrane –induced by glutamate and neuropeptides– increases the action potential response to each stimulus as neurotransmitters accumulate.
- **Long-term potentiation** (LTP) has been detected in various parts of the central nervous system. In the spinal dorsal horn consists of activity-dependent long-lasting nociceptor synaptic facilitation.

2.3. Glial cells: neuron-glia and glia-glia interactions.

Neuron-glia interactions have an essential role in enabling the nervous system to function properly. The more complex and efficient a nervous system is, the more glial cells are present (Edenfeld *et al*., 2005; Austin and Moalem-Taylor, 2010; Eroglu and Barres, 2010).

[8] Until that date, works referred to CTb labelling as an indisputable evidence for sprouting into lamina II from large myelinated fibres (Aβ) in adjacent laminae. CTb was considered to selectively label large and medium size neurons so far (Ma *et al*., 2000; White and Kocsis, 2002).

[9] Some additional hypotheses suggested are: (1) inputs from large myelinated fibres to lamina II may be via excitatory interneurons; (2) high-frequency stimulation can provoke a failure of synaptic release mechanisms and neurotransmitters could actually being also captured by adjacent neurons; (3) aberrant branches of damaged C fibres could make contact with large myelinated fibres (Kohno *et al*., 2003).

Glia, also known as neuroglia, was first described in 1859 by German physician Rudolf Virchow and derives etymologically from the greek *γλία* "glue". They are non-conducting cells that modulate neurotransmission at the synaptic level and make up over 70% of the total cell population in the human CNS (Hertz, 2004; Romero-Sandoval *et al*., 2008b). Glia can be divided into two types: microglia and macroglia (astrocytes and oligodendrocytes[10]). Main functions of glial cells consist on providing structural, trophic and metabolic support to the neurons they surround, offering space compartmentalisation at synapses and removing cellular debris (Raghavendra and DeLeo, 2003). However, after a growing body of scientific research throughout the past 15 years, it can nowadays be stated that glial cells have integral roles in maintaining CNS homeostasis, and in chronic pain aetiology and progression far beyond the mere role of physical support for neurons they were originally attributed (Scholz and Woolf, 2007). In fact, experiments carried out in simple nervous systems such as those from invertebrates have shown that glia is able to sculpt neuron functional circuits by modifying the efficacy of synaptic connections, what enables to form and remove nerve projections (Edenfeld *et al*., 2005).

Further works in various models of chronic neuropathic pain in rodents report that peripheral nerve injury induces spinal glia activation[11] (Ito *et al*., 2009; Sagar *et al*., 2011). Activation of microglia is the first step in a cascade of immune responses in the CNS. Furthermore primary afferent neuron terminals are flanked by microglial cells that maintain and survey the environment in the spinal dorsal horn. Microglia expresses the same surface markers as macrophages/monocytes[12] and, in response to injury, it triggers

[10] Astrocyte and oligodendrocyte lineage cells are derived from neural stem cells, whereas microglia originates from the immune system. In the peripheral nervous system, there are two classes of Schwann cell (myelinating and non-myelinating), which functionally and antigenically resemble the glia of the CNS (Eroglu and Barres, 2010). Oligodendrocytes and Schwann cells form the myelin sheath of axonal fibres in the central and peripheral nervous system (respectively). However, unlike Schwann cells, a single oligodendrocyte can wrap several axons at a time.

[11] Proinflammatory cytokines have postulated as common mediators of allodynia and hyperalgesia, since they encourage nociceptive transmission between neurons. These algic molecules are in fact current products released by activated glia, what suggests that glial cells may be important modulators of nociception and hence, potential targets to treat neuropathic pain.

[12] In early embrionary stages, monocytic precursors are recruited by the CNS before closure of the blood-brain barrier (BBB). Subsequently, they differentiate first into macrophage-like amoeboid microglia and then into ramified microglia. This explains why microglia expresses the same surface markers as macrophages/monocytes.

the neuroinflammatory response, while astrocytes undergo astrogliosis (Marchand *et al*., 2005).

Activated microglia exhibits a ramified star-shaped morphology visually contrasting to the original amoeboid shape when inert. They also undergo hyperplasia and up-regulation of certain genes related to migration, phagocytosis, cytokines, chemokines, growth factors, nitric oxide and prostaglandins (Nakagawa and Kaneko, 2010). Controversially, microglial activation in the CNS provides both neuroprotective and neurodegenerative roles *(Patro et al*., 2010). Pro- and anti-inflammatory cytokines can apparently polarize microglia to distinct activation states, however there is still intense debate and the topic is yet far from being fully understood (Guadagno *et al*., 2013; Cherry *et al*., 2014).

Astrocytes are the most abundant cells in the CNS and modulate synaptic transduction through astrocyte–neuron interactions. Activated astrocytes exhibit hypertrophic morphology with thick ramifications. Given the crucial roles of astrocytes in brain development, metabolism, and function, it is not surprising that astrocytes are involved in almost every disease of the central nervous system.

The time course of spinal microglial and astrocytic activation varies following nerve injury. Hence, even after microglial activation decreases, astrocytic activation persists, as does neuropathic pain (Nakagawa and Kaneko, 2010). Summarising, microglia might be responsible for the initiation of neuropathic pain states, and astrocytes may be involved in their maintenance (**Fig.9**). Despite the scarce literature, especial emphasis must be also placed on glial anti-nociceptive properties, that is, glial activation is not always bad (Milligan and Watkins, 2009).

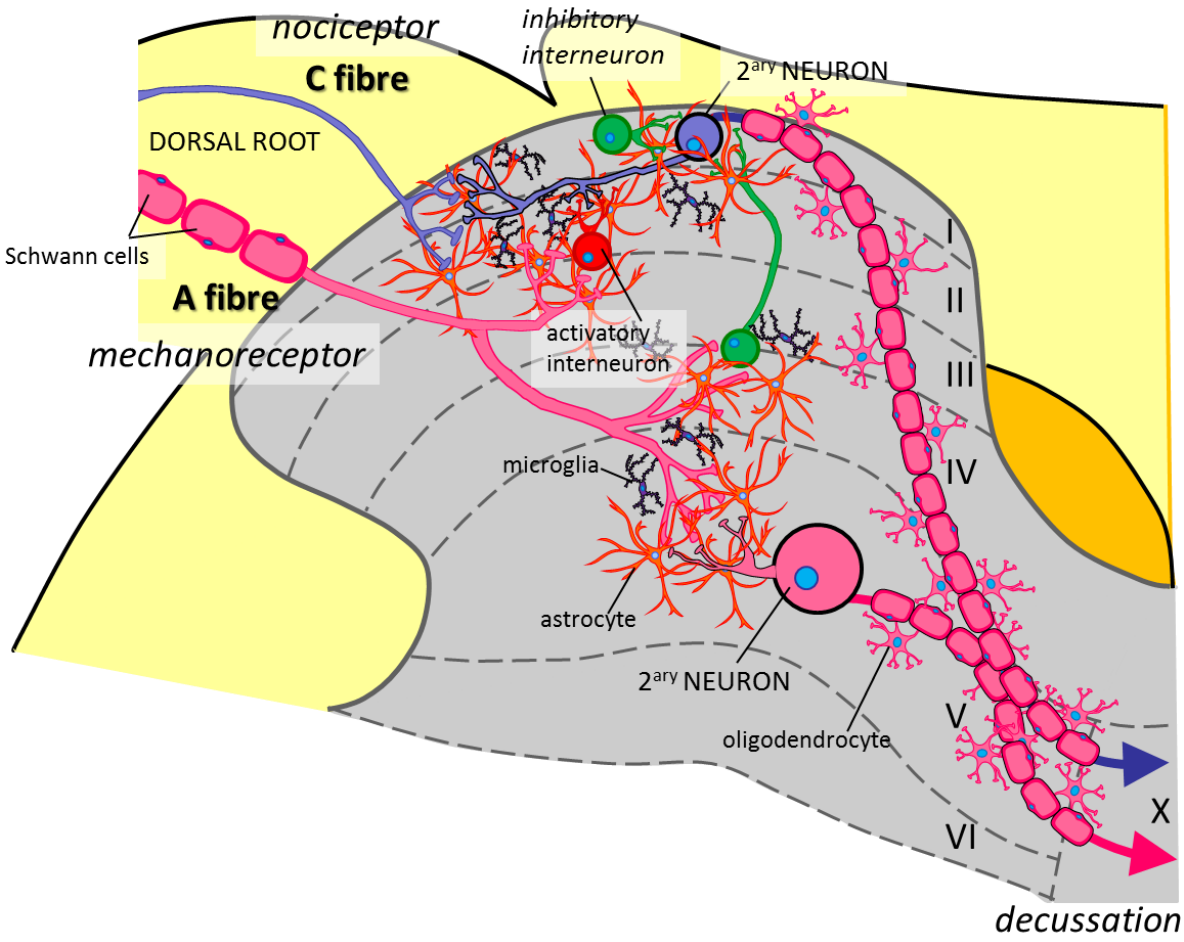

Figure 9. Modulation of pain-processing by glial cells in the spinal dorsal horn. Under continuous and increased firing from the periphery, activated microglia releases several pro-inflammatory cytokines, chemokines and other agents that modulate pain processing by affecting either presynaptic release of neurotransmitters and/or postsynaptic excitability. Additionally, glial cells also have an important role in the cross-talking between non-nociceptive (A fibres) and nociceptive neurons (central sensitisation). The release of inflammatory mediators initiates a self-propagating mechanism of enhanced cytokine expression by microglial cells assisted by an increasing population of activated astrocytes, which maintain the neuroinflammatory process even after the cease-fire of microglial cells.

Most available analgesics for pathological pain are still symptomatic. Conventional treatments have a scarce efficiency for neuropathic pain. Traditionally, coadjuvant drugs such as antidepressants and anticonvulsants, have demonstrated to be more efficient than opioids in some types of neuropathy (Watkins *et al*., 2007a). Recently, a few analgesics based on pathological mechanisms aimed to modulate the biochemical reactions that take place in neuron-to-astrocyte, neuron-to-microglia or microglia-to-astrocyte communication at definite times (once upon ingested) (**Fig.10**).

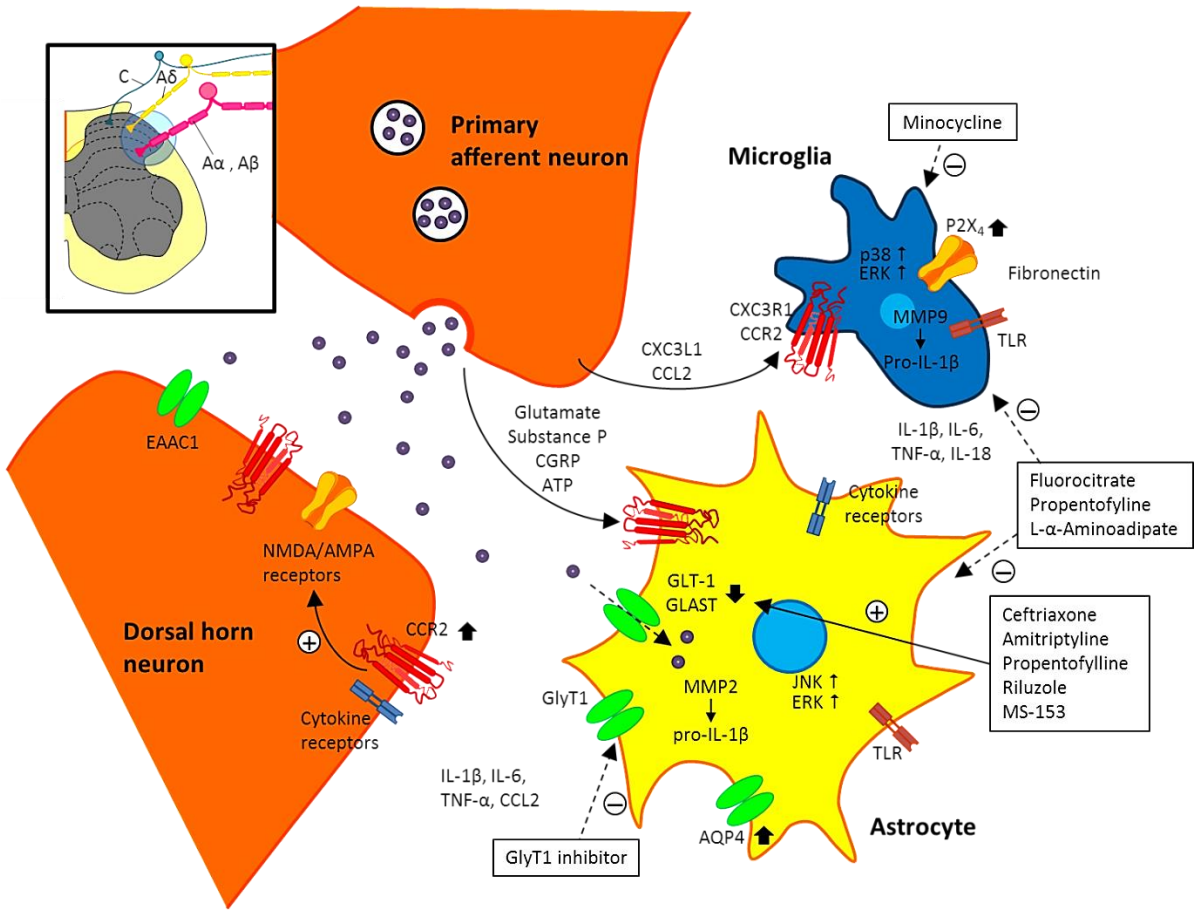

Figure 10. Signals involved in the activation of spinal microglia and astrocytes[13]**.** Ceftriaxone, amitriptyline, propentofyline, riluzole and MS-153 have been reported to modulate glutamate external levels by means of glutamate transporters (GLT-1 and GLAST) in astrocytes. Fluorocitrate, propentofylline (again) and L-α-aminoadipate have shown to act on internal signalling pathways disrupting the metabolism of astrocytes and microglia. Genes' labels are merely testimonial. AQP4: aquaporin 4, ERK: extracellular signal-regulated kinase, GlyT: glycine transporter, JNK: c-Jun N-terminal kinase, MMP: matrix metalloprotease, TLR: toll-like receptor. Modified from (Nakagawa and Kaneko, 2010).

Several changes have been noted to occur in the dorsal horn with central sensitisation. Firstly, pain-associated molecules such as substance P (SP), calcitonin gene-related peptide (CGRP) and other ligands targeting ion channels (ATP) are released at the synapse bottom by primary afferent neurons. Following increased firing, some of these surplus molecules may not be able to bind the receptors on the post-synaptical neuron but target the surrounding neuroglia. As a consequence, upregulation of cytokines (e.g. IL-1β, IL-6, TNF-α, IL-18) and chemokines (e.g. CCL2, CXC3L1) levels increase in glial cells, leading to further attraction and activation of immune glial cells and encouraging nociceptive transmission between neurons. Under this overexcited state, afferent dendrites release additional

[13] For further reading on pharmacological attenuation of glial activation see (Mika, 2008).

excitatory aminoacids and chemokines creating a vicious cycle that intercommunicates neurons, microglia and astrocytes at the dorsal horn (Norimoto *et al*., 2014).

3. Toll-like receptor.

3.1. Systematic discovery and distribution of Toll-like receptors.

Human toll-like receptors (TLR) are homologues of Drosophila toll proteins[14]. Eleven members of the TLR family have been identified in humans so far (designated TLR1 to 11) (Oda and Kitano, 2006) and they are distinguished by belonging to a protein superfamily with interleukin-1 receptor (IL-1R) homologous regions: the *toll/IL-1R (TIR) family* (reviewed in (Leon *et al*., 2008; McCormack *et al*., 2009)). TLR4 is probably the most studied among them all, as it presents two unique features that distinguishably set it apart: the requirement of a co-receptor for ligand recognition and the ability to signal through two different adaptor protein systems according to its cellular location –MyD88- and TRIF-dependent pathways, inducing either inflammatory cytokine or IFNβ production, respectively[15] – (Tanimura *et al*., 2008; Gangloff, 2012).

TLR4 is a type I transmembrane glycoprotein[16] with a highly polymorphic extracellular leucine-rich repeat (LRR)[17] N-terminal domain, and an intracellular signaling TIR[18] C-terminal domain (Gómez *et al*., 2014) implicated in both innate and adaptive immune responses in vertebrates (Sorge *et al*., 2011). The cytoplasmic TIR domain modulates interactions with the adaptor proteins involved in the signal transduction cascade, what in simple terms consists in downstream recruitment of protein kinases, which activate transcription factors such as nuclear factor-κB (NFκB), activating protein 1 (AP-1) and interferon (IFN)-regulatory factor 3 (IRF3) (Hoshino *et al*., 1999; Kawai and Akira, 2006). The final result is the up-regulation of diverse inflammatory mediators such as cytokines,

[14] To read more on *Drosophila* toll proteins see (Bilak *et al.*, 2003).

[15] Biological activity of TLR4 depends on their membrane localization. Plasma membrane MyD88-dependent pathway gives rise to cytokine production, whilst endosome TRIF-dependent pathway results in type I IFN.

[16] A Type I membrane protein refers to a single-pass membrane protein (crosses the membrane only once) with its hydrophilic N-terminal segment on the extracellular side of the membrane.

[17] Leucine-rich repeat domain consists in a typical conserved arc-shaped structure with multiple leucine residues that provides an optimal scaffold for the formation of protein-protein interactions.

[18] Toll/interleukin-1 receptor consists in a conserved cytoplasmic domain with a central five-stranded parallel β-sheet surrounded by five α-helices on both sides that makes it attractive for specific protein binding.

chemokines, tissue-destructive enzymes and the expression of costimulatory molecules on antigen-presenting cells (APC). This signifies the induction of the adaptive immune response (Abdollahi-Roodsaz *et al*., 2007).

As key players of the innate immune system, TLR can recognize pathogen-associated molecular patterns (PAMP) such as bacterial endotoxin, Gram-negative bacterial lypopolysaccharides (LPS) and lipooligosaccharides (LOS) (Peri and Calabrese, 2013). However, they can also detect endogenous molecules resulting from injury known as damage associated molecular patterns (DAMP) or alarmins. That said, TLR4 is overexpressed in damaged tissues and may be activated by necrotic cells, injured axons and components of the extracellular matrix. Some endogenous ligands of TLR4 are several heat shock proteins (Lasarte *et al.*, 2007; Ohara *et al*., 2013), the alternatively spliced type III repeat extra domain A of cellular fibronectin (FNIII EDA) (Okamura *et al*., 2001; Lefebvre *et al.*, 2011) and a plasma proteins (Sohn *et al*., 2012). They all cause cytokine production mediated by TLR4.

As mentioned before, TLR4 requires a co-receptor for ligand recognition. To this respect, two binding proteins have been identified so far. The myeloid differentiation 2 receptor (MD-2), a small glycoprotein that interacts as a monomer with an exogenous PAMP leading to its activation (Teghanemt *et al*., 2008), and an additional co-receptor named cluster of differentiation 14 (CD14) (**Fig.11**). In fact, a PAMP such as LPS has been reported to fail to produce allodynia, supporting the idea of an alternative via for TLR4 signaling that induces enhanced nociception[19] in absence of bacterium-derived factors (Cao *et al*., 2009; Hutchinson *et al*., 2009). Additionally, it has been described that CD14 is upregulated upon exposure to inflammatory molecules, as it is required for the internalisation of TLR4 (Zanoni *et al*., 2011).

[19] TLR4 activation is necessary but not sufficient to induce spinally mediated pain enhancement. This can be explained by a dual mechanism of antigen presentation to TLR4 (as the one cited in the paragraph) leading to two different effects (sepsis or allodynia). But another explanation could be that TLR4 is only one of the many molecular players in the development of pain behaviours (Smith, 2010).

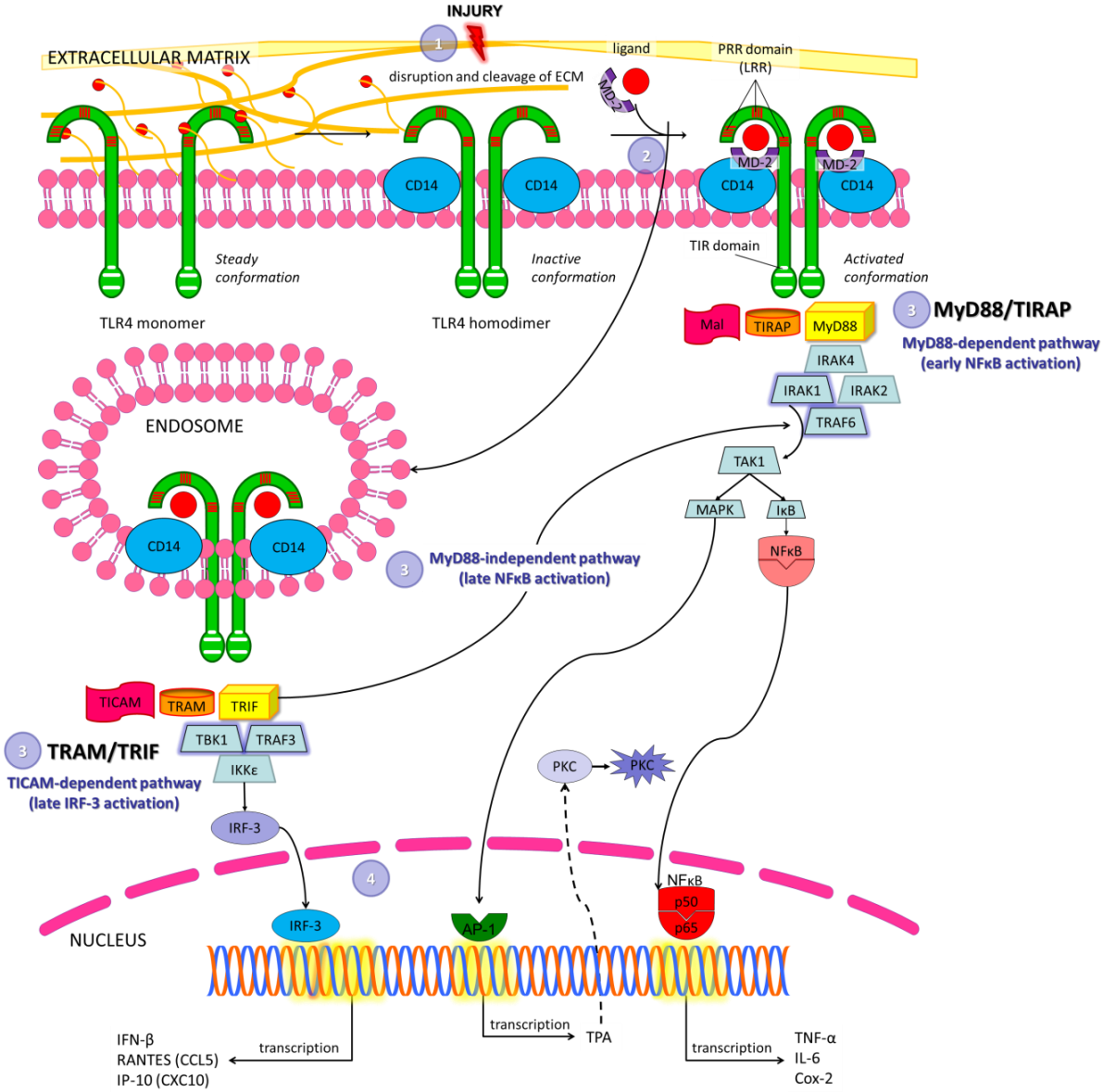

Figure 11. TLR4 intracellular signaling pathway: innate and adaptive immune response. (**1**) Interaction between ECM components and TLR4 ectodomain prevent dimerization of the cytosolic TIR domains, essential for maintaining the receptor in an inactive state prior to the recognition of the ligand. Tissue disruption liberates TLR4 from restraint, thus allowing endogenous ligands to stimulate the receptor. (**2**) Ligand recognition by TLR leads to the association of cytosolic TIR domains, as only dimeric TIR provide the scaffold for the recruitment of cytosolic adapters and assembly of signalosome. (**3**) Activation of intracellular transmission via signalling cascade initiates. The first downstream step requires the interaction between TLR and adaptor molecules containing TIR domain. Association with the different adaptors will depend on TLR4 membrane localization. Thus it can bind MyD88 and TIRAP/Mal (on the one side) or TRIF/TICAM-1 and TRAM/TICAM-2 (on the other side). TLR4 signals through the MyD88-dependent pathway from the cell membrane to produce proinflammatory cytokines and is internalized into late endosomes to signal through the TICAM-dependent pathway to produce IFN. Alternatively, proinflammatory cytokines can also be upregulated through a MyD88-independent pathway. Additionally to these transcription products, both MyD88-dependent and –independent pathways can induce the transcription of TPA, which is a potent protein kinase C (PKC) activator. (**4**) In brief, the activation and translocation of NFκB, AP-1 and IRF-3 transcription factors to the nucleus promotes the production of a wide variety of inflammatory mediators such as cytokines (TNFα, IL6, IL1β), chemokines, type 1 interferon (IFN), tissue-destructive enzymes. These costimulatory molecules provide a second signal to T cells to initiate the adaptive immune response. *IRF-3 = interferon regulatory factor-3; AP-1 = activator protein-1; TPA = 12-O-tetradecanoylphorbol-13-acetate; IFN-β = interferon-β; RANTES = regulated on activation normal T Cell expressed and secreted; IP-10 = interferon-γ-induced protein 10; COX-2 = cyclooxygenase-2*. Modified from (Owen M et al., 2015).

3.2. Role of Toll-like receptors in dorsal horn plasticity.

TLR4 antagonists have been traditionally conceived as ideal molecules triggering therapeutic effects on rodent sepsis models (Piazza *et al*., 2009; Takashima *et al*., 2009). However, later discoveries on the predominant expression of TLR4 by microglia[20] in the CNS –also resident and recruited macrophages – (Olson and Miller, 2004) and on the presence of these receptors in peripheral sensory neurons (Wadachi and Hargreaves, 2006) suggested a role for TLR4 also in nociception. Further experiments using TLR4 antagonists in rodent models of neuropathic pain confirmed this hypothesis as repeated administration resulted in relief of both thermal hyperalgesia and mechanical allodynia (Bettoni *et al*., 2008). Notwithstanding, in addition to this, TLR4 receptors have been described on the surface of a large number of distinct cell types: immune cells (Gondokaryono *et al*., 2007; Huang *et al*., 2007), dendritic cells (Takagi, 2011), glial cells (Li et al., 2015), the articular cartilage (Meng *et al.*, 2010; Gómez *et al.*, 2014), neurons (Ohara *et al*., 2013), fibroblasts (Ospelt *et al.*, 2008), Sertoli cells (Winnall *et al*., 2011) and endothelial and epithelial cells (Erridge, 2010).

In their basal state, glia play important roles in maintaining the health and normal functioning of the nervous system. However under altered physiological states, such as chronic pain, glia becomes activated, releasing a variety of substances involved in the initiation and maintenance of neuropathic pain including prostaglandins, excitatory aminoacids, growth factors and proinflammatory cytokines (Watkins and Maier, 2003). This contributes to the dysregulation of neuronal functioning. In this regard, the involvement of TLR4 in these neuroimmune interactions has been increasingly reported in the past decade (Bettoni *et al*., 2008; Saito *et al*., 2010). Furthermore, knock-out and knock-down assays of TLR4 expression have shown an attenuation of behavioural hypersensitivity, decreased glial activation and decreased expression of proinflammatory cytokines (Tanga *et al*., 2005; Lan *et al*., 2010).

[20] Expression of TLR4 on the microglial cell surface is of particular concern to us since they grow in numbers as they massively activate under sustained pain conditions, contributing to central sensitization –the main adaptive change involved in pain chronification–.

3.3. Morphine and Opioid-induced Hypersensitivity (OIH).

Opioids are the benchmark for treating moderate to severe pain and together with non-steroidal anti-inflammatory drugs (NSAID) the spearhead of the WHO analgesic ladder (Clark, 2002; Angst and Clark, 2006). Although originally designed for alleviating cancer-related pain, its potent analgesia made them popular for treating any chronic pain[21]. However, neuropathic pain has been reported to be resistant to morphine treatment.

In the past century it was yet known that opposing analgesia opiates could intriguingly induce immunosuppressive side effects coursing along with the loss of antinociception (West *et al.*, 1997). This convergent scenario was traditionally explained by means of a tolerant mechanism (de Conno *et al.*, 1991; Sjøgren *et al.*, 1993; Aley and Levine, 1997). Striking similarities in mechanisms underlying chronic pain and opioid tolerance led to the discovery of a possible role for spinal glia in modulating opioid counter-regulatory mechanisms. Furthermore, several studies on repeated morphine administration demonstrated a proinflammatory response opposing morphine analgesia (Song and Zhao, 2001).

Over the last few years, an emerging concept has been steadily gaining ground as a valid alternative to explain this crossroads: the phenomenon of *opioid-induced hypersensitivity* (OIH), also known as *opioid-induced hyperalgesia* (Ocasio *et al*., 2004). This theory achieved rapid and detailed clinical broadcasting especially by the hand of Dr Wolfgang Koppert (Koppert, 2004;Koppert and Schmelz, 2007) and Dr J David Clark (Angst and Clark, 2006; Chu *et al.*, 2006; Low *et al*., 2012). To this respect, acute and chronic[22] high doses of opioids have been reported to induce spontaneous pain, allodynia and thermal hyperalgesia in humans (Raffa and Pergolizzi, 2013) and rodents (Li *et al*., 2001; Chang *et al.*, 2007). Nevertheless, it is still difficult to differentiate between morphine tolerance and induced

[21] Opioids mediate their pharmacological effects via activation of three types of G-protein coupled receptors (GPCR): mu opioid receptor (MOR), delta opioid receptor (DOR) and kappa opioid receptor (KOR). Recently, a new opioid-like receptor ORL-1 has been proposed. Opioid receptors are found in cell membranes at multiple sites in the CNS and PNS. Morphine, the gold standard among strong opioids, is a potent μ agonist.

[22] Until very recently, it was assumed that chronic use of opioids could lead to opioid-induced abnormal pain sensitivity only if followed by abrupt reduction or withdrawal of dosage; however this position was definitely knocked down in the past decade as reviewed in (DuPen et al., 2007;Mao, 2006).

hyperalgesia and various mechanisms have been proposed to be implicated in the development of OIH based on plastic changes occurring in the PNS and CNS.

a) Counter-regulation hypothesis. According to the *counter-regulation hypothesis*[23], a balance between anti- and pro-nociceptive effects is apparently dependent on the type, dose, pattern and route of opioid administration (Chu *et al.*, 2006) and is thought to occur as a compensatory mechanism in an attempt to reach homeostasis (Freye, 2010). Chronic administration of intrathecal or systemic morphine may produce a sustained imbalance at spinal and supraspinal levels and therefore act also on some other opioid receptors coupled to excitatory cholera toxin-sensitive G_s-proteins (stimulative regulative G protein) located on pre- and post-synaptic neurons and on glial cells. Subsequently, intracellular levels of cAMP increase and enable the activation of protein kinases and the opening of calcium channels leading to increased intracellular Ca^{2+} levels and membrane depolarization. As a consequence, multiple neurotransmitters (Substance P, CGRP) are released. Calcium may also act on nNOS leading to NO production and on conventional PKC, which will phosphorylate and inactivate opioid receptors and activate NMDA-receptors (Koppert and Schmelz, 2007; Marion Lee *et al.*, 2011; Raffa and Pergolizzi, 2013; Pal and Das, 2013) (**Fig.12**). It is worth mentioning that opioid receptors exist as dimers or oligomers of same or different opioid receptor subtypes and that potency of morphine is attenuated in δ-containing opioid receptors, since they display decreased G-protein coupling and signaling compared to μ-homodimers; corresponding to what seen in cases of neuropathic pain as well (Gupta *et al.*, 2010).

[23] The *counter-regulation hypothesis* is also referred to as the *opponent process theory* (Solomon and Corbit, 1974).

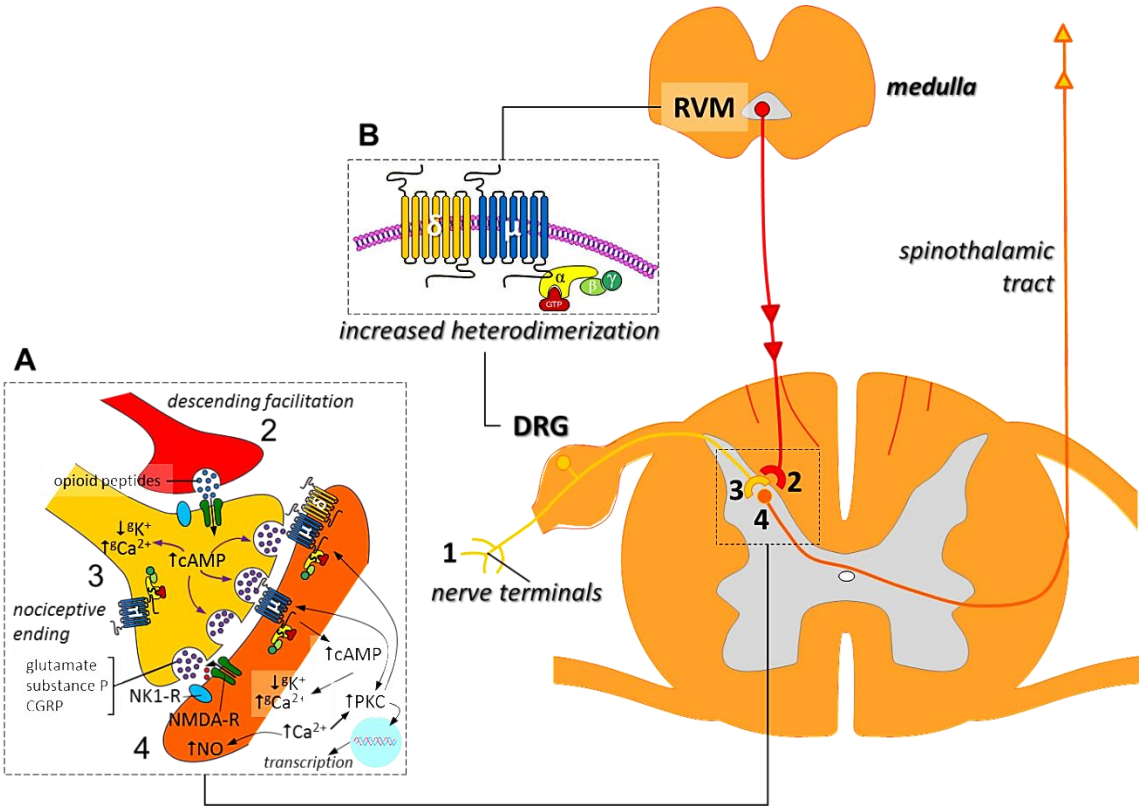

Figure 12. Schemtatic representation of the different mechanisms implicated in the development of OIH. When an opioid binds to a receptor, an excitatory or inhibitory response may occur. The activation of opioid receptors can inhibit transmission of pain impulses in the brain and spinal cord and in peripheral sensory nerves. Opioids can also modulate noxious stimuli via descending inhibitory pathway. However opioids can also lead to pro-nociceptive mechanisms, which may differ depending on the chosen site along the nervous system: (**1**) sensitisation of peripheral nerve endings; (**2**) enhanced descending facilitation of nociceptive signal transmission; (**3**) enhanced production and release as well as diminished reuptake of nociceptive neurotransmitters; (**4**) sensitisation of second-order neurons to nociceptive neurotransmitters; (**5**) Neuroplastic changes in the RVM medulla that may increase descending facilitation via *on cells*. **Box A (dotted line).** Activation of $G_{i/o}$-coupled opioid receptors reduces intracellular levels of cAMP. However, upon long-term application of μ-agonists other less common G_s-coupled opioid receptors may also become activated and act on adenylyl cyclases increasing the levels of intracellular cAMP at the primary nerve endings in the spinal dorsal horn. This will result in the activation of protein kinases and the opening of calcium channels leading to increased intracellular Ca^{2+} levels and membrane depolarization. Consequently, a heightened release of excitatory amino acids and neuropeptides acting on the postsynaptic neuron (e.g. NK1-R) will also occur. Morphine-induced activation of G_s-coupled opioid receptors can also happen at the postsynaptic neuron. Increased intracellular levels of Ca^{2+} can induce the activation of a conventional PKC causing the phosphorylation of NMDA-receptors and therefore increased influx of Ca^{2+}. Simultaneously, PKC can also act on opioid receptors rendering them inactive. In addition to all this, increased levels of intracellular Ca^{2+} induce heightened production of NO, which reduces the antinociceptive potency of μ-agonists. Further increased levels of opioids might be maintained by facilitative descending pathways. **Box B (dotted line).** Additionally, following morphine chronic treatment μ-δ heterodimer is increased in the DRG, RVM and other regions in the brain. Potency of morphine is attenuated in δ-containing opioid receptors, since they display decreased G-protein coupling and signaling compared to μ-homodimers. *DRG = dorsal root ganglia, RVM = rostral ventromedial medulla, cAMP = cyclic adenosine monophosphate, PKC = protein kinase C, NO = nitric oxide.* Figure modified from (Angst and Clark, 2006;Koppert and Schmelz, 2007).

Despite this approach, opioids can exert non-stereoselective effects on other receptors (Hutchinson *et al*., 2010a; Due *et al*., 2012). This is sustainable with the fact that opioid

hyperalgesia was still observed in μ-, δ- and κ-opioid receptor triple knockout mice, which again is suggestive of the existence of a non-classical opioid receptor whose non-stereoselective activation opposes analgesia (Juni *et al*., 2007).

b) TLR4 and opioids tinckering.

Opioids are currently obtained by isolation from opium for the low cost that it represents (Rinner and Hudlicky, 2012). Some opioids (e.g. codeine, heroin) produce metabolites chemically identical to morphine after systemic administration (Smith, 2009). In this regard morphine is primarily metabolised in the liver into two major metabolites: morphine-6-glucuronide (M6G) and morphine-3-glucuronide (M3G); the former, an analgesic active compound, and the latter, devoid of analgesic activity (Komatsu *et al*., 2009). Morphine derivative M3G (Lewis *et al*., 2010; Due *et al*., 2012) presents a lack of binding to opioid receptors and has been reported to mediate, single-handedly, the activation of the TLR4/MD-2 heterodimer on microglial surfaces, as inferred from *in vitro*, *in vivo* and *in silico* studies[24] (**Fig.13**). To this respect, researcher Linda R. Watkins and her team (Hutchinson *et al*., 2010a; Hutchinson *et al*., 2010b; Hutchinson *et al.*, 2012) advocate for considering TLR4 receptors as the missing link that connects the concepts of immune system, antinociception loss and use of opioids. According to Watkins, opioids might activate TLR4 on glial surfaces leading to a mechanism that opposes classical opioid analgesia (Watkins *et al*., 2005; Watkins *et al.*, 2007a; Watkins *et al*., 2009). In fact, although TLR4 might not be the only receptor for glial activation, some glial inhibitors (*propentofylline, pentoxifylline, minocycline, ibudilast*) are potential useful agents for the treatment of neuropathic pain and for the prevention of tolerance to morphine analgesia (Mika, 2008), and particularlly *ibudilast* has been recently described as a TLR4 singalling inhibitor. Ibudilast showed to increase the clinical efficacy of opioids by inhibiting glial activation (based on microglial and astrocyte activation marker suppression) and to possess the ability of enhancing the production of anti-inflammatory cytokines, in addition to suppressing proinflammatory ones. That is, TLR4 can recognize opioids as foreign xenobiotic substances leading to proinflammatory immune signaling (Watkins *et al.*, 2007a). In fact, TLR4 knockout mice

[24] A wide list of TLR4 agonist and antagonist molecules are described in (Li, 2012).

fail to display hyperalgesia following M3G administration (Due *et al.,* 2012) and OIH is not reversed by administration of an opioid antagonist (Chu *et al*., 2006).

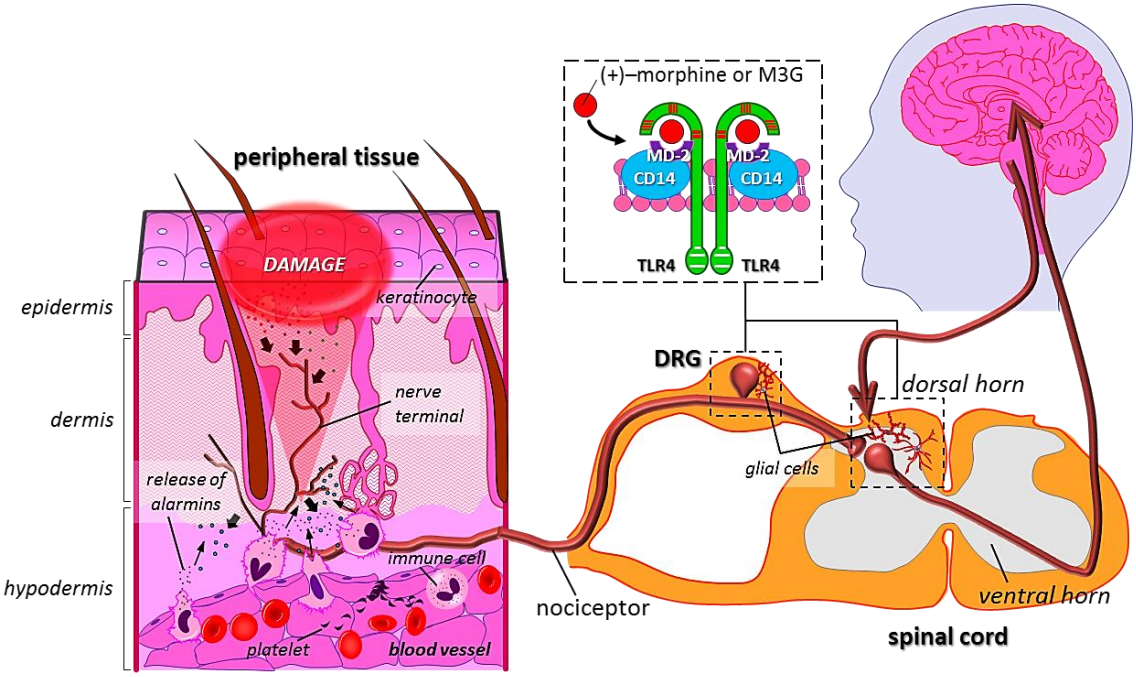

Figure 13. TLR4 stimulation as an underlying mechanism for opioid-induced hyperalgesia. Although the molecular mechanisms underlying OIH still remain to be clarified, it is thought to result from alterations in the PNS and CNS. To this respect, a wide range of opioids and opioid metabolites have been reported to bind and activate TLR4, whose main representative are the opioid metabolite morphine-3-glucuronide (M3G) and the unnatural isomer (+)–morphine, both of which have no effect on opioid receptors but elicit increased nociception. TLR4 is predominantly expressed in sensory neurons in the DRG and in microglia in the spinal dorsal horn, and overlapping mechanisms based on TLR4 non-stereoselective activation have been suggested to regulate both surgical incision induced-nociception and OIH.

To the best of our knowledge, the only existing opposition to these findings is based on the work of a Japanese group, stating that TLR4-knockout mice present microglial activation (assessed by CD11b mRNA levels[25]) and reduced tail-flick[26] latencies when morphine is daily given for five consecutive days (Fukagawa *et al*., 2013).

4. Animal models for the study of pain.

4.1. Osteoarthritic pain.

[25] Despite the traditional use of CD11b, Iba1 and GFAP as protein markers of glial cell activation, as suggested in (Horvath *et al*., 2010), this is being increasingly questioned.

[26] The tail-flick test consists in a radiant heat light source that sends out a light beam focused to the tail of the rat. The reaction is detected automatically when a digital timer that started counting up when the light switched up stops as the animal withdraws its tail from the light beam. The recorded time is registered as the withdrawal latency for that animal.

Osteoarthritic Pain (OA) is currently defined as a chronic degenerative disorder of multifactorial aetiology that affects the entire diarthrosis leading to a same pathologic state: degeneration of the joint elements with eventual restricted movement and pain (Pomonis *et al*., 2005; Aigner *et al*., 2010). Risk factors associated with the development of OA include genetic, ethnical, gender, ageing, obese and occupational based reasons among others. In fact, OA affects differently to men and women, being hand and knee OA more commun in women and hip OA similar in both genres (Solís *et al*., 2007).

According to the International Association for the Study of Pain (IASP), osteoarthritis (OA) is the most common joint disorder worldwide, affecting aproximately 37% of senior citizens (IASP, 2009). Large scale studies on the prevalence of osteoarthritis in Spain are carried out by the Spanish Society for Rheumatology (SER). This Society estimated a similar prevalence of 43% in the general Spanish population in year 2000 (Cano Montoro and Cases Gómez, 2002). To this respect, only knee and hand OA exhibit well-documented national data, remaining other locations (e.g. hip, neck or column) undocumented, extrapolated from foreign studies or only partially analysed in small cohort of patients by individual groups (Alegre De Miquel *et al*., 2011; Garriga, 2014) (**table 3**).

		Age						
Affected joint		40-49	50-59	60-69	70-79	>80	general	
knee OA	prevalence in men	2.4%	5.5%	18.1%	16.7%	14.3%	5.7%	10.3%
	prevalence in women	4.4%	13.3%	37.2%	44.1%	29.1%	14.0%	
hand OA	prevalence in men						2.3%	6.2%
	prevalence in women						9.5%	

Table 3. Study on the prevalence and impact of rheumatic diseases carried out by the Spanish Society for Rheumatology (EPISER 2000 project[27]). There might be variations in OA prevalence depending on the different diagnosis criteria (e.g. symptomatic, radiologic or both) used in population-based studies (Comas et al., 2010). All the data herein mentioned come from the EPISER 2000 project.

Until very recently, pre-clinical research on OA was mainly focused on the study of the progression of the disease rather than on the chronic pain associated to this condition (Ayala and Fernández-López, 2007). Nowadays pain is just considered the major symptom of OA and also the major determinant of functional loss. Factors proposed for contributing

[27] EPISER 2000 project consisted on a study to determine the prevalence of lumbalgia, hand and knee OA, rheumatoid arthritis, fibromialgia and osteoporosis in the Spanish population. It also counted on the development of a pilot study on the prevalence of systemic lupus erythematosus. Basically, a population-based survey was conducted in 20 Spanish cities to 2.998 individuals over an age of 20, random selected and clasified according to age and sex. Subjects were also examined in minute detail by trained rheumatologists according to a standardised protocol and criteria in accordance to the American College of Rheumatology and the WHO were applied (Carmona, 2001).

to this complex pain syndrome include biological, psychological and social framework, the sum of which may explain the discrepancies found between the degree of joint damage and the severity of pain in different patients (Hunter *et al.*, 2009) (**table 4**).

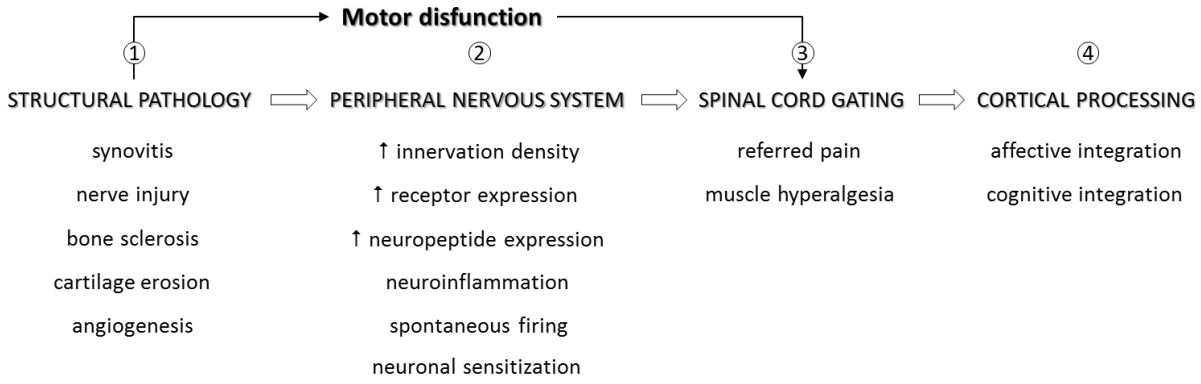

Table 4. Biological and psychological factors contributing to OA pain. (**1**) ***Structural pathology***. Under certain conditions knee structure undergoes cartilage erosion, disrupted bone metabolism and local proinflammatory processes that lead to synovitis and vascular and nerve remodelling. (**2**) ***Peripheral nervous system*****.** Neuro -inflammation and -sensitisation at the peripheral terminals may cause hyperexitability of nerve afferent fibres leading to spontaneous firing. (**3**) ***Altered spinal cord gating***. Continuous discharge at the spinal dorsal horn might result in synapse plasticity and cause disruptive phenomena such as referred pain and muscle hyperalgesia even though the pain source originates at the knee joint. (**4**) ***Altered cortical processing***. Past experiences and sociocultural background may influence subjective judgment of pain and lead to dysfunction of descending noxious inhibitory control. **Motor disfunction**. Tissue injury and consequent release of proinflammatory molecules may lead to changes in the environment bathing nociceptor terminals, resulting in lowered thresholds and increased responsiveness to stimuli. Additionally, hypertrophy of the capsule causes movement restriction and during the healing feedback response, this immobilization can originate developing small fibres to adhere with the surrounding tissue leading to ectopic discharge and stimuli misinterpretation by the spinal cord and brain.

Despite the underlying chronic pain condition, whether OA has a neuropathic or a rather nociceptive component has long been subject of debate (Combe *et al*., 2004; Hochman *et al*., 2010; Kelly *et al*., 2013). National (Oteo *et al.*, 2013) and international (Hochman *et al*., 2010) clinical studies have recently shown up the presence of a neuropathic component in not less than 33% of all cases diagnosed as chronic knee joint pain caused by knee osteoarthritis. That said, both peripheral and central sensitisation are relevant elements in the pathology as elicited for clinical evidence in the recent years (Arendt-Nielsen *et al*., 2010; Finan *et al*., 2013). In fact, all indicators of pain sensititisation (both peripheral and central) have been observed in patients with knee osteoarthritis to a greater or lesser extent: hyperalgesia, allodynia, spatial summation, temporal summation (wind-up) and aftersensations (Harden *et al*., 2013; Skou *et al*., 2013). On the one hand, peripheral sensitisation is normally related to local and neurogenic inflammation, which shows up mainly as primary hyperalgesia and aftersensations but only little primary allodynia. On the other hand central sensitisation is characterised by allodynia and hyperalgesia spread to

adjacent and remote sites from the affected joint (spatial summation) and may involve impared descending pain modulation mechanisms (Courtney *et al*., 2012).

4.1.1. Pain associated with osteoarthritis of the knee.

During osteoarthritis, the impediment of articular mobilization makes the pressure exerted by the synovial liquid in the articular space to be too much to allow the nutrients to get into the chondrocytes; hence the cell cannot produce the fibres needed for repairing the ECM of the cartilage (Beyreuther *et al*., 2007).

The knee receives a nerve supply from cutaneous nerves in the overlying skin, branches of peripheral nerves passing near the joint (primary nerves) and branches of intramuscular nerves crossing the joint capsule (accessory nerves) **(Fig.14)**. Most afferent fibres in articular nerves are unmyelinated, comprising C and sympathetic nerve fibres. Heavily myelinated Aβ fibres and thinly myelinated Aδ fibres comprise about 20% of the total fibres (Kidd, 1996). These sensory nerves respond to mechanical stimuli such as stretching of the joint capsule but also to chemical inflammatory mediators, which may directly stimulate silent nociceptive fibres or sensitise them to mechanical stimuli. All types of afferences (nociceptors or not) may be implicated in the pathophysiology of osteoarthritic pain by means of peripheral sensitisation and neurogenic plasticity may operate at both, peripheral and spinal levels.

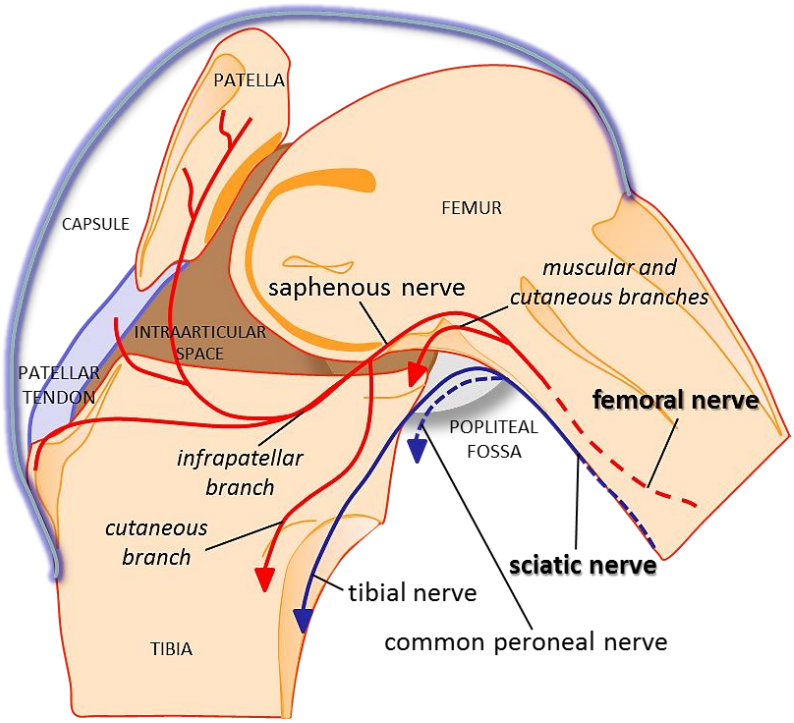

Figure 14. Knee joint innervation. The femoral nerve innervates muscular and cutaneous tissues of the upper tight and leg. The terminal cutaneous branch of the femoral nerve is the saphenous nerve. Saphenous nerve divides into three branches at the knee joint, all gathered in the infrapatellar branch, but also continues downstream to the feet basically innervating skin tissues. Sciatic nerve innervates the lower leg and foot and devides in two branches at the *popliteal fossa*: the tibial and the common peroneal nerves. The tibial nerve gives rise to articular, muscle and skin branches, whereas the common peroneal nerve gives off articular and cutaneous (lateral sural nerve) branches.

In the rat, 80% of all knee joint afferent nerve fibres are nociceptive. Nociceptors are located throughout the entire joint, including the capsule (McDougall, 2006), ligaments (McDougall *et al*., 1997), tendons, menisci, periosteum and subchondral bone (Mach et al., 2002). Even the synovium contains a good supply of large-(Aβ), middle-(Aδ) and small-diameter (C) axons (Wenham and Conaghan, 2009). The former are especially located around the larger blood vessels and responsible for the control of articular blood flow, while the middle- and small-sized are basically silent and responsible for pain transmission only during tissue damage or when sensitised during an inflammatory response (McDougall *et al*., 1997). Paradoxically, the cartilage (McCormack *et al*., 2009), the primary site of injury in OA, is avascular and aneural (Bora and Miller, 1987; Henrotin *et al*., 2005). This may explain why in the early states, the joint is usually asymptomatic.

However, innervation of the diarthrosis under pathologic conditions is notably different from that of normal state. Under pathological conditions, the sensory and sympathetic

nerve fibres are absent in the superficial synovia and in areas of intense inflammation, whilst deeper synovia keeps its innervation around the vessels (Im *et al.*, 2010). Contrary to this, nerve and vascular ingrowth have been reported to occur in damaged osteoarthritic cartilage (**Fig.15**) (Ashraf and Walsh, 2008). This may suggest that the *inflammatory soup* straining from the nearby vessels may produce different effects depending on the tissue phenotype where it is released.

Osteoarthritic pain initiates with a mild intraarticular inflammation and degeneration of the articular cartilage and the subchondral bone (Beyreuther *et al.*, 2007). Overexpression of matrix-degrading proteases and pronflammatory cytokines contribute to the progression of the pathology by diverse mechanisms involving down-regulation of anabolic processes and up-regulation of catabolic and inflammatory responses (Kapoor *et al*., 2010). As a result, high-threshold mechanoreceptors, polymodal nociceptors, and "silent" nociceptors in the joint capsules and ligaments become sensitised, reducing their activation thresholds and increasing the firing rate of action potentials to the spinal dorsal horn.

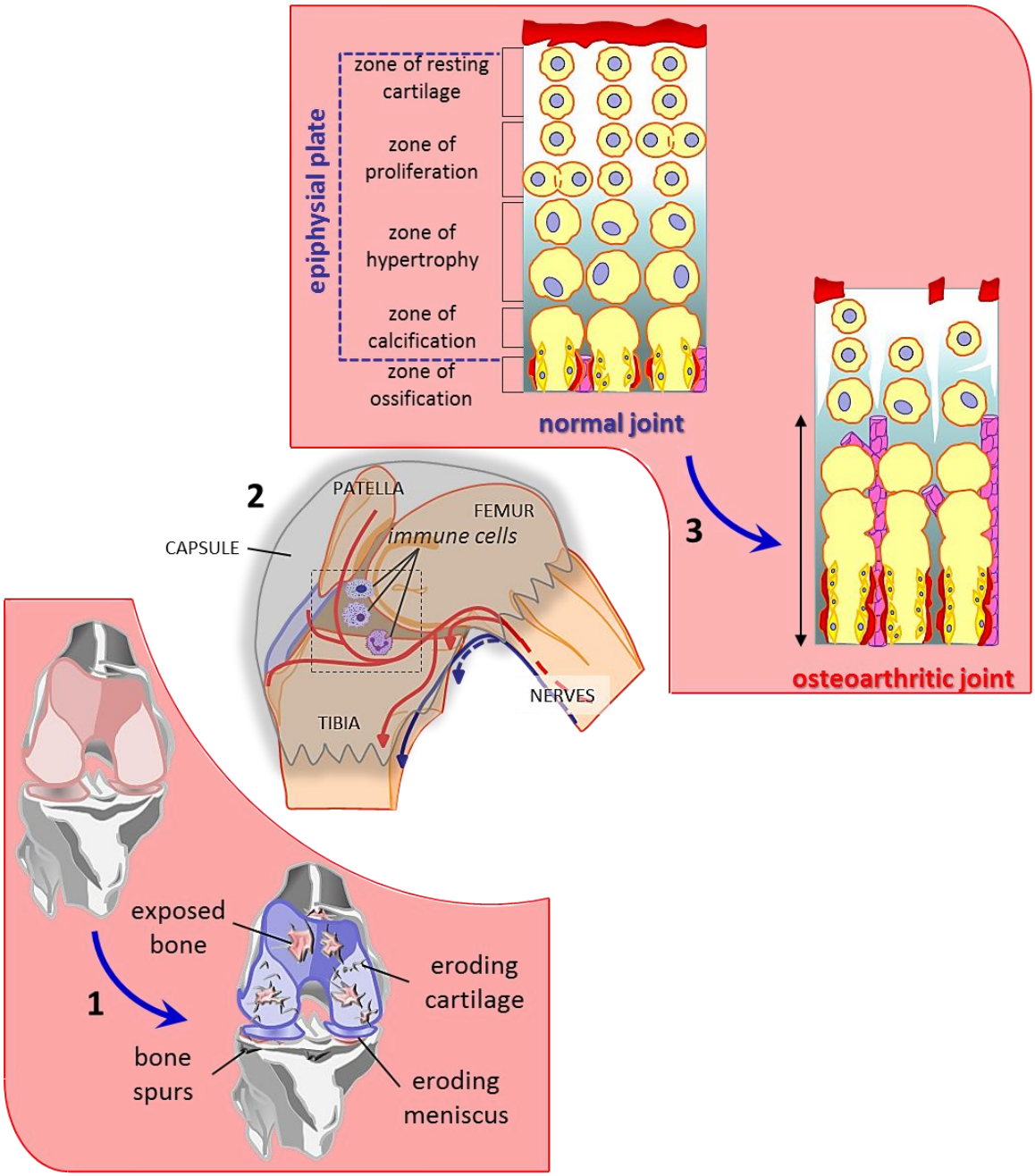

Figure 15. Vascularization and innervation of the articular cartilage in the knee under normal and pathological conditions. The degradation of cartilage results of the combination of mechanical stress and biochemical factors. (**1**) OA generally initiates with mechanical erosion. (**2**) Particles released from the knee cartilage to the interstitial fluid provoke a "knock on effect" on immune cells causing the joint cavity to swell up, thus increasing the tension at the connective tissue and causing the articular space to distend the capsule. Initial thickening of the synovial membrane and capsule causes the knee cartilage to stop being lubricated, being deprived of the nutritional supply. (**3**) Thus, the cartilage loses its capacity to tolerate tensions, breaks up and thins, remaining in turn the subchondral bone exposed. Next, there is an increase of the emerging bone mass all along the articular line, together with angiogenesis and nerve growth at the epiphyseal plate of the metaphysis. Fissures in the cartilage on the one side and subchondral angiogenesis on the other side increase permeability allowing further plasma cells to enter the cartilage-bone unit.

Despite the clear evidence for a central role on pain production in OA, current treatments are chiefly palliative and aimed at peripheral mechanisms (Jordan *et al*., 2003; Barron and Rubin, 2007; Benito *et al.*, 2008) (**table 5**). There are, additionally, a

few drawbacks associated with many of the drugs being used. For instance, analgesia induced by peri- or intra-articular knee infiltration with corticorsteroids (Wittich *et al*., 2009; Ertürk *et al*., 2014) or local anaesthetics (Creamer *et al.*, 1996; Eker *et al.*, 2008; Jorgensen *et al.*, 2014) lasts only 2-3 weeks and requires multiple injections. Intra-articular hyaluronic acid for its part has not proved to achieve greater effects and results from different studies show to be controversial (Lo *et al.*, 2003; Arrich *et al.*, 2005). Other conventional treatments such as NSAID have shown both insufficient efficacy and gastrointestinal or cardiovascular side effects (Caldwell *et al*., 1999; Brandt, 2003; van Laar *et al*., 2012;). On the other hand, topic capsaicin (Kosuwon *et al.*, 2010; Laslett and Jones, 2014) and oral SYSADOA[28] (Clegg *et al*., 2006) have recently postulated as good alternatives as presenting more remnant analgesia and avoiding secondary effects of NSAID. However, physicians usually turn to the use of combined therapies for treating osteoarthritis-knee pain[29].

Type of administration	Treatment
ORAL	paracetamol (acetaminophen)
	NSAID
	opioids*
	tramadol
	SYSADOA (glucosamine sulfate, chondroitin sulfate, diacetylrhein)
TOPICAL	local anaesthetics (lidocaine)
	NSAID
	capsaicin
INTRA-ARTICULAR	corticosteroids
	hyaluronan (SYSADOA)
	local anaesthetics

Table 5. Current pharmacological treatment on knee osteoarthritis. Treatments for OA-knee pain are chiefly palliative and aimed at peripheral mechanisms, except the use of tramadol and opioids, which can bind receptors located in the CNS. Treatment guidelines recommend starting with paracetamol as the first-line therapy for oral administration, followed by NSAID, opioids and tramadol. Patients not responding to paracetamol nor willing to undergo further systemic therapy are prescribed topical administration as a stand-alone therapy or in combination with oral drugs. Condroprotective drugs (SYSADOA) may be also given as coadjuvants to oral paracetamol. While paracetamol achieves acute pain relief, these medicines provide long-therm acting but prolonged effect and are considered as disease-modifying drugs. The latter effect can also be appreciated with intra-articular therapy however, this is an invasive technique and requires both aseptic conditions and spaced-time administrations.

[28] SYSADOA = symptomatic slow action drugs for osteoarthritis.

[29] A consensus document on pharmacological treatment of OA elaborated by the SER is recommended for further reading (Blanco and de la Sociedad, Panel de Expertos, 2005).

4.1.2. *A model of osteoarthritic pain chemically induced by monosodium iodoacetate.*

Experimental animal model systems are intended to best imitate syndromes and pathologies currently occurring in patients and to this purpose, they are decisive to complement osteoarthritic studies from clinicians in human beings. They provide a means for studying the pain mechanisms involved in such a heterogeneous disease and give cause to survey correlating symptoms in other chronic pain conditions in order to develop more efficient therapies.

However, despite the robust similarities to the human disease, achieving identical overlapping is a matter out of reach. To this regard, infiltration of the chemical agent monosiodium iodoacetate (MIA) into the articular cavity of the rat knee reproduces the knee degenerative disease observed in clinics in a very precise way. Since the articular cartilage lacks vascularization, the metabolism in chondrocytes acts at low oxygen tensions, being the majority of the energetic requirements satisfied by anaerobic glycolysis. In the MIA model, MIA binds the active site of glyceraldehyde-3-phosphate dehydrogenase (GAPDH) enzyme rendering the enzyme useless. As a consequence, the following steps in glycolysis are inhibited. Therefore, the blockade of glycolisis leads to their own cellular death and subsequent disruption of articular cartilage (Lefebvre *et al*., 2011).

Attending to a physiological context, MIA induces hind paw distal tactile allodynia and thermal hyperalgesia (Procházková *et al.*, 2009), and knee proximal mechanical hyperalgesia that correlate with the presence of activated spinal microglia and astroglia typical in central sensitisation (Sagar *et al.*, 2011)

From a clinical point of view, MIA induces synovitis followed by cartilage thinning, development of fissures and disruption of deeper zones in direct contact with the subchondral bone. Inflammation of the synovium and capsule is apparently resolved by day 3-7 and is not considered to play a role any more in pain production. This first phase mainly consists in the interaction of plasmatic proteins and inflammatory products with resident fibroblasts to restore the cartilage surface. Hence, while neutrophils and macrophages remove the dead tissue and cellular debris, other incoming cells together with resident fibroblasts form a granulation tissue, which starts as a laxe connective

tissue that ends up by progressively densifying and even producing cartilage in some areas in order to patch the damaged area (**Fig.16A**). Subsequently, patches of new-forming tissue extend to the calcified cartilage and repair of the deep zone occurs during the second week post-MIA (Bove *et al*., 2003; Combe *et al*., 2004). During this process, remodelling of the superficial zone can however cause an excess of deposits that may turn towards an outgrown, thickened fibrotic phenotype, leading to aberrant architecture and function of the normal tissue. That is, the development of a fibrocartillaginous callus or fibrous pannus that, in case of a natural normal fracture would serve to join the bone fragments but, in this case (chemically induced OA), it often makes the femoral and tibial condiles to stick together (**Fig.16B**).

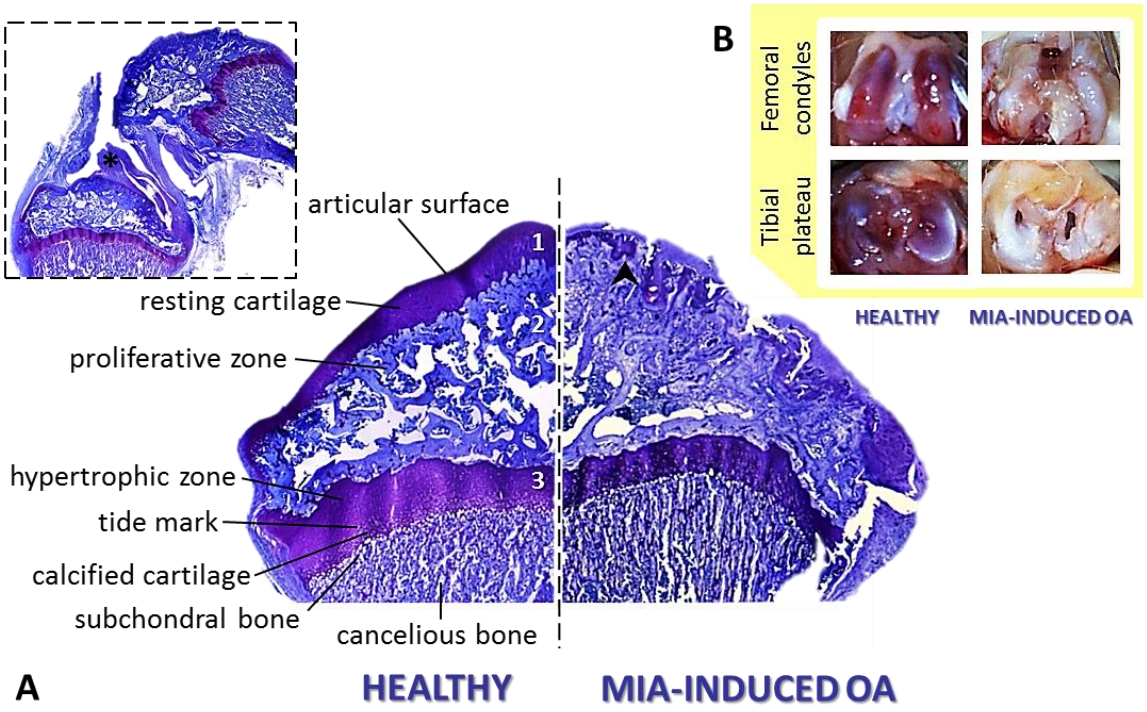

Figure 16. A. Representative micrograph of a toluidine-blue stained section of the tibial plateau in a healthy (left side) and MIA-induced osteoarthritic (right side) knee, 22 days post-injection. Healthy cartilage is made up of three well-diferentiated zones: (**1**) superfitial tangential zone (10-20%), (**2**) middle zone (40-60%), (**3**) deep zone (30%). Proportion of each of these zones is altered in the pathological cartilage. During OA process, the superficial zone, consisting in the resting cartilage (navy blue), thins or completely fades away. Structural disruption of the synovial membrane allows plasma to massively enter the intra-articular space and the wound (before, referred as articular surface) is covered by a wave of formed elements secreting cytokines, growth factors and plasmatic proteins that serve as the basis for the resident cells to adhere and start to repair the wound (light blue). During the repairing process, resident cells in the middle zone (proliferative zone) start to proliferate together with the invading cells that infiltrated into its clefts and fissures; then migrate to the surface and occasionally produce new cartilage (➤). Marked damage can also affect the deep zone from the calcified cartilage and show decreased thickness. The tidemark—the demarcation line between calcified and articular cartilage—shifts upwards, representing a thinning of the overall articular cartilage. Note excess pannus (✱) formed in the joint between femur and tibia with the disruption of the synovium (dotted-line box). **B. Gross appearance of the knee joint following surplus fibrosis, 22 days post-MIA.**

4.2. Postsurgical pain.

Nearly every surgery evokes postoperative pain. This is often classified within the acute pain category regarding the ailment duration, which in many cases in more or less short order resolves, but may shift into a rather outlasting subchronic pain state in some therapy-resistant cases (Deumens *et al*., 2013). To this respect, the IASP defined persistent post-operative pain as the pain state that generally lasts more than two months after surgical intervention and cannot be explained by other causes (Schug and Pogatzki-Zahn, 2011).

During the last decade an increasing number of articles enhanced transition into chronic post-surgical pain as a not so uncommon event involving physical remodelling of the neuronal network structure. In fact, plastic changes such as temporal and spatial summation at distant sites to the wound have been reported, whence peripheral (Brennan *et al*., 1996) and central (Obata *et al.,* 2006; Ito *et al.*, 2009; Chen *et al.*, 2012) sensitisation are considered important hallmarks of this long-lasting postoperative (PO) pain.

Despite the existence of guidelines to surgically proceed on the basis of consensus and introduction of new interventional and anaesthetic techniques, postoperative pain continues to be largely undermanaged (Wu and Raja, 2011) and insufficiently represented in clinical literature (Kissin and Gelman, 2012).

In order to investigate the pathophysiological mechanisms of this persistent postsurgical pain and to evaluate novel analgesic therapeutics, preclinical models of postsurgical pain have been developed.

4.2.1. Incisional model of pain.

The typical model of incisional pain was first characterised by Brennan and colls. (Brennan *et al*., 1996). Considering that pain caused by inflammation, nerve injury or incision is constructed by different pathophysiologic mechanisms, the authors designed an incisional model for postoperative pain able to sensitise on the one hand primary afferences (Aδ and C-fibres) and on the other hand wide dynamic range (WDR) neurons in the spinal dorsal horn (Pogatzki *et al.*, 2002; Zahn *et al*., 2002; Banik and Brennan, 2004). This model is based on a surgical incision performed on

the plantar aspect of the animal's hind paw. Information is transmitted by both sural and tibial nerves (**Fig.17**) and results in an increased responsiveness to tactile and/or heat stimuli at sites immediately adjacent (both) and remote (only the former) to the incision (Zahn and Brennan, 1999). In other words: the development of primary and secondary hyperalgesia.

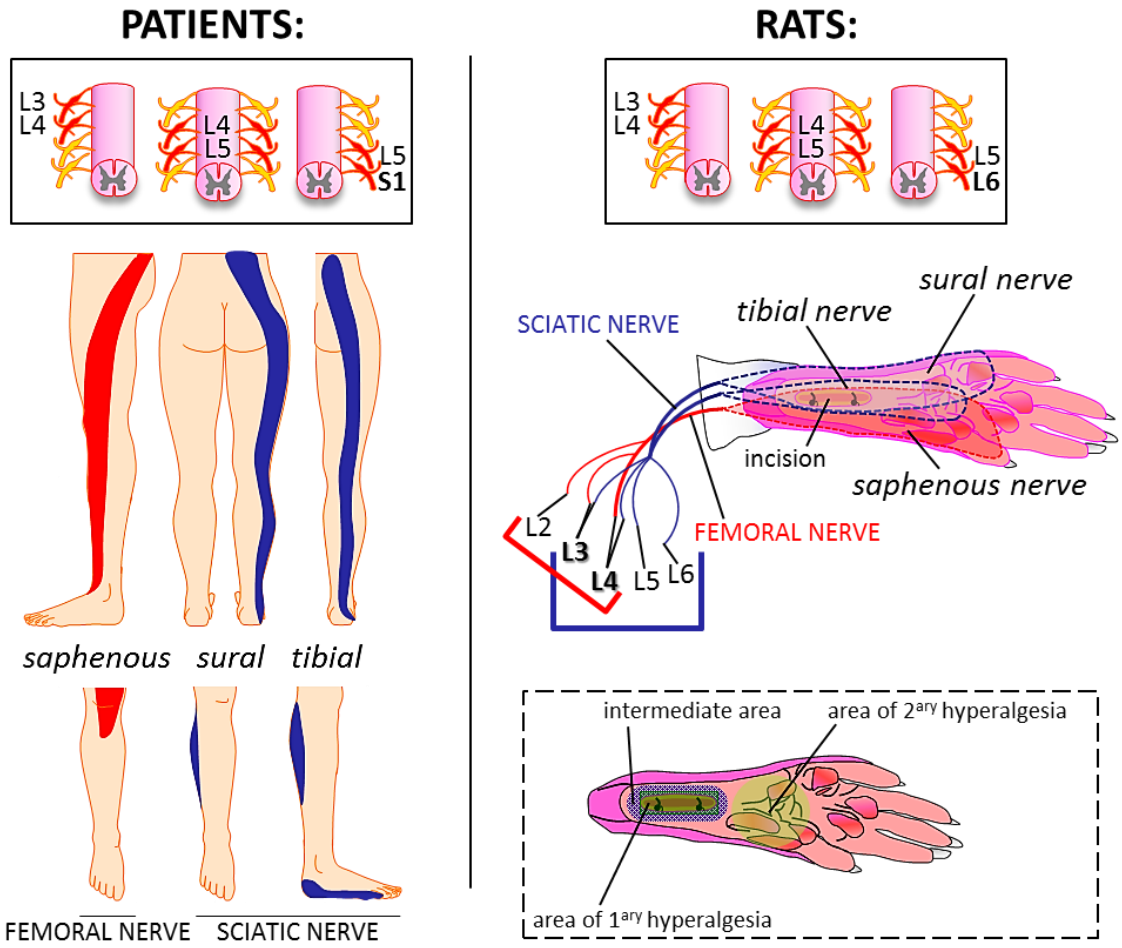

Figure 17. Cutaneous innervation on the sole of the foot in human patients and on the plantar aspect of the hind paw in rats. Saphenous, sural and tibial branches of the femoral (the former) and sciatic (the latters) nerves are shown. Areas of primary and secondary hypersensitivity detected in the model after incision onto the rat's paw are also shown (dotted line box). L2 to L6 correspond to lumbar sections of the spinal cord, whilst S1 matches the sacral region. Note that S1 region in human patients corresponds to L6 in rats.

Immune cells play a controversial dual role at the incision site in surgical wounds, as they not only contribute to the inflammatory and nociceptive response during wound healing but may also initiate the sensitisation of peripheral nociceptors (Magerl and Klein, 2006; Voscopoulos and Lema, 2010).

Observations derivative from this model may lead to test theories of sensitisation and plasticity in postoperative pain but also to assess the contribution of different analgesic drugs and therapies to the management of incisional pain.

Regarding a basic science context, the pain incisional model in rodents is a well-characterised method to assess morphine-derived pro- or anti-nociceptive effects. Regarding this last point in particular, diverse studies seem to indicate that reading of opioid induced hypersensitibility (OIH) apparently depends on the nature of the model and on the tests used for measuring the experimentally evoked pain. To cite but a couple of examples, a single medium/low-dose of morphine administered subcutaneously into the skin of the back prior to the surgery (Clark *et al.*, 2007) has shown to reduce early proinflammatory cytokines levels within the wound environment, with the consequent although short-lasting anti-nociception. In the same line, an intrathecal administration of high-dose morphine (Nagakura *et al*., 2008) results in supression of surgically induced pain immediately after incision. However, information about chronic morphine administration is still confusing. To our knowledge, Sinatra and Ford suggested for the first time the hypothesis that chronic (but not acute) high doses of opiates in animals with peripheral nerve damage could negatively affect the proliferation of Schwann cells (and other immune cells) and induce the inhibition of myelin debris removal (Sinatra and Ford, 1979). This was later followed by the discovery of opiates affecting other immune-like cells such as the glia. For instance, studies on repeated administration of high systemic doses of morphine show hypertrophy and overexpression of several molecular markers in spinal glial cells, what is related to facilitation of pain transmission (Song and Zhao, 2001; Cui *et al*., 2006). Furthermore, chronic subcutaneous administration of medium/high doses of morphine starting prior to surgery fails to reduce hypersensitivity, slowing down the course of recovery and enhancing molecular changes in microglia during several days as evidence of changes in neural plasticity (Horvath *et al*., 2010). Additionally, enhanced levels of proinflammatory cytokines at the peri-incisional skin area have also been reported under chronic high doses of morphine (Liang *et al*., 2008). This could be explained by the development of a physiological tolerance to morphine immunosuppressive effects (West *et al.*, 1997).

II. OBJECTIVES

Animal pain models are basically used for two reasons: **to explore the mechanisms that underlie both physiological and pathological pain**, and to study or develop currently existing or new synthetic analgesic drugs. According to this:

- On the one hand the present work intended to accurately **assess the nociceptive thresholds in** animals suffering from **osteoarthritis**-induced knee joint **pain**,
  1. to achieve therefore a better **understanding of** the chronic **pain state**
  2. to **study the role of** toll-like receptor 4 (**TLR4**) by means of a TLR4 blocking molecule **on**:
     a. **hampering the development of the disease**,
     b. **diminishing nociception** once the disease is developed.

- On the other hand, the work also aimed to **evaluate** the **nociceptive thresholds in** a rat model of **incisional pain** to **study the role of** toll-like receptor 4 (**TLR4**) by means of a TLR4 blocking molecule **on time recovery and** the **mechanisms involved** in such an acute pain state.

- An additional objective consisted in **studying the involvement of glia** in the maintenance of both, osteoarthritic and surgical pain.

III. MATERIAL AND METHODS

1. Experimental animals.

Adult male Wistar rats obtained from Harlan Interfauna Ibérica (Spain) were used for all experiments. The animals were housed in clear plastic cages (4-6 rats/cage) under standard laboratory conditions: temperature- (23 ± 1ºC), humidity- (50-55%) and light- (12/12-h light/dark cycle; lights on at 7.30) controlled rooms with standard rodent chow and water available *ad libitum*. All rats were left at least for five days to be acclimatized in the environment of our animal facilities before the initiation of any experiment in accordance with animal protection standards (BOE, 2005; Capdevila *et al*., 2007). After observation of spontaneous behaviour in order to ensure there was no anomalous response, animals were randomly assigned to treatment or control groups. An observer who was blind to drug treatment conducted all the behavioural assays. All animal procedures were carried out following a protocol that was approved by the Ethical Committee of Universidad Rey Juan Carlos (URJC) and in agreement with the guidelines of the International Association for the Study of Pain (IASP) (Zimmermann, 1983).

2. Surgical procedures.

2.1. MIA model of osteoarthritic pain.

OA was induced in rats (weighing 200–250 g or 250–300 g for i.p. or i.t. administration respectively) by intra-articular infiltration of monosodium iodoacetate (MIA) into the knee cavity. As it has been previously reported (Schuelert and McDougall, 2008; Schuelert *et al.*, 2010), iodoacetate produces a very persistent degeneration of the knee articulation that reaches its maximum state on week two up to four.

Briefly, animals were anaesthetised with 0.3 ml / 100 g (i.p.) Equithesin (176 mM $MgSO_4.7H_2O$, 5.6% Dolethal Vétoquinol S.A., 5.62 mM propylene glycol Codex®, 254 mM chloral hydrate Sigma-Aldrich®, 11.4% absolute ethanol)[30]. A single intraarticular injection of 2 mg MIA (Sigma-Aldrich®) in 50 µl (Pomonis et al., 2005; Cifuentes *et al*., 2010) physiological saline

[30] For animals receiving intrathecal (i.t.) drug administration, MIA was given under isoflurane anaesthesia. The main reasons for this decision were: (1) chloral hydrate was forbidden in year 2013, (2) i.t. administration was performed subsequent to intraperitoneal (i.p.), and (3) during the Thesis we found out in the literature that isoflurane induced less side effects than any other anaesthetic.

(0.9% NaCl) was given through the infra-patellar ligament of the right knee[31] (**Fig.18**). The dose of MIA was based on the previous literature (Fernihough *et al*., 2004; Kalff *et al*., 2010). Control contralateral hind paw received a single intra-articular injection of normal saline (50 µl) (Bove *et al*., 2003; Cialdai *et al*., 2009). 50 µl saline was also intra-articularly administered into both knee joints in a distinct control naïve group. All injections were executed by means of a 30 G insulin syringe (Becton Dickinson) (Clements *et al*., 2009).

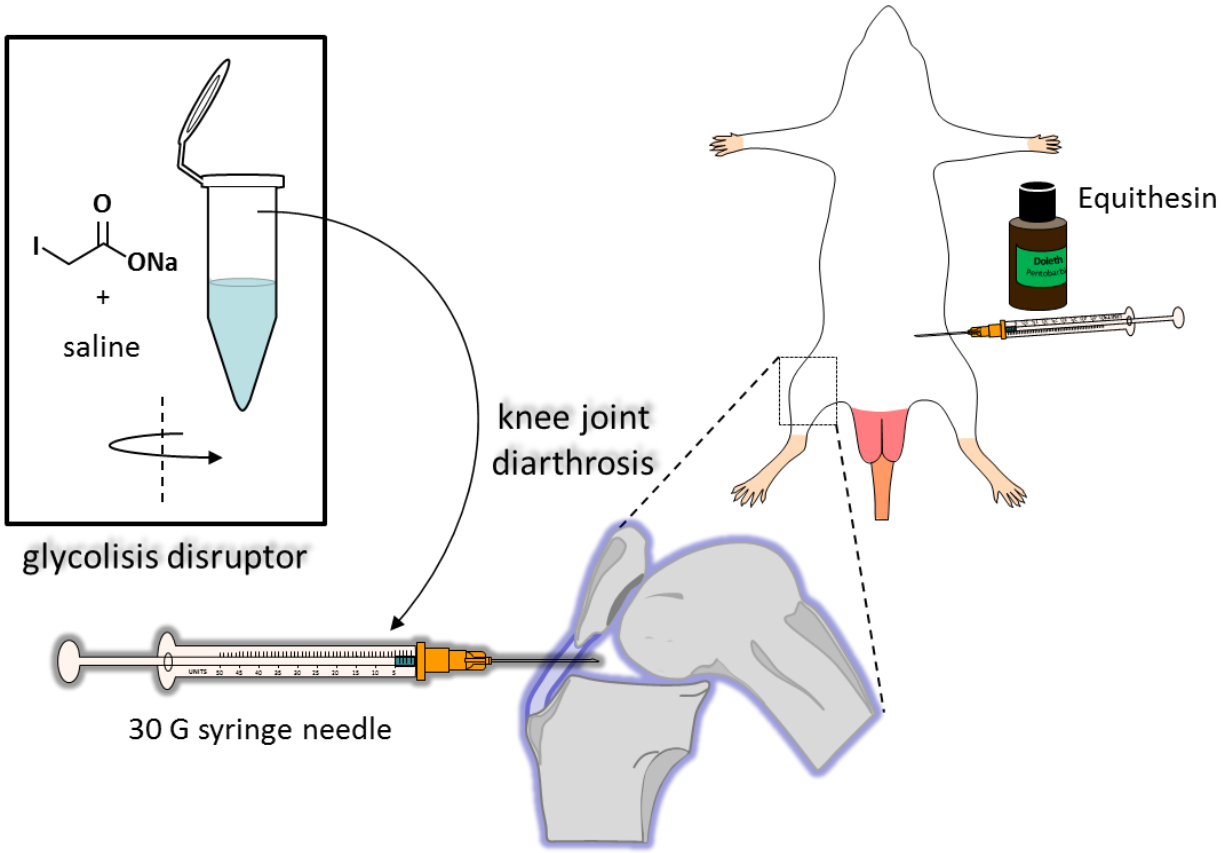

Figure 18. Chemical-induced model of osteoarthritic pain: knee joint injection.

2.2. Intrathecal surgery: osteoarthritic pain.

Intrathecal surgery was performed as previously described (Matsunaga *et al*., 2007; Avila-Martin *et al*., 2011) with slight modifications. Briefly, rats were surgically prepared under pentobarbital (Dolethal, 0.225 ml·kg^{-1}, i.p., Vetóquinol) and 2% xylazine (Xilagesic, 0.43 ml·kg^{-1}, i.p., Calier) anaesthesia, followed by an atropine dose (0.05 ml·kg^{-1}, B. Braun) in order to avoid spasms and bradycardia. In addition 0.1 ml of antibiotic was administered (Enrofloxacin, 2.5% Baytril®, Bayer) after surgery, followed by daily doses up to four days. A commercially

[31] In Portugal knee joint injection was performed into the left knee in a volumen of 25 µl with a 26 G needle, and contralateral knees received no injection.

available polyethylene tube (I.D.: 28 mm O.D.: 61 mm; PE-10, Becton Dickinson) was purchased for catheter implantation and externalized to the back of the neck. Immediately before surgical implantation the catheter was sterilized with absolute ethanol, and thoroughly washed with sterile physiological saline. Following skin incision and blunt dissection of the muscle layers overlying the vertebrae, a small hemi-laminectomy at the vertebral L5 level was performed (spinal Co3). The exposed Co3 dura was subjected to a small durectomy with iris-type scissors so that the tip of the intrathecal catheter could be inserted rostrally and medially on top of the spinal cord with a final position just below the intended L5 delivery site (vertebral L1). The area was cleaned to permit catheter fixture with cyanoacrylate glue to the L6 vertebrae. The percutaneous end of the intrathecal catheter was finally secured by inserting it through a small cutaneous incision at the base of the cranium, whereupon it was filled with sterile saline and tapped with a custom-made steel wire. Artificial dura mater (Neuropatch, B. Braun) was placed on top of the small tear and the overlying muscle layers were ligated with a continuous 4-0 polyglycolic acid absorbable suture. Skin was finally closed with individual 2-0 silk suture stitches (**Fig.19**). Rats were housed individually and carefully observed during recovery. Animals showing neurological deficits after surgery were not used. Four days following implantation of intrathecal catheters, new baseline measurements were taken and rats were given a single intra-articular injection of MIA (Liu *et al.*, 2011) or saline accordingly under isoflurane anaesthesia.

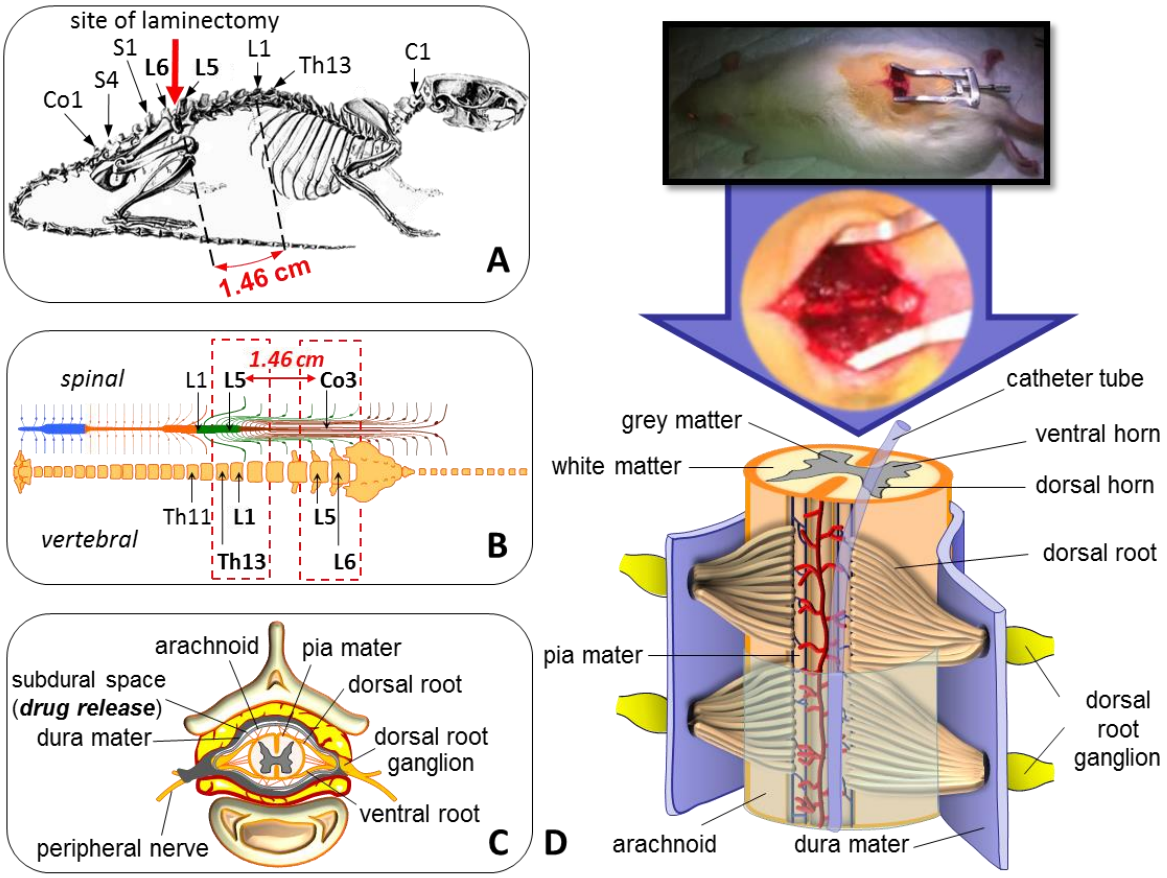

Figure 19. Intrathecal surgery. A. Representation of the skeleton of a rat. **B.** Schematic representation of topographic relations of spinal cord and vertebral column. **C.** Cross section of the spinal cord. **D.** Laminectomy and catheterisation performed on a rat. Since nomenclature of the vertebral bodies does not correlate in space to the same spinal segments, catheter tubes had to be introduced 1.46 cm upwards through the subdural space in order to reach the desired site for the release of the drugs (as shown in **A** and **B**).

2.3. Surgical incision: incisional pain.

Surgery was performed according to the rat model of incisional pain developed by Brennan *et al.*(Brennan *et al.*, 1996) with slight modifications (**Fig.20**). Rats (weighing 250–300 g) were anaesthetised with 2% isoflurane delivered via a nose cone. The right hind paw was prepared in a sterile manner applying a 10% povidone-iodine solution (Betadine®) onto its plantar aspect and a 1–cm longitudinal incision was made through skin and fascia, starting 0.5 cm from the proximal edge of the heel and extending toward the digits. The plantaris muscle was then elevated on a 23 G hypodermic needle and likewise incised longitudinally. Haemostasis was achieved with gentle pressure and the skin was gathered with 2 mattress sutures of 5-0 nylon. Finally the wound site was covered with topical antibiotic ointment (0.2% nitrofurazone, Furacin®) and the animals were then allowed to recover in their cages. The left contralateral paw remained intact.

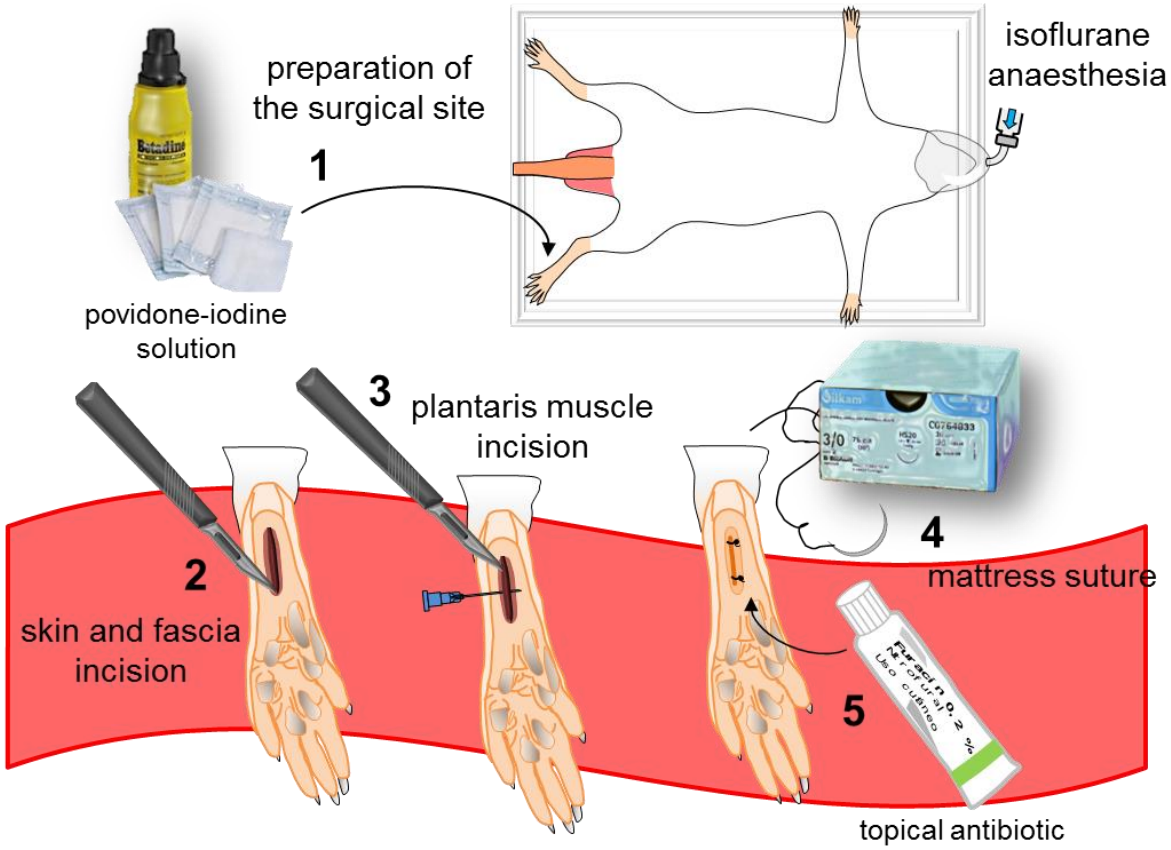

Figure 20. Surgical incision.

3. In vivo assays.

Behavioural experiments.

Limb nociception was assessed by tactile, thermal and mechanical sensory testing as described in the following lines.

3.1. Von Frey test.

During the Thesis, depending on the model being used, von Frey filaments or electronic von Frey were used for an optimal characterisation (**Fig.21**).

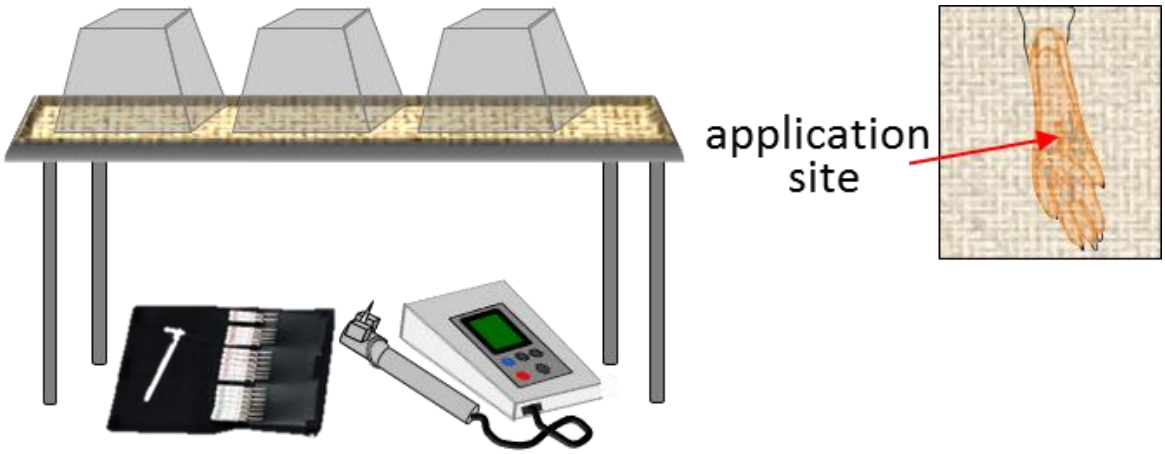

Figure 21. Von Frey test.

During two days previous to behavioural assessment and every test day before the experiment, animals were placed in a Perspex chamber with a mesh metal floor and allowed to acclimatize. When using von Frey filaments, a five-try paradigm was assumed. Essentially, von Frey filaments where applied five times in a row perpendicular to the mid plantar surface of the hind paw while the animal standing still on its four paws. The five-trial process was repeated three times only if four out of five trials achieved a response; if not, we moved on to the next filament (from low weight to high weight) until we achieved four-five responses in a three-serial-row. That is, we pursued an all or nothing response (Ferreira-Gomes *et al.*, 2008). When using automated electronic von Frey, (Ugo Basile), the response threshold to innocuous light touch on either hind paw was measured as previously described with minor modifications (Whiteside *et al.*, 2004). Electronic von Frey monofilament was applied perpendicular to the mid plantar surface of the hind paw and held until a response was achieved. The mechanical stimulation was maintained for 2 s and a total of three readings were taken for each rat at each time point. Average of these three readings was determined and used for subsequent analyses.

3.2. Paw-flick test.

The response to noxious thermal stimulus was determined using a thermal plantar devise (Ugo Basile, Italy) in a modified Bennett and Hargreaves' method (Bennett and Hargreaves, 1990) (**Fig.22**). Briefly, similarly to the previous test, rats were allowed to acclimatize to the test conditions two days preceding the experiments and ten minutes on every test day before behavioural assessment by being placed within a plastic

compartment on a glass floor. A light source beneath the floor was then aimed at the mid plantar surface of the hind paw. The withdrawal reflex interrupted the light and automatically turned it off remaining the time for latency withdrawal recorded. Average of three measures 2-5 min apart was recorded. The intensity of the heat source was adjusted such that baseline latencies to withdrawal were 8-10 s, with a 15 s cut off to avoid tissue damage.

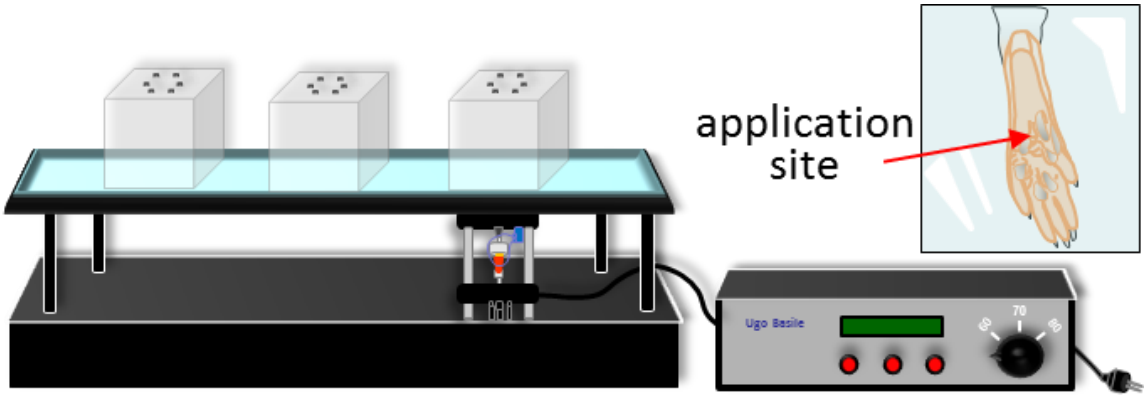

Figure 22. Paw-flick test.

3.3. Knee bend test.

To assess the sensitivity to a natural mechanical stimulus such as the knee-bend movement and therefore, to elucidate the existence of proximal hyperalgesia, a knee-bend test was performed as described by Ferreira-Gomes *et al*. (Ferreira-Gomes *et al*., 2008) in a rat model of MIA-induced osteoarthritic pain. All animals were habituated to the experimenter and to the test for a period of one week before recording any value. The test consisted on recording the number of squeaks and/or struggle reactions in response to five extensions and five flexions of the knee joint **(Fig. 23)** and scored as follows:

Score	*Type of reaction*
0	No response
0.5	Struggle occurs to maximal flexion/extension
1	Struggle occurs to moderate flexion/extension Vocalisation occurs to maximal flexion/extension
2	Vocalisation occurs to moderate flexion/extension

The sum of the recorded reactions (with a maximal feasible value of 20) represents the knee-bend score.

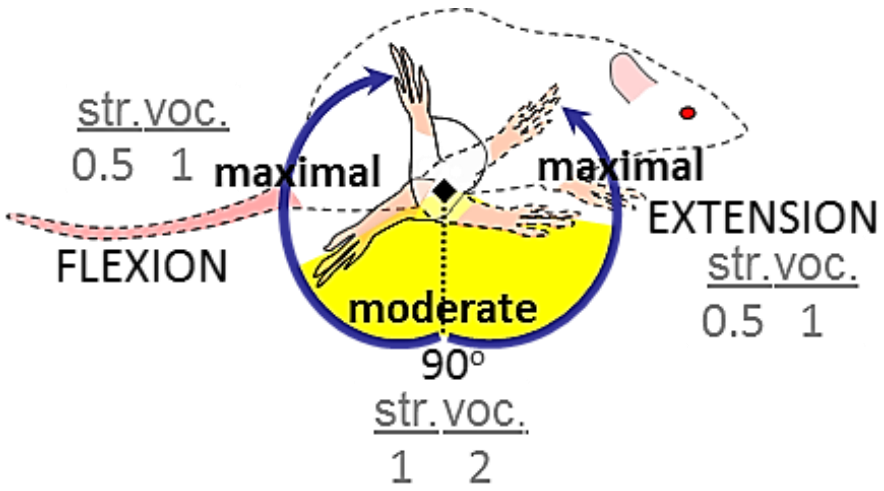

Figure 23. Knee bend test. Str. = struggle; voc. = vocalisation.

3.4. Catwalk test.

The Catwalk test was used to evaluate the disability induced by the OA model and the disconformity after receiving the treatment (Ferreira-Gomes *et al.*, 2012). OA animals show a decreased weight bearing in the osteoarthritic limb probably due to increased sensitivity. In this test animals are placed in a glass platform located in a dark compartment and allowed to walk freely. The surface is mildly water sprayed and a light beam from a tubular fluorescent lamp illuminates the platform in order to reflect the light downwards only at the points of contact of each paw area with the glass platform, resulting in a bright sharp image of the paw print (**Fig.24**). The intensity of the paw print signal increases with the area of the paw in contact with the platform and with the pressure applied by it. Therefore, the total ipsilateral paw print intensity is quantified by determining the area of the paw in contact with the platform, in number of pixels, and multiplying it by the mean intensity of each pixel, giving us the overall intensity of the paw print.

The platform was monitored by a video camera with a wide-angle objective, placed under the glass platform and connected to a computer equipped with video acquisition software (Ulead Video Studio, USA). Six random frames of the videos recorded during the rat evaluation were obtained: 3 frames with the animal walking (corresponding to spaced time steps of consecutive contralateral and ipsilateral footprints) and 3 frames corresponding to distant trials with the animal standing still. The number and intensity of pixels above a defined threshold were quantified using ImageJ 1.47, allowing the

comparison between the area/pressure applied by each paw. Results were expressed in total intensity of the ipsilateral hind paw as a percentage of the total intensity of both hind paws.

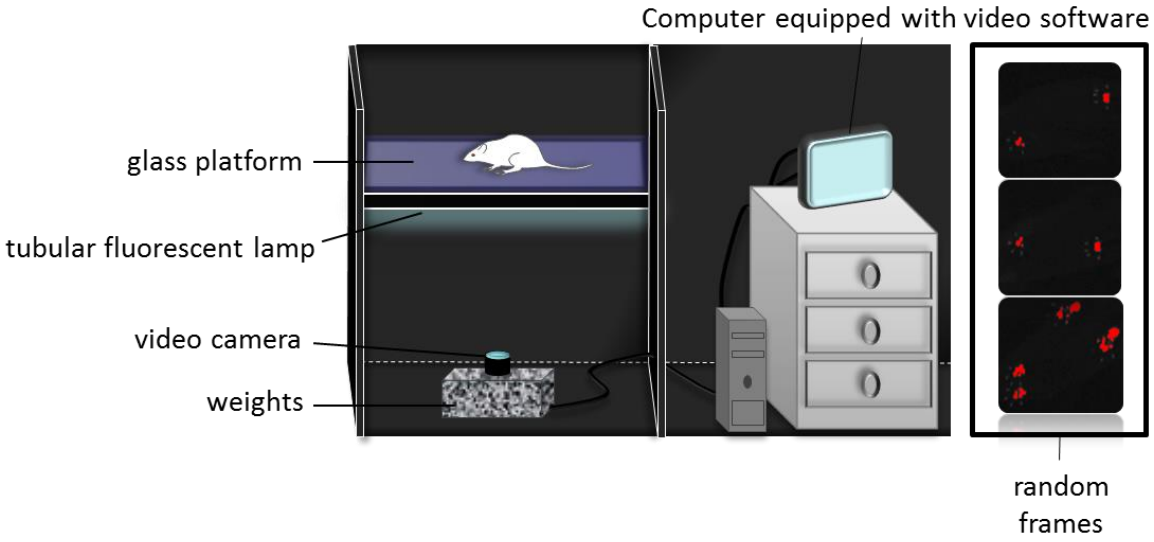

Figure 24. Catwalk test.

4. Drugs used.

4.1. TLR4-A1.

Based on the studies carried out by Piazza *et al*. (Piazza *et al*., 2009) on *in vitro* cell cultures and *in vivo* sepsis model in mice, we reproduced a benzylammonium lipid to be tested in our *in vivo* rat model systems that we named as "TLR4 antagonist 1" (TLR4-A1). A TLR4 inhibitor molecule (TLR4-A1) with target on its co-receptor CD14 protein (Arroyo-Espliguero et al., 2004) was synthesized as previously described (Piazza *et al.*, 2009; Peri and Piazza, 2012) and presented in a 9:1 ratio of 0.9% saline and ethanol. For intrathecal administration, TLR4-A1 was diluted only in sterile saline.

TLR4-A1 synthesis was modified by Dr Quesada starting from a commercially available and inexpensive compound (methyl-β-D-glucopyranoside) (**Fig.25**). The identity and purity of the compound was confirmed and verified by HPLC analysis and NMR.

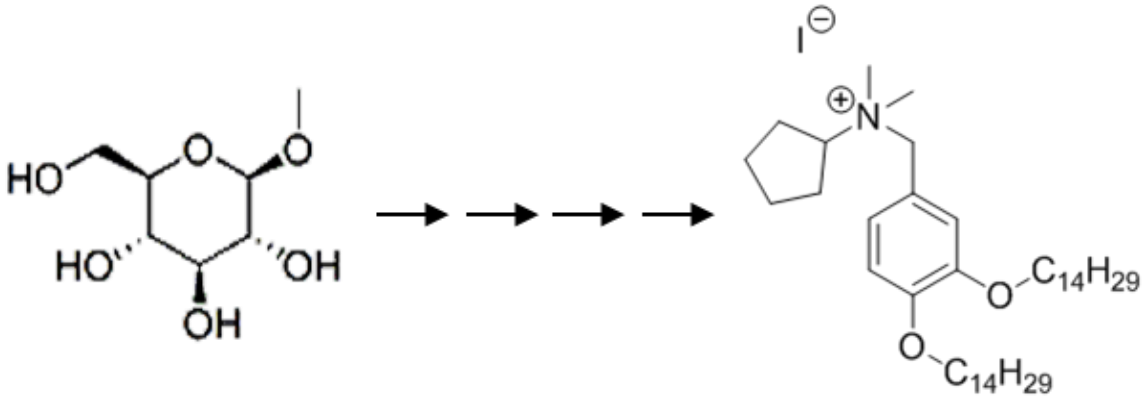

Figure 25. TLR4-A1 molecule.

4.2. Other drugs.

Morphine sulphate was purchased from Sigma-Aldrich Química (Spain) and diluted in 0.9% innocuous saline.

All i.p. administrations consisted on a total volume of 0.5 ml. On its part, i.t. administrations consisted on volumes of 0.01 ml preceded and followed by 0.01 ml sterile saline. All drugs were freshly prepared on the day of the experiment.

Experimental and drug administration protocols.

a) MIA-induced model of osteoarthritic pain.

   In order to assess the time course and chronicity of pain in the model, behavioural assessment was first performed during a 50-day period after the infiltration of 2 mg MIA. The role of TLR4 targeting chronic or nociceptive pain was investigated using a new synthetic experimental compound: TLR4-A1 (**Table 6**). Intraarticular injection was given subsequent to habituation to the test environment and after recording baseline values (day 0). Data were then registered from postoperative day 7 onwards as follows: on days 7, 14 and 21, and alternatively on days 28, 35, 40 and 50 too.

1. Acute administration of TLR4-A1 upon the development of osteoarthritis
• blank group → control • MIA group → control • MIA group + 10 mg·kg^{-1} TLR4-A1 (i.p.) on day 14
2. Chronic administration of TLR4-A1 upon the development of osteoarthritis
• blank group → control • MIA group → control • MIA group + 15-day treatment with 10 mg·kg^{-1} TLR4-A1 (i.p.)
3. Chronic administration of TLR4-A1 parallel to the induction of the osteoarthritis
i.p.administration • blank group → control • MIA group → control • MIA group + 5-day treatment with 10 mg·kg^{-1} TLR4-A1 (i.p.) **i.t. administration** • blank group + surgery → control • MIA group + surgery → control MIA group + surgery + 5-day treatment with 0.1 mg·kg^{-1} TLR4-A1 (i.t.)

Table 6. Pharmacological treatments evaluated in the MIA-induced model of osteoarthritic pain.

a.1) Acute systemic administration.

In order to determine the anti-nociceptive properties of the TLR4-A1 compound after the onset of the pathology, animals were given a single dose on day 14 after MIA injection. This also enabled us to characterize the time course of drug effect. TLR4-A1 acute treatment consisted on a single dose (10 mg·kg^{-1}) on day 14 and animal behaviour was evaluated before and 30 min, 60, 1 h 30 min, 2 h and 3 h following the administration **(Fig.26A)**.

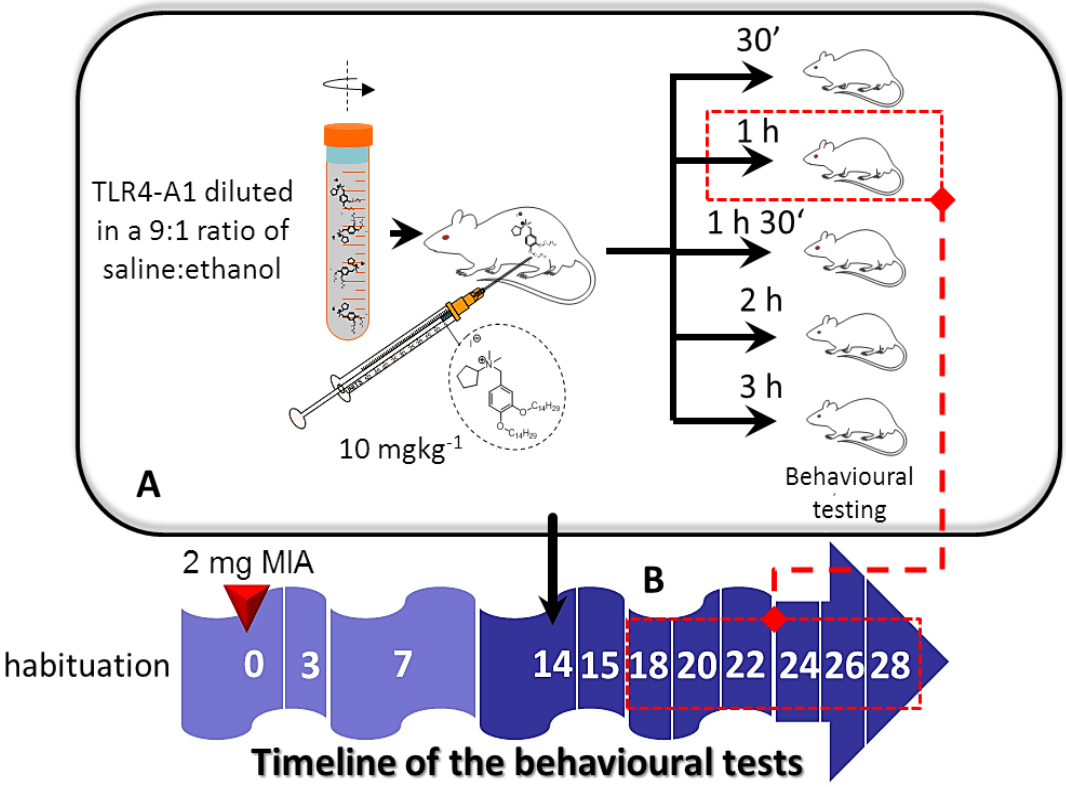

Figure 26. Experimental protocol followed at the FMUP. A. Acute administration. **B.** Chronic administration.

a.2) Chronic systemic administration.

In the protocol followed at the FMUP, chronic treatment with vehicle TLR4-A1 or TLR4-A1 (10 mg·kg^{-1}) itself consisted on daily administrations during 15 days starting on day 14. Behavioural tests were carried out on days 3, 7, 14 and 15 post-MIA injection and on days 18, 20, 22, 24, 26 and 28 before and 1 h after drug administration **(Fig.26B)**.

In the protocol followed in Universidad Rey Juan Carlos (FCS-URJC), vehicle of TLR4-A1 or TLR4-A1 alone (10 mg·kg^{-1}, i.p.) was daily administered during five consecutive days starting on day 0 post-MIA injection. Withdrawal thresholds for tactile allodynia (electronic von Frey) and heat hyperalgesia (paw-flick test) in 2 mg MIA- and sham saline-treated knees were evaluated on the aforementioned days **(Fig.27A)**.

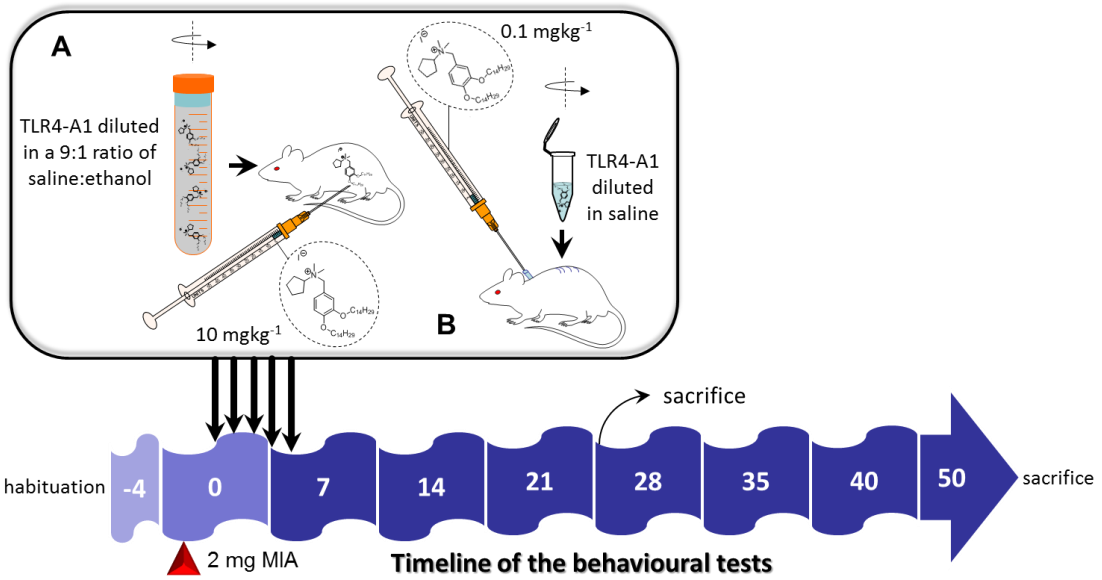

Figure 27. Experimental protocol for chronic administration of TLR4-A1 followed at the FCS-URJC. A. i.p. administration. **B.** i.t. administration.

a.3) Chronic intrathecal administration.

Two different baseline thresholds were recorded for groups undergoing intrathecal surgery: just before catheterisation and four days after the surgery was performed. Rats with no motor or sensitive impairment were classified into control naïve or osteoarthritic group and received innocuous saline or TLR4-A1 (0.1 mg·kg^{-1}) during the first five days immediately after 2 mg MIA- or saline-infiltration. Withdrawal threshold and thermal latency were assessed every 7 days during the following three weeks (**Fig.27B**).

b) Model of incisional, postoperative pain.

Von Frey and paw-flick tests were performed during 10 consecutive days to determine the time course of tactile allodynia and heat hyperalgesia on operated animals and to evaluate the effect of the administration of three different treatments on their nociceptive thresholds (**Table 7**).

Chronic administration of vehicle, morphine or/and TLR4-A1 (two doses of 5 mg·kg^{-1}·day^{-1})
• blank group → control
• incisional group → control → 9-days vehicle (i.p.)
• incisional group → 9-days 10 mg·kg^{-1} morphine (i.p.)
• incisional group → 9-days 10 mg·kg^{-1} TLR4-A1 (i.p.)
• incisional group → 9-days 10 mg·kg^{-1} TLR4-A1 + morphine (i.p.)

Table 7. Pharmacological treatments evaluated in the postoperative model of incisional pain.

Every compound was i.p. injected twice a day (5 mg·kg^{-1}), since higher doses of morphine were seen to produce sedation. Each administration was separated by 6 hours for 9 consecutive days and tested starting 24 h following plantar incision twice a day: 2 hours before and 45 min following the first administration of the day. In the case of animals receiving both drugs, TLR4-A1 was administered 15 min prior to morphine and behaviour was assessed 30 min after the latter **(Fig.28)**. In sum, every animal had received at the end of the day 10 mg·kg^{-1} morphine or/and TLR4-A1.

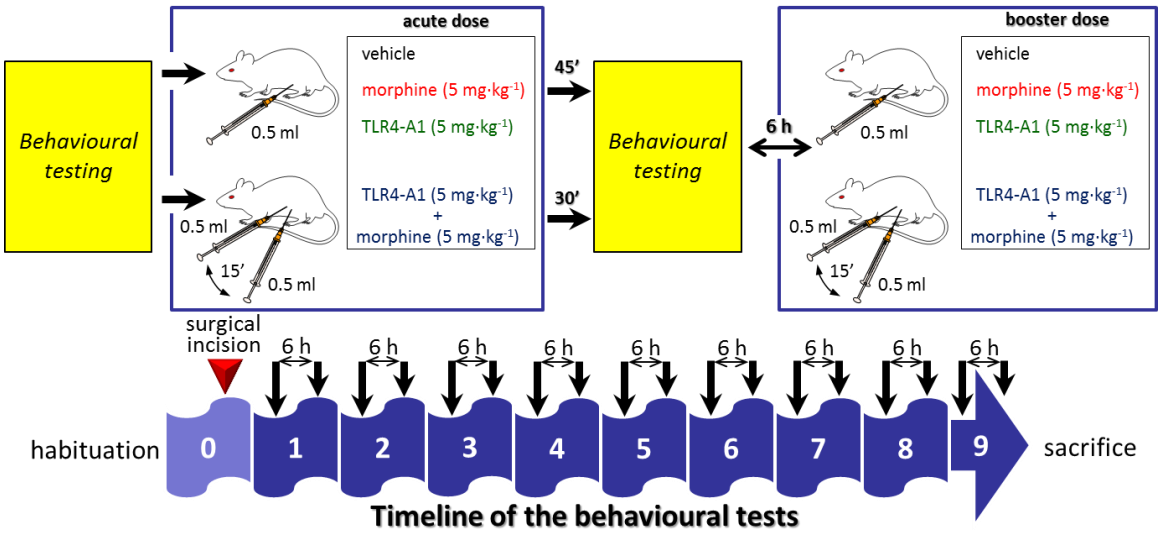

Figure 28. Experimental protocol for chronic administration of morphine and/or TLR4-A1: a 9-day treatment starting one day following surgical incision.

Doses for TLR4-A1 were obtained comparing to previous works carried out by F Peri and M Piazza (Piazza *et al*., 2009) on a mice sepsis model.

5. *In vitro* assays.

5.1. General histological methods.

5.1.1. Immunohistochemical study for glial activity.

5.1.1.1. Collection of spinal cords.

Animals were sacrified 22 or 10 days after surgery (OA and PO model respectively; n = 4-5 rats for each group). Deep pentobarbital (60 mg·kg^{-1}, i.p.) anaesthetised rats were intracardially perfused via the left ventricle with 200 ml of normal saline (pumped by means of a peristaltic pump at a constant flow rate of approximately 20 ml·min^{-1}) followed by fresh-prepared 4% paraformaldehyde (PFA) fixative in 0.1

M phosphate buffer saline (PBS), pH 7.4, 4ºC (referred to as *fixative solution* from now on), once upon blood was cleared from the circulatory system (**Fig.29**).

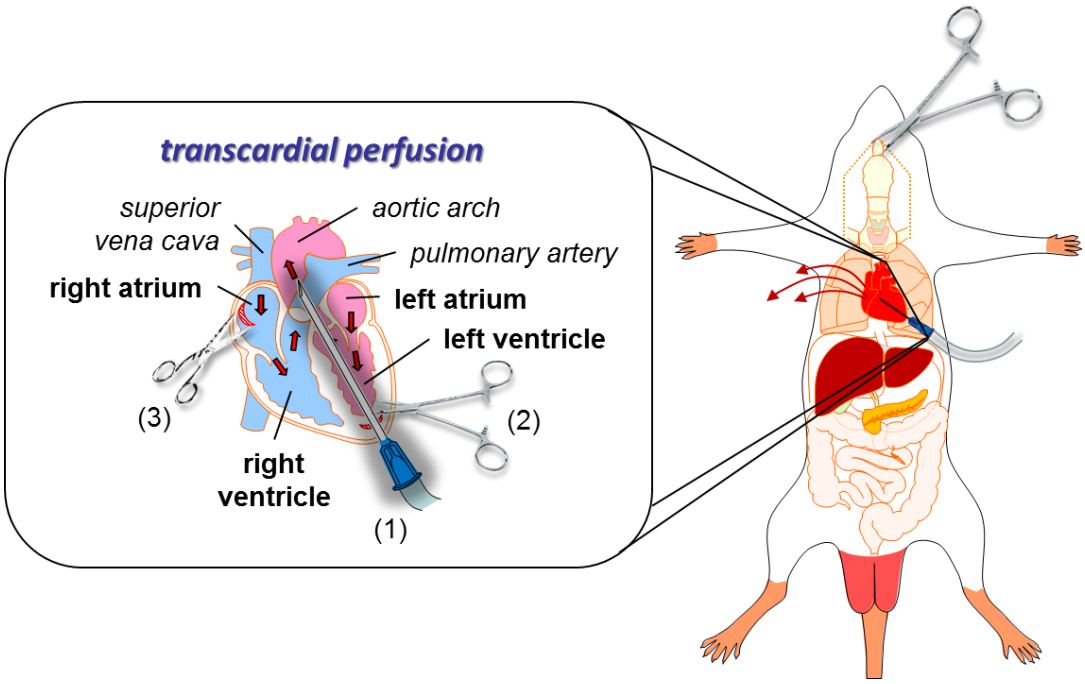

Figure 29. Transcardial perfusion.

A laminectomy of the entire thoracic and lumbar spinal cord was performed and a L3-L5 spinal segment was excised and kept in the aforementioned fixative solution for four extra hours at room temperature. Then cryopreserved in 0.1 M PBS (pH 7.4) supplemented with 30% sucrose and 0.05% azide (*cryopreservative solution*) at 4ºC until further processing[32]. Alternatively, the knees or saphenous nerves were also collected.

5.1.1.2. Tissue processing.

Following post-fixation treatment spinal cord specimens were transferred through serial increasing concentrations of water miscible ethanol; then replaced with xylene, which can be mixed with paraffin (**Fig.30**). In order to ease and hasten the dehydratation protocol, samples were introduced into numbered cassettes and placed into a basket located in a tissue-transfer processor for an automated

[32] A similar protocol was followed in Portugal at the FMUP with minor modifications; using 0.2 ml of heparin prior to perfusing the animal and starting the perfusion with Tyrodes' solution instead of saline.

performance. After dehydration, samples were placed in moulds which were filled up with hot liquid paraffin. Once paraffin cooled down, blocks were ready to cut.

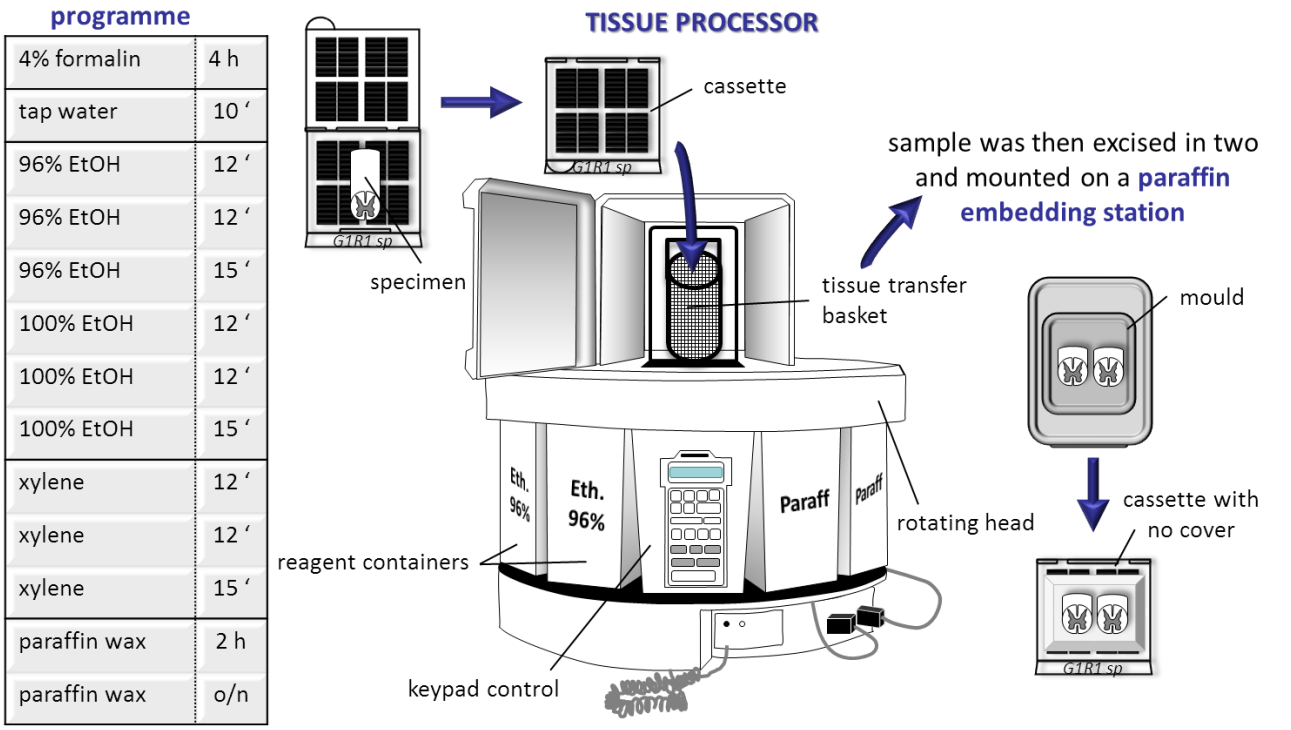

programme	
4% formalin	4 h
tap water	10 ‘
96% EtOH	12 ‘
96% EtOH	12 ‘
96% EtOH	15 ‘
100% EtOH	12 ‘
100% EtOH	12 ‘
100% EtOH	15 ‘
xylene	12 ‘
xylene	12 ‘
xylene	15 ‘
paraffin wax	2 h
paraffin wax	o/n

Figure 30. Grading-up concentrations of ethanol for specimens dehydration. On the left side of the image, a table shows the programme entered into the tissue processor, consisting on grading-up concentrations of ethanol for specimens dehydration (initial task on top).

Paraffin wax blocks of spinal sections corresponding to lumbar segments 3 to 5 were thaw-mounted in a Minot rotatory microtome and serial 5 µm transverse sections collected on 0.02% poly-L-lysine coated slides.

In order to not waste too much time nor materials, it was important to think about a strategy. Each segment of spinal cord was too large to be placed onto a cassette, so we placed it in two halves (as seen in **Fig.30**). Every spinal fragment was then mounted on four different slides as 20 consecutive sections placed in order. Since we aimed to obtain serial cuts for L3, L4 and L5 sections, after cutting, we could have a series of possibilities: L4-L4, L3-L5, L4-L3 o L5-L4, depending on how we placed the spinal cord segments (**Fig.31**). This disposal enabled thus comparison of each section with the previous and following so the specific lumbar section could be determined corroborating typical grey matter shapes specific for each lumbar section on an anatomy atlas.

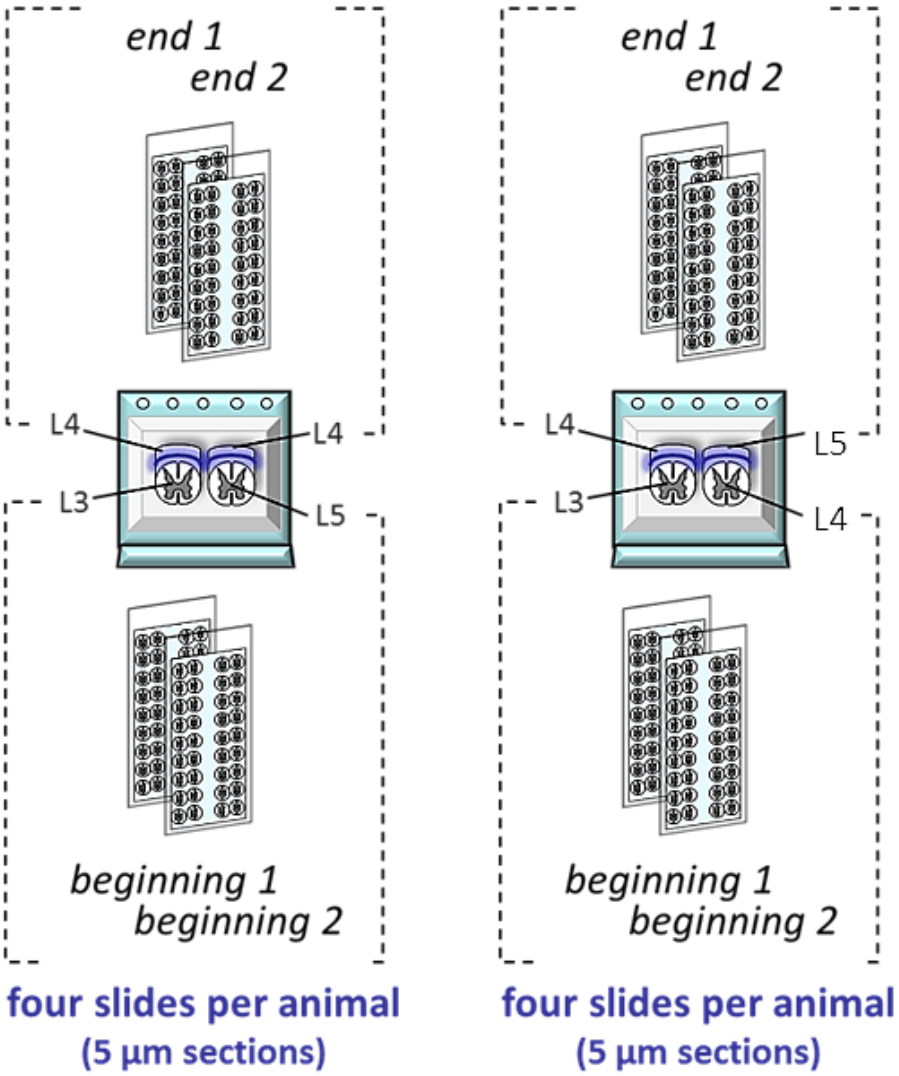

Figure 31. Disposal of paraffin wax-mounted spinal cord samples.

5.1.1.3. Immuno-staining.

All samples were immune-stained by the *indirect peroxidase-labeled antibody method* (**Fig.32**).

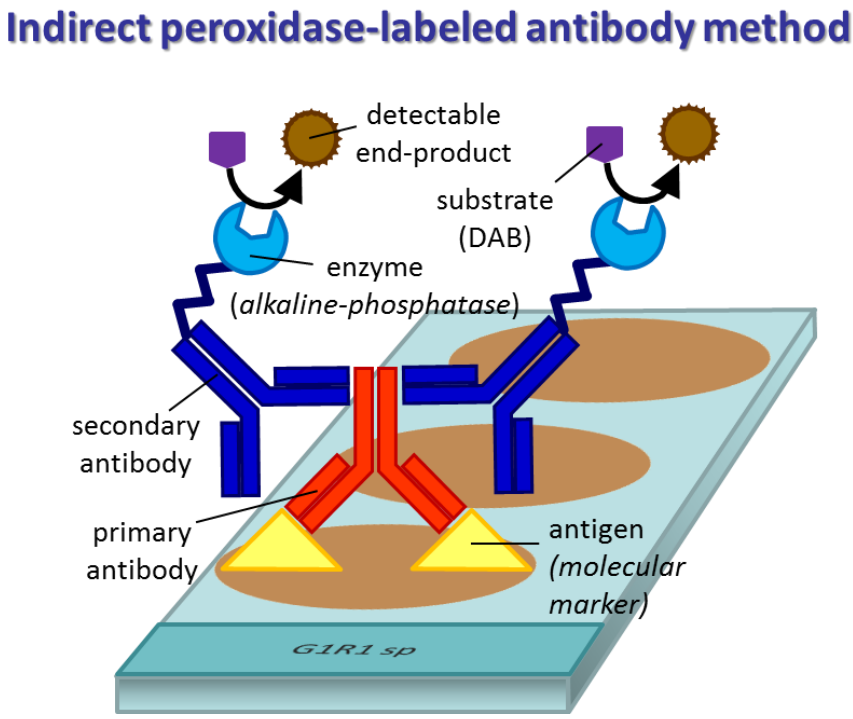

Figure 32. Indirect peroxidase-labeled antibody method. DAB = 3,3'-diamino-benzidine-tetrahydrochloride.

Briefly, after deparaffinization samples followed an antigen retrieval-microwave method in citrate buffer. Then treated with a fresh 3% solution of hydrogen peroxide (H_2O_2) in sterile water for 15 min[33] in order to block the activity of endogenous peroxidase, followed by a 30 min incubation with fetal calf serum (FCS) or bovine serum albumin (BSA) as appropriate to reduce non-specific background staining. Sections were then treated for 1 hour with optimally diluted *Abcam7260* rabbit anti-GFAP (1:5000) or *Abcam5076* goat anti-Iba-1 (1:500) serum immunoglobulins, washed and treated for an additional hour with one drop of histofine kit® (Cy^{TM}2-conjugated) anti-rabbit or *Jackson ImmunoReasearch711225152* alkaline-phosphatase (AP)-conjugated donkey anti-goat serum immunoglobulin diluted 1:350. Samples were then washed to remove any excess of antibody and treated with a freshly prepared solution of 0.05% 3,3'-diamino-benzidine-tetrahydrochloride (DAB, Sigma®) for 5 min. A dark brown end-product became then visible at the site of the antigen as the DAB reaction took place (**Fig.33**).

[33] The protocol for immuno-staining had slight variations at the FMUP: 0.5% of H_2O_2 in methyl alcohol for 30 min was used.

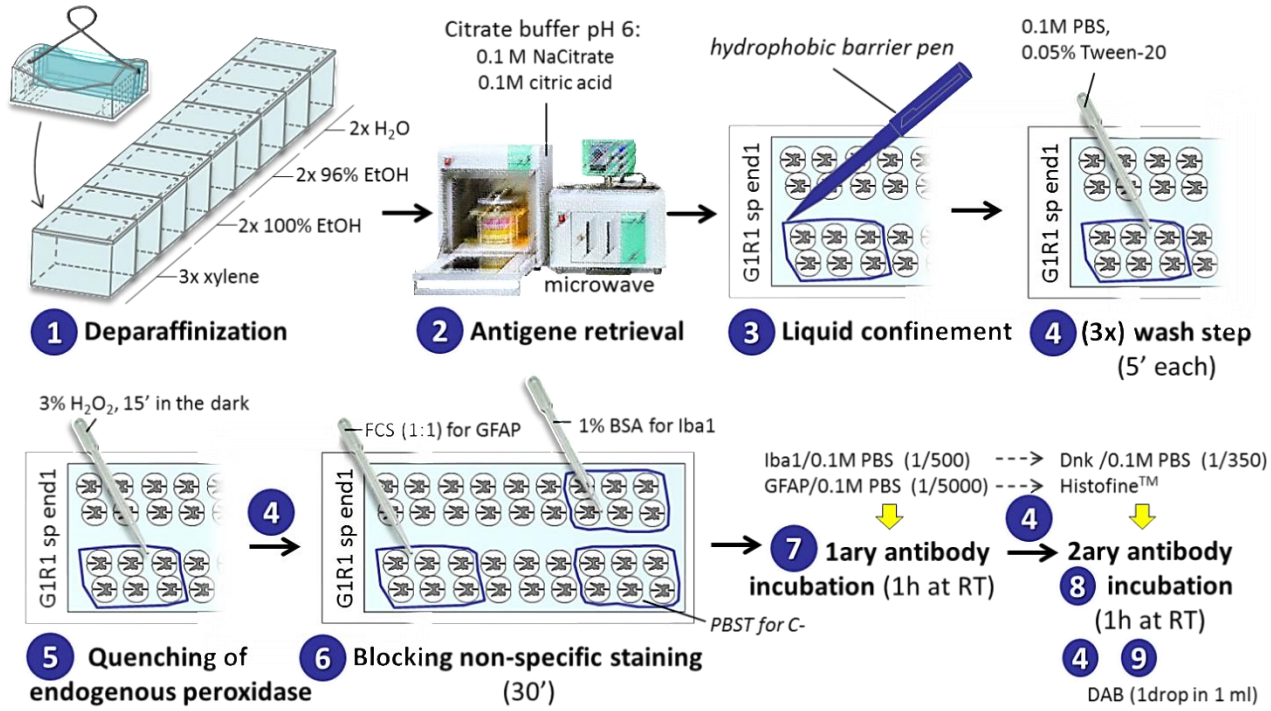

Figure 33. Immunostaining protocol.

Eventually, sections were washed well in tap water and followed a staining-dish system of grading-up concentrations of ethanol inverse to the one just seen in the previous figure (**table8**). A drop of Eukitt™ mountaing medium (miscible with xylene but not with water) was added onto the microscope slide and protected with a cover-slip.

H_2O
H_2O
96% ethanol
96% ethanol
Absolute ethanol
Absolute etanol
Xylene
Xylene
Xylene

Table 8. Grading-up concentrations of ethanol.

5.1.1.4. Method for counting immunoreactive receptors: microscopic examination.

For each section corresponding to every lumbar region, total stained-cells were counted separately in laminas I-II, III-IV and V-VI. Identification of spinal cord layers was made according to the classification by Rexed (Rexed, 1952) and

photomicrographs were recorded to make montages of the entire spinal cord at a final magnification of 20x.

5.1.2. Macroscopic examination of the knees: osteoarthritic pain.

Regarding the MIA-induced model of osteoarthritic pain, rat knee joints were exposed in order to verify correlation between the damaging action of MIA with the results observed when behavioural testing. After sacrificing, ligaments were excised and the tibial and femoral articular faces were exposed (**Fig.34**).

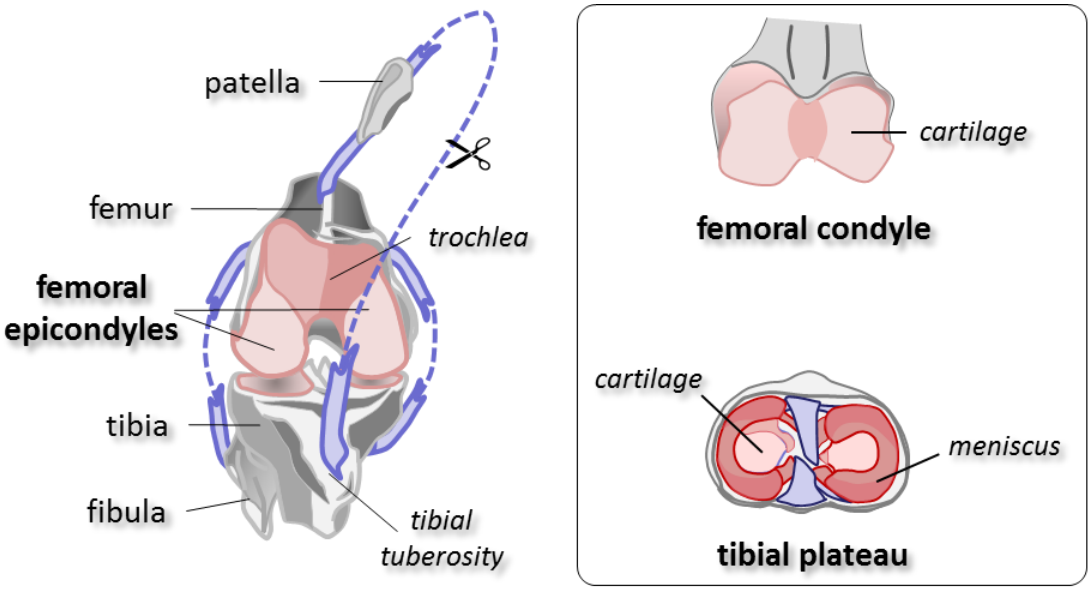

Figura 34. Schematic frontal and cross sectional view of the right knee.

5.1.3. Processing and microscopic examination of the knees: osteoarthritic pain.

5.1.3.1. Bone decalcification.

Dissection and tissue processing of rat knee joints was performed as previously described (Memon *et al*., 2010) with slight modifications. Because of the calcium salts contained in the bone, a specific protocol for the preparation of sections was needed. The articulating bones were cut as proximal to the knee joint as possible and immediately transferred to cold fixative solution for additional 72 h. Specimens were then replaced in cryoprotective solution and kept at 4ºC until further use. Removal of the mineral content was carried out by immersion of the knee samples in a decalcifying fluid containing a chelating agent, EDTA, and leaving the samples rotate in that fluid at room temperature (5% EDTA / 10% PFA)

on a shaker run at low speed. Solution was renewed weekly for 4-5 weeks. A cotton bud was provided in the solution as a scaffold for the withdrawing calcium.

5.1.3.2. Staining.

Following decalcification, tissues were washed, dehydrated in grading-up ethanol series, and embedded in paraffin wax (**Fig.35**). Tissue sections were cut at 5 µm thickness on a rotary Minot microtome and used for 0.5% toluidine blue O containing 1% sodium borate.

programme	
4% formalin	o/n
tap water	10 '
96% EtOH	35 '
96% EtOH	35 '
96% EtOH	40 '
100% EtOH	35 '
100% EtOH	35 '
100% EtOH	40 '
xylene	35 '
xylene	35 '
xylene	40 '
paraffin wax	4 h
paraffin wax	24 h

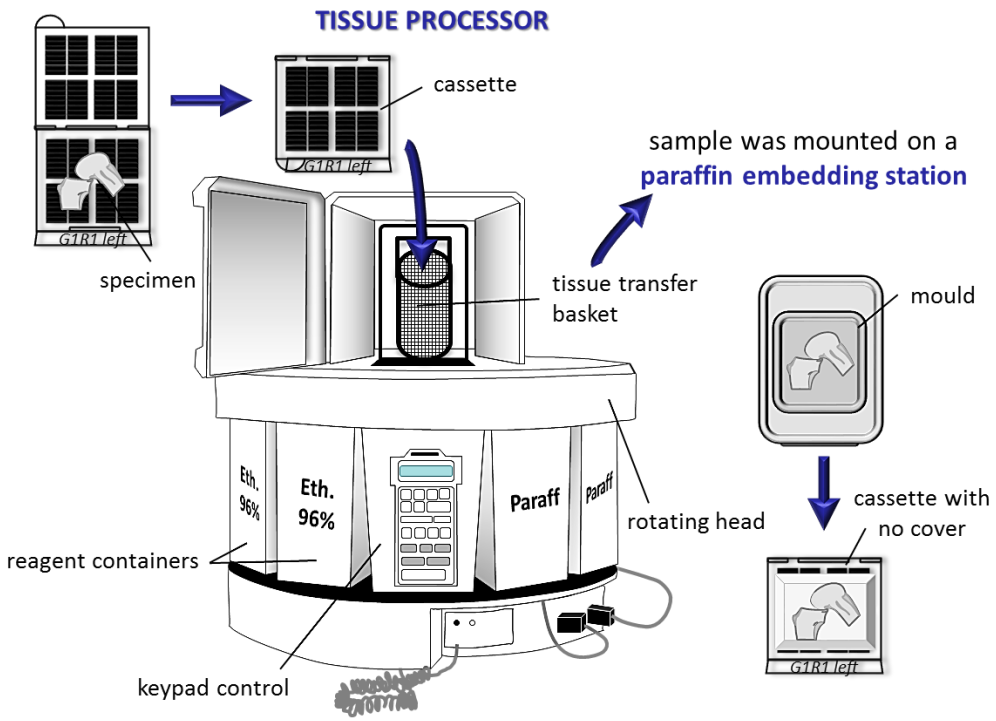

Figure 35. Grading-up concentrations of ethanol for knee specimens dehydration: paraffin-embedded tissue protocol.

5.1.3.3. Microscopic examination.

Photomicrographs of the 5 µm sections were recorded to make montages of the entire knee at a final magnification of 2.5x. 8-10 montages were made of each 4 experimental groups. OA pathology scores were determined by histologic analysis. Toluidine blue-stained sections were used to assess the structures, cells and tidemarks of the articular cartilage (Hagiwara et al., 2009) by means of the Pritzker-score (Pritzker *et al*., 2006) (see section IV.2.1).

5.1.4. Saphenous nerve biopsy and microscopic examination.

One centimetre segments of ipsilateral (injured side) and contralateral (uninjured side) saphenous nerve corresponding to the groin-knee (OA model) or knee-hip (PO model)

extent were removed 22 or 10 days post-surgery, respectively, and immediately post-fixed in the fixative solution. After 4 hours, sections were immersed in cryoprotective solution and kept at 4ºC until further use. Tissue samples were fixated and embedded in resin according to a protocol ran by a Service Request. The resulting resin blocks were mounted in an Ultramicrotome Leica EM UC7 and serial transverse semithin sections of 800 nm–thickness were cut. Since prolonged heating enables toluidine blue staining, sections now displayed on microscope slides were warmed up and stained with toluidine blue for morphological and morphometrical study. Image acquisition was performed using optical microscopy. Micrographs were recorded to make montages of entire saphenous nerve transverse sections at a final magnification of 63.5x. Six montages per nerve were made for every animal of each experimental group (n = 2-4 animals). Myelinated nerve fibre, myelin sheath and axonal diameters, and percentage of total endoneurial area were measured (Costa *et al*., 2005). The parameters were analysed on digitised pictures using the ImageJ 1.47 software.

5.2. Protein determination by biochemical assays.

5.2.1. Collection of spinal cords.

Spinal cord collection was performed as previously described (Butt *et al.,* 2007; Gil-Dones *et al.*, 2008) with modifications. Briefly, rats were decapitated and the spinal cord tissue was extracted using hydraulic pressure by inserting an 18-gauge needle into the caudal end of the vertebral canal and flushing the spinal cord out with ice-cold saline. A 0.5–cm segment corresponding to the medial part of the lumbosacral enlargement (LI-LV) (Gilerovich *et al.*, 2008) was excised from the isolated spinal cord, flash frozen on liquid nitrogen and immediately stored at –80 ºC for further processing.

5.2.2. Enzyme-Linked ImmunoSorbent Assay (ELISA).

Spinal cord homogenization was adapted from the method of Sweitzer *et al*. (Sweitzer *et al.*, 2001; Sweitzer and DeLeo, 2002). In brief, spinal cord sections were weighed and then mechanically disrupted in 0.5 ml of ice-cold lysis buffer (**table 9**) using a Polytron homogenizer (Kinematica, Switzerland) at high speed for pulses of 10 s.

Lysis buffer (pH 7.4)	supplemented with
50 mM NaCl 10 mM Tris 2.5 mM $MgCl_2 \cdot 6H_2O$ 2.5 mM $MgCl_2$	protease inhibitor cocktail

Table 9. Lysis buffer for tissue homogenization and posterior disruption. Buffer cannot include any detergent among its components in order to avoid altering absorbances when reading the ELISA plate.

Lysates were ultracentrifuged at 16,000 x g for 30 min at 4ºC and the resulting supernatant (soluble protein fraction) was divided equally: a 200 µl aliquot for IL-1β and IL-6 and a 200 µl aliquot for TNF-α ELISA quantification.

Protein concentrations for IL-1β, IL-6 and TNF-α were determined using Diaclone® rat ELISA kits according to the manufacturer's directions and comparing samples to the standard curve generated from the respective kits. Protein levels in treated and untreated operated animals were compared to those from control naïve animals (n = 4-6).

6. Statistical analysis.

GraphPad Prism5 software was used for all statistical analysis. Two-way repeated-measures ANOVAs with Bonferroni post-hoc tests were used to determine statistical significance between groups in all experiments. One-way ANOVA followed by Dunnett's or Newman-Keuls Multiple Comparison test was also used for comparing the different time-points of each group to their respective baseline values (day 0). For all analyses, $P<0.05$ was considered as statically significant.

IV. RESULTS

1. *In vivo* assays: behavioural experiments.

1.1. Implementation of the osteoarthritic model of pain.

As previously mentioned, a thorough investigation on dose-finding studies was performed before making any choice of the volume and quantity of MIA administration to be used. We concluded that a 2 mg-dose was ideal for causing irreversible damage and severe chronic pain. Two different volumes of 25 and 50 µl were tested and the latter was chosen, which actually corresponded to the maximum intake volume allowed by the knee joint space[34].

In order to test if saline injection into the contralateral knee joint space caused any alteration on the withdrawal threshold or latency values, behavioural tests were carried out in parallel in a separate untreated group of rats. In this respect, test days were chosen at random (**Fig.36**).

[34] During the stay in the Faculty of Medicine at Universidad do Porto (FMUP), we assumed the volume they were currently using (2 mg–MIA in 25 µl–saline).

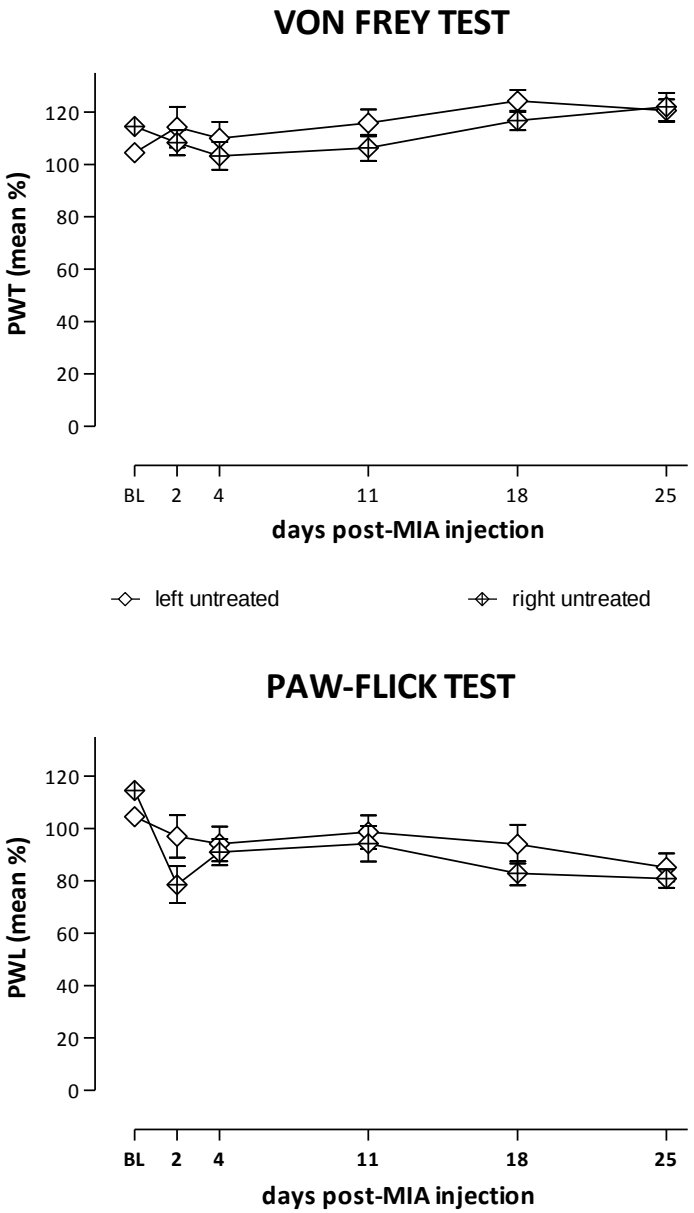

Figure 36. Time-course response to tactile (von Frey test) and heat (paw-flick test) acute stimuli applied on the plantar aspect of the paw in a control untreated set of animals. Data represent the mean percentage of the modification of the response ± Standard Error of the Media (SEM). N = 10 animals per group. PWT = paw withdrawal threshold; PWL = paw withdrawal latency.

As concerns the injected animals, limping was visible in most animals right on the following day to MIA administration and decreased paw withdrawal thresholds and latencies were observed along 50 days. A flattened time-threshold curve was perceptible for both tests: MIA induced thermal hypersensitivity with withdrawal latencies always under the baseline levels and produced significant tactile allodynia in the ipsilateral hindpaw ($P<0.001$ ipsilateral *vs*. contralateral paw) (**Fig.37**).

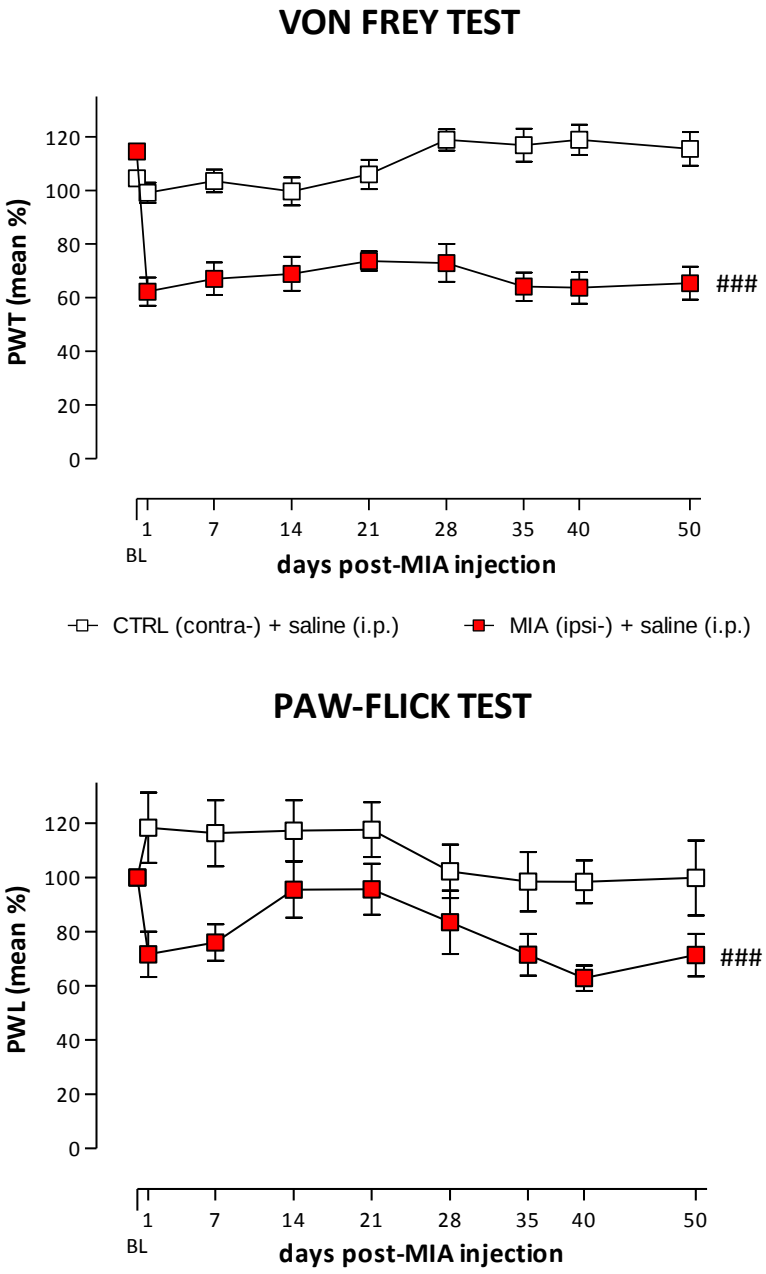

Figure 37. Time-course response to tactile (von Frey test) and heat (Hargreaves' test) acute stimuli plantarly applied in rats' innocuous saline or 2 mg MIA infiltrated-knees. Data represent the mean percentage of the modification of the response ± SEM of the responses. # contralateral vs. ipsilateral paw. 2-way ANOVA, Bonferroni post-hoc test. (●P<0.05, ●●P<0.01, ●●●P<0.001). N = 10 animals per group.

1.1.1. TLR4-A1 acute anti-nociceptive effect.

To evaluate the antinociceptive effect of TLR4-A1, drug was acutely administered on day 14 after saline or MIA infiltration. Ethanol:saline (1:9, i.p.) was given as vehicle. Three different tests were used: von Frey test (tactile stimulus) at a distal site of the injury, knee bend test (mechanical stimulus) at the precise site of the injury and

Catlwalk test (no stimulus applied). Behavioural assessment was evaluated before and 30 min, 1 h, 1 h 30 min, 2 h and 3 h following administration.

MIA produced significant tactile allodynia in the ipsilateral hindpaw (**Fig.38A**). Intraperitoneal TLR4-A1 (10 $mg \cdot kg^{-1}$) attenuated MIA-induced tactile allodynia, with peak effect at 1 h (75.00% ± 7.82) post-administration (**Fig.38A**). Movement-induced nociception was evaluated through the knee-bend and CatWalk tests. MIA induced an increase in the knee-bend score for the injected knee significantly different (**Fig. 38B**) from those for the control group. On its part, intraperitoneal TLR4-A1 (10 $mg \cdot kg^{-1}$) attenuated mechanical allodynia with peak effect at 30 min (3.13U ± 0.87) – 1 h (3.13U ± 0.86) post-administration (**Fig. 38B**). MIA also induced spontaneous pain from day 3 onwards as inferred from a decrease in the total ipsilateral paw print intensity assessed by the Catwalk test. Intraperitoneal TLR4-A1 (10 $mg \cdot kg^{-1}$) partially recovered control baseline with peak effect at 30 min (47.61% ± 2.31) and 3 h (50.05% ± 0.64) post-administration (**Fig. 38C**).

In control rats, PWT, scores for the knee-bend test and intensity for the paw print throughout the study did not significantly differ from the baseline values.

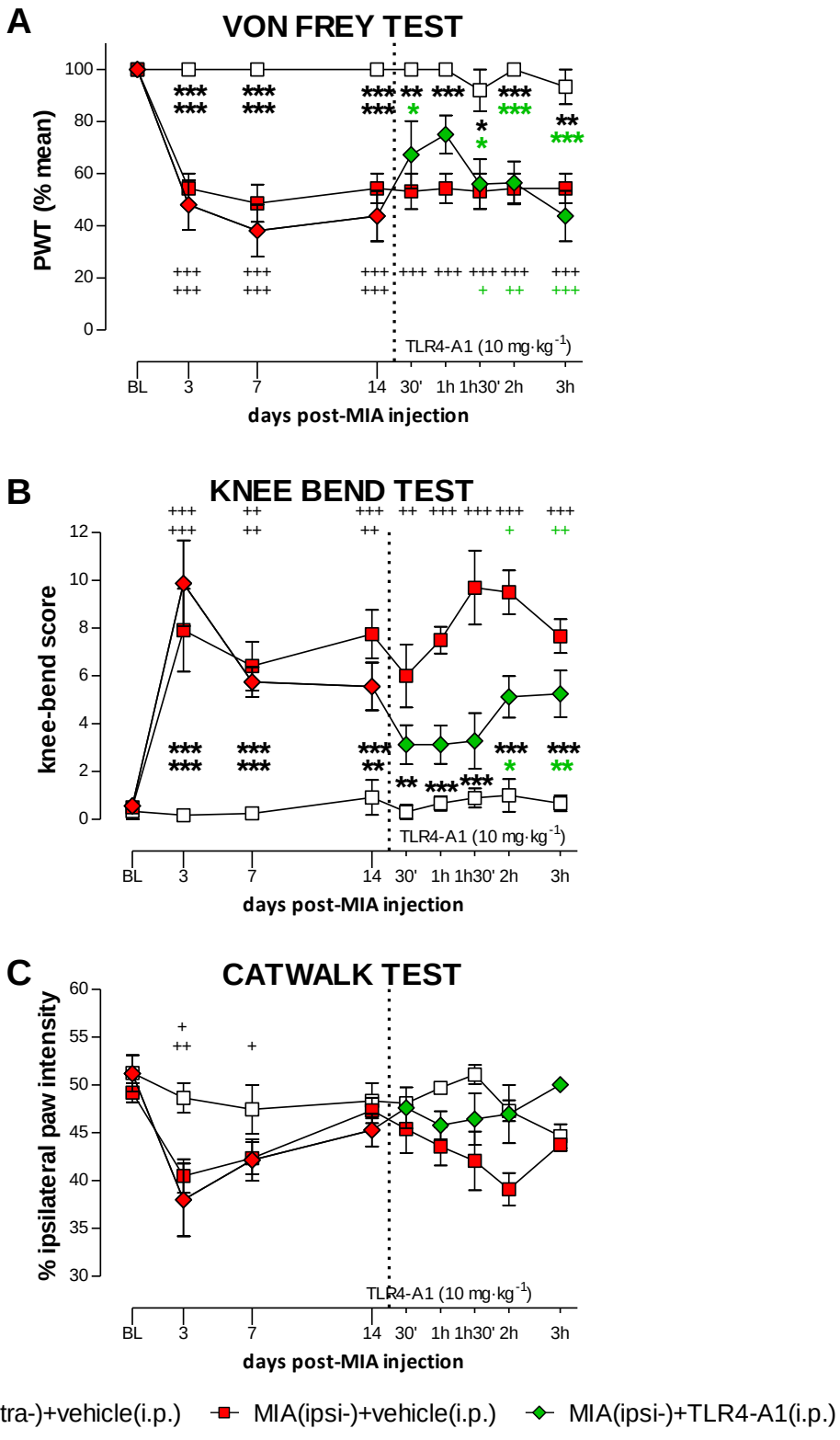

Figure 38. Immediate time course of TLR4-A1 acute effect administered once the pathology is developed. (**A**) Von Frey test. (**B**) Knee-bend test. (**C**) Catwalk test. * vs. CTRL (contra-) + vehicle (i.p.); 2-way ANOVA, Bonferroni post-hoc test. + vs. respective baseline (day 0). 1-way ANOVA, Dunnett's Multiple Comparison test (●P<0.05, ●●P<0.01, ●●●P<0.001). N = 6-8 animals per group.

1.1.2. TLR4-A1 chronic anti-nociceptive effect.

In order to assess if TLR4-A1 effect was different when acutely or chronically given, two different protocols on chronic administration were performed.

a. 5-day treatment

A 5-day intraperitoneal treatment with TLR4-A1 (10 $mg \cdot kg^{-1} \cdot day^{-1}$) partially attenuated MIA-induced tactile allodynia. During an initial phase (first 14 days post-MIA), there were no statistically significant differences between TLR4-A1- and control-groups. However later the effect of TLR4-A1 disappeared and a nociceptive response became clear (day 21), appearing statistically significant differences with the control group ($P<0.001$) and its baseline (day 0, $P<0.01$) (**Fig.40A**). On the contrary, 5-day TLR4-A1 (10 $mg \cdot kg^{-1} \cdot day^{-1}$) caused an overall blockage of MIA-induced thermal hyperalgesia as compared to baseline and the control group (**Fig.40B**).

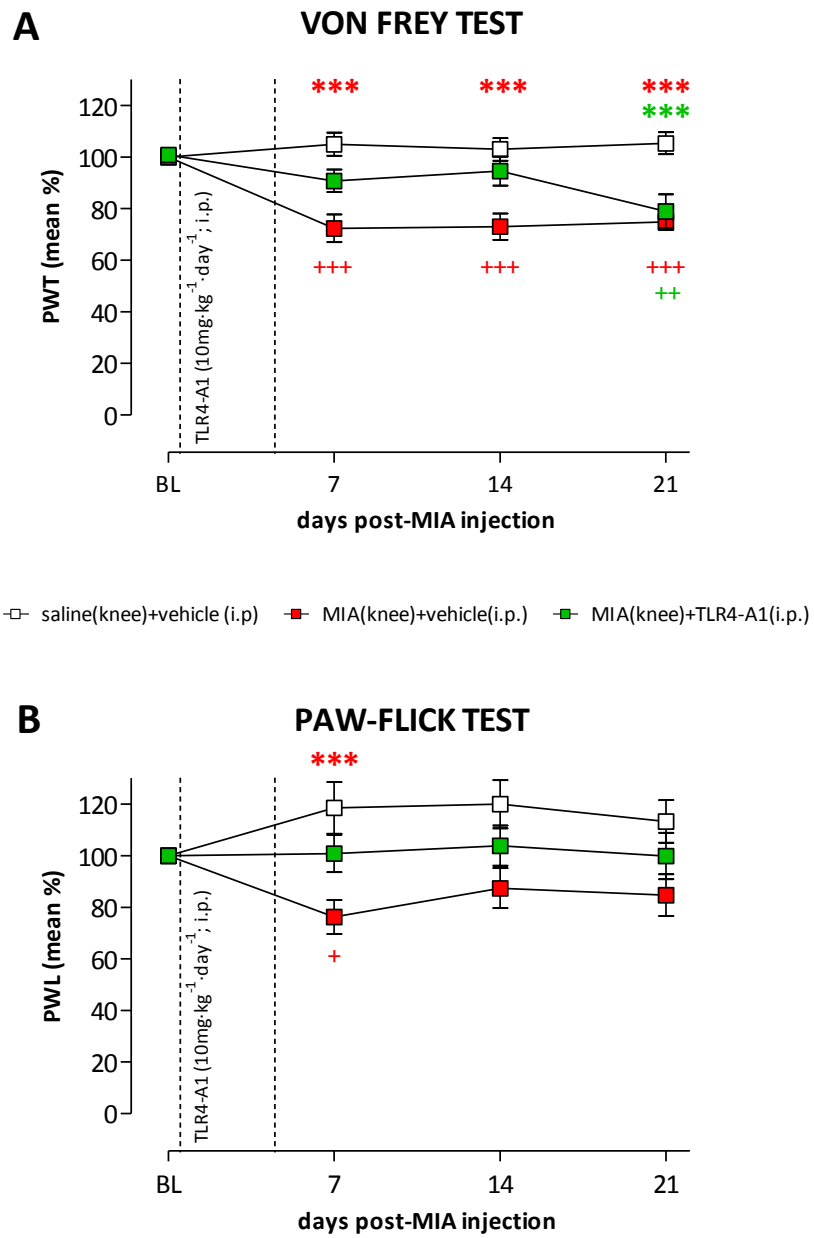

Figure 40. A short (5-day) TLR4-A1 treatment at the outbreak of the pathology. Data represent the mean percentage of the modification of the response ± SEM of the responses. * vs. different treatments (2-way ANOVA, Bonferroni post-hoc test); $^{+}$ different treatments compared to their respective day 0 (1-way ANOVA, Newman-Keuls Multiple Comparison test) (● P<0.05 , ●● P<0.01, ●●● P<0.001). N = 6-8 animals per group.

b. 15-day treatment (once the pathology has settled).

A second protocol of administration was designed starting once the pathological condition was evident. All behavioural tests were performed before and 1 hour following 10 mg·kg^{-1} TLR4-A1 daily administration.

Chronic effect of TLR4-A1 shows a trend to recover baseline threshold levels when light touch stimuli was applied on the mid-plantar aspect of the paw, with a

sustained effect all along the 15 days. Acute effect, that is, response studied 1 hour right after daily administration, also showed an attenuation of MIA-induced tactile allodynia, peaking on day 18 onward. These values were slightly closer to control thresholds, showing a more defined trend to recover baseline threshold levels (**Fig.41A**).

As previously mentioned, movement-induced nociception was evaluated through the knee-bend and CatWalk tests. When the stimuli was applied right on the damaged point (mechanical flexion and extension of the knee joint), chronic effect of TLR4-A1 showed a curve that close resembled that from the control group. Acute effect showed a similar pattern with a more noticeable attenuation of MIA-induced effects on days 18, 20 and 22 though. Despite the difference existing between both effects and the control group, no statistical differences were appreciated (**Fig.41B**).

Chronic effect of TLR4-A1 seemed not to affect MIA-induced spontaneous pain, remaining a similar pattern on the line graph. In the same way, acute effect of TLR4-A1 did not seem to differ much from the values registered for the MIA-group (**Fig.41C**).

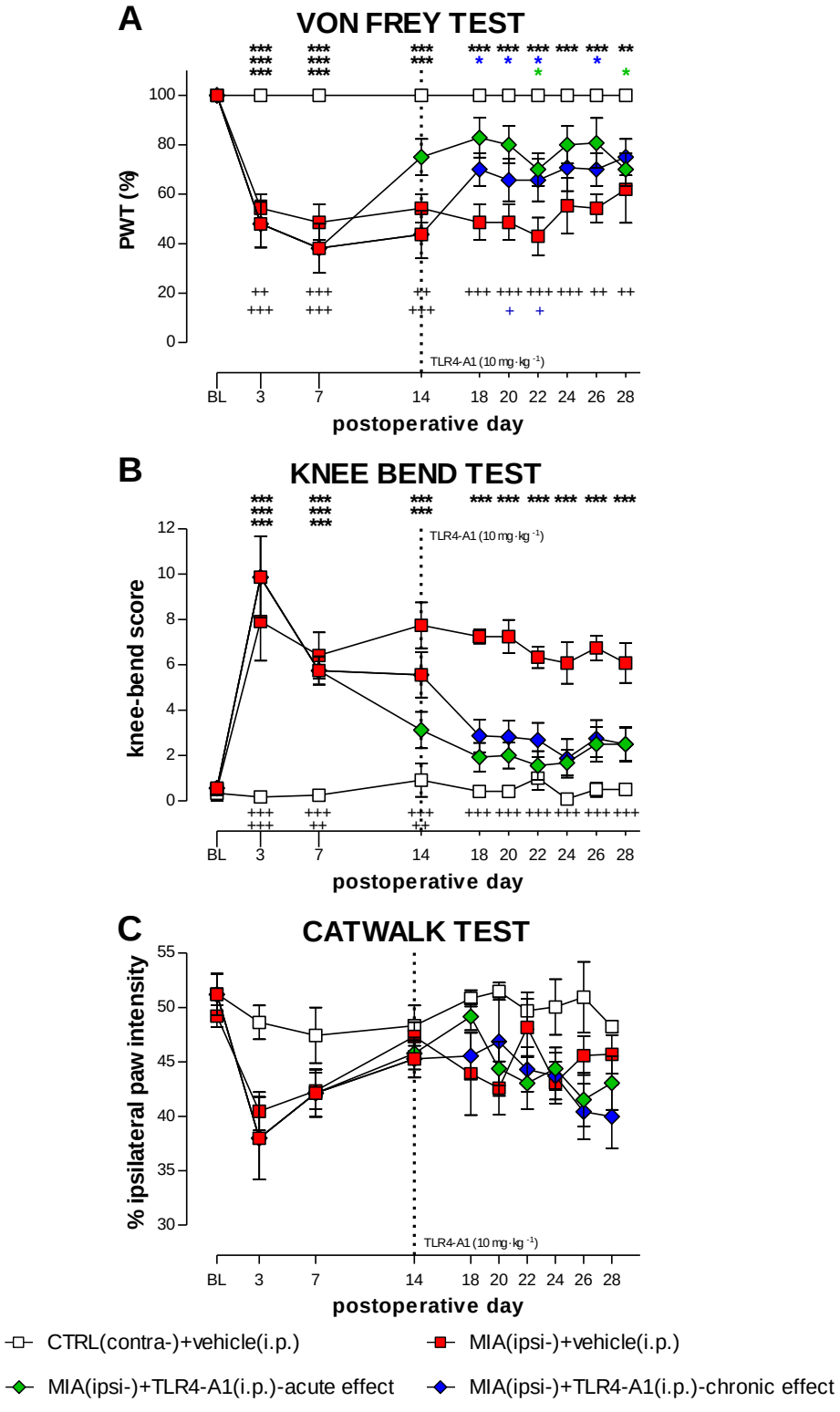

Figure 41. A 15-day TLR4-A1 treatment once the pathology is developped. A. Von Frey test. **B**. Knee-bend test. **C**. Catwalk test. * control contralateral paw vs. different treatments (2-way ANOVA, Bonferroni post-hoc test); + different treatments vs. corresponding day 0. 1-way ANOVA, Dunnett's Multiple Comparison test (●P<0.05, ●●P<0.01, ●●●P<0.001). N = 6-8 animals per group. Data are represented as the mean percentage ± % SEM. Dotted line represents the time point TLR4-A1 starts being administered at a ratio of 10 mg·kg^{-1}·day^{-1} during 15 consecutive days.

1.1.3. Intrathecal administration of TLR4-A1.

In sham animals (animals with catheter but not MIA-treated), saline-treatment[35] did not modify mechanical nor thermal thresholds during 3 weeks of experiments. MIA infiltrations on catheterised saline-treated animals produced however significant decrease on withdrawal thresholds at days 7 (55.6% ± 11.3, P<0.01) and 14 (57.4 ± 12.9, P<0.01) and on withdrawal latencies also at day 7 (72.7% ± 4.7, P<0.05) and 14 (70.9 ± 7.5, P<0.05) as compared to their corresponding baselines (day 0) (**Fig.42A,B**); just similar to what happened in MIA-treated animals with no catheter (**Fig.40**). On its part, 5-day intrathecal TLR4-A1-treatment (0.1 $mg \cdot kg^{-1} \cdot day^{-1}$) in MIA-treated rats reduced tactile-allodynia and values returned to baseline on days 14 (92.9% ± 7.6) and 21 (94.7% ± 5.6) after a decreasing initial phase (67.3% ± 13.4 on day 7, P<0.05 vs. baseline). On the contrary, TLR4-A1 did not modify heat-hyperalgesia: day 14 (67.0% ± 4.4, P<0.001 vs. baseline), day 21 (82.5% ± 7.2, no significant levels) (**Fig.42A,B**). This is at odds with what seen for intraperitoneally TLR4-A1 (10 $mg \cdot kg^{-1} \cdot day^{-1}$) OA animals: an initial phase with no tactile allodynia and complete recovery from heat hyperalgesia (**Fig.40**).

[35] In this case, the vehicle used was saline since etanol causes spinal toxicity.

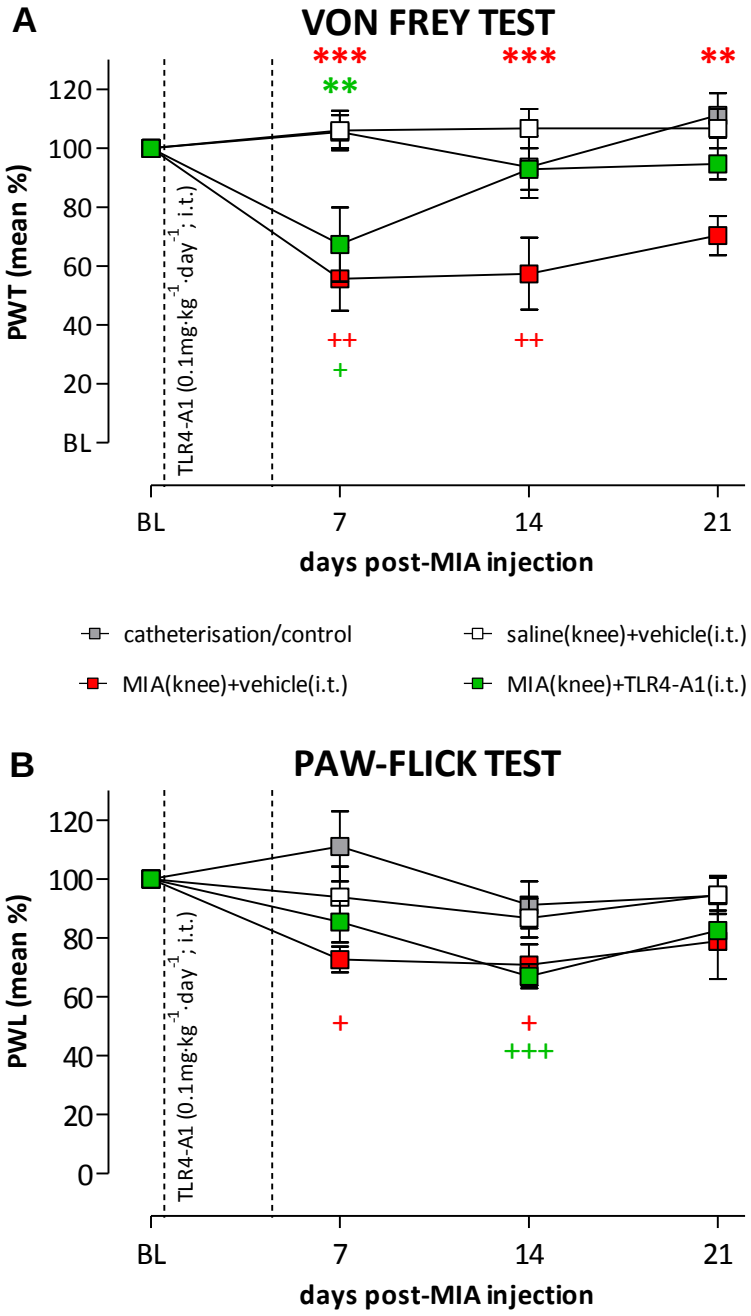

Figure 42. Effect of intrathecal administration of TLR4-A1 on a same protocol of 5-day treatment at the outbreak of the pathology. (**A**) Von Frey test. (**B**) Paw-flick test. * control contralateral paw vs. different treatments (2-way ANOVA, Bonferroni post-hoc test); $^{+}$ different treatments compared to their respective day 0 (1-way ANOVA, Dunnett's Multiple Comparison test). (●P<0.05, ●●P<0.01, ●●●P<0.001). Data represent the mean % ± SEM % of ≥ 8 animals per group.

1.1.4. Body weight.

Control- and MIA-group did not present any visible difference when compared with each other in any of the vehicle given groups (intraperitoneal or intrathecal). However, there were statistically significant differences when comparing

catheterised and non-catheterised animals, remaining the weight gain rate lower in the former ($P<0.01$ and $P<0.001$ for days 14 and 21 respectively). A short (5-day) TLR4-A1 treatment at the outbreak of the pathology also hampered weight gain during the first days when intrathecally ($P<0.001$, days 7 and 14) but not when intraperitoneally administered. However, by the end of the experiments the percentage weight increase matched in all catheterised rats, no matter it was vehicle or TLR4-A1 what given (**Fig.43A**). On its part, even though a long (15-day) TLR4-A1 treatment once the pathology has fully developped also hindered weight gain for several days, animals finally reached same weight levels as the control- and MIA-groups by the end of the experiment (**Fig.43B**).

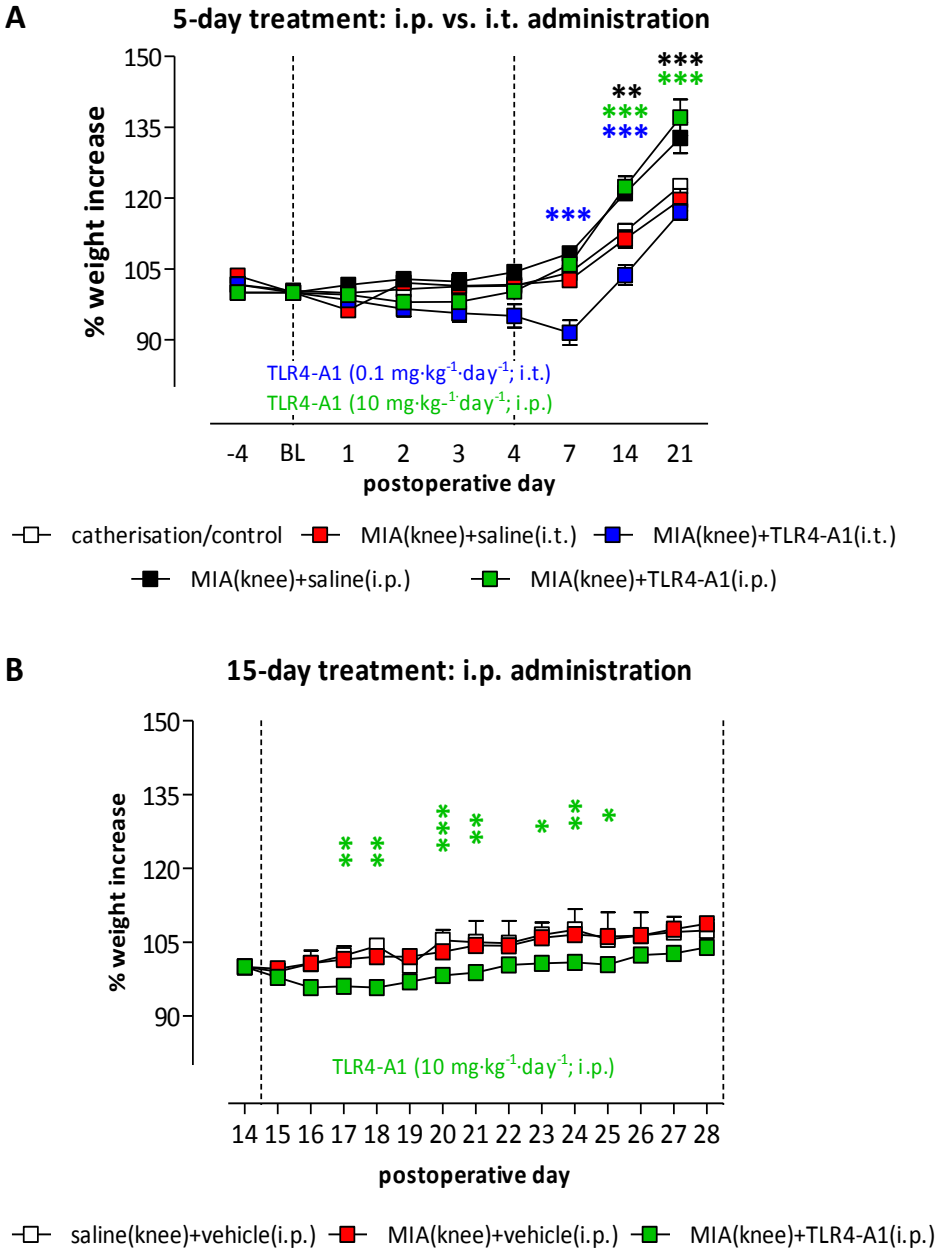

Figure 43. Comparison of percentage weight increase among untreated and treated animals for all of the groups tested. A. Comparison of catheterised and non-catheterised animals. **B.** 15-day TLR4-A1 intraperitoneally administered. * vs. control group (2-way ANOVA, Bonferroni test) (P<0.05 , ●● P<0.01, ●●● P<0.001). Data represent the mean % ± % SEM of n = 8-10 rats per group.

1.2. Incisional model of surgical pain.

As previously described, in order to carry out an incisional model of nociceptive pain, we focused on Brennan's model and stimulated three different areas in the nearby of the wound selecting the one we felt the most at ease with, which was also the one being stimulated for the OA model.

1.2.1. Pharmacological acute vs. cumulative chronic effects.

Daily drug 10 mg·kg^{-1} (i.p.) administration was divided in two: a first 5 mg·kg^{-1} dose to assess animal behaviour and a booster dose to achieve the 10 mg·kg^{-1}day^{-1}. Behavioural tests were performed before and right after daily drug administration.

a. TLR4-A1 and morphine acute effect.

The mid-plantar surface of each hind paw was stimulated during 9 consecutive days and responses to electronic von Frey stimuli were registered. Incision-induced tactile allodynia gradually attenuated from day 1 to 9. Incised animals recovered baseline thresholds by day 9. Statistical significant differences between contra- and ipsi-lateral paws were present during the first 8 days, vanishing the following day (**Fig.43A-C**). Acute intraperitoneal morphine (5 mg·kg^{-1}) totally reversed incision-induced tactile allodynia, overlapping with the values registered for the contralateral paw of untreated animals. Responses to electronic von Frey registered statistical significant differences from day 1 to day 6 (also isolated day 9) when comparing ipsilateral paws of morphine-treated to untreated animals (**Fig.43A**).

Acute TLR4-A1 (5 mg·kg^{-1}; i.p.) also achieved a reversion of tactile-induced allodynia. Statistical significant differences between contra-(vehicle) and ipsi-lateral (TLR4-A1) paws were present on postoperative days 1 ($P<0.01$) and 4 ($P<0.05$) and during all four first days when compared to the ipsilateral paw of the untreated-group (vehicle) (**Fig.43B**). On its part, TLR4-A1 (5 mg·kg^{-1}) + morphine (5 mg·kg^{-1}) reversed incision-induced tactile allodynia, exisiting no statisitical significant differences when comparison was made to the contralateral paw of untreated animals (**Fig.43C**). Similar to morphine-treated group, significant differences to ipsilateral paw of untreated-group were present all along the 9-day period.

When a noxious thermal stimulus was applied, statistically significant differences were found until day 2 between the contra- and ipsi-lateral hind paws of the innocuous vehicle-treated (i.p.) group (untreated-group) (**Fig.43D-F**). Contrary to the ipsilateral paw of the untreated-group, thresholds in all treated groups

exceeded the values observed for the contralateral paw at all time-points; presenting the TLR4-A1 + morphine-treated group the greater degree of antinociception (**Fig.43F**), followed by morphine (**Fig.43D**) and TLR4-A1 (**Fig.43E**).

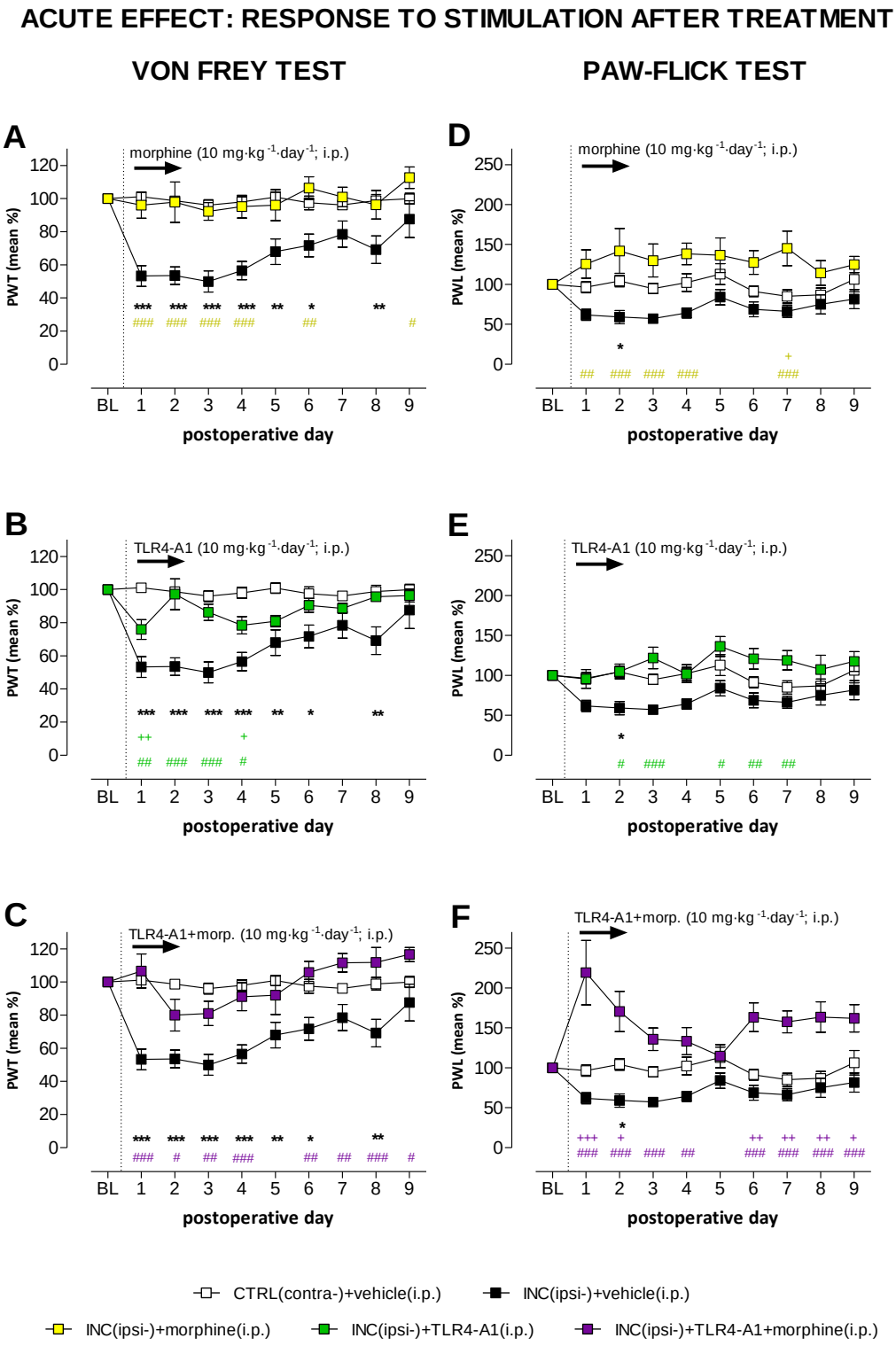

Figure 43. Response to a non-noxious (von Frey test, A-C) or noxious (paw-flick test, D-F) stimulus registered 45 min following vehicle, morphine, TLR4-A1 or TLR4-A1+morphine administration. Incision-induced tactile allodynia was

detectable throughout the first 8 days of experiments. Morphine (A) and TLR4-A1+morphine (C) administrations exhibited no statistical significant differences compared to the contralateral paw of untreated animals. For TLR4-A1 administrations (B) significant differences existed on two isolated days (P<0.01 for day 1 and P<0.05 for day 4). Comparison between ipsilateral paws of untreated and treated groups showed statistical significant differences throughout all 9 days for morphine- and morphine+TLR4-A1-treated groups, and for the first four days post-incision for the TLR4-A1-group. **Incision-induced heat hyperalgesia** only presented statistical significant differences compared with contralateral paw during the first two days post-incision. All of the treated groups exhibited antinociception after administrations (D,E,F). * contra- vs. ipsi-lateral paw (untreated-group); $^{+}$ ipsilateral paw (treated-group) vs. control contralateral paw (untreated group); $^{\#}$ ipsilateral paw (treated-group) vs. ipsilateral paw (untreated-group).Two-way ANOVA, Bonferroni post-hoc test (● P<0.05 , ●● P<0.01, ●●● P<0.001). Data represent mean ± SEM of 10 rats. The dotted line represents the time point when the treatments were started to be administered from. That is, treatment had been already administered to the rats by day 1 on the graph. Electronic von Frey and not calibrated monofilaments was used.

b. TLR4-A1 and morphine chronic effects.

Withdrawal thresholds and latencies following stimulation of the mid plantar aspect of the paw were also assessed before daily administrations.

Similar to what previously reported, incision-induced tactile allodynia gradually attenuated from day 1 to 9 when electronic von Frey was applied onto the mid plantar aspect of the hind paw. Statistical significant differences between contra- and ipsi-lateral paws of incised animals were present until day 5, vanishing the following day (**Fig.44A-C**). Register before daily intraperitoneal morphine on the other hand showed a long-lasting tactile allodynia with statistical significant differences (P<0.001 for all days) that extended over day 9 when comparing with the contralateral paw of the control group. Even registers corresponding to ipsilateral paws of untreated animals broke away from morphine-treated values existing statistical significant differences from day 7 on (**Fig.44A**). Data before daily i.p. TLR4-A1 showed a shorter recovery time compared to the control group, existing statistically significant differences only until day 4 (**Fig.44B**). Eventually, register before daily i.p. TLR4-A1+morphine showed once again a similar time course recovery as the untreated group. Statistically significant differences compared to the contralateral paw (untreated-group), resembled those seen for the ipsiltateral paw of the untreated group; that is, repeated TLR4-A1+morphine administration had no effect on time course recovery following plantar incision (**Fig.44C**).

As regards withdrawal latencies, the untreated-group showed similar results to what previously reported for the register after vehicle administration.

Withdrawal latencies gradually recovered baseline and significant differences between the contra- and ipsilateral paws remained visible until day 3 (**Fig.44D-F**). Data before daily i.p. morphine showed withdrawal latencies that did not recovered baseline and significant differences were seen on day 7 ($P<0.01$) compared to the contralateral paw of the control group (**Fig.44D**). On the contrary, register before daily intraperitoneal TLR4-A1 showed latencies closer to what seen for the contralateral paw of the untreated (vehicle)-group (**Fig.44E**). Furthermore, significant differences regarding the ipsilateral paw of the untreated group were seen (days 3, 4, 6 and 8). Finally, time-course recovery daily assessed before everyday TLR4-A1+morphine administration was comparable stimulating with electronic von Frey and a heat beam. Latencies practically overlapped the curve described by the ipsilateral paw of vehicle-treated animals (**Fig.44F**).

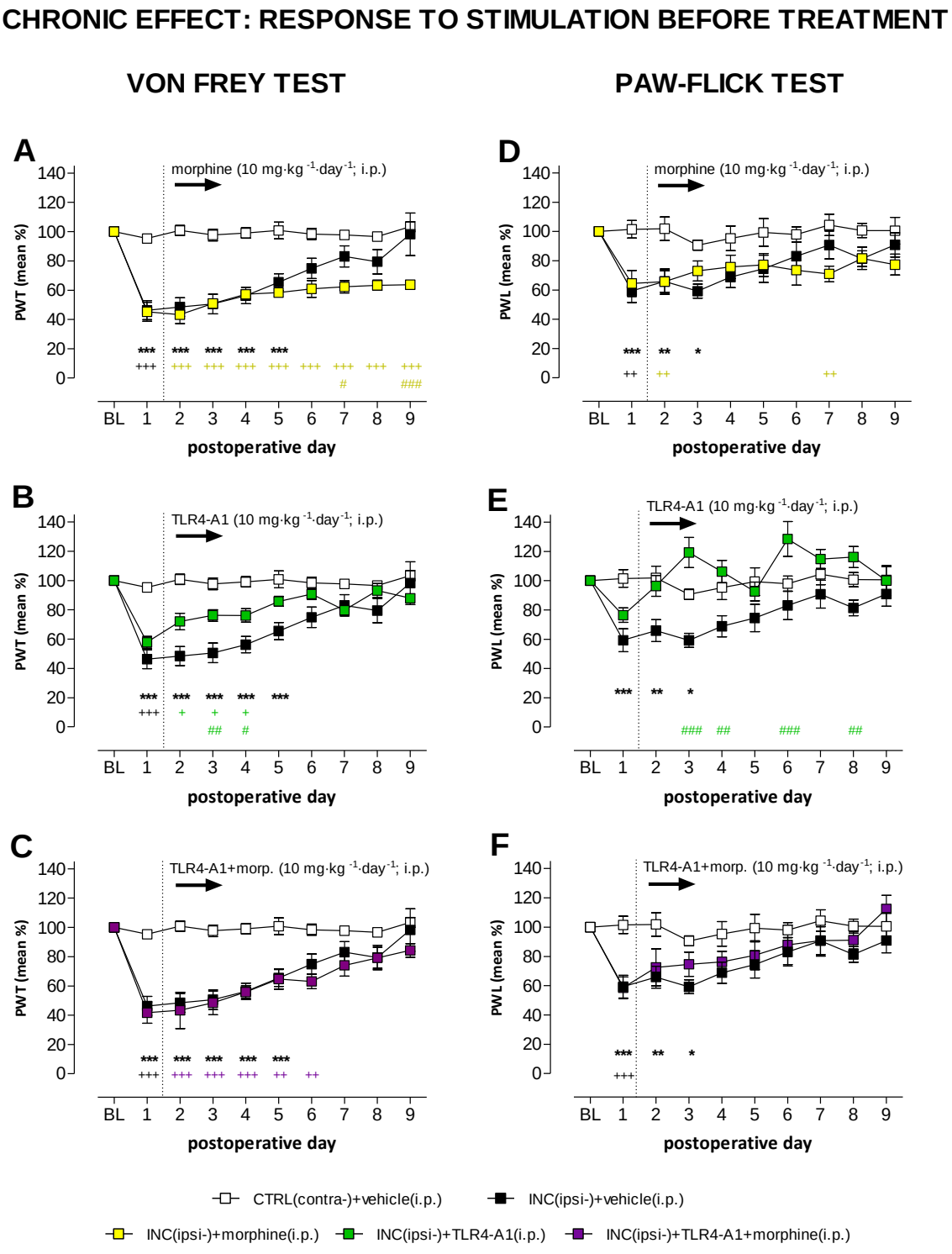

Figure 44. Response to a non noxious (von frey test) or noxious (paw-flick test) stimulus registered during a 9-day treatment protocol right before daily administration of any dose. Figure shows registers before morphine (A,D), TLR4-A1 (B,E) and TLR4-A1+morphine (C,F) administrations. * contra- vs. ipsi-lateral paw (untreated-group); $^{+}$ ipsilateral paw (treated-group) vs. control contralateral paw (untreated group); $^{\#}$ ipsilateral paw (treated-group) vs. ipsilateral paw (untreated-group). Two-way ANOVA, Bonferroni post-hoc test (● P<0.05, ●● P<0.01, ●●● P<0.001). Data represent mean ± SEM of 10 rats. The dotted line represents the time point when the treatments were started to be administered from. That is, by day 1 on the graph, no treatment had been administered to the rats yet. Electronic von Frey was used.

c. Body weight.

In all analysed groups there were statistically significant differences compared to the control group. Incised TLR4-A1- and TLR4-A1+morphine-treated groups counted on the greatest significant differences, starting right after two days post-incision. Morphine-treated group drifted apart from postoperative day 6 on and the incised untreated-group (innocuous saline) showed significant differences at days 8 and 9. Therefore, both incision and treatment affected general discomfort along the 9-day observational period (**Fig.46**).

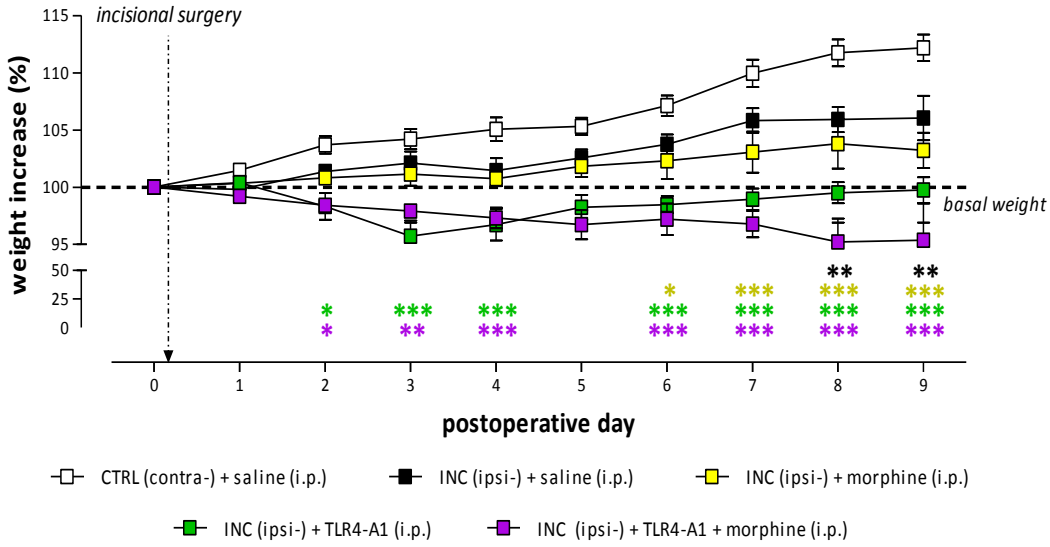

Figure 46. Comparison of percentage weight increase among untreated and treated animals for all of the groups tested. Weight increase represented as percentage increase considering the baseline measurement as 100%. * Comparison of ipsilateral paws of any group *vs*. contralateral paw of the untreated-group. Two-way ANOVA followed by Bonferroni post-hoc test (● p<0.05 , ●● p<0.01, ●●● p<0.001).

2. *In vitro* assays.

2.1. Macroscopic evaluation and histologic analysis of the knee joint.

After sacrificing the animals, both knees were immediately examined macroscopically. 22 days after saline infiltration into the left knee revealed translucent and pearly pink condyles, with an apparently smooth intact surface **(Fig.47A)**. On the other hand, 2 mg MIA-infiltrated knees showed a rather white and opaque aspect with surface undulation, striking fibrillation and erosion **(Fig.47B)**. Features observed for the left knee of vehicle-treated animals equally described the aspect of the left knee of animals receiving TLR4-A1 (10 $mg \cdot kg^{-1}$, i.p.) during five consecutive days starting soon after the moment infiltrations

were given **(Fig.47C)**. On the contraty the right knee (MIA-injected) of TLR4-A1-treated animals does not exactly correspond to the features observed for the right knee of vehicle-treated rats, but rather shows an intermediate state with soft surface roughness and slight glassy appearance **(Fig.47D)**.

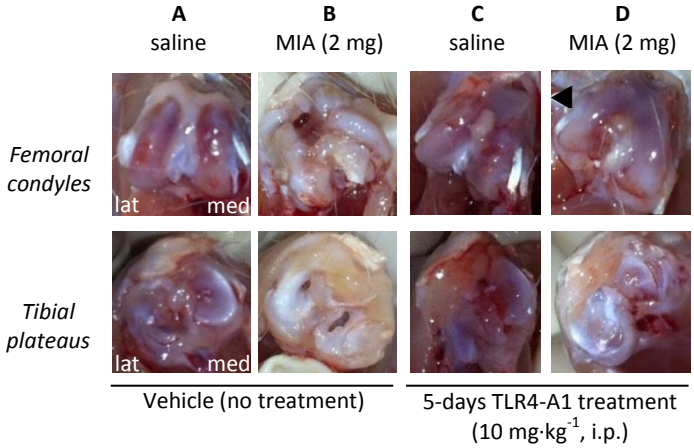

Figure 47. Comparison of gross appearance of unstained tibia and femur articular cartilage surfaces in the MIA-induced osteoarthritic model of pain at 4 weeks (22 days) following infiltrations. Representative images of the contralateral saline-infiltrated joint (**A**) and the MIA-infiltrated joint (right knee) of the same animal (**B**). Contralateral (**C**) and ipsilateral (**D**) knee joints of animals receiving TLR4-A1 (10 mg·kg-1, i.p.) during five consecutive days starting soon after the moment infiltrations were given. The medial condyle of the distal femur exhibited an osteophyte formation at the intercondylar space (arrowhead).

Structural changes in the rat knee joint were microscopically assessed in the different groups of rats and graded according to the Pritzker-score (Pritzker *et al*., 2006) **(Tab. 11)**.

Parameter (key feature)	*Grade*	*Description*
Surface and cartilage morphology intact	0	Normal matrix architecture and intact cells
Surface intact	1	Oedema and/or superficial abrasion in the matrix; death, proliferation and/or hypertrophy of cells.
Surface discontinuity	2	Matrix discontinuity at superficial zone; death, proliferation and/or hypertrophy of cells
Vertical fissures	3	Matrix vertical fissures and branched fissures into mid zone; death, regeneration and/or hypertrophy of cells
Erosion	4	Cartilage matrix loss
Denudation	5	Sclerotic bone within denuded surface
Deformation	6	Bone remodeling: fibrocartilaginous and osseous cells invading microfractures

Table 11. Cartilage degeneration score. OA cartilage histopathology grade assessment. Grade = depth progression into cartilage.

For better analysing the cartilage status, toluidine blue staining was performed. At first glance, toluidine blue stained sections obtained from control group (**Fig.48A**) showed continuous intact surface layer with normal matrix architecture. On the contrary, injection

of MIA into the femorotibial joint caused erosion and deformation of the subchondral bones (**Fig.48B**). Nevertheless, a 5-day TLR4-A1 (10 $mg \cdot kg^{-1} \cdot day^{-1}$; i.p.) treatment apparently had no influence on saline (**Fig.48C**) nor MIA injections (**Fig.48D**). However, even though ipsilateral knees (MIA-treated) of rats receiving TLR4-A1 showed irregular surfaces with focally extensive area of cartilage loss and degeneration, inflammatory cells remained focal in the cartilage matrix and did not extend as fibrosis areas outside the femoral condyle nor the tibial plateau. Contrary to these findings, sections from MIA-treated knees of rats receiving sterile saline showed a femoro-tibial unit where femur and tibia were stuck together.

Subsequently, the tibial plateau was analysed and divided into three zones of equal width: Z1, Z2 and Z3. A score was given to each cartilage zone and represented as a bar graph (**Fig.48E**). A more detailed examination showed intact surface with no matrix loss for contralateral tibiae (left knees) of saline-treated (i.p.) rats: Z1 = 0.7, Z2 = 0.7 and Z3 = 0.6. Ipsilateral tibiae (right knees) in the same group displayed degeneration scores more suitable for an erosional state in all three zones: Z1 = 3.8, Z2 = 4.3 and Z3 = 4.1. On the other hand, contralateral knees of TLR4-A1-treated animals showed superficial abrasion in zone 1 (1.7), and intact surface with no matrix loss for zones 2 and 3: Z2 = 0.4 and Z3 = 0.3. Ipsilateral knees in the same group exhibited a wider range of scores corresponding to matrix discontinuity and incipient fissures in zone 1 (2.6), matrix vertical fissures and incipient erosion in zone 2 (3.5), and complete erosion in zone 3 (4.5).

The mean of all three scores was plotted in a second bar graph (**Fig.48F**). Assuming the mean score of the three zones as a realistic distribution of MIA solution into the articular cavity, intact surface with no matrix loss was observed for contralateral saline-treated tibiae (left knees) of both saline- and TLR4-A1-treated groups (grades 0.7 and 0.8 respectively). In flat opposition, tibiae corresponding to 2mg MIA-treated knees (right knees) showed a complete loss of cartilage matrix (grade 4.1) for intraperitoneally saline and an incipient erosion (grade 3.5) for TLR4-A1-treated animals (i.p.).

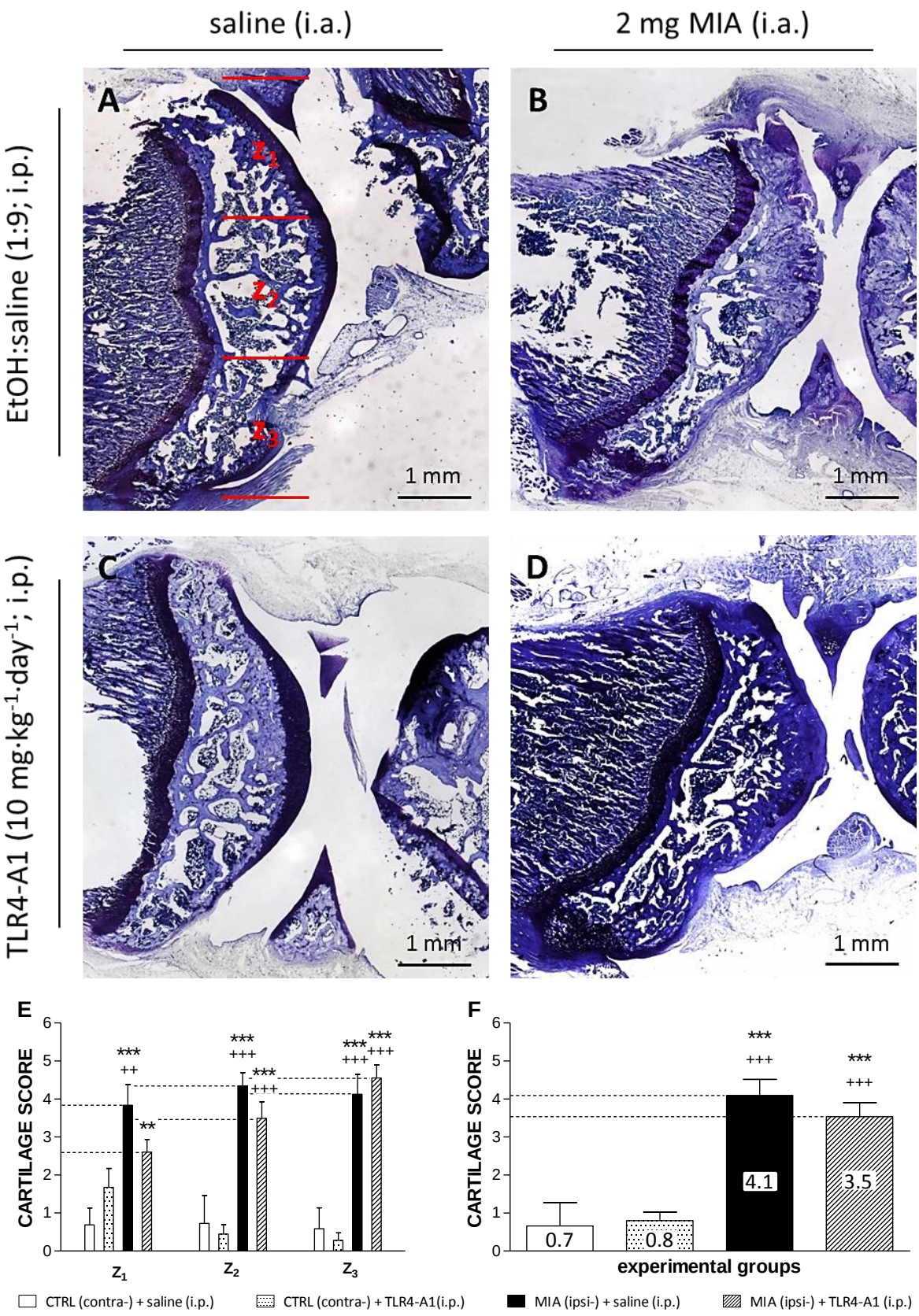

Figure 48. Representative sagittal histologic sections from rat joints in the MIA-induced osteoarthritic model of pain after 22 days following MIA or saline infiltration. Even columns (A and C) correspond to contralateral knees of i.p. vehicle or TLR4-A1-treated groups respectively. Odd columns (B and D) correspond to MIA-treated knees of i.p. vehicle or TLR4-A1-treated groups respectively. For better evaluation, only the tibial plateau was analysed and divided into three zones of

equal width (marked by red lines): Z1 as the anterior part of the joint, Z2 in the middle and Z3 as the posterior part. A numeric score was assigned based on the physical aspect of the cartilage tissue (**E**). The mean value of the three zones is represented as well (**F**). Intact surface with no matrix loss was observed for contralateral saline-treated tibiae (left knees) of both saline- and TLR4-A1-treated groups (grade 0-1). Tibiae corresponding to 2mg MIA-treated knees (right knees) showed a completely loss of cartilage matrix (grade 4) for intraperitoneally saline and an incipient erosion (grade 3-4) for TLR4-A1-treated animals (i.p.). * ipsilateral knees vs. contralateral knee + saline (i.p.); $^{+}$ ipsilateral knees vs. contralateral knee + TLR4-A1 (i.p.). Two-way ANOVA, Bonferroni post-hoc test. (● p<0.05 , ●● p<0.01, ●●● p<0.001). Sample size of 7-11 animals per group. Micrographs correspond to individual 2.5x images gathered together by Microsoft® Image Composite Editor (ICE).

2.2. Microscopic examination of the saphenous nerves.

2.2.1. Morphological analysis

a) <u>Osteoarthritic model of pain.</u>

In all samples analysed nervous tissue is mainly staining the colour of toluidine blue and, at a first glance, all histological sections seem morphologically normal. Groups exhibited a similar distribution of small- and large-diameter myelinated and unmyelinated nerve fibres and Schwann cells, each surrounded by a well-defined endoneurium, and regular proportions between myelin sheath thickness and fibre diameter (**Fig.49**). However, various mast cells exhibiting the dark purple colour of toluidine blue (metachromasia) were appreciated in sections corresponding to MIA treated group under innocuous saline. On the contrary, the rest of the nerves only showed occasionally a lonesome mast cell.

No striking differences regarding the nerve or connective (endoneurium) tissues were appreciated among groups.

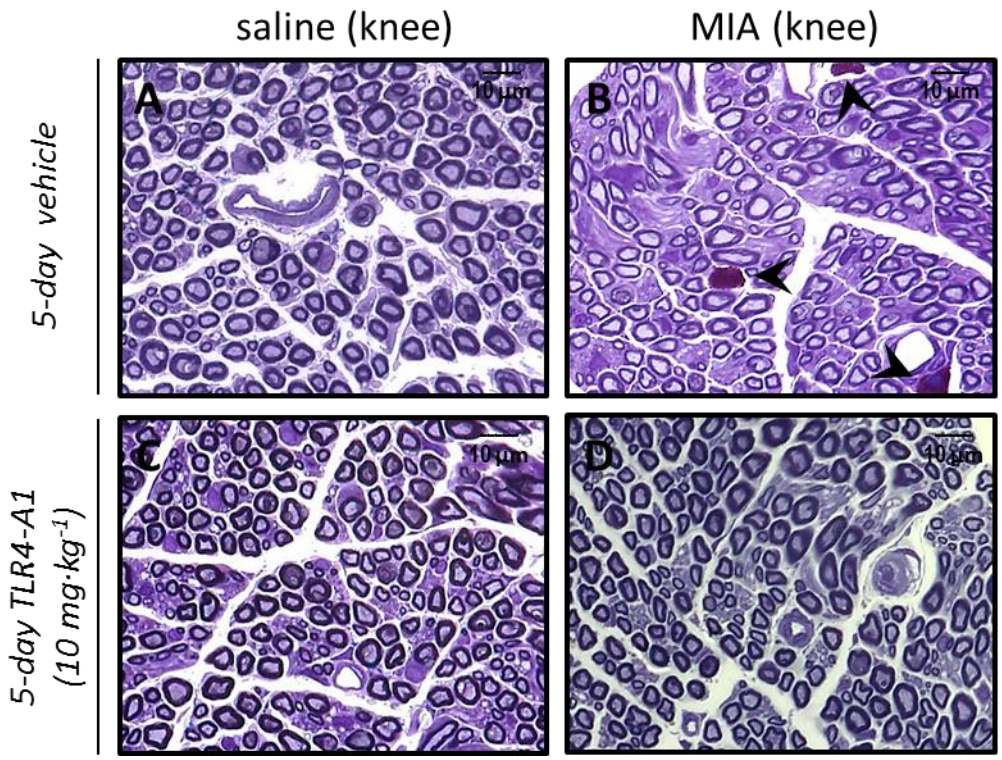

Figure 49. Light micrographs from saphenous nerve of rat in the MIA model of pain. (A) Contralateral and (B) ipsilateral nerves of vehicle-treated animals. (C) Contalateral and (D) ipsilateral nerves of 5-day TLR4-A1-treated rats. Note intensely stained mast cells exhibiting a metachromatic reddish-purple colour in the MIA group receiving innocuous vehicle (arrowheads in B). Micrographs correspond to individual 63.5x images. Postoperative day 22.

b) <u>Incisional model of pain.</u>

No big differences were seen in the histological nerve sections from ipsilateral paws (incised) concerning the distance between perineurium and the bundle of nerve fibres or the endoneurium area as compared to their respective contralateral controls. No obvious difference was either seen in the specimens analysed with respect to demyelination or axonal injury as compared to the vehicle-treated control contralateral tissue (**Fig.50**). Sections of all groups occasionally showed a mast cell.

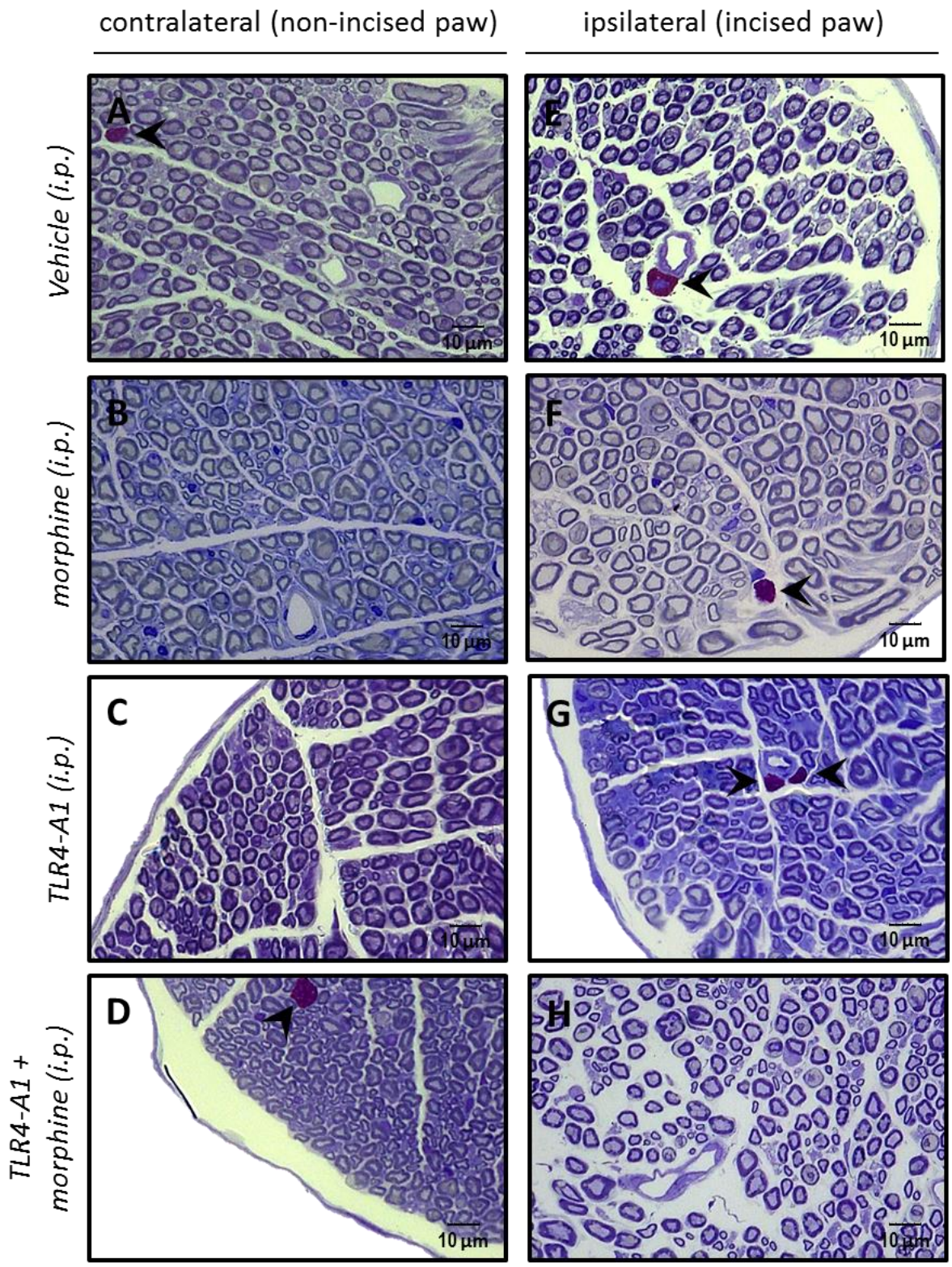

Figure 50. Light micrographs from saphenous nerve of rat in the PO model of pain. (A-D) Contralateral and (E-H) ipsilateral nerves of vehicle, morphine, TLR4-A1 and TLR4-A1+morphine treated animals. Note the presence of scarce (arrowheads) or none mast cells in the endoneurium of any section. Micrographs correspond to individual 63.5x images. Postoperative day 10.

2.2.2. Morphometrical analysis

a) Osteoarthritic model of pain.

The morphometrical analysis showed that no striking differences were observed among groups for all the parameters studied. Notwithstanding, a more detailed morphometrical analysis on different easily measurable parameters showed that sections corresponding to the ipsilateral paw (MIA-treated) of intraperitoneally vehicle-treated rats separated from the rest of groups (**Table 12**).

a.1. *Fibre diameter.* The diameter of myelinated nerve fibres was of greater magnitude for the vehicle-treated group (contra-: 4.70 µm ± 0.04; ipsi-: 4.43 µm ± 0.06) than for the TLR4-A1-treated group (contra-: 4.33 ± 0.03; ipsi-: 4.36 ± 0.03). Comparisons made between the contra- and ipsilateral nerves of each group showed a statistically significant decrease for the ipsilateral nerve (MIA, $P<0.001$) of the vehicle-treated group. Diameters did not differ within the TLR4-A1-treated group, although both were significatively shorter than that of the contralateral nerve from the vehicle-treated group ($P<0.001$).

a.2. *Axonal diameter.* In a similar way, the axonal diameter was also greater for the vehicle-treated group (contra-: 2.41 µm ± 0.03; ipsi-: 2.52 µm ± 0.04) than for the TLR4-A1-treated group (contra-: 2.37 ± 0.03; ipsi-: 2.34 ± 0.03). However the only axonal diameter showing a statistically significant increase with regard to the others was the ipsilateral nerve (MIA, $P<0.001$) from the vehicle-treated group.

a.3. Myelin sheath thickness was determined by the following formula: (D-d)/2, where D corresponds to the fibre diameter and d to the axonal diameter. Comparisons made between the contra- and ipsilateral nerves of each group showed a statistically significant decrease for the ipsilateral nerve (MIA, $P<0.001$) of the vehicle-treated group. Myelin sheath thickness did not differ within the TLR4-A1-treated group; it was significatively thinner than that of the contralateral nerve and thicker than that of the ipsilateral nerve from the vehicle-treated group ($P<0.001$).

a.4. *G ratio.* The G-ratio was calculated as follows: d/D. MIA-treated paws from the vehicle group exhibited statistically significant greater G-ratios than all the other nerves.

That is, the axoplasma's size was increased and the fibre size diminished in MIA-treated paws of the vehicle group, whereas in the TLR4-A1-treated group just the diameter of nerve fibres was decreased.

	vehicle (0.9% NaCl; i.p.)		**TLR4-A1** (10 mg·kg-1; i.p.)	
	contralateral	**ipsilateral (MIA)**	**contralateral**	**ipsilateral (MIA)**
diameter of nerve fibres (mean ± S.E.M., µm)	4.70±0.04	4.43±0.06***	4.33±0.03+++	4.36±0.03+++
diameter of axons (mean ± S.E.M., µm)	2.41±0.03	2.52±0.04*	2.37±0.03	2.34±0.03
myelin sheath thickness (mean ± S.E.M., µm)	1.15±0.01	0.95±0.02***	0.98±0.01+++	1.01±0.01+++
G ratio	0.51±0.00	0.56±0.00***	0.54±0.01+++	0.53±0.00+++

Table 12. Morphometrical analysis of nerve cross-sections 22 days post-infiltration. ∗ vs. corresponding contralateral paw; **+** vs. contralateral paw of the vehicle-treated group. Statistical significance between conditions was determined by one-way ANOVA test followed by Newman-Keuls Multiple Comparison test. (● p<0.05 , ●● p<0.01, ●●● p<0.001). N = 6 sections from 2-4 saphenous nerves in each case.

b) Incisional model of pain.

The morphometrical analysis showed no statistically significant differences among groups (**Table 13**).

	contralateral				**ipsilateral (incision)**			
	vehicle	**morphine**	**TLR4-A1**	**T + M**	**vehicle**	**morphine**	**TLR4-A1**	**T + M**
diameter of nerve fibres (mean ± S.E.M., µm)	4.0 ± 0.5	4.4 ± 0.1	4.2 ± 0.1	4.1 ± 0.2	3.7 ± 0.6	4.0 ± 0.1	4.1 ± 0.0	4.4 ± 0.3
diameter of axons (mean ± S.E.M., µm)	2.0 ± 0.2	2.2 ± 0.1	2.1 ± 0.1	2.0 ± 0.1	1.9 ± 0.4	2.2 ± 0.0	2.3 ± 0.0	2.3 ± 0.2
myelin sheath thickness (mean ± S.E.M., µm)	1.0 ± 0.2	1.1 ± 0.1	1.1 ± 0.1	1.1 ± 0.1	0.9 ± 0.1	0.9 ± 0.0	0.9 ± 0.0	1.0 ± 0.1
G ratio	0.50 ± 0.1	0.50 ± 0.0	0.49 ± 0.0	0.49 ± 0.0	0.50 ± 0.0	0.54 ± 0.0	0.54 ± 0.0	0.52 ± 0.0

Table 13. Morphometrical analysis of nerve cross-sections 10 days post-surgery. N = 6 sections from 2-4 saphenous nerves in each case.

2.3. Inmunohistochemical study for glial activity.

2.3.1. Osteoarthritic model of pain.

2.3.1.1. Microglial expression of ionized calcium binding adapter molecule 1 (Iba1).

Intraarticular injection of MIA increased the numbers of Iba-1 positive activated microglia in the ipsilateral spinal cord at day 22; it was statistically significant for the superficial (I-II) laminae of L3 (P<0.01) and L4 (P<0.01) sections and for the deeper (V-VI) laminae of the former (P<0.001). Aditionally, total microglia counting in the overall ipsilateral dorsal horn of L3 sections was increased for MIA-treated animals (P<0.05). Iba-1 in the ipsilateral dorsal horn of 5-day TLR4-A1-treated rats showed on the contrary a similar pattern to the contralateral dorsal horn; that is, TLR4-A1 prevented activation of microglia (**Fig.51&52**).

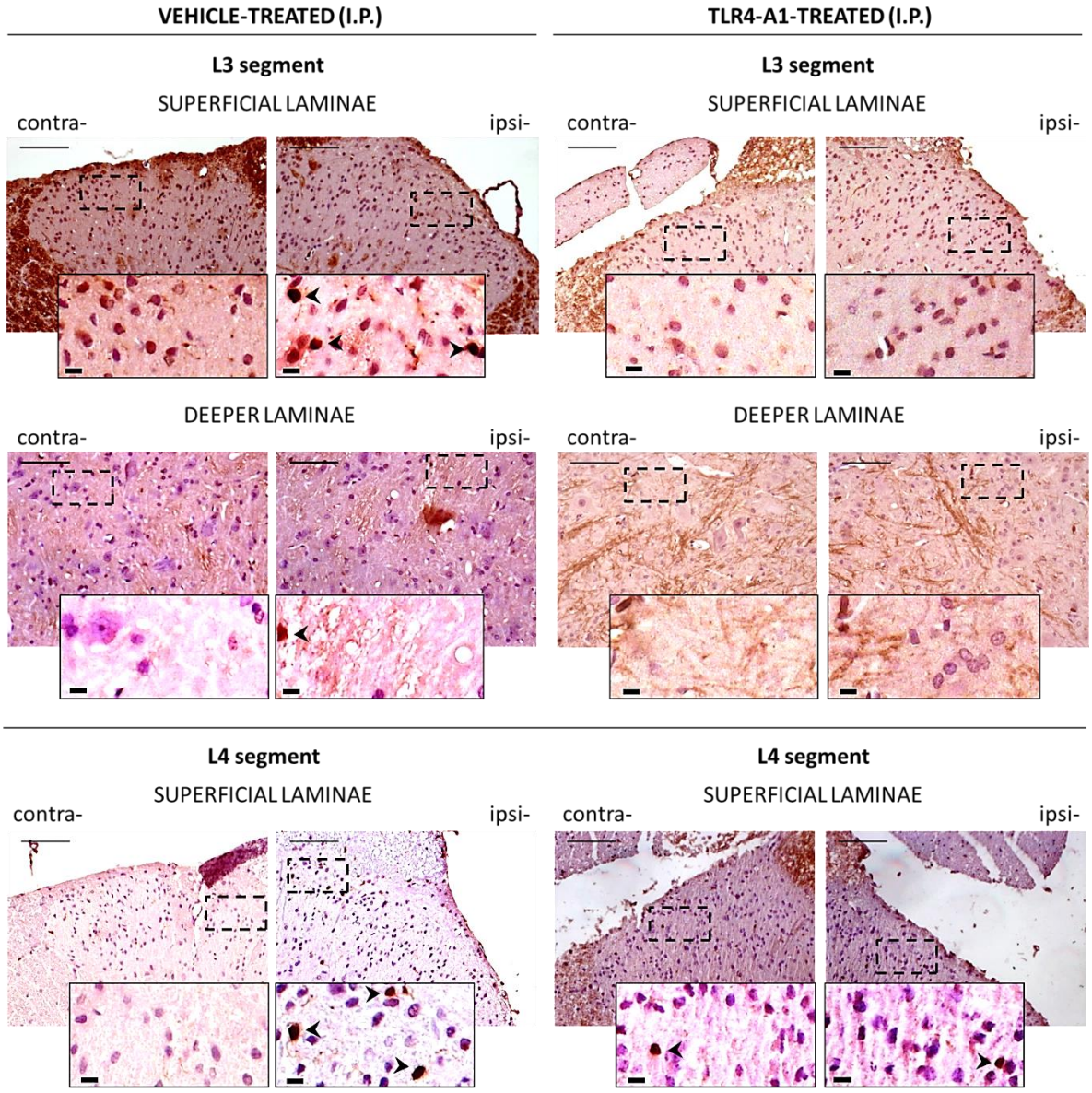

Figure 51. Representative images of microglial activation in the contralateral and ipsilateral spinal cord 22 days following unilateral MIA injection. Iba-1 immunoreactivity in L3 superficial (upper row) and deeper laminae (middle row), and in L4 superficial lamina (bottom row). The results shown are representative of experiments performed using six animals per group (with three sections per lumbar segment for each animal). Arrowheads indicate Iba-1 immunoreactive cells. Scale bar = 100μm and 10μm in insets.

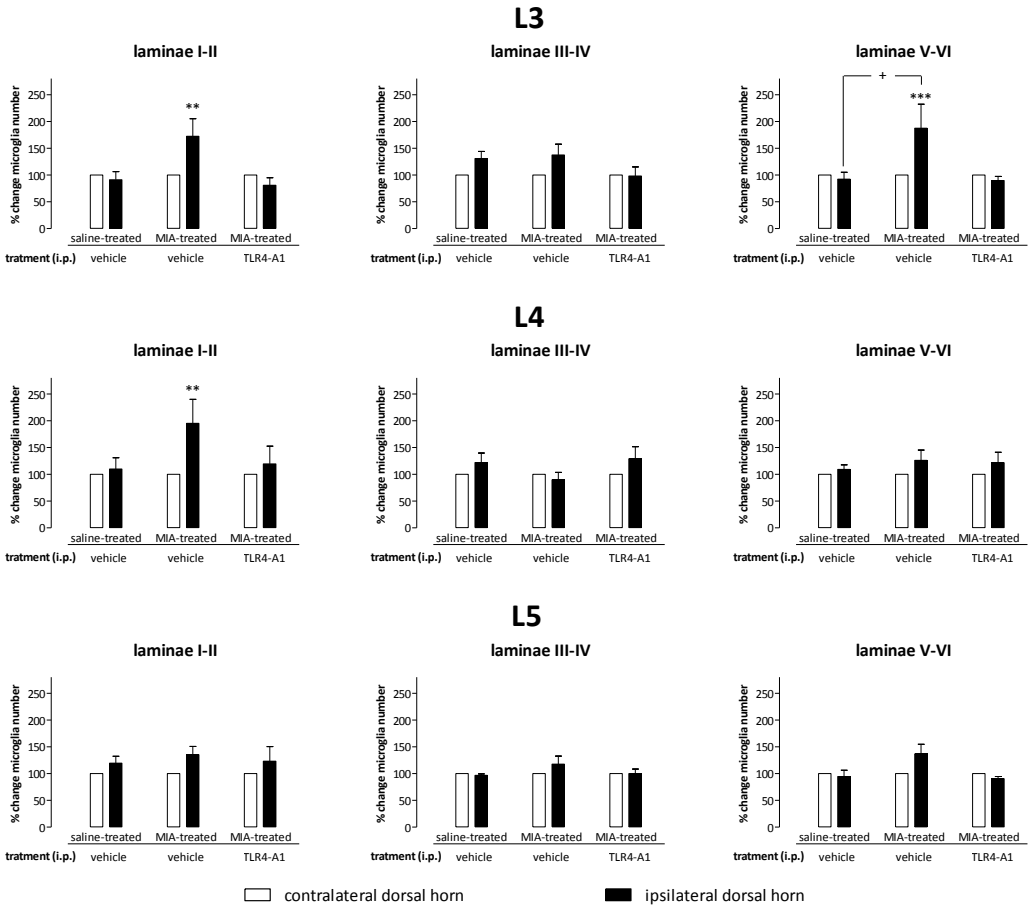

Figure 52. Quantification of microglia activation through laminae I-VI in the dorsal horn of rat lumbar spinal cord after MIA injection. The number of Iba-1–positive microglia was counted in laminae I-VI for each lumbar section and treatment. Data are expressed as mean % ± % S.E.M. of the number of activated microglia in contralateral dorsal horn (100% baseline). * vs. contralateral dorsal horn; + vs. ipsilateral dorsal horn of saline-treated intact group. Two-way ANOVA, Bonferroni post-hoc test. (● $p<0.05$, ●● $p<0.01$, ●●● $p<0.001$). All rats were sacrificed 22 days following MIA-induced osteoarthritis. The results shown are representative of experiments performed using six animals per group (with three sections per lumbar segment for each animal).

2.3.1.2. Astrocyte expression of glial fibrillary acidic protein (GFAP).

Intraarticular injection of MIA also increased the numbers of GFAP postitive activated astrocytes in the ipsilateral spinal cord at day 22; in this case, it was statistically significant for the superficial (I-II; $p<0.01$) and middle (III-IV; 0.001) laminae of L3 sections. Moreover, total astrocyte counting in the overall ipsilateral dorsal horn of L3 sections was increased for MIA-treated animals. On the other hand, GFAP in the ipsilateral dorsal horn of 5-day TLR4-A1-treated rats showed once again a similar pattern to the contralateral dorsal horn (**Fig.53&54**). That is, TLR4-A1 prevented activation of astroglia.

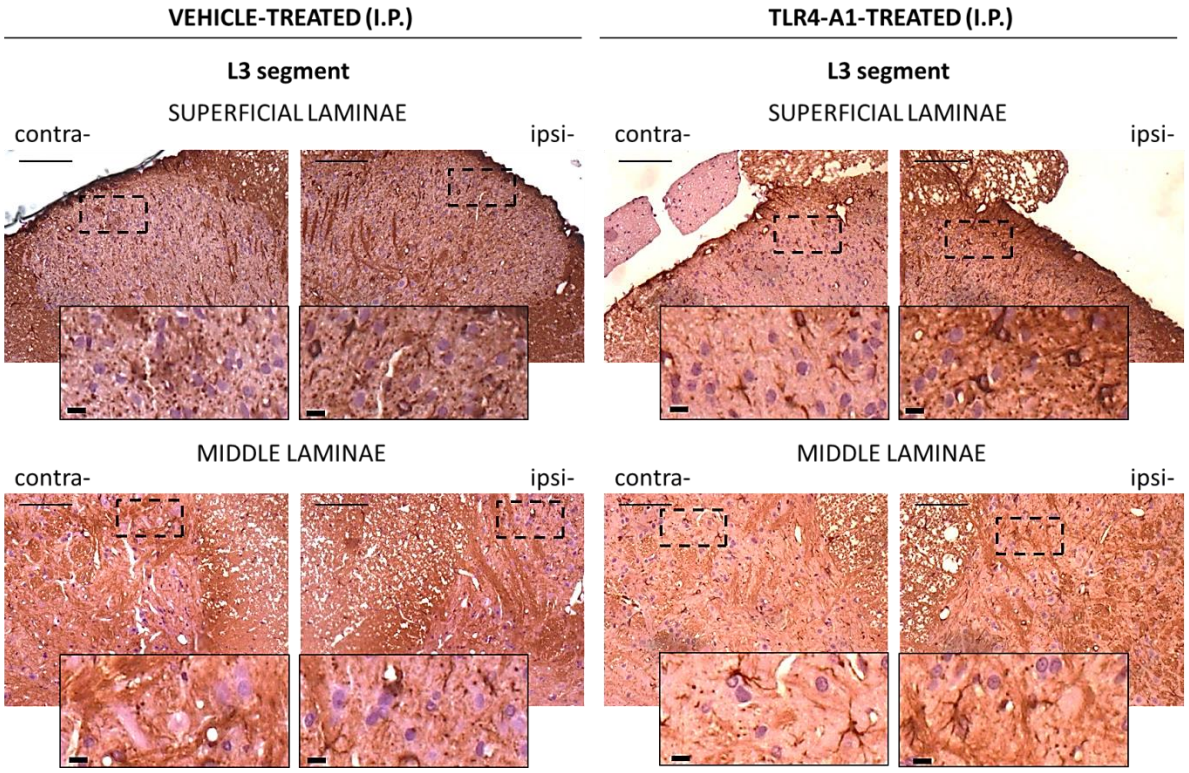

Figure 53. Representative images of astrocyte activation in the contralateral and ipsilateral spinal cord 22 days following unilateral MIA injection. GFAP immunoreactivity in L3 superficial (upper row) and middle laminae (bottom row). The results shown are representative of experiments performed using six animals per group (with three sections per lumbar segment for each animal). Scale bar = 100µm and 10µm in insets.

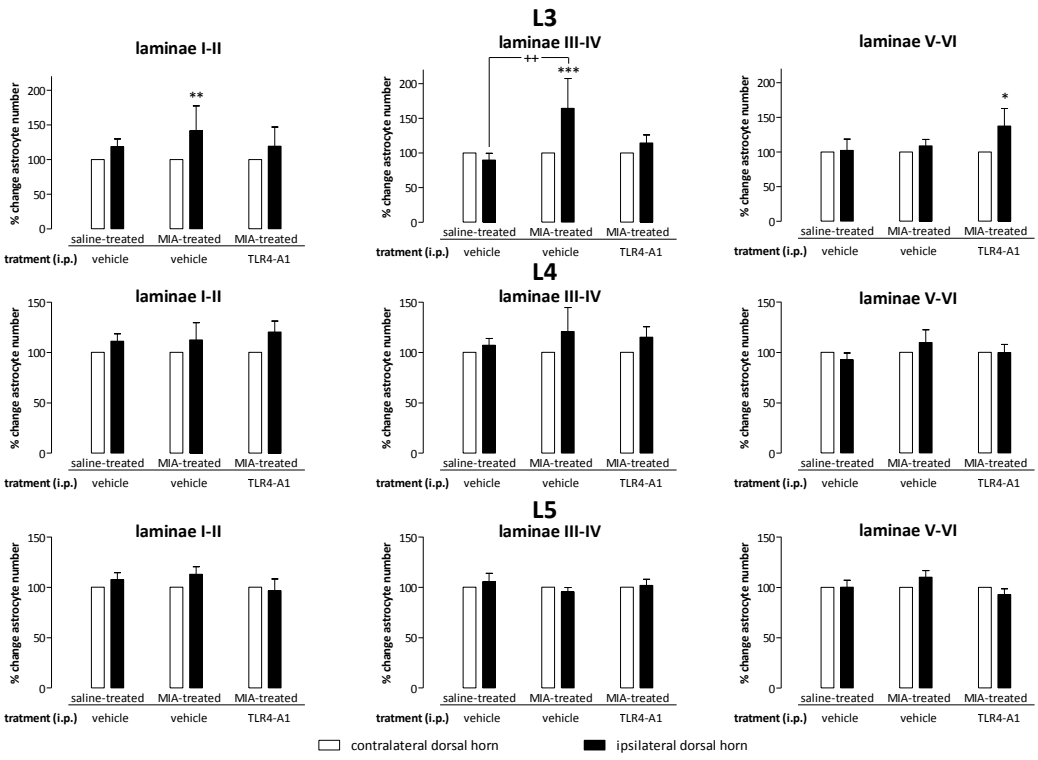

Figure 54. Quantification of astrocyte activation through laminae I-VI in the dorsal horn of rat lumbar spinal cord after MIA injection. The number of GFAP–positive astrocytes was counted in laminae I-VI for each lumbar section and treatment. Data are expressed as mean % ± % S.E.M. of the number of activated astrocytes in

contralateral dorsal horn (100% baseline). * vs. contralateral dorsal horn; + vs. ipsilateral dorsal horn of saline-treated intact group. Two-way ANOVA, Bonferroni post-hoc test. (● p<0.05 , ●● p<0.01, ●●● p<0.001). All rats were sacrificed 22 days following MIA-induced osteoarthritis. The results shown are representative of experiments performed using six animals per group (with three sections per lumbar segment for each animal).

2.3.2. Incisional model of pain.

2.3.2.1. Microglial expression of ionized calcium-binding adapter molecule 1 (Iba1).

Numbers of Iba-1 positive activated microglia in the ipsilateral spinal cord of 9-day saline-treated rats 10 days following surgical incision showed increased immunoreactivity for the superficial (I-II; $p<0.05$) laminae of L3 sections and for the superficial (I-II; $p<0.001$) and middle (III-IV; 0.05) laminae of L4 sections. Moreover, although not statistically significant, total microglia counting in the overall ipsilateral dorsal horn of L3 and L4 sections was increased for incised animals. None of the other treatments showed increased Iba-1 immunolabelling, with the sole exception of TLR4-A1 + morphine treatment, which showed increased Iba-1 positive activated microglia for the superficial (I-II; $p<0.01$) laminae of L3 sections (**Fig.55&56**).

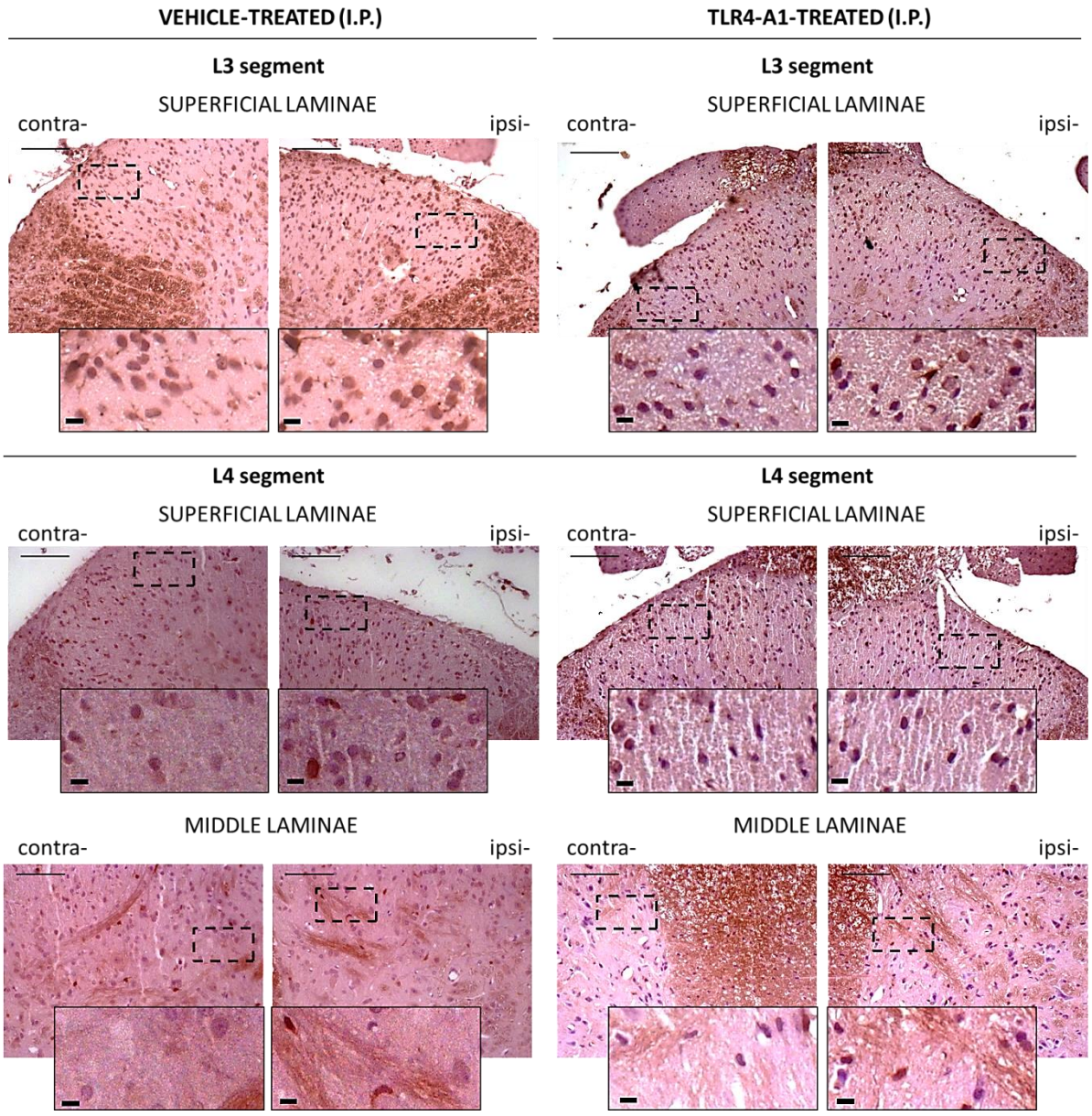

Figure 55. Representative images of microglial activation in the contralateral and ipsilateral dorsal horn of the spinal cord 10 days following unilateral incisional surgery. Iba-1 immunoreactivity in L3 superficial laminae (upper row) and L4 superficial (middle row) and middle laminae (bottom row) The results shown are representative of experiments performed using six animals per group (with three sections per lumbar segment for each animal). Scale bar = 100µm and 10µm in insets.

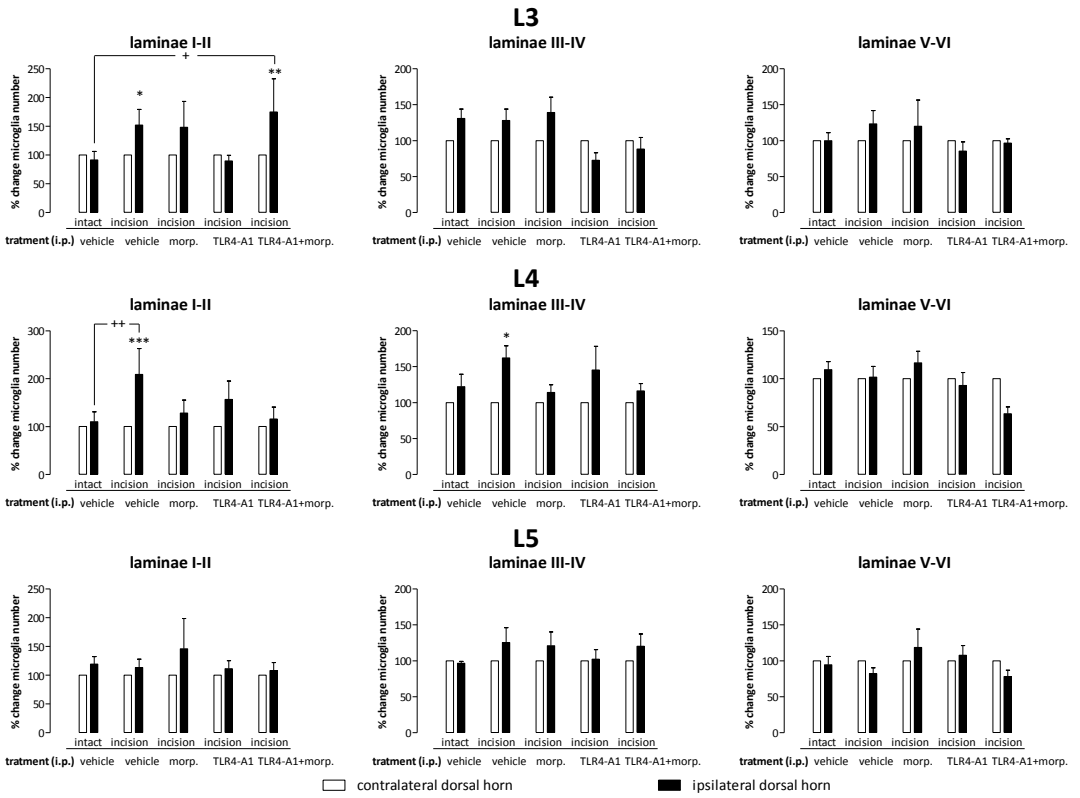

Figure 56. Distribution of Iba-1 binding sites through laminae I-VI of the dorsal horn of rat lumbar spinal cord. The number of Iba-1–positive microglia was counted in laminae I-VI for each lumbar section and treatment. Data are expressed as mean % ± % S.E.M. of the number of activated microglia in contralateral dorsal horn (100% baseline). * vs. contralateral dorsal horn; + vs. ipsilateral dorsal horn of saline-treated intact group. Two-way ANOVA, Bonferroni post-hoc test. (● p<0.05 , ●● p<0.01, ●●● p<0.001). All rats were sacrificed 22 days following MIA-induced osteoarthritis. The results shown are representative of experiments performed using six animals per group (with three sections per lumbar segment for each animal).

2.3.2.2. Astrocyte expression of glial fibrillary acidic protein (GFAP).

In general terms, no statistical significant differences were found between ipsilateral and contralateral sides in any of the groups. However, middle (III-IV) laminae of ipsilateral dorsal horns in L5 sections showed a slight significant increase ($p<0.05$) compared to the contralateral side in morphine-treated animals and, although not statistically significant, total astrocyte counting in the overall ipsilateral dorsal horn of L5 was also increased (**Fig.57&58**).

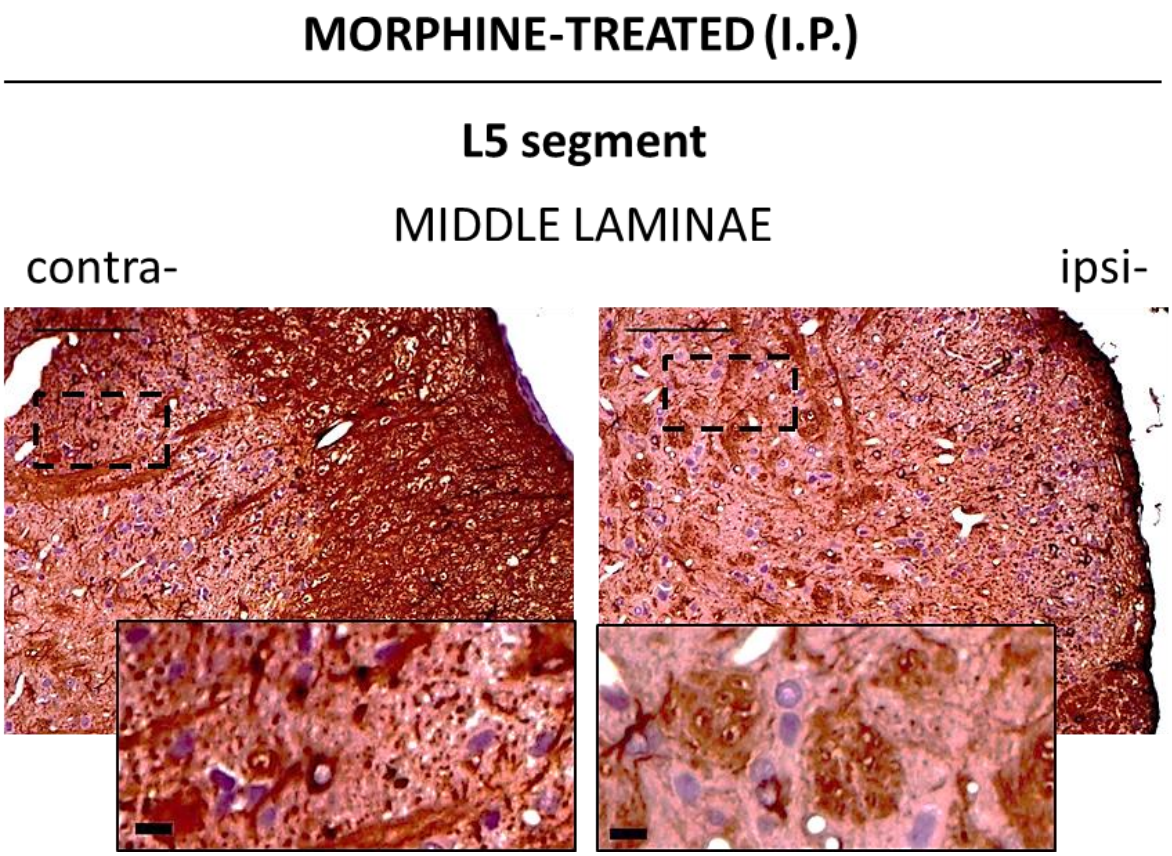

Figure 57. Representative images of astrocyte activation in the contralateral and ipsilateral spinal cord after hind paw incision. Immunohistochemical labeling of L5 middle lamina of morphine-treated rats. The results shown are representative of experiments performed using six animals per group (with three sections per lumbar segment for each animal). Scale bar = 100µm and 10µm in insets.

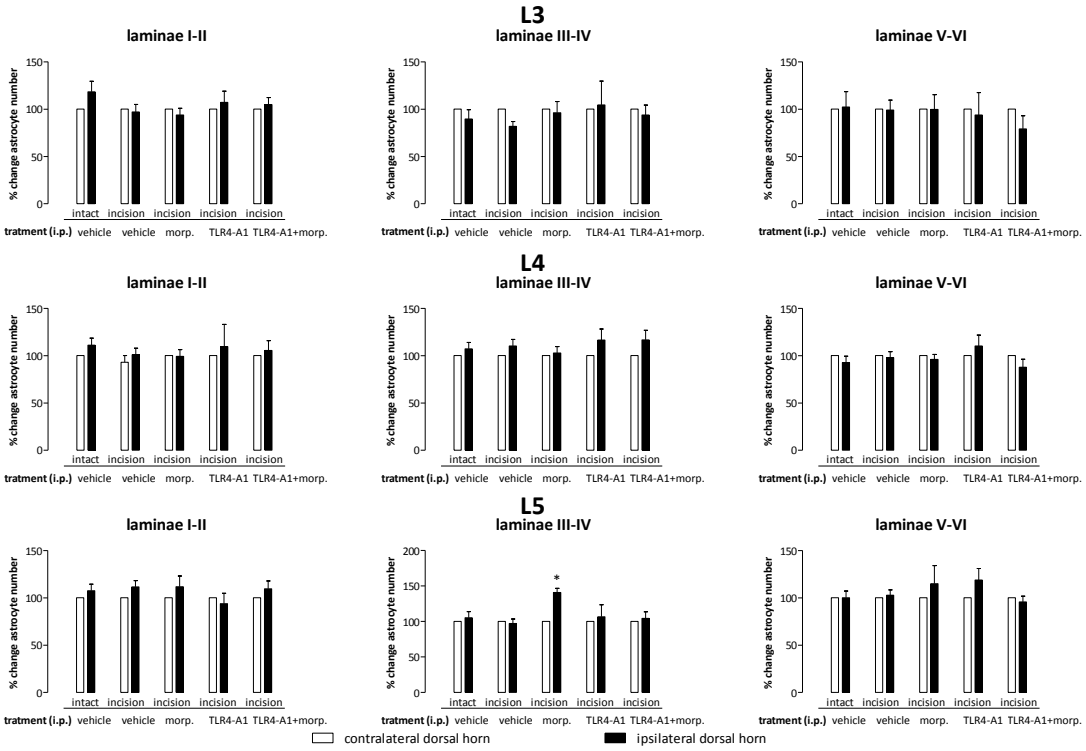

Figure 58. Distribution of GFAP binding sites through laminae I-VI of the dorsal horn of rat lumbar spinal cord. The number of GFAP–positive astrocytes was counted in laminae I-VI for each lumbar section and treatment. Data are expressed as mean % ± % S.E.M. of the number of activated astrocytes in contralateral dorsal horn (100% baseline). * vs. contralateral dorsal horn; + vs. ipsilateral dorsal horn of saline-treated intact group. Two-way ANOVA, Bonferroni post-hoc test. (● p<0.05 , ●● p<0.01, ●●● p<0.001). All rats were sacrificed 22 days following MIA-induced osteoarthritis. The results shown are representative of experiments performed using six animals per group (with three sections per lumbar segment for each animal).

2.4. Enzyme-Linked ImmunoSorbent Assay (ELISA).

2.4.1. Osteoarthritic model of pain.

The effects of long-lasting osteoarthritic pain on spinal tumor necrosis factor-α (TNF-α) levels were studied 22 and 50 days following MIA-induced knee osteoarthritis. No statistical significant differences were observed in the lumbar spinal cord when compared to normal healthy animals. No significant differences were either seen in the 5-day TLR4-A1 (10 $mg \cdot kg^{-1} \cdot day^{-1}$) group. However, MIA-treated group displayed the lowest TNF-α levels among all the three groups analysed (**Fig.59**).

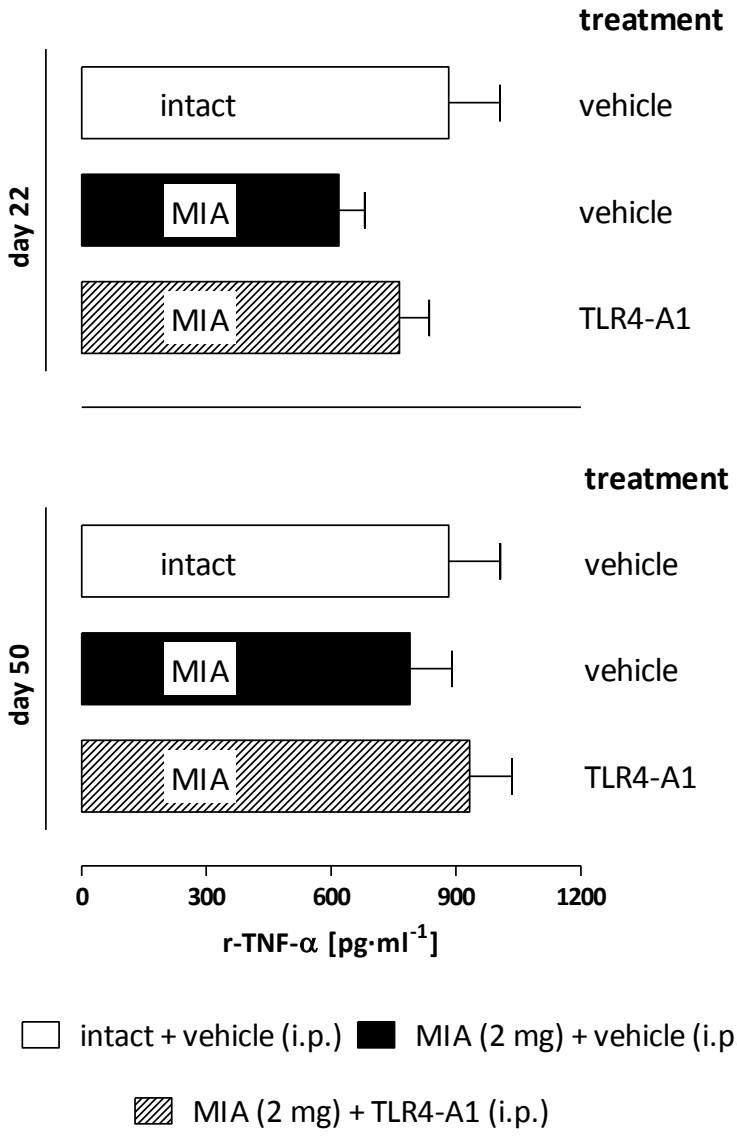

Figure 59. Comparison of TNF-α cytokine levels at the spinal cord among control, MIA-treated and MIA-treated + 5-day TLR4-A1 treatment groups. Control healthy animals first and MIA-treated animals next were taken as controls for comparison with the remaining group (receiving 5-day TLR4-A1 treatment right at the onset of the pathology). TNF-α levels of each experimental group were also compared on two different days (22 and 50 post-saline or –MIA injection). No statistical significant differences were seen among groups. Significance was determined using a Multiple Comparison Newman-Keuls post hoc test following a one-way ANOVA. For all groups an homogenate of lumbar 2 (L2) to 6 (L6) spinal cord sections was loaded (n = 6 rats per group).

2.4.2. Incisional model of pain.

The effects of acute postoperative pain arising from an incisional procedure on spinal TNF-α and on the early proinflammatory cytokines interleukin-6 (IL-6) and interleukin-1b (IL-1b) levels were analysed at an earlier stage (day 4 and day 10) (**Fig.60**). All experimental groups presented similar levels of each proinflammatory protein by day 4.

On day 10, only IL-6 levels displayed statistical significant differences in all groups when compared to healthy control (intact). Besides, IL-6 levels of morphine- and TLR4-A1-treated groups were even significantly higher than those of the incisional group. All groups except intact control displayed higher IL-6 levels on day 10 vs. day 4.

On the other hand, even though not statistically significant, IL-1b levels were also higher on day 10. No clear difference was observed among the experimental groups though.

As regards TNF-α, levels remained stable for all groups by day 4. However, all incised groups experienced a decrease by day 10, especially visible in the treated groups (morphine, TLR4-A1 and TLR4-A1 + morphine). Error bars might certainly have impeded significant levels between both days analysed.

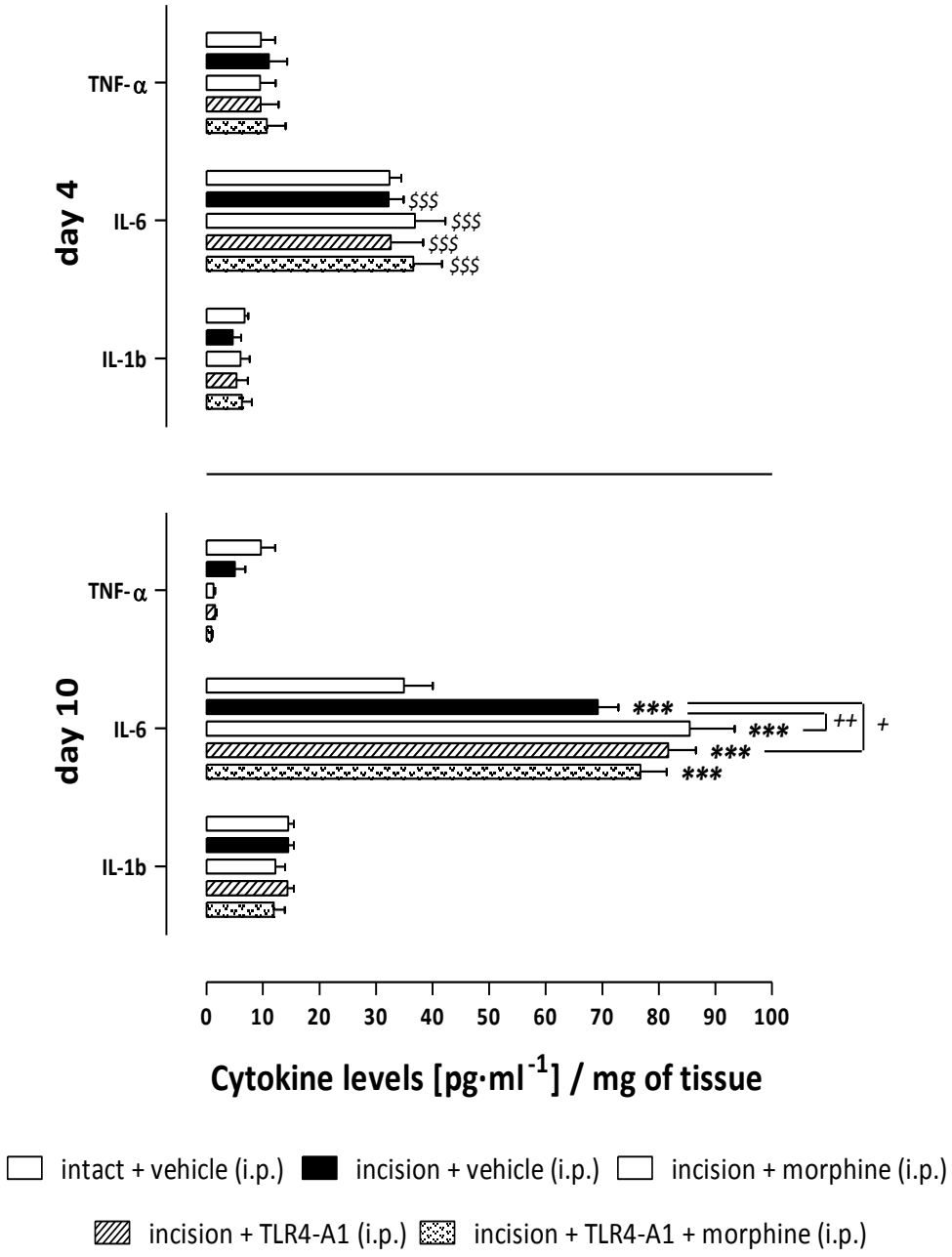

Figure 60. – Comparison of IL-1b, IL-6 and TNF-α cytokine levels at the spinal cord among different treatment groups. Control healthy animals first and incised animals next were taken as controls for comparison with the remaining treated groups. Cytokine levels of each experimental group were also compared on two different days (4 and 10 post-incisional surgery). Only day-10 IL-6 levels displayed statistical significant differences in all groups when compared to healthy controls. IL-6 levels of morphine- and TLR4-A1-treated groups were significantly higher than those of the incisional group. All groups except intact control displayed higher IL-6 levels on day 10 vs. day 4. And even though not statistically significant, IL-1b levels were also higher on day 10. ***P<0.001 vs. negative control (intact) group (significance was determined using a Bonferroni post hoc test following a two-way ANOVA); $^{+}$P<0.05 and $^{++}$P<0.01 vs. positive control (incision) group (significance was determined using a Bonferroni post hoc test following a two-way ANOVA); $^{\$\$\$}$P<0.001 represent comparison of cytokines levels on day 4 vs. day 10 (Multiple Comparison Newman-Keuls post hoc test following a one-way ANOVA). For all groups an homogenate of lumbar 2 (L2) to 6 (L6) spinal cord sections was loaded (n = 6 rats per group).

V. DISCUSSION

General discussion.

In the past decade several studies have reported that glial cells in the spinal cord are critically involved in the development and maintenance of chronic pain and Toll-like receptor 4 (TLR4) has postulated its candidature as a pivotal element in this connection (Bettoni *et al*., 2008; Milligan and Watkins, 2009). Binding of endogenous ligands to TLR4 activates these cells, which start to produce and release a variety of substances (e.g. prostaglandins, excitatory aminoacids, growing factors and proinflammatory cytokines) that enhance pain by increasing the excitability of nearby neurons (Tanga *et al*., 2005; Sauer *et al*., 2014). In this regard, we endeavour to study and compare the physiological changes that may occur at peripheral and spinal levels in two different models of pain in experimental animals: one capable of generating mixed pain (neuropathic and nociceptive) and one in principle only nociceptive.

A classic model of mixed pain in rat on the generation of an osteoarthritic disease state was chosen for inducing high reproducible behavioural changes. In order to assess the reliability of a synthetic TLR4 blocker (TLR4-A1) in unmasking presumable TLR4-mediated nociceptive signalling pathways, three different administration protocols were followed: (1) intraperitoneally or (2) intrathecally, during the first five days immediately after inducing the pathology; and (3) intraperitoneally, after the pathology was fully developed. This part represents a continuation of a previous work carried out in our laboratory on the analgesic action of two different TLR4 blocking compounds (TAK-242 or CLI-095 and TLR4-A1) in a model of neuropathic pain induced by a chemotherapeutic agent (Goicoechea *et al*., 2011; Pascual *et al.*, 2011; Rincón Carvajal *et al*., 2011). As previously described, TLR4 may participate in the development of behavioural hypersensitivity and the hystopathologic characteristics of the joint disease in an animal model of iodoacetate-induced osteoarthritic pain. Since spinal glial cells have been reported to contribute to this chronic pain behaviour (Sagar *et al*., 2011), our purpose consisted first to determine the degree of involvement of TLR4 receptor in this hypersensitivity, and second to distinguish TLR4–peripheral from –central mediated nociception through the integrative study of the many physiological and histological changes occurring at different locations (peripheral nerve and spinal cord).

A second objective was to analyse the involvement of TLR4 receptors in transitory postoperative nociception in a typical model of nociceptive pain that courses with allodynia and hyperalgesia. In

this case, besides the acute analgesic effect of a TLR4 blocker, time recovery after repeated administrations was also assessed. The aim was basically addressed to determine the contribution of TLR4 receptors in short-term nociception. The effect of repeated daily morphine on time recovery after surgery and the phenomena of tolerance and opioid induced hypersensitivity were also studied. Repeated morphine administration has been reported to potentiate the duration of allodynia in peripheral inflammatory and neuropathic pain models and activate spinal glia (Loram *et al*., 2012), and in this respect we aimed to look into what happens in a postsurgical model of pain. Physiological and histological changes occurring at different locations (peripheral nerve and spinal cord) were also assessed.

1. A model of osteoarthritic knee pain chemically induced with monosodium iodoacetate.

a) Comprehension of the "chronic pain state" and its mechanisms in the rat osteoarthritic model.

During the growth process, mammalian epiphyses produce and incorporate new cartilage matrix to the end of the long bones, whereas it is reabsorbed and ossified nearby their diaphyses. That is, ossification and cartilage depletion in bones such as tibia and femur advances from the medial zone of their diaphyses towards their epiphyses. Once the epiphyses have replaced their entire cartilage matrix with bone, growth stops (Geneser, 2000). In humans, such growth process starts on the second trimester of gestation and ends up when the adult state is fully accomplished, around the twenties (García Poblete *et al*., 2006). However in rats at this same equivalent age we use, the potential for long bone growth still exists (Poole *et al*., 2010). In fact, the growth plates in adult rodents remain open despite sexual maturity age is achieved (Aigner *et al*., 2010). This is probably the reason why we observe a raising tendency that stabilises in a plateau after induction of osteoarthritis when assessing the nociceptive behaviour of the animals. We suspect that a remodelling of the joint might be happening possibly due to the chondrocytes arising from the cordons in the mineralised bone. In fact, the histological sections of knees collected 22 days after MIA injection showed cartilage-bone unit remodelling with occasional new cartilage synthesis near the articular surface (Fig.16). Therefore, despite the good approach to the human OA disease the MIA model might represent, as long suggested, an optimal

rodent model system for human OA may be rather impossible to achieve. At least not if expecting long-term assessment.

All that said, the intra-articular injection of MIA creates an acute model for the study of cartilage degradation and joint pain. Since OA is an active process resulting in the breakdown of the balance between cartilage formation and destruction, taking a leaf out of growth plates in rodents can be useful to understand how to fight imbalance of the articular cartilage metabolism in human OA. In this connection, histomorphometric measurements of cartilage and bone changes herein were, to the extent possible, assessed and scored according to the procedures established by the OARSI in order to achieve better standardisation of the assessment of structural change.

As previously reported (Ferreira-Gomes *et al*., 2008; Procházková *et al*., 2009), 2 mg intraarticular MIA injection into the knee joint resulted in decreased nociceptive thresholds as compared to the contralateral paw after both, acute mechanical stimulation of the knee joint (knee-bend test) and tactile or heat stimulation of the plantar aspect of the hind paw (von Fey and Hargreaves' test respectively). However, this reduction was more pronounced for the knee-bend and von Frey test (greater statistical significant differences) than for the paw-flick (Hargreaves') test. Actually, it is considered an established fact that following a peripheral injury, there is an increased responsiveness to a normally innocuous mechanical stimulus in the uninjured tissue surrounding the site of injury, but no change in the threshold to thermal stimuli (Cousins *et al*., 2008; Kam and Power, 2008). Additionally, an imbalance in weight bearing in favour of the not MIA-treated paw was also plausible (Catwalk test), making obvious the existence of spontaneous nociception. These changes are believed to be the result of processes that occur in the dorsal horn of the spinal cord following injury, the watchword of central sensitisation.

Subsequently, an analysis of the gross appearance of the articular cartilage surfaces was performed in order to correlate MIA-induced joint pain with structural alteration in the knee joint components. Macroscopic evaluation of the knee joints showed extensive damage of the tibial and femoral cartilage surfaces in the MIA-treated knees, in the form of profuse degeneration and fibrosis, which in effect seemed to correlate with what observed in the behavioural tests. Based on the principle that when only a part of a section is scored

does not truly represent the entire section and when analysing an overview much detail is lost, the tibial plateau was submitted to further histologic analyses under the microscope and divided into three zones for precise examination. Once again, as previously reported (Ferreira-Gomes *et al*., 2008), histology of the knee was in accordance to what assessed with behavioural tests, showing profuse degeneration and completely loss of the cartilage matrix all along the articular surface (from the outer lateral part to the inner medial part).

Peripheral sensitisation is characterised by the interplay between peripheral nociceptors and inflammation, and may initiate typical osteoarthritic joint pain via central sensitisation. Correlation of behavioural testing with quantitative peripheral neurophysiological parameters may provide objective and further information on the pathophysiological processes of pain generation. There is a very limited number of studies on changes in the morphological composition of peripheral nerves in rats, perhaps on account of the relative ease of electrophysiological studies compared to histological. As previously described in the literature, the saphenous nerve, known to innervate the knee structure, is a purely sensory nerve (Porr *et al.*, 2013; Tassone and Raghavendra, 2015). The questions of whether A- or C-fibres, and whether injured or uninjured fibres, are more important for the generation of spontaneous pain, still remain unanswered. In the study carried out herein, thick myelinated sensory nerve fibres (low-threshold tactile sensitive and proprioceptive) and thinly myelinated (thermoreceptive) were evaluated. Unmyelinated C-fibres remained unstudied. Peripheral axons are not quiescent structures. Their morphology (and also physiological functions) is subjected to the myelinating Schwann cells that wrap them around. Schwann cells seem to determine the packing density of axonal neurofilaments and hence the axonal caliber. Myelination locally enlarges the axonal caliber whereas hypomyelination of the axons results in a reduction of axonal diameter. Additionally, increased neurofilament density (low axonal caliber) has been seen in certain cases of neuropathies (Cole *et al*., 1994). Bearing this in mind, under normal conditions the saphenous nerve consists of a single bundle (fascicle) of afferent nerve fibres. Inside this fascicle, every single nerve fibre (myelinated or not) is surrounded by a loose connective supporting tissue named endoneurium. In turn, the fascicle is surrounded by a collagen layer coated by epithelial cells, that is, the perineurium. In the nerve sections corresponding to MIA-injected knees, the percentage of endoneurium area showed no

apparent differences compared to its contralateral, however an extensive oedema in the sub-perineurial space and increased presence of mast cells were clearly evident. The most feasible explanation is that inflammatory conditions confer a disruption of the perineurial and/or endoneurial capillary barriers (Antonijevic *et al*., 1995), what would allow immune cells to assidously patrol the endoneurium. Nerve fibre diameters and myelin sheath thickness were reduced, whereas axonal diameters increased compared to the control contralateral nerve. The ratio of the axon diameter to the total fibre diameter (G ratio) was also calculated and showed increased values. This means the overall myelinated nerve fibre size was reduced (hypomielinated), coursing with axoplasmic swelling that resulted in an inflammatory milieu –as inferred from the numerous mast cells observed herein–.

Peroxidase-positive microglia or astrocytes were assayed using a combination of diaminobenzidine (DAB) histochemistry and immunolabeling for the microglia-specific marker Iba-1 or for the astrocyte-specific marker GFAP as corresponding. Increased labelling of Iba-1, indicative of microglial activation, was observed at day 22 in MIA-treated rats. Iba-1 immunolabelling was significantly increased in superficial and deeper laminae of the ipsilateral dorsal horn in lumbar section L3 and in superficial laminae of the ipsilateral dorsal horn in lumbar section L4 of MIA-treated rats, compared to the contralateral dorsal horn. Numbers of GFAP positive activated astrocytes were also significantly increased in the superficial and middle laminae of the ipsilateral dorsal horn in lumbar section L3 of MIA-treated rats, compared to the contralateral dorsal horn. Superficial laminae in the dorsal horn are thought to receive inputs from thinly myelinated (Aδ) and unmyelinated (C) fibres of thermoreceptors and nociceptors (mechanosensitive nociceptors), whilst deeper laminae receive their input from heavily myelinated (A) fibres known as low-threshold mechanosensitive afferents (tactile receptors that signal vibration, touch and pressure) (Lu, 2008; Watson *et al*., 2012). Therefore, increased Iba-1 and GFAP-labelling of superficial laminae is consistent with the marked nociceptive behaviour seen for the paw flick test, whilst increased Iba-1-labelling in deeper laminae is consistent with the more marked nociceptive behaviour seen for von Frey and Knee-bend tests. Microglial activation is considered the first stage of CNS inflammation. The absence of increased GFAP-labelling in deeper laminae might attend to earlier activation of Iba-1. Activation in lumbar section L5 remained unaltered for both types of glial cells, compared to the contralateral spinal cord

and the ipsilateral spinal cord of saline-treated rats. This may be due to the fact that the femoral nerve, which receives the articular branch of the saphenous nerve at the knee joint, triggers L3 and L4 spinal sections but not L5, which is a domain exclusively of the sciatic nerve. Therefore, at this point, the reproducibility of the model was considered proven in our facilities.

b) *Study on the role of TLR4 in the rat osteoarthritic model.*

The analgesic effect of acute TLR4-A1 administration occurred within 30 minutes, with maximum effect between 30 minutes and 1 hour and duration up to 60 minutes – 1 hour 30 minutes, as elicited by acute stimulation tests. However the effects seemed to carry on when no stimulus was applied (Catwalk test). This can be explained as follows. Neuropathic pain is characterised by spontaneous pain, allodynia and hyperalgesia, with a crucial role for inflammatory mediators in afferent sensitisation (Djouhri *et al*., 2006). The chemical structure of the TLR4-A1 compound, which presents a quaternary ammonium cation, presumably impedes the drug to pass across the blood brain barrier. However, a small portion might succeed in crossing from the periphery into the central nervous system; hence the first effects to fade away correspond to those opposing the stimuli applied at a remote site from the source of injury (von Frey test). The vast majority of the TLR4-A1 molecules might remain in the periphery; hence the next effects to disappear match those opposing stimuli applied at or immediately adjacent to the site of injury (knee-bend test). Deletion of spontaneous pain is the last effect to cease. This makes particular sense for two reasons: first, the absence of external stimulation; and second, being an amphiphilic compound, TLR4-A1 is prone to aggregate, existing thus the probability of a small residual effect as the aggregates dissolve.

Repeated administration of TLR4-A1 did not result in tolerance, as inferred from the results obtained from acute stimulation tests: the acute effect, assessed daily 1 hour following intraperitoneal administration over the course of 15 days, showed similar analgesia for every tested day. However, with the exception of the first day, TLR4-A1 seemed not to have any effect on spontaneous nociception at any day.

A 5-day intraperitoneal administration of TLR4-A1 compound starting soon after intra-articular injection of MIA showed a two-fold analgesic profile. During an early phase (first

two weeks) allodynia was completely counteracted; however during a second phase (next two weeks) there was a trend to the results obtained for MIA animals under no pharmacological treatment. This might be explained as follows: during the first two weeks, TLR4-A1 repetitively administered during nearly one week blocks the pull effect for immune cells that would have caused a rapid sensitisation of the afferent nerve fibres. However, the damage (chondrocytes death) is evident. When TLR4-A1 presence ceases, the reparation of the tissue progressively resumes, sensitising the peripheral nerve. No difference is observed compared to the control contralateral paw when stimulating with a heat beam. As stated before, the existence of increased responsiveness to a non noxious mechanical (tactile) stimulus but absence of response to thermal stimuli in a remote zone from the site of injury indicates the existence of central sensitisation. Since only pre-existing heat hyperalgesia is completely blocked, this TLR4-A1 treatment seems therefore to be blocking the nociceptive but not the neuropathic component of pain. This is consistent with the aforementioned hypothesis suggesting the predominance of a peripheral role when systemically administered. TLR4-A1 effect was also sustained during the 15 days of treatment when both the knee joint and a remote area were stimulated, although analgesia was more marked for the former. Additionally, this pharmacological protocol seemed not to have effect on spontaneous nociception. The presence of spontaneous nociception together with scarce anti-allodynic effects when a remote site to the wound was stimulated underscored the peripheral (but not central) effect that systemic administration had. This was further corroborated with the results obtained from intrathecal administration: a 5-day intrathecal administration of TLR4-A1 compound starting soon after intra-articular injection of MIA confined the drug to the central nervous system. The drug could not cope with the massive inflammatory pull effect generating at the periphery, therefore, during the first week allodynia was increased. However, as time went by, no central sensitisation was observed, as elicited from the absence of distal allodynia following the first week. On the contrary, nociception was evident throughout the three weeks as elicited from thermal hyperalgesia. In this case, the neuropathic but not the nociceptive component of pain seemed to be blocked. We can state that our assumptions on that TLR4-A1 molecule would practically not cross the blood brain barrier seem to be proven at this moment.

Macroscopic examination of the knee joints showed TLR4-A1 protected somehow from extensive damage. Even though the structures of the ipsilateral paws and their contralateral were notably different at a first glance, the state seemed not to be as bad as appreciated with the rats not receiving TLR4-A1. The scarce presence of osteocytes on the femoral condyles and white opaque appearance of the tibial plateaus made us thought that MIA was exerting its apoptosis-induced action, but no massive inflammatory response was attracted to the damage tissue as no vast degree of fibrosis was seen. Indeed, when examining the knee stained sections under the microscope, erosion of the cartilage together with new cells filling and proliferating in the fissures of the cartilage matrix were seen, however no uncontrolled pannus formation outside the articular surface (synovitis) was appreciated. This more organised proliferation of cells in TLR4-A1-treated rats might be explained by its peripheral action during the five days it was promptly systemically administered.

Similar to the nerve sections corresponding to MIA-injected knees of saline-treated animals, the percentage of endoneurium area in 5-day TLR4-A1 treated animals showed no apparent differences compared to its contralateral, and an extensive oedema was also evident in the sub-perineurial space. However, no increased presence of mast cells was observed. The diameters of myelinated nerve fibres, their corresponding axons and the myelin sheath thickness remained unvaried as compared to the contralateral nerve. Same for the G ratio. That is, early TLR4-A1 administration somehow protected the nerve from axonal or myelin impairment, what just matched the absence of glial activation in the ipsilateral dorsal horn. This was also in accordance with what provided by the behavioural tests: lack of heat hyperalgesia and only late tactile allodynia when a remote site from the knee joint was stimulated.

As a final remark, TNF-α level in spinal cord sections corresponding to L2-L6 was also examined and as expected, no significant differences in the protein expression of this cytokine were observed for any of the groups at the studied days (22 and 50).

2. A model of postoperative pain surgically induced by an incision on the plantar aspect of the paw.

The postoperative pain model that has been used herein was first developed by Brennan and colls. two decades ago. The model has been repeatedly used over the years by different groups varying it with slight modifications. Tactile stimulation at a 1 cm-remote site from the wound (area of secondary hyperalgesia) led to differences (compared to the control group) that extended until day 9 for the von Frey test and until day 3-4 for the paw-flick test. This presumable peripheral sensitisation may contribute to pain hypersensitivity and inflammation. However, analyses of peripheral nerve fibres rarely showed a macrophage ambulating in the endoneurium in both contralateral and incised paws, and when so, they were considered as normal patrolling immune cells present in every healthy tissue. Since the gross appearance of the nerves can address us to wrong conclusions, a series of parameters were analysed to be more objective. The diameter of myelinated nerve fibres and their corresponding axons, the myelin sheath thickness and the G-ratio did not vary much among the different groups. That is, the incision on the plantar aspect of the hind paw resulted after ten days in no measurable changes of the nerve.

Regarding the analyses in search of activated microglia in the spinal dorsal horns, significantly increased labeling of Iba-1 was observed at day 10 in lumbar section L3 superficial laminae and L4 superficial and middle laminae of the ipsilateral dorsal horn from vehicle-treated incised rats (compared to the contralateral dorsal horn). On the contrary, no significant changes were observed for GFAP immunolabelling. Astrocytes contribute to maintain chronic pain and the absence of activation by day 10 would be consistent with the acute condition of the pain model. The substantial increased activation for microglia only in superficial laminae is suggestive of nociceptive pain. This is consistent with the findings carried out by a different group (Romero-Sandoval et al., 2008), stating that enhanced expression of the microglial marker Iba1 and the astrocytic marker GFAP in the dorsal horn of the lumbar spinal cord is associated with behavioural allodynia following paw incision surgery. However, as they mentioned, following resolution of behavioural hypersensitivity Iba1 and GFAP expression returned to baseline expression levels, so that significant increase expression of Iba1 and GFAP could be evident in the whole dorsal horn, or solely in the superficial or deeper laminae depending upon the time after paw incision surgery.

IL-6 level in an homogenate of spinal cord section L2-L6 was markedly increased on postoperative day 10 as compared to postoperative day 4 and to the healthy control group. Any other cytokine (TNF-α or IL-1β) showed similar levels to control group, slightly reduced though on postoperative day 10 for TNF-α. High levels of IL-6 have been reported in some chronic inflammatory conditions, especially related to the inflammatory process following nerve injury, and the initiation and maintenance of neuropathic pain (Starkweather, 2010). Elevated IL-6 activity has been likewise associated to the increased production of NGF in astrocytes, as also found in some neuropathies (Vargas *et al*., 2004).

a) *Study on the role of TLR4 in the rat postoperative model.*

Following the same test scheduling system on the mid-plantar surface of the hind paw as mentioned above, the effect of chronic, systemic TLR4-A1 treatment caused the dissipation of any significant tactile allodynic sign from the fifth day onwards, five days earlier than it did without treatment (vehicle group). Besides, heat hyperalgesia disappeared after the first administration, two or three days earlier than it did in the untreated group. On the other hand, acute effect of TLR4-A1, that is, responses assessed soon after daily systemic administration, proved to be analgesic. Only two intermittent days (4 and 5) showed significantly decreased withdrawal thresholds compared to baseline, whereas the rest of the days practically overlapped the data obtained for the intact paw. As for the paw-flick test, an anti-hyperalgesic effect was observed for most of the days. This could suggest an anti-inflammatory effect for TLR4-A1 in the periphery, as inflammatory pain models are characterised by decreased latency thresholds (Ren and Dubner, 1999; Huang *et al.*, 2006). However, the other component, tactile stimulation was only partially blocked, suggesting that surgical pain is different from strict inflammatory pain, but also from neuropathic pain.

Peripheral nerves did not look at a first glance very different from those of the untreated group. Myelinated nerve fibre and axonal diameters, myelin sheat thickness and G-ratio remained practically invariant compared to the contralateral nerve. That is, TLR4-A1 seemed to have a protective effect.

In regards to the immunohistological labelling for glial activation, no statistical significant differences were observed in the ipsilateral dorsal horn of incised rats, compared to the

contralateral side. The cytokine profile was similar to that from the untreated animals undergoing incision of their hind paws.

b) *Comprehension of the mechanisms underlying the transition from an acute to a sub-chronic pain state after repeated administration of systemic morphine.*

Opiates are thought to activate pain inhibitory and facilitative systems, and the predominance of one over the other would lead to anti- or pro-nociceptive mechanisms (Freye, 2010). There is major interest in development approaches driven to use concomitant administration of drugs with opioids (e.g. NMDA-antagonist, NSAID, α-2-agonist) or opioid rotation, so that the patient can enjoy the beneficial (analgesic) effects of opioids preventing OIH (Herrera *et al*., 2009). However there are not full effective strategies to avoid OIH at the present date (Horvath RJ, Romero-Sandoval EA, De Leo JA., 2010). The use of minutely detailed opioid-induced hyperalgesia protocols (attending to acute or chronic exposure, high or low doses, type of opioid and route of administration) are essential for obtaining observable and measurable responses since even when animal models are employed, OIH may resemble tolerance or be confused with opioid withdrawal. And more importantly, different mechanisms might underlie the phenomenon in each specific circumstance (Low *et al*., 2012).

OIH is normally referred as to opiate high doses but little is said about lower doses. Therefore we took as a reference the dosage given in (Loram *et al*., 2012). We considered 5 $mg \cdot kg^{-1}$ as the limiting dose for producing analgesia without sedation and hence, the boundary between low and high morphine dosage. Morphine was intraperitoneally administered twice daily for nine consecutive days at 12 h and 18 h (Horvath *et al*., 2010). Besides we counted on the knowledge that mice receiving chronic morphine treatment (10 $mg \cdot kg^{-1}$, s.c. twice daily for 4 days) did not develop tolerance in an inflammatory model of pain (Zollner *et al.*, 2008).

As stated before for the two other groups, the withdrawal threshold to von Frey filaments and the withdrawal latency to radiant heat were measured before surgery and then twice daily through postoperative day 9. Chronic effect of morphine in response to tactile stimuli showed no recovery of baseline thresholds and was even far from the results obtained for the incised paw of untreated animals. Similar occurred to withdrawal latencies to radiant

heat, which can particularly be divided into two phases: an early phase with latencies overlapping those from untreated animals, and a second phase where all groups leave the morphine treated animals far behind, which achieves no recovery. Exactly in the same manner as what just reported, no recovery was appreciated when stimuli were applied immediately adjacent to the incision. Repeated morphine visibly slowed down normal time recovery.

On the other hand, acute effect of morphine was preserved. Sustained antiallodynic effects were observed all along the nine days, overlapping with healthy control thresholds throughout the whole course of the experiment. Analgesia (that is, latencies over the baseline) was also evident and maintained at all time points. We can conclude therefore that no tolerance to morphine administration was developed, and hampered recovery might correspond to physical dependence or opioid induced hypersensitivity.

The analysis of the nerve sections showed similar values for the fibre and axonal diameter of myelinated nerve fibres, as well as for the myelin sheath thickness and G-ratio. That is, morphine did not visibly affect to the paw. A previous study (Horvath *et al*., 2010) reported that no changes in Iba1 or GFAP expression are observed in the spinal dorsal horn between groups when morphine is chronically given. In the same line, we observed no statistical significant differences in the ipsilateral dorsal horn of incised rats, compared to its corresponding contralateral side. Once again, the cytokine profile was similar to that from the untreated animals undergoing incision of their hind paws.

c) *Study on time recovery when repeated morphine is given with adjuvant administration of TLR4-A1.*

We initiate the discussion of this section bearing in mind the idea that modulation of glia could attenuate neuropathic pain symptoms and enhance morphine effectiveness (Mika, 2008). According to Due and colls. (Due *et al.*, 2012) activation of TLR4/MD2 complex by morphine metabolite M3G is likely responsible for induction of tactile but not thermal nociceptive behaviour. Therefore we used a TLR4 blocker molecule as a coadjuvant of morphine administration in order to compare what we saw with the morphine-treated group previously described. When the TLR4 blocker molecule preceded the administration of morphine, the chronic effect on recovery times closely resembled that of the incised

animals in the untreated group. That is, none of the administered compounds seem to have any effect on the normal recovery time of rats undergoing hind paw surgeries. However when examining the daily acute effect, it did have an acute antiallodynic effect resulting from the synergy between the threshold patterns of TLR4-A1 and morphine treated rats. Acute analgesia in response to heat stimulation was also quite evident and consistent with the synergistic effect of these two agents. Therefore, the combination of the TLR4-A1 blocking compound with morphine resulted in the beneficial (analgesic) effects of morphine without worsening/impeding the average short-term recovery time. That is, it was confirmed that none of the administered compounds seem to have any effect on the normal recovery time of rats undergoing hind paw surgeries when given as a combination of both and, which is more, in clear opposition to Due and colls., morphine-triggered activation of TLR4 seemed to be responsible for induction of both tactile and thermal nociceptive behaviour.

The nerve sections also showed unvariable fibre and axonal diameters in comparison to the contralateral nerve. Myelin sheath thickness and G-ratio also remained unmodified. In regards to glial immunolabelling, we observed no statistical significant differences in the ipsilateral dorsal horn of incised rats, compared to the contralateral spinal cord. As described for the other two treated groups, the cytokine profile was similar to that from the untreated animals undergoing incision of their hind paws.

We can therefore conclude that incision altered IL-6 levels in a similar way in all groups regardless of the treatment given.

CONCLUSIONS

Based on the results derived from the **model of osteoarthritic knee pain chemically induced with monosodium iodoacetate**, we can assert that:

1. TLR4 blockade can prevent the development of OA-induced sensitisation, since TLR4-A1 diminishes heat hyperalgesia when intraperitoneally administered and allodynia when intrathecally administered.

2. In accordance with behavioural results, blocking TLR4 also prevents histological and immunohistochemical alterations related with OA.

From the results obtained in the **model of postoperative pain surgically induced by an incision on the plantar aspect of the paw**, we can sustain that:

1. Peripherally TLR4 blockade diminishes behavioural signs of central and peripheral sensitisation.

2. Morphine administration induced analgesia but does not reduce recovery time.

3. Since morphine and TLR4-A1 co-administration do not induce any summative effect on pain behaviour, opioid and TLR4 receptors do not seem to share common mechanisms of action.

Together, results from both models indicate that TLR4 is an interesting target to develop new analgesic drugs focused to avoid central and peripheral sensitisation.

RESUMEN

1. INTRODUCCIÓN

1.1. Introducción al dolor.

De acuerdo con la definición dada por la Asociación Internacional para el Estudio del Dolor (IASP, de su acrónimo en inglés *International Association for the Study of Pain*), el dolor es una "experiencia sensorial y emocional desagradable, asociada principalmente a daño tisular o descrita en términos de dicho daño" (Merskey 1986). No obstante, la presencia de una sensación desagradable confinada a un área anatómica concreta no es suficiente para categorizarla como dolor, sino que ha de coexistir con componentes cognitivos y emocionales que escapan al ojo del observador. Por tanto, el dolor es una experiencia personal y subjetiva (Melzack and Katz 2001).

En términos generales, el dolor es un mecanismo natural que trabaja en pro del organismo para evitar estímulos que puedan suponer un daño a la integridad del mismo. Este mecanismo de defensa se conoce como dolor agudo o fisiológico y actúa desencadenando los comportamientos que alejan o minimizan el foco de la amenaza (IASP Scientific Program Committee 2014). En resumidas cuentas, un estímulo nocivo, esto es, de alta intensidad térmica, mecánica o química, pone en marcha un sistema que se activa en las terminales sensoriales de las neuronas aferentes primarias en la periferia (los llamados nociceptores o nocirreceptores). Dicho estímulo viaja entonces a lo largo de todo el nervio en forma de impulsos eléctricos hasta el sistema nervioso central (SNC), donde se producen relevos a nivel espinal y supra-espinal (bulbo raquídeo y tálamo). Finalmente, con el último relevo, una matriz de áreas corticales asociadas con las múltiples dimensiones conscientes del dolor es activada. Esta descripción constituye en realidad un complejo proceso modulado por diversos actores y sus dianas en diferentes puntos de las vías sensoriales (Kitahata 1993).

Por su parte, el dolor crónico constituye un grupo de desórdenes del sistema nervioso producido por uno o más mecanismos de señalización celular que funcionan de manera anormal. A este respecto, los cambios de tipo inmunológico (células inmunes) o de tipo electrolítico (pH) que ocurren en un tejido tras una lesión, pueden dar lugar a una sensibilización periférica y al desarrollo de hiperalgesia primaria. De hecho, la inflamación en las terminales nerviosas periféricas puede ejercer un efecto de reclutamiento de nociceptores que se hallaban en un estado silente, o incluso provocar la conversión de

fibras mecánicas no sensoriales en sensoriales. Esto incrementa significativamente la señal nociceptiva que llega a la médula espinal y, en parte, puede explicar el fenómeno de la sensibilización central y del desarrollo de alodinia; esto es, porqué estímulos que en situaciones normales no nos resultan nocivos pueden sentirse como dolorosos (Schaible 2006).

1.2. Fisiopatología del dolor.

MODULACIÓN DEL ESTÍMULO NOCICEPTIVO.

La información procedente de estímulos nocivos originados en la periferia es transferida a centros superiores del cerebro a través de dos vías nociceptivas ascendentes diferentes: el tracto espinotalámico –recibe las señales entrantes de fibras primarias Aδ y C, encargadas de conducir la temperatura y la nocicepción– y el tracto del lemnisco –recibe señales entrantes desde las fibras nerviosas primarias Aα, Aβ y Aδ, encargadas de conducir el tacto y la propiocepción– (Dubuc *et al*. 2013).

Por otra parte, el SNC presenta también vías nociceptivas descendentes, que pueden ser de carácter facilitador o inhibidor. Éstas se diferencian en su anatomía y actividad farmacológica, y probablemente se activen de manera simultánea cuando ocurra un fenómeno nociceptivo de tipo agudo. Las vías descendentes facilitadoras están confinadas a los funículos ventrolaterales mientras que las vías descendentes inhibidoras descienden en los funículos dorsolaterales (Mulak *et al*., 2012). Dichas vías expresan diferentes receptores que son activados de manera específica por distintos tipos de transmisores químicos. La presencia continuada de un estímulo nocivo podría dar lugar a un desequilibrio en la activación entre estas vías moduladoras, resultando en cambios anatómicos y/o bioquímicos a nivel de la médula espinal. Precisamente, se piensa que esta condición subyace en algunos estados de dolor crónico, en los que la sensación dolorosa se ve incrementada al producirse cierto grado de neuroplasticidad en favor de las vías descendentes facilitadoras.

PLASTICIDAD EN EL ASTA DORSAL.

Las fibras nerviosas de las raíces dorsales varían en grosor, lo que representa una función directa de su velocidad de conducción. Estimulaciones eléctricas de baja intensidad

producen solo la activación de las fibras mielínicas de mayor grosor (Aα), y con forme aumenta la intensidad del estímulo, las fibras de menor calibre van siendo también reclutadas de manera progresiva: Aβ, Aδ y C, en este orden (Brodal, 2010b). Por consiguiente, puede deducirse fácilmente que bajo condiciones normales de estimulación, los nociceptores permanecen silentes. Sin embargo, si la intensidad del estímulo es lo suficientemente alta, como ocurre después de una lesión nerviosa o tisular, los nociceptores pueden activarse y, si el estímulo continúa, las fibras Aβ podrían incluso establecer comunicaciones cruzadas con fibras Aδ o C a nivel medular, lo que convertiría señales sensoriales inocuas en señales nocivas (Cui y Fu, 2014). Esto se puede explicar de la manera que se describe a continuación. Las terminaciones centrales de las neuronas sensoriales primarias en mamíferos se encuentran organizadas en planos horizontales (dorsoventrales) en la sustancia gris de la médula espinal, cada uno de los cuales codifica topográficamente un área específica de la superficie del cuerpo (Doubell et al., 1997). Rexed elaboró una clasificación de diez láminas diferentes de acuerdo a la heterogénea distribución de los cuerpos neuronales presentes en la sustancia gris de la médula espinal (Rexed, 1952). Las neuronas aferentes somatosensoriales, capaces de transmitir información nociceptiva, terminan en el asta dorsal de la médula (Brown, 1982), organizado en seis láminas. Las láminas I, II y V albergan sinapsis con neuronas de pequeño y medio calibre, esto es, fibras C y Aδ (conductoras de temperatura y nocicepción). Por el contrario, las fibras de mayor tamaño, Aβ, envían sus proyecciones a las láminas III, IV y VI (relacionadas con el tacto y la propiocepción). Alteraciones en la naturaleza de estas últimas fibras de gran calibre pueden dar lugar por consiguiente a las comunicaciones cruzadas mencionadas anteriormente, lo que permitiría interpretar un suave estímulo táctil como una señal nociceptiva (Cui y Fu, 2014).

INTERACCIONES NEURONA-GLIA Y GLIA-GLIA.

Las interacciones recíprocas entre neurona y glía juegan un papel esencial en garantizar la precisión del procesamiento de la información en el sistema nervioso. A tal efecto, el número de células gliales aumenta de manera directa con forme lo hace la complejidad y eficiencia del sistema nervioso (Edenfeld *et al*., 2005; Austin y Moalem-Taylor, 2010; Eroglu y Barres, 2010). La glía en el SNC puede clasificarse en dos tipos celulares: microglía y macroglía (astrocitos y oligodendrocitos).

Las células gliales participan de manera activa en el mantenimiento de la homeostasis en el SNC, así como en la etiología y progresión del dolor crónico (Scholz y Woolf, 2007). Se ha demostrado en diferentes modelos de dolor neuropático en roedores que lesiones en nervios periféricos inducen una activación glial en la médula espinal (Ito *et al.*, 2009; Sagar *et al*., 2011). El tiempo y duración de la activación microglial y astrocítica varía tras la lesión nerviosa. La microglía parece ser responsable de la iniciación del estado de dolor neuropático, mientras que los astrocitos estarían implicados en el mantenimiento de la condición (Nakagawa y Kaneko, 2010). Ambos tipos celulares presentan al activarse un aumento de la expresión de los genes que codifican para citoquinas (ej.: IL-1β, IL-6, TNF-α, IL-18) y quemocinas (ej.: CCL2, CXC3L1), lo que da lugar a una mayor atracción y activación de células gliales. Bajo este estado de sobreexcitación, las neuronas liberarían también aminoácidos excitadores y quemocinas que estimularían la transmisión nociceptiva, creándose un círculo vicioso que pondría en intercomunicación neuronas, microglía y astroglía en las astas dorsales de la médula espinal (Norimoto *et al*., 2014).

1.3. Receptores de tipo Toll (TLR).

DISTRIBUCIÓN DE LOS RECEPTORES TLR Y SU IMPLICACIÓN EN LA PLASTICIDAD ESPINAL.

Los receptores de tipo toll (TLR) en humanos se distinguen por pertenecer a una superfamilia de proteínas con regiones homólogas al receptor de interleuquina-1 (IL-1R) (Leon *et al*., 2008; McCormack *et al*., 2009). De entre todos los receptores TLR, TLR4 es probablemente el más estudiado al presentar dos características singulares que lo diferencian del resto y lo hacen por ende más atractivo para su estudio: el requerimiento de un correceptor para el reconocimiento del ligando, y la capacidad de señalizar a través de dos sistemas de proteínas adaptadoras diferentes según su localización en la célula (Tanimura *et al*., 2008; Gangloff, 2012).

Los receptores TLR4 juegan un papel clave en el reconocimiento de patrones moleculares asociados a patógenos y de moléculas endógenas producidas tras una lesión (Peri y Calabrese, 2013). Han sido descritos en la superficie de un amplio número de distintos tipos celulares, que incluyen: células inmunes (Gondokaryono *et al.*, 2007; Huang *et al*., 2007), células dendríticas (Takagi, 2011), células gliales (Li *et al*., 2015), el cartílago articular (Meng et al., 2010; Gómez et al., 2014), neuronas (Ohara *et al*., 2013), fibroblastos (Ospelt

et al., 2008), células de Sertoli (Winnall *et al.*, 2011), células endoteliales y células epiteliales (Erridge, 2010). Esta amplia ubicuidad y su evidente papel en la inflamación (Piazza *et al*., 2009; Takashima et al., 2009) han llevado a que, en los últimos años, el receptor TLR4 se esté teniendo especialmente en cuenta como un actor importante en la nocicepción. De hecho, se ha descrito una expresión predominante del receptor en la microglÍa del sistema nervioso central (Olson y Miller, 2004) y en neuronas sensoriales periféricas (Wadachi y Hargreaves, 2006). Además, el empleo de antagonistas de los receptores TLR4 han confirmado un alivio de la hiperalgesia térmica y de la alodinia mecánica en modelos de dolor neuropático en roedores (Bettoni *et al*., 2008).

En condiciones normales, la glía juega un papel clave en mantener la salud y el funcionamiento normal del sistema nervioso. Sin embargo, cuando se produce una condición patológica, tal como las alteraciones producidas en estados de dolor crónico neuropático, la glía se activa y comienza a liberar una variedad de sustancias implicadas en la iniciación y el mantenimiento de dicho dolor (Watkins y Maier, 2003). A este respecto, durante la pasada década se ha ido describiendo progresivamente la implicación de los receptores TLR4 en las interacciones neuroinmunes que tienen lugar a nivel medular en situaciones de dolor neuropático (Bettoni *et al*., 2008; Saito *et al*., 2010). Además, ensayos *knock-out* y *knock-down* para el receptor TLR4 han demostrado una atenuación de la hipersensibilidad, así como un descenso de la activación glial y una disminución de la expresión de citoquinas proinflamatorias (Tanga *et al*., 2005; Lan *et al*., 2010).

HIPERSENSIBILIDAD INDUCIDA POR OPIOIDES.

Los opioides constituyen la segunda prescripción en términos de frecuencia para el tratamiento del dolor crónico, tan solo superados por los AINE (Clark, 2002; Angst and Clark, 2006). Sin embargo, el dolor neuropático se caracteriza por activación incontrolada de células gliales y parece ser resistente al tratamiento con morfina. Ya en el siglo pasado era conocido que, en oposición a su potente efecto analgésico, los opioides podían también inducir efectos secundarios inmunosupresores cursando junto con la pérdida de antinocicepción (West *et al.*, 1997). Este escenario convergente fue explicado tradicionalmente por un mecanismo de tolerancia (de Conno *et al*., 1991; Sjøgren *et al*., 1993; Aley y Levine, 1997). No obstante, con el inicio de este siglo, ha emergido un concepto que ha ido ganando poco a poco terreno como alternativa válida para explicar

esta controversia: el fenómeno de la hipersensibilidad inducida por opioides (OIH, de su acrónimo en inglés *opioid induced hypersensitivity*), también llamada hiperalgesia inducida por opioides (Ocasio *et al*., 2004). A este respecto, el tratamiento agudo y/o crónico con altas dosis de opioides ha demostrado inducir dolor espontáneo, alodinia e hiperalgesia térmica en humanos (Raffa y Pergolizzi, 2013) y roedores (Li *et al*., 2001; Chang *et al.*, 2007). Sin embargo, todavía hoy en día se hace difícil diferenciar entre tolerancia analgésica a la morfina e hiperalgesia inducida por morfina.

1.4. Modelos animales para el estudio del dolor.

A. Dolor artrósico.

De acuerdo con la Asociación Internacional para el Estudio del Dolor (IASP), la artrosis es el desorden articular más común en todo el mundo, afectando aproximadamente al 37% de los ciudadanos de edad avanzada (IASP, 2009). La Sociedad Española de Reumatología (SER) estimó una prevalencia similar del 43% en la población española en general en el año 2000 (Cano Montoro y Cases Gómez, 2002).

La artrosis se define como un desorden degenerativo, de etiología multifactorial, que afecta de manera crónica a toda la diartrosis, dando lugar a la degeneración de los elementos de la articulación con la consecuente restricción de movimientos y dolor (Pomonis *et al.*, 2005; Aigner *et al*., 2010). La rodilla recibe un aporte de nervios desde los nervios cutáneos en la piel superficial, ramas de nervios periféricos que pasan cerca de la articulación (neuronas primarias) y ramas de nervios intramusculares que cruzan la cápsula de la articulación (nervios accesorios). La mayoría de las fibras aferentes en los nervios articulares son amielínicas (fibras nerviosas C y simpáticas). Por su parte, las fibras mielínicas Aβ y Aδ comprenden en torno al 20% del total de fibras (Kidd, 1996). Estos nervios sensoriales responden a estímulos mecánicos como estiramientos de la cápsula de la articulación pero también a mediadores inflamatorios químicos, que estimulan directamente fibras nociceptivas silentes o las sensibilizan a estímulos mecánicos. Por tanto, el dolor se considera hoy en día el mayor síntoma de la artrosis y también el mayor determinante de la pérdida de funcionalidad, actuando una suma de componentes de origen biológico, psicológico y social (Hunter *et al*., 2009).

A pesar de la clara condición de dolor crónico, el hecho de si la artrosis tiene un componente neuropático o más bien nociceptivo ha sido un tema de debate durante

mucho tiempo (Combe et al., 2004; Hochman *et al.*, 2010; Kelly *et al*., 2013). Recientemente, estudios clínicos de ámbito nacional (Oteo et al., 2013) e internacional (Hochman *et al.*, 2010) han revelado la presencia de un componente neuropático en la artrosis de rodilla en más de un 33% de todos los casos diagnosticados como dolor crónico de articulación de la rodilla. Dicho esto, tanto la sensibilización periférica como central parecen ser elementos relevantes en la patología (Arendt-Nielsen et al., 2010; Finan *et al*., 2013). De hecho, todos los indicadores de sensibilización al dolor (tanto periféricos como centrales) se han observado en pacientes con artrosis de rodilla en un mayor o menor grado: hiperalgesia, alodinia, sumación espacial, sumación temporal (*wind-up*) y sensación persistente (*aftersensations*) (Harden *et al*., 2013; Skou *et al.*, 2013). Por un lado, la sensibilización periférica se relaciona normalmente con las inflamaciones local y neurogénica que cursan con la hiperalgesia primaria y sensación persistente observadas en los ensayos de conducta. Por otro lado, la sensibilización central se caracteriza por la presencia de alodinia e hiperalgesia distal (sumación espacial) y puede implicar mecanismos dañados de modulación nociceptiva descendente (Courtney *et al.,* 2012). Sin embargo, a pesar de la evidencia del papel central de la producción del dolor en la artrosis, los tratamientos actuales son principalmente paliativos y enfocados a mecanismos periféricos (Jordan *et al*., 2003; Barron and Rubin, 2007; Benito *et al*., 2008).

MODELO DE DOLOR ARTRÓSICO.

En la rata el 80% de todas las fibras nerviosas aferentes en la articulación de la rodilla son nociceptivas. Los nociceptores están localizados a lo largo de toda la articulación (McDougall *et al*., 1997; Mach *et al.*, 2002; McDougall, 2006; Wenham y Conaghan, 2009), a excepción del cartílago (Bora y Miller, 1987; Henrotin *et al*., 2005). Esto puede explicar por qué en los primeros estadíos de la artrosis la articulación es normalmente asintomática. Sin embargo, la inervación de la diartrosis en estado normal y bajo condiciones patológicas es notablemente diferente, habiéndose descrito un crecimiento nervioso y vascular en el cartílago artrósico (Ashraf y Walsh, 2008).

La infiltración del agente químico monosodio iodoacetato (MIA) en la cavidad articular de la rodilla reproduce la enfermedad degenerativa de la rodilla observada en la clínica de una manera muy precisa, interrumpiendo el metabolismo de los condrocitos y

dando lugar a la muerte celular y consiguiente degeneración del cartílago articular (Lefebvre *et al.*, 2011). Atendiendo a un contexto fisiológico, MIA es capaz de inducir hiperalgesia mecánica en la propia rodilla afectada, pero también alodinia táctil e hiperalgesia térmica a nivel plantar de manera distal a la rodilla (Procházková *et al.*, 2009). Este comportamiento se correlaciona con la típica presencia de microglía y astroglía espinal activada en la sensibilización central (Sagar *et al*., 2011). Desde un punto de vista clínico, MIA produce una marcada sinovitis seguida de un adelgazamiento del cartílago, el desarrollo de fisuras y la alteración de zonas más profundas en contacto directo con el hueso subcondral. La sinovitis e inflamación de la cápsula parecen remitir para el día 3-7 y no se considera que jueguen ya más un papel en la producción de dolor. Esta primera fase consiste principalmente en la interacción de las proteínas plasmáticas y los productos inflamatorios con los fibroblastos residentes para restaurar la superficie del cartílago. Sin embargo, durante este proceso la remodelación de la zona superficial puede causar un exceso de depósitos, que conducirán a un fenotipo fibrótico y engrosado del tejido.

B. ***Dolor postoperatorio.***

Prácticamente cualquier cirugía produce dolor postoperatorio. Éste es a menudo clasificado dentro de la categoría de dolor agudo de acuerdo con el tiempo de convalecencia, el cual remite en muchos casos con mayor o menor rapidez, pero que puede también convertirse en un dolor persistente en algunos casos de resistencia a la terapia (Deumens *et al.*, 2013). A este respecto, la IASP define el dolor postoperatorio persistente, como aquel estado que dura generalmente más de dos meses después de una intervención quirúrgica y que no puede ser explicado por otras causas (Schug y Pogatzki-Zahn, 2011). Se han descrito cambios plásticos como la sumación temporal y espacial en sitios distantes a la herida, por lo que la sensibilización periférica (Brennan *et al*., 1996) y central (Obata *et al*., 2006; Ito *et al*., 2009; Chen *et al.*, 2012) pueden ser consideradas importantes distintivos de este dolor postoperatorio de larga duración. Con el objeto de investigar los mecanismos fisiopatológicos del dolor postquirúrgico persistente y de evaluar nuevos analgésicos dirigidos contra el dolor postoperatorio, se han desarrollado modelos preclínicos de dolor postquirúrgico.

MODELO DE DOLOR POSTOPERATORIO.

El modelo típico de dolor por incisión fue descrito por primera vez por Brennan y cols. (Brennan *et al*., 1996). Considerando que el dolor causado por inflamación, lesión nerviosa o incisión está compuesto por diferentes mecanismos fisiopatológicos, los autores diseñaron un modelo de dolor postoperatorio capaz de sensibilizar por un lado las aferencias primarias (fibras Aδ y C) y por otro lado las neuronas de amplio rango dinámico (WDR, de su acrónimo en inglés *wide dynamic range*) en el asta dorsal de la médula espinal (Pogatzki *et al*., 2002; Zahn *et al*., 2002; Banik y Brennan, 2004).

El modelo está basado en una incisión quirúrgica realizada en la planta de la pata trasera del animal. La información procedente de la incisión es transmitida por medio del nervio sural y tibial, y resulta en un aumento de la respuesta en lugares adyacentes y distales a la incisión frente a estímulos caloríficos y/o táctiles (Zahn y Brennan, 1999). En otras palabras, el desarrollo de hiperalgesia primaria y secundaria. Observaciones derivadas de este modelo pueden conducir a comprobar teorías de sensibilización y plasticidad en el dolor postoperatorio pero también a evaluar la contribución de diferentes fármacos analgésicos y terapias en el tratamiento del dolor postquirúrgico, como los efectos derivados de la morfina.

2. OBJETIVOS.

Los **modelos de dolor animal** se utilizan básicamente por dos razones: **explorar los mecanismos que subyacen tanto al dolor fisiológico como patológico**, y estudiar o desarrollar fármacos anágesicos ya existentes o de nueva síntesis. De acuerdo con esto:

- Por un lado este trabajo intentó **evaluar** de manera detallada **los umbrales de nocicepción en** animales con **dolor de** la articulación de la rodilla inducido por **artrosis**:

  3. para conseguir un mejor **entendimiento del** estado de **dolor crónico**

  4. para **estudiar el papel del** receptor de tipo toll 4 (**TLR4**) por medio de una molécula bloqueante del TLR4 **en**:

  a. **impedir/dificultar el desarrollo de la enfermedad**,

  b. **disminuir la nocicepción** una vez se ha desarrollado la enfermedad.

- Por otro lado, el trabajo también trató **evaluar** los **umbrales de nocicepción** en un modelo de **dolor por incisión** en rata para **estudiar el papel de** los receptores de tipo toll 4 (**TLR4**) por medio de una molécula bloqueante del TLR4 **en el tiempo de recuperación y en los mecanismos implicados**,
- Un objetivo adicional consistió en **estudiar la implicación de la glia** en el mantenimiento de ambos, el dolor artrósico y el dolor quirúrgico.

3. MATERIALES Y MÉTODOS.

3.1. Animales de experimentación.

Ratas macho Wistar adultas obtenidas de Harlan Interfauna Ibérica (España) fueron empleadas para todos los experimentos. Los animales fueron distribuidos a su llegada a nuestras instalaciones en jaulas de plástico transparente (4-6 ratas/jaula) bajo condiciones estándar de laboratorio: habitaciones con temperatura (23 ± 1ºC), humedad (50-55%) y luz (ciclos de luz/oscuridad de 12 horas) controlados de manera constante, con agua y comida disponible *ad libitum*. Seguidamente se les mantuvo durante un período de cinco días de aclimatación antes de la iniciación de cualquier experimento, de acuerdo con los estándares de protección animal de la Unión Europea (BOE, 2005; Capdevila *et al*., 2007).

Con objeto de constatar que no había respuestas anómalas en su comportamiento, los animales fueron observados cuidadosamente y, a continuación, fueron asignados al azar a grupos control o de tratamiento. Un observador ciego a los tratamientos farmacológicos realizó todos los ensayos de comportamiento. Todos los procedimientos animales se llevaron a cabo siguiendo un protocolo que fue aprobado por el Comité Ético de la Universidad Rey Juan Carlos (URJC) y de acuerdo con las pautas establecidas por la Asociación Internacional para el Estudio del Dolor (IASP) (Zimmermann, 1983).

3.2. Procedimientos quirúrgicos.

A. Modelo de dolor artrósico inducido por MIA.

La artrosis fue inducida en ratas (con pesos de 200-250 g o 250-300 g para administración i.p. o i.t. respectivamente) mediante la infiltración intraarticular de monosodio iodoacetato (MIA) en la cavidad articular de las rodillas. Como se ha

descrito con anterioridad (Schuelert y McDougall, 2008; Schuelert *et al.*, 2010), el iodoacetato produce una degeneración persistente de la articulación de la rodilla que alcanza su estado máximo entre la segunda y la cuarta semana tras su administración.

Los animales fueron anestesiados con 0,3 ml / 100 mg (i.p.) de Equithesin[36], tras lo cual se administró una única inyección intraarticular de 2 mg MIA (Sigma-Aldrich®) en 50 µl de suero salino fisiológico (Pomonis *et al*., 2005; Cifuentes *et al.*, 2010) a través del ligamento infrapatelar de la rodilla derecha[37]. La dosis de MIA fue escogida de acuerdo con la literatura cotejada (Fernihough *et al.*, 2004; Kalff *et al*., 2010). La pata trasera contralateral recibió una única inyección de suero salino normal (50 µl) (Bove et al., 2003; Cialdai *et al.*, 2009). También se administró 50 µl de salino en ambas rodillas en un grupo control distinto. Todas las inyecciones fueron llevadas a cabo por medio de una jeringuilla de insulina de 30 G (Becton Dickinson) (Clements *et al.*, 2009).

B. Cirugía intratecal: dolor artrósico.

La cirugía intratecal se realizó del mismo modo a como han descrito otros autores (Matsunaga *et al*., 2007; Avila-Martin *et al.*, 2011), con ligeras modificaciones. Las ratas se prepararon quirúrgicamente bajo anestesia con pentobarbital (Dolethal, 0,225 ml·kg^{-1}, i.p., Vetóquinol) y 2% xilacina (Xilagesic, 0.43 ml·kg^{-1}, i.p., Calier), seguido de una dosis de atropina (0.05 ml·kg^{-1}, B. Braun) con objeto de evitar espasmos y bradicardia. Además, se administró 0,1 ml de un antibiótico (Enrofloxacina, 2,5% Baytril®, Bayer) después de la cirugía. Un tubo de polietileno disponible comercialmente (I.D.: 28 mm O.D.: 61 mm; PE-10, Becton Dickinson) fue utilizado para su implantación como catéter y externalizado en la parte posterior del cuello. Inmediatamente antes de la implantación, el catéter fue esterilizado con etanol absoluto, y minuciosamente lavado con suero salino fisiológico estéril. Tras la incisión en la piel y la disección roma de las capas musculares superpuestas a las vértebras, se realizó una pequeña hemi-

[36] En los animales preparados para recibir administración intratecal (i.t.), el MIA se administró bajo anestesia con isoflurano al 2%. La razón principal consistió en que (1) el hidrato de cloral fue prohibido en el año 2013, (2) el protocolo de administración intratecal fue llevado a cabo después del intraperioneal (i.p.), y (3) durante la tesis descubrimos en la literatura que el isoflurano inducía menores efectos adversos que cualquier otro anestésico.

[37] En Portugal, la inyección intraarticular se realizó en la rodilla izquierda, en un volumen de 25 µl, con una jeringuilla de 26 G, y las rodillas contralaterales no recibieron inyección.

laminectomía a nivel L5 vertebral (Co3 espinal). La duramadre Co3 expuesta fue sometida a una pequeña durectomía con tijeras de tipo-iris de manera que la punta del catéter intratecal pudiera insertarse de manera rostral y medialmente por encima de la médula espinal con una posición final justo por debajo del sitio L5 de liberación del fármaco (L1 vertebral). El área fue limpiada para permitir la fijación del catéter con un adhesivo de cianocrilato a la vértebra L6. El extremo percutáneo del catéter fue finalmente asegurado insertándolo a través de una pequeña incisión cutánea en la base del cráneo, el cual se rellenó con suero salino y se tapó el orificio de entrada con ayuda de un alambre personalizado. Una duramadre artifical (Neuropatch, B. Braun) se colocó sobre la pequeña abertura realizada a nivel Co3 espinal y las capas de músculo sobre ésta fueron unidas con una sutura continua de ácido poliglicólico absorbible de 4-0. Las ratas fueron entonces enjauladas individualmente y observadas cuidadosamente durante la recuperación. Los animales que mostraron déficits neurológicos después de la cirugía quedaron descartados. Cuatro días después de la implantación de los catéteres intratecales, se tomaron nuevas medidas basales y las ratas recibieron una inyección intraarticular de MIA (Liu *et al*., 2011) o salino, como correspondiese, bajo anestesia con isoflurano al 2%.

C. Incisión quirúrgica: dolor incisional.

La cirugía se desarrolló de acuerdo al modelo de dolor incisional en rata desarrollado por Brennan y cols. (Brennan et al., 1996), con ligeras modificaciones. Las ratas (con pesos entre 250-300 g) fueron anestesiadas con isoflurano al 2% administrado por medio de un cono nasal. La pata trasera derecha fue esterilizada con una solución de povidona yodada al 10% (Betadine®) y una incisión longitudinal de 1 cm fue realizada a través de la piel y fascia en la planta de la pata del animal, comenzando a 0,5 cm del extremo proximal del talón en dirección hacia los dedos. El músculo *plantaris* fue entonces elevado con ayuda de una aguja hipodérmica de 23 G e igualmente cortado de manera longitudinal. Haciendo algo de presión con una gasa o torunda de algodón se consiguió la hemostasis de la zona y los dos pliegues de piel fueron finalmente unidos con dos suturas maestras de nylon de 5-0. Finalmente la herida fue cubierta con una untura de antibiótico tópico (0.2% nitrofurazona, Furacin®) y se permitió que los

animales se recuperaran en sus respectivas jaulas. La pata izquierda contralateral permaneció intacta.

3.3. Ensayos *in vivo*:

A. Ensayos de conducta.

La nocicepción fue evaluada mediante la comprobación de la sensibilidad a estímulos táctiles, térmicos y mecánicos como se describe en las siguientes líneas.

1. Test de von Frey.

Durante la tesis, se utilizaron filamentos de von Frey o von Frey electrónico para una mejor caracterización. Durante dos días, previos a la evaluación conductual, y cada día de evaluación antes del experimento, los animales fueron colocados en una caja de polimetilmetacrilato con una malla metálica como suelo y se les permitió aclimatarse. Cuando se usaron los filamentos de von Frey, se asumió un paradigma basado en cinco intentos. Los filamentos de von Frey fueron aplicados cinco veces seguidas de manera perpendicular a la superficie media de la planta de la pata trasera mientras el animal permanecía apoyado con las cuatro patas sobre el suelo. El proceso, de cinco intentos, fue repetido tres veces solo si cuatro de cinco intentos lograban una respuesta; si no, pasábamos al siguiente filamento (desde el de menor al de mayor calibre) hasta que se conseguían cuatro/cinco respuestas en una misma serie. Esto es, se trató de perseguir una respuesta de todo o nada (Ferreira-Gomes *et al.*, 2008). Cuando utilizamos el von Frey electrónico automatizado (Ugo Basile), el umbral de respuesta al tacto inocuo del filamento en cada pata trasera era medido como se ha descrito anteriormente (Whiteside *et al.*, 2004), con ligeras modificaciones. El microfilamento de von Frey electrónico se aplicó perpendicularmente a la superficie de la mitad de la planta de la pata trasera y se mantuvo presionado hasta que se consiguió una respuesta. La estimulación mecánica fue mantenida durante 2 s y se tomó un total de tres lecturas para cada rata en cada tiempo testado. La media de estas tres medidas fue determinada y utilizada para análisis posteriores.

2. *Test de retirada de la pata.*

La respuesta a un estímulo calorífico nocivo fue determinada por medio de un aparato térmico plantar (Ugo Basile, Italia) mediante el método modificado de Bennett y Hargreaves (Bennett and Hargreaves, 1990). De manera similar a lo descrito para el test anterior, las ratas fueron aclimatadas a las condiciones del test dos días antes de los experimentos y diez minutos cada día de evaluación justo antes de los ensayos conductuales, colocando las ratas en un compartimento de plástico sobre un suelo de cristal. Una fuente de luz bajo el suelo fue dirigida a la superficie media plantar de la pata trasera con objeto de calentarla, de manera que el reflejo de retirada de la pata interrumpía la luz y automáticamente apagaba un contador, quedando registrado el tiempo de latencia de retirada de la pata. La media de tres medidas separadas 2-5 min entre sí fue registrada. La intensidad de la fuente de calor fue ajustada de tal manera que las latencias basales de retirada fueran de 8-10 s con un tiempo de corte de 15 s para evitar el daño tisular.

3. *Test de knee-bend.*

Para evaluar la sensibilidad a un estímulo mecánico natural como el movimiento de flexión de la rodilla y por consiguiente, para elucidar la posible existencia de hiperalgesia proximal, se empleó un test de flexión de la rodilla descrito por Ferreira-Gomes y cols. (Ferreira-Gomes *et al*., 2008) en un modelo de rata de dolor artrósico inducido por MIA. Todos los animales fueron habituados al experimentador y al test durante un período de una semana antes de registrar cualquier valor. El test consistió en registrar el número de vocalizaciones y/o reacciones de forcejeo en respuesta a cinco extensiones y cinco flexiones de la articulación de la rodilla y se puntuó como sigue:

puntuación	*Tipo de reacción*
0	Sin respuesta
0.5	El forcejeo ocurre ante el grado máximo de flexión/extensión
1	El forcejeo ocurre ante un grado moderado de flexión/extensión La vocalización ocurre ante el grado máximo de flexion/extensión
2	La vocalización ocurre ante un grado moderado de flexión/extensión

La suma de las reacciones registradas (con un hipotético máximo valor de 20) representa la puntuación del test de la flexión de la rodilla.

4. *Test del catwalk.*

El test del catwalk fue utilizado para evaluar la discapacidad inducida por el modelo artrósico y el discomfort después de recibir tratamiento (Ferreira-Gomes *et al*., 2012). Los animales con artrosis muestran una disminución de la distribución del peso sobre la extremidad con artrosis probablemente debido a un aumento de la sensibilidad. Los animales son colocados en una plataforma de cristal localizada en una habitación oscura y se les permite deambular libremente. La superficie es rociada con algo de agua y un tubo fluorescente ilumina la plataforma para reflejar la luz hacia abajo solo en los puntos en los que exista contacto entre el área de cada pata con la plataforma de cristal, resultando en una acusada imagen de la huella de la pata. La intensidad de la señal de la impresión de la pata aumenta con el área de contacto de la pata con la plataforma y con la presión aplicada por ésta. Por consiguiente, la intensidad total de la impresión de la pata ipsilateral es cuantificada determinando el área de la pata en contacto con la plataforma, en número de píxeles, y multiplicándola por la intensidad media de cada píxel, dándonos la intensidad general de la impresión de la pata.

La plataforma de cristal fue monitorizada por medio de una videocámara con un objetivo gran angular dispuesta bajo ésta. Un ordenador equipado con un programa de vídeo (Ulead Video Studio, USA) daba cuenta del registro obtenido a través de la cámara. Se obtuvieron seis fotogramas al azar de los vídeos grabados durante la evaluación de las ratas: 3 fotos con el animal caminando (correspondientes a pasos, espaciados en el tiempo, de huellas contralaterales e ipsilaterales consecutivas) y 3 fotos correspondientes a posturas, distantes en el tiempo, del animal sobre sus cuatro patas. El número y la intensidad de los píxeles por encima de un umbral definido fueron cuantificados utilizando el programa Image J 1.47, permitiendo la comparación entre el área/presión ejercida por cada pata. Los resultados fueron expresados en intensidad total de la pata trasera ipsilateral como porcentaje de la intensidad total de ambas patas traseras.

B. Compuestos utilizados.

TLR4-A1.

Basado en estudios llevados a cabo por Piazza y cols.(Piazza et al., 2009) en cultivos celulares *in vitro* e *in vivo en modelos de* sepsis en ratones, reprodujimos un lípido benzilamonio para ser testado en nuestros modelos *in vivo* de rata, al que llamamos como "TLR4 antagonista 1" (TLR4-A1). Este inhibidor del receptor TLR4 con diana en su correceptor CD14 (Arroyo-Espliguero *et al*., 2004) fue sintetizado como se ha descrito previamente (Piazza *et al.*, 2009; Peri y Piazza, 2012) y presentado en una proporción 9:1 de suero salino y etanol. Para la administración intratecal, el TLR4-A1 fue diluido solo en suero salino estéril.

OTROS COMPUESTOS.

La morfina sulfato fue adquirida a Sigma-Aldrich Química (España) y diluida en suero salino inocuo. Todas las administraciones i.p. consistían en volúmenes totales de 0,5 ml. Por su parte, las administraciones i.t. consistieron en volúmenes de 0,01 ml precedidos y continuados por 0,01 ml de suero salino estéril. Todos los compuestos fueron preparados en el día del experimento.

Protocolos de administración de fármacos.

1. *Modelo de dolor artrósico inducido por MIA.*

   El papel del receptor de tipo toll 4 (TLR4) dirigido contra el dolor crónico o nociceptivo fue investigado utilizando un nuevo compuesto experimental sintético diseñado únicamente para fines de investigación: el TLR4-A1. La inyección intraarticular se administró tras la habituación al ambiente del test y después de registrar los valores basales (día 0). Los datos fueron registrados desde el día postoperatorio 7 en adelante como sigue: en los días 7, 14 y 21, y de manera alternativa en los días 28, 35, 40 y 50 también.

Administración aguda de TLR4-A1 una vez establecida la artrosis
• grupo blanco → control • grupo MIA → control • grupo MIA +10 mg·kg^{-1} TLR4-A1 (i.p.) en día 14
Administración crónica de TLR4-A1 una vez establecida la artrosis
• grupo blanco → control • grupo MIA → control • grupo MIA +15 días de tratamiento con 10 mg·kg^{-1} TLR4-A1 (i.p.)
Administración crónica de TLR4-A1 paralelamente a la inducción de la artrosis
a) Administración i.p. • grupo blanco → control • grupo MIA → control • grupo MIA+5 días de tratamiento con 10 mg·kg^{-1} TLR4-A1 (i.p.) **b) Administración i.t.** • grupo blanco + cirugía → control • grupo MIA + cirugía → control • grupo MIA + cirugía + 5 días tratados con 0,1 mg·kg^{-1} TLR4-A1 (i.t.)

- Administración sistémica aguda.

  El tratamiento agudo con TLR4-A1 consistió en una única dosis (10 mg·kg^{-1}) en el día 14 y el comportamiento animal fue evaluado antes y 30 min, 1h, 1h 30 min, 2 h y 3h tras la administración.

- Administración sistémica crónica.

  En el protocolo seguido en la FMUP, el tratamiento crónico con el vehículo o el propio TLR4-A1 (10 mg·kg^{-1}) consistió en una administración diaria durante un período de 15 días, una vez la patología se había establecido (a partir del día 14). Los tests de conducta se llevaron a cabo los días 3, 7, 14 y 15 después de la inyección de MIA y en los días 18, 20, 22, 24, 26 y 28 antes y 1h después de la administración del compuesto.

  En el protocolo de la Universidad Rey Juan Carlos (FCS-URJC), el vehículo o el propio TLR4-A1 (10 mg·kg^{-1}) fueron administrados i.p. de manera diaria durante cinco días consecutivos, desde el día 0 hasta el día 4 después de la inyección de MIA. Los umbrales de retirada para la alodinia táctil y la hiperalgesia térmica se evaluaron en los días anteriormente citados.

- Administración intratecal crónica.

  Se registraron dos umbrales basales diferentes para los grupos con cirugía intratecal: justo antes de la cateterización y cuatro días después de la cirugía. Las ratas sin descoordinación motora o sensitiva en el segundo de estos días, fueron clasificadas en grupo control o artrósico y recibieron suero salino inocuo o TLR4-A1 (0,1 $mg \cdot kg^{-1}$) durante los primeros cinco días inmediatamente después de la infiltración con 2 mg MIA o salino. Los umbrales de retirada o latencias térmicas fueron evaluados cada 7 días durante las siguientes tres semanas.

2. *Modelo postoperatorio de dolor incisional.*

Los tests de von Frey y de retirada de la pata se emplearon para determinar el curso temporal de la alodinia táctil y de la hiperalgesia térmica durante 10 días consecutivos en animales operados quirúrgicamente. Posteriormente se evaluó también el efecto de la administración de tres tratamientos distintos en los umbrales de nocicepción.

Administración crónica de suero salino, morfina y/o TLR4-A1 (dos dosis de 5 $mg \cdot kg^{-1} \cdot día^{-1}$)
• grupo blanco →control
• grupo incisional→control → 9 días de suero salino (i.p.)
• grupo incisional→9 días de 10 $mg \cdot kg^{-1}$ morfina (i.p.)
• grupo incisional→9 días de 10 $mg \cdot kg^{-1}$ TLR4-A1 (i.p.)
• grupo incisional→9 días de 10 $mg \cdot kg^{-1}$ TLR4-A1+morfina (i.p.)

Cada compuesto fue administrado de manera diaria como dos dosis intraperitoneales de 5 $mg \cdot kg^{-1}$, cada una separada por 6 horas durante 9 días consecutivos y testados 24 h después de la incisión plantar dos veces al día durante toda la duración del tratamiento: 2 horas antes y 45 minutos después de la primera administración del día. En el caso de los animales que recibieron ambos fármacos, TLR4-A1 fue administrado 15 min antes de la morfina y el comportamiento se evaluó 30 min después de esta última. Esto permitió evaluar ambos, el efecto resultante del tratamiento crónico (efecto crónico seriado) e inmediatamente después de la administración (efecto agudo seriado). La segunda administración fue considerada como una dosis de recuerdo. En resumen, cada animal recibió al final de cada día 10 $mg \cdot kg^{-1}$ de morfina y/o de TLR4-A1.

3.4. Ensayos *in vitro*:

A. Métodos histológicos generales.

Estudio inmunohistoquímico para la actividad glial.

1. *Recogida de médulas espinales.*

   Los animales se sacrificaron a los 22 o 10 días después de la intervención quirúrgica (modelo de artrosis y modelo postoperatorio respectivamente; n = 4-5 ratas por grupo). Las ratas fueron anestesiadas con pentobarbital (60 $mg \cdot kg^{-1}$, i.p.) y perfundidas intracardialmente a través del ventrículo izquierdo con 200 ml de suero salino normal, seguido de paraformaldehído al 4% en tampón salino fosfato (0,1M, pH 7,4, 4ºC) (referido como solución fijadora a partir de ahora). Se realizó una laminectomía de la médula espinal torácica y lumbar y se recogieron las secciones espinales L3-L5 para guardarlas en la solución fijadora durante cuatro horas a temperatura ambiente. A continuación se criopreservaron en tampón salino fosfato (0,1M, pH7,4) suplementado con 30% de sacarosa y 0.05% de azida sódica a 4 ºC hasta su posterior procesamiento. De manera alternativa, las rodillas y los nervios safenos fueron también recogidos.

2. *Procesamiento de tejidos.*

   La deshidratación de los especímenes se llevó a cabo mediante concentraciones gradualmente crecientes de etanol. Posteriormente se cambiaron a un medio con tolueno y finalmente se incluyeron en parafina. Los bloques de parafina de las secciones espinales fueron montados en un micrótomo rotatorio de tipo Minot. Se realizaron cortes seriados de 5 µm de grosor y se recogieron sobre portaobjetos tratados con 0.02% de poli-L-lisina. Dado que la parafina es poco permeable a las tinturas, las muestras ya montadas fueron desparafinadas en concentraciones gradualmente decrecientes de etanol.

3. *Inmunodetección.*

   Después de la desparafinación, las muestras siguieron un método para la exposición de antígenos enmascarados por la parafina y a continuación fueron inmunoteñidas por el método indirecto de la peroxidasa. Las muestras fueron tratadas con una solución al 3% de peróxido de hidrógeno en agua estéril durante 15 min con el fin de bloquear la actividad peroxidasa endógena, seguido de una incubación de 30 min con suero bovino fetal o seroalbúmina bovina, como correspondiera, para

reducir el ruido de fondo. Las secciones fueron entonces tratadas durante 1 hora con los anticuerpos anti-GFAP o anti-Iba-1 debidamente diluidos, lavadas y tratadas durante una hora adicional con un kit o anticuerpo secundario conjugado para amplificar la señal. Las muestras fueron entonces lavadas para retirar el exceso de anticuerpo y tratadas con una solución de DAB (Sigma®) durante 5 min. Finalmente las secciones fueron lavadas con agua corriente y siguieron una batería de concentraciones crecientes de etanol (justo inversa a la descrita anteriormente) para permitir su montaje. Por último las preparaciones fueron cubiertas con un cubreobjetos y observadas al microoscopio.

4. *Método para el contaje de las células marcadas: examinación microscópica.*

   Para cada sección correspondiente a cada región lumbar (L3, L4 o L5), el número total de células marcadas fueron contadas de manera separada en láminas I-II, III-IV y V-VI. La identificación de las láminas del asta dorsal de la médula espinal se realizó de acuerdo a la clasifcación de Rexed (Rexed, 1952) y se tomaron fotografías de las secciones para hacer montajes de la médula espinal completa a una magnificación final de 20x.

Examinación macroscópica de las rodillas.

Después de su sacrificio, las rodillas de las ratas de los animales en el modelo de dolor artrósico inducido por MIA fueron expuestas para verificar la correlación entre la acción dañina del MIA con los resultados observados durante la evaluación conductual. Para ello, los ligamentos fueron cuidadosamente escindidos y las caras articulares de la tibia y el fémur expuestas.

Procesamiento y examinación microscópica de las rodillas: dolor artrósico.

1. *Descalcificación ósea.*

   La disección y procesamiento del tejido en las articulaciones de las rodillas fue realizada como se ha descrito previamente (Memon *et al.*, 2010) con ligeras modificaciones. Los huesos fueron cortados lo más próximo a la articulación de la rodilla posible e inmediatamente transferidos a una solución fijadora durante 72 horas adicionales. Los especímenes fueron entonces dispuestos en una solución crioprotectora y mantenidos a 4ºC hasta su uso. La retirada del contenido mineral se llevó a cabo mediante la inmersión de las rodillas en una solución de descalcificación (5% EDTA / 10% PFA) y dejándolas rotar a temperatura ambiente en

un agitador a baja velocidad. La solución fue renovada semanalmente durante 4-5 semanas. Una torunda de algodón en la solución sirvió de estructura para atrapar el calcio que se retiraba del hueso.

2. Tinción.

Después de la descalcificación, los tejidos fueron lavados, deshidratados en series de concentración de etanol gradualmente creciente e incluidos en parafina. Posteriormente, se cortaron secciones de tejido de 5 µm de grosor en un micrótomo de rotación de Minot y se utilizaron para tinción con azul de toluidina al 0,5% (con borato de sodio al 1%).

3. Examinación microscópica.

Fotografías de las secciones de rodilla fueron grabadas para hacer montajes de la rodilla entera a una magnificación final de 2,5x. El objeto de la tinción con azul de toluidina consistió en facilitar la evaluación de las estructuras del cartílago mediante el uso de la puntuación de Pritzker (Pritzker *et al.*, 2006).

Biopsia y examinación microscópica de los nervios safenos.

Segmentos de un centímetro de longitud de nervios safenos ipsilateral (lado dañado) y contralateral (lado no dañado) correspondientes a la extensión ingle-rodilla (modelo de artrorsis) o espinilla-rodilla (modelo postoperatorio) fueron retiradas 22 o 10 días tras la cirugía (respctivamente), e inmediatamente fijadas en una solución fijadora. Después de 4 horas, se incluyeron en una solución crioprotectora y se mantuvieron a 4ºC hasta su uso. Las muestras fueron fijadas e incluidas en resina de acuerdo a un protocolo llevado a cabo por el Servicio de Apoyo Tecnológico. Los bloques resultantes de resina fueron montados en un Ultramicrotomo Leica EM UC7 y se hicieron secciones transversales semifinas de 800 nm de grosor. Las secciones se calentaron entonces para permitir su tinción con azul de toluidina para su estudio morfológico y morfométrico (Sghirlanzoni *et al*., 2005). Se grabaron imágenes para realizar montajes del nervio safeno entero a una magnificación final de 63,5x. Finalmente, distintos parámetros fueron analizados en fotografías digitalizadas utilizando el software ImageJ.

B. Determinación de proteínas mediante ensayos bioquímicos.

Recogida de médulas espinales.

La recogida de las médulas espinales se realizó como se ha descrito previamente (Butt *et al*., 2007; Gil-Dones *et al.*, 2008) con ligeras modificaciones. Las ratas fueron

decapitadas y las médulas espinales se extrajeron del animal utilizando presión hidráulica insertando una aguja de calibre 18 en el extremo caudal del canal vertebral y descargando suero salino frío en su interior. Un segmento de 0,5 cm correspondiente a la parte media del engrosamiento lumbar (LI-LV) (Gilerovich *et al.*, 2008) fue cortada de la médula espinal aislada, congelado en nitrógeno líquido e inmediatamente almacenado a -80ºC para su posterior procesamiento.

ELISA.

La homogenización de las médulas espinales fue adaptada del método de Sweiter *et al*. (Sweitzer *et al*., 2001; Sweitzer y DeLeo, 2002). Los segmentos medulares que se guardaban congelados fueron recogidos y pesados; a continuación, se homogenizaron en 0,5 ml de tampón de lisis frío por medio de un homogenizador Polytron (Kinematica, Suiza) a pulsos de alta velocidad de 10 s. Los productos resultantes fueron entonces ultracentrifugados a 16.000x g durante 30 min a 4ºC y el sobrenadante (fracción de proteína soluble) fue dividido igualmente en: una alícuota de 200 µl para la cuantificación de IL-1β e IL-6 y una alícuota de 200 µl para la cuantificación de TNF-α.

Las concentraciones de proteína para IL-1β, IL-6 y TNF-α fueron determinadas utilizando kits de ELISA para rata de Diaclone® de acuerdo a las indicaciones del fabricante y comparando las muestras con la curva patrón generada para cada kit. Los niveles de proteína en los animales operados tratados y no tratados fueron comparados con aquellos de los animales control (n =4-6).

3.5. Análisis estadístico.

El *software* GraphPad Prism5 se utilizó para todos los análisis estadísticos. Para determinar la existencia de diferencias estadísticamente significativas entre los distintos grupos se usó el test de ANOVA de dos vías seguido por el análisis posthoc de Bonferroni en todos los experimentos. Un test de ANOVA de una vía seguido por el test de Dunnett o el test de comparación múltiple de Newman-Keuls fue usado para comparar los diferentes tiempos con sus respectivos valores basales (día 0). En todos los análisis se consideró una diferencia estadísticamente significativa a partir de una $P<0,05$.

4. RESULTADOS

4.1. Ensayos *in vivo*: ensayos de conducta.

4.1.1. Modelo de dolor artrósico.

Como se ha mencionado anteriormente, se llevó a cabo una minuciosa investigación sobre estudios de determinación de dosis antes de elegir cualquier volumen o cantidad de MIA. Concluimos que 2 mg era ideal al causar un daño irreversible y dolor crónico severo. Dos diferentes volúmenes (25 y 50 µl) fueron utilizados, decantándonos finalmente por 50 µl por su facilidad de administración. La cojera era evidente justo al día siguiente de la inyección de MIA en la mayoría de los animales y se mantuvieron umbrales de latencia y de retirada de la pata disminuidos a lo largo de 50 días, más marcados en respuesta al tacto suave con filamentos de von Frey que frente a un estímulo calorífico. La inyección de suero fisiológico en la pata contralateral no causó alteración alguna en el comportamiento del animal, como se deduce de su comparación con un grupo aparte de animales con las rodillas intactas.

ii. Efecto antinociceptivo agudo de TLR4-A1.

Para estar seguros de la duración del efecto del compuesto, se utilizaron tres tipos de test diferentes el día postoperatorio 14: el test de von Frey (estímulo táctil) en un lugar alejado de la rodilla, el test del knee bend (estímulo mecánico) en la misma rodilla y el test del Catwalk (sin aplicación de estímulo), que informaba sobre dolor espontáneo.

MIA producía alodinia táctil significativa en la pata trasera ipsilateral todos los días testados. La administración intraperitorneal de TLR4-A1 (10 $mg \cdot kg^{-1}$) atenuaba dicha alodinia, con un efecto máximo pasada 1 h de la administración. La nocicepción inducida por el movimiento fue evaluada por medio de los tests de flexión de la rodilla (knee-bend) y del Catwalk. MIA inducía un aumento en la puntuación para el test de la flexion de la rodilla a lo largo de todos los tiempos estudiados; mientras que la administración intraperitoneal de TLR4-A1 (10 $mg \cdot kg^{-1}$) atenuaba la alodinia mecánica con un efecto máximo entre los 30 min y 1 h tras la administración. El MIA también inducía dolor espontáneo desde el día 3 en adelante y la administración intraperitoneal de TLR4-A1 (10 $mg \cdot kg^{-1}$) recuperaba parcilamente el umbral basal con un efecto máximo a los 30 min y 3 h tras la administración.

iii. Efecto antinociceptivo crónico de TLR4-A1.

TRATAMIENTO CORTO (5 DÍAS) AL COMIENZO DE LA PATOLOGÍA. Durante una fase inicial, los primeros 14 días después de la inyección del MIA, existían diferencias estadísticamente significativas entre los grupos tratados con TLR4-A1 y sin tratar. Sin embargo, con forme el efecto de TLR4-A1 desaparecía, la respuesta nociceptiva se hacía evidente (días 21), desvaneciéndose las diferecias significativas existentes entre ambos grupos y apareciendo con respecto al grupo control. Por el contrario, la administración intraperitoneal de TLR4-A1 (10 $mg \cdot kg^{-1} \cdot día^{-1}$) producía un bloqueo total de la hiperalgesia térmica.

TRATAMIENTO LARGO (15 DÍAS) UNA VEZ LA PATOLOGÍA SE HA DESARROLLADO. La respuesta estudiada antes de la administración diaria de TLR4-A1 muestra una tendencia a recuperar los umbrales basales cuando se aplica un estímulo táctil en la planta de la pata, con un efecto mantenido a lo largo de los 15 días. A pesar de existir diferencias manifiestas con el grupo control, se observaba uno u ocasionalmente ningún nvel de significancia. El efecto una hora después de la administración diaria del compuesto mostraba también una atenuación de la alodinia táctil, haciéndose máxima a partir del día 18. Cuando el estímulo se aplicaba justo sobre la rodilla (test de flexión de la rodilla), el efecto crónico mostraba una curva que se asemejaba mucho a la del grupo control; mientras que el efecto agudo mostraba incluso una atenuación aún mayor, especialmente los días 18, 20 y 22. TLR4-A1 sin embargo parecía no tener efecto sobre el dolor espontáneo (test del Catwalk).

iv. Administración intratecal de TLR4-A1.

La administración intratecal durante 5 días de TLR4-A1 (0,1 $mg \cdot kg^{-1} \cdot día^{-1}$) en ratas tratadas con MIA mostraban una reducción en la alodinia táctil y los valores volvían a los umbrales baseles la segunda y tercera semana. Por el contrario, TLR4-A1 no modificaba la hiperalgesia térmica; justo lo contrario de lo que pasaba con los animales que recibían administraciones intraperitoneales.

v. Incremento del peso corporal.

Los grupos control y MIA no presentaban diferencias de peso en ninguno de los grupos tratados con vehículo. Sin embargo, existían diferencias estadísticamente significativas cuando se comparaban animales cateterizados y no cateterizados. La caterización reducía la velocidad de increment de peso. El

tratamiento corto (5 días) con TLR4-A1 al inicio de la patología también dificultaba la ganancia de peso durante los primeros días cuando se administraba de manera intratecal pero no así cuando se administraba de manera intraperitoneal. Sin embargo, al final de los experimentos, el incremento de peso en todos los animales cateterizados coincidía con independencia de haber recibido salino o TLR4-A1. Por su parte, aunque el tratamiento largo (15 días) con TLR4-A1 una vez la patología se ha desarrollado también dificultaba la ganacia de peso durante varios días, finalmente alcanzaba niveles de peso similares a los de los grupos control y MIA.

4.1.2. Modelo de dolor quirúrgico por incisión.

Efecto farmacológico agudo vs. acumulativo crónico.

Con objeto de evitar posibles efectos indeseables como discomfort general o sedación que enmascarían la analgesia real, la administración diaria de los compuestos (10 $mg \cdot kg^{-1}$) fue dividida en dos: una primera dosis de 5 $mg \cdot kg^{-1}$ para evaluar el comportamiento del animal y una dosis de reserva para alcanzar la dosis final diaria de 10 $mg \cdot kg^{-1}$. Los ensayos de conducta fueron realizados antes y justo después de cada administración diaria.

1. Efecto antinociceptivo agudo del TLR4-A1 y de la morfina.

Los animales con incisón recuperaban gradualmente los umbrales basales hacia el noveno día cuando se estimulaba el punto medio de la superficie de la planta de la pata trasera con un aparato de von Frey electrónico. La administración intraperitoneal de morfina (5 $mg \cdot kg^{-1}$) revertía completamente la alodinia táctil durante todos los días testados. La administración de TLR4-A1 (5 $mg \cdot kg^{-1}$) también conseguía la reversion de la alodinía táctil aunque de una manera más sutil. Por su parte, TLR4-A1 (5 $mg \cdot kg^{-1}$) + morfina (5 $mg \cdot kg^{-1}$) revertía igualmente la alodinia táctil de manera similar a la morfina.

Cuando se aplicaba un estímulo calorífico, se apreciaban diferencias estadísticamente significativas hasta el día 3 u 8 al comparar con la pata contralateral o con la medida basal respectivamente en el grupo con incisión tratado con vehículo. Por el contrario, todos los grupos tratados presentaban valores que sobrepasaban los umbrales basales en todos los

tiempos analizados, siendo el grupo TLR4-A1 + morfina el que presentaba mayor grado de analgesia, seguido por mofina y finalmente TLR4-A1.

2. Efecto crónico antinociceptivo del TLR4-A1 y pronociceptivo de la morifina.

La alodinia táctil se atenuaba gradualmente desde el día 1 al 9 cuando se aplicaba el filamento electrónico de von Frey, recuperando niveles basales para el día 7. Sin embargo, diferencias estadísticamente significativas entre ambas patas se mantenían hasta el día 9, desapareciendo al día siguiente. Los registros antes de la administración diaria de morfina, mostraron por el contrario una alodinia táctil de larga duración con diferencias estadísticamente significativas que se extendían hasta el día 9 cuando se comparaban con el umbral basal o con la pata contralateral. Los datos recogidos antes de la administración diaria de TLR4-A1 mostraban un tiempo de recuperación similar a los no tratados. El registro antes de la administración intraperitoneal de TLR4-A1 + morfina mostraba una vez más un tiempo de recuperación similar al grupo no tratado, solapando incluso con sus valores.

En cuanto a los umbrales de latencia, diferencias con el día basal eran visibles hasta el día 5 en animales no tratados o hasta el día 4 al comparar con la pata contralateral. Los datos antes de la administración diaria con morfina mostraban latencias que no se recuperaban a lo largo de los 9 días. Contrariamente a esto, los registros obtenidos antes de la administración intraperitoneal de TLR4-A1 mostraban latencias similares a la pata contralateral. De hecho la recuperación ocurría de manera más rápida que en animales tratados con el vehículo. Finalmente, el tiempo de recuperación evaluado diariamente antes de cada administración de TLR4-A1 + morfina mostraba latencias que practicamente solapaban la curba descrita para los animales tratados con vehículo.

Incremento del peso corporal.

En todos los grupos analizados había diferencias estadísticamente significativas en comparación con el grupo control (sin incision). Los grupos tratados con TLR4-A1 o TLR4-A1 + morfina contaban con las mayores diferencias significativas, empezando ya desde el segundo día tras la incisión. El grupo tratado con morfina presentaba

diferencias significativas a partir del día seis, mientras que el grupo tratado con vehículo mostraba diferencias significativas a partir del día 8. Por lo tanto, tanto la incisión como el tratamiento afectaban al discomfort general a lo largo de los 9 días estudiados.

4.2. Ensayos *in vitro*.

4.2.1. Evaluación macroscópica y análisis histológico de la articulación de la rodilla.

22 días después de la infiltración de la rodilla derecha con 2 mg de MIA revelaron, rodillas izquierdas con cóndilos translucidos y rosa perlados, con superficie aparentemente intacta y lisa. Por otro lado, la rodillas infiltradas con MIA mostraban un aspecto más blanco y opaco con superficie ondulosa, marcada fibrosis y erosión. Esto se ajustaba a lo descrito previamente (Williams y Brandt, 1984; Im *et al.*, 2010; Takeshita *et al.*, 2011).

Los cambios estructurales en la articulación de la rodilla de la rata fueron evaluados microscópicamente en los diferentes grupos de ratas y puntuados de acuerdo a la puntuación de Pritzker (Pritzker *et al.*, 2006). Para analizar mejor el estado del cartílago, se realizaron tinciones con azul de toluidina y hematosina y eosina. En un primer vistazo, las secciones teñidas con azul de toluidina del grupo control mostraron una superficie articualr intacta y continua con una arquitectura normal de la matriz. Por el contrario, la inyección de MIA en la articulación femorotibial causaba erosión y deformación de los huesos subcondrales. Sin embargo, el tratamiento de 5 días con TLR4-A1 (10 $mg \cdot kg^{-1} \cdot día^{-1}$; i.p.) no parecía influir en las inyecciones intraarticulares de salino o MIA. Sin embargo, aunque las patas ipsilaterales (tratadas con MIA) de ratas tratadas con TLR4-A1 mostraban superficies articulares irregulares con un amplio área de pérdida de cartílago y degeneración, las células inflamatorias permanecían localizadas en la matriz cartilaginosa y no se extendía en forma de fibrosis fuera del cóndilo del femur o de la meseta tibial. De manera contraria a esto, las secciones de las rodillas tratadas con MIA de ratas recibiendo salino estéril mostraban una unidad femoro-tibial donde el fémur y la tibia permanecían pegados entres sí. En la tinción hematosilina y eosina, la pérdida de cartílago articular (reducción de engrosamiento) y la infiltración de células inmunes a través de fisuras verticals a través de la matriz cartilaginosa hacia el hueso subcondral se hicieron apreciables en las rodillas

ipsilaterales. Las secciones de las rodillas contralaterales mostraron cartílago articular y hueso subcondral normales de la meseta de la tibia y del cóndilo femoral, sin síntomas de discontinuidad cartilaginosa.

El análisis de la meseta tibial en tres zonas independientes de igual amplitude mostró una superficie intact sin pérdida de matriz para las tibias contralaterales (tratadas con salino) de ambos grupos, tratados con vehículo o con TLR4-A1. En clara oposición, las tibias correspondientes a rodillas tratadas con 2 mg MIA mostraron una pérdida complete de la matriz cartilaginosa para aquellos animales tratados intraperitonealmente con salino y una erosion incipiente para los animales tratados con TLR4-A1.

4.2.2. Evaluación microscópica del nervio safeno.

a) Análisis morfológico.

MODELO DE DOLOR ARTRÓSICO. En un primer vistazo, las secciones histológicas parecían morfológicamente normales. Los grupos exhibían una distribución similar de fibras nerviosas mielínicas de pequeña y amplio diámetro y de fibras no mielínicas. Las proporciones entre el grosor de la banda de mielina y los diámetros de las fibras parecían también regulares. Sin embargo, se apreciaban varios mastocitos exhibiendo metacromasia en secciones correspondientes al grupo tratado con MIA bajo tratamiento con salino inocuo. Por el contrario, solo la pata contralateral infiltrada con salino de ratas tratadas con salino intraperitoneal mostraba ocasionalmente algún mastocito solitario patrolando el endoneuro.

Los animales que recibieron MIA también exhibían síntomas claros de edema extensivo en el espacio subperineural: una clara extensión entre el perineuro y el fascículo de fibras nerviosas. Estos efectos se extendían a ambos grupos de animales: aquellos que recibían salino intraperitoneal y aquellos recibiendo TLR4-A1 durante 5 días. Por el contrario, en las patas contralaterales tratadas con salino se observaban axones apretados en estrecha asociación con el perineuro.

MODELO DE DOLOR POSTOPERATORIO. No se apreciaron grandes diferencias entre las secciones histológicas de los nervios de las patas ipsilaterales (con incisión) en referencia a la distancia del perineuro del fascículo de fibras nerviosas o el área

del endoneuro comparado con sus respectivos controles contralaterales. Tampoco se apreciaban diferencias obvias en los especímenes analizados respecto a la demielinación o daño axonal en comparación con los tejidos control contralaterales de ratas tratadas con vehículo. Las únicas excepciones a lo anteriormente citado parecían ser las patas con incisión de los grupos tratados con salino y TLR4-A1+morfina, quienes aparentemente presentaban menos densidad axonal por área de tejido nervioso (mayor endoneuro) y un fascículo de fibras nerviosas en estrecha asociación con el perineuro respecto a las patas contralaterales. Sin embargo, cualquier fibra puede resultar diferente dependiendo de la altura y del ángulo a la que se ha cortado. Las secciones de todos los grupos ocasionalmente presentaron algún mastocito solitario patrullando el endoneuro.

Cabe mencionar que los núcleos de las células de Schwann en las secciones correspondientes a ambos nervios safenos de animales tratados con morfina vinieron marcadas por una alta intensidad de la tinción con azul de toluidina.

b) Análisis morfométrico.

MODELO DE DOLOR ARTRÓSICO. El análisis morfométrico mostró la ausencia de marcadas diferencias entre los grupos para todos los parámetros utilizados. Sin embargo, todos los parámetros de las secciones correspondientes a la pata ipsilateral (tratada con MIA) de ratas tratadas intraperitonealmente con TLR4-A1 se distanciaban del resto de los grupos.

- Diámetro de la fibra. El diámetro de las fibras mielínicas era de mayor magnitud para el grupo tratado con vehículo (contra-: 4,70 µm ± 0,04; ipsi-: 4,43 µm ± 0,06) que para el grupo tratado con TLR4-A1 (contra-: 4,33 ± 0,03; ipsi-: 4,36 ± 0,03). La comparación entre los nervios contra- e ipsa-lateral de cada grupo mostraba una reducción estadísticamente significativa para el nervio ipsilateral (MIA, $P<0,001$) del grupo al que se le administró el vehículo. Los diámetros no diferían dentro del grupo tratado con TLR4-A1, aunque ambos nervios eran significativamente menores que el nervio contralateral del grupo tratado con vehículo ($P<0,001$).
- Diámetro del axón. De una manera similar, el diámetro de los axones también era de mayor magnitud para el grupo tratado con vehículo (contra-:

2,41 µm ± 0,03; ipsi-: 2,52 µm ± 0,04) que para el grupo tratado con TLR4-A1 (contra-: 2,37 ± 0,03; ipsi-: 2,34 ± 0,03). Sin embargo, el único diámetro que presentaba un aumento estadísticamente significativo en comparación con los otros era aquel del nervio ipsilateral (MIA, P<0,001) del grupo al que se le administró el vehículo.

- Grosor de la banda de mielina. Determinado por la fórmula: (D/d)/2, donde D corresponde al diámetro de la fibrea y d al diámetro del axón. La comparación entre los nervios contra- e ipsi-lateral de cada grupo mostraba una reducción estadísticamente significativa del grosor de la banda de mielina del nervio ipsilateral (P<0,001) del grupo al que se le administró el vehículo. El grosor de la banda de mielina no difería dentro del grupo tratado con TLR4-A1; estaba reducido de manera estadísticamente significativa respecto al del nervio contralateral y aumentado respecto al del nervio ipsilateral del grupo tratado con vehículo (P<0,001).
- G-ratio (d/D). Los valores para la pata ipsilateral de animales tratados con vehículo eran significativamente mayores que los de cualquier otro grupo.

  Por consiguiente, el tamaño del axoplasma estaba aumentado y el de la fibra disminuido en las patas infiltradas con MIA del grupo tratado con el vehículo, mientras que en el grupo tratado con TLR4-A1 solo el diámetro de las fibras se veía disminuido.

MODELO DE DOLOR POSTOPERATORIO. El análisis morfométrico no mostraba diferencias estadísticamente significativas entre grupos para ninguno de los parámetros estudiados.

4.2.3. Estudio inmunohistoquímico para la actividad glial.

MODELO DE DOLOR ARTRÓSICO.

- *Expresión de la molécula adaptadora de unión a calcio ionizado 1 (Iba1) en microglia.* La inyección intraarticular de MIA aumentó los niveles de microglía activada positiva para Iba-1 en la médula ipsilateral a día 22; aunque solo de manera estadísticamente significativa para las láminas superficiales (I-II) de L3 (P<0,01) y L4 (P<0,01) y para las láminas profundas (V-VI) de L3 (P<0,001). Además, el número de microglía en el asta dorsal ipsilateral en general de las secciones L3 estaba incrementado para los animales tratados con MIA (P<0,05).

El marcaje para Iba-1 en el asta dorsal ipsilateral de las ratas tratadas con TLR4-A1 durante 5 días por el contrario mostraban una patrón similar al del asta dorsal contralateral; esto es, el TLR4-A1 prevenía la activación de la microglía.

- *Expresión de la proteína ácida fibrilar glial (GFAP) en astrocitos.* La inyección intraarticular de MIA también incrementaba los números de astrocitos activados positivos para GFAP en la médula ipsilateral a día 22; aunque en este caso, solo era estadísticamente significativo para las láminas superficiales (I-II; $p<0,01$) y medias (III-IV; $p<0,001$) de las secciones L3. Además, el número total de astrocitos en el asta dorsal ipsilateral en general en las secciones L3 estaba incrementado para los animales tratados con MIA. Por otro lado, el marcaje para GFAP en el asta dorsal ipsilateral de las ratas tratadas con TLR4-A1 durante 5 días mostraba una vez más un patrón similar al del asta contralateral. Esto es, el TLR4-A1 prevenía la activación de la astroglía.

MODELO DE DOLOR POSTOPERATORIO.

- *Expresión de la molécula adaptadora de unión a calcio ionizado 1 (Iba1) en microglia.* El número de microglía activada postivia para Iba-1 en el asta dorsal ipsilateral de las ratas tratadas con salino 10 días tras la incisión quirúrgica mostraba un aumento del marcaje para las láminas superficiales (I-II; $p<0,05$) de las secciones L3 y para las láminas superficiales (I-II; $p<0,001$) y medias (III-IV; 0,05) de las secciones L4. Además, aunque no de manera estadísticamente significativa, el marcaje total de microglía en el asta dorsal ipsilateral en general de las secciones L3 y L4 estaba aumentado para los animales con incisión. Ninguno de los otros tratamientos mostraba marcaje aumentado para Iba-1, con la solo excepción del tratamiento con TLR4-A1+morfina, que mostraba un aumento de la microglía positiva para Iba-1 en las láminas superficiales (I-II; $p<0,01$) de las secciones L3.
- *Expresión de la proteína ácida fibrilar glial (GFAP) en astrocitos.* En general, no se apreciaron diferencias estadísticamente significativas entre los lados ipsilateral y contralateral para ninguno de los grupos. Sin embargo, las láminas medias (III-IV) de las astas dorsales ipsilaterales en las secciones L5 mostraban un aumento ligeramente significativo ($p<0,05$) comparado con el lado contralateral en los animales tratados con morfina y, aunque no de manera

significativa, el número total de astrocitos en el asta dorsal ipsilateral en general de la sección L5 estaba también aumentado.

4.2.4. ELISA (ensayo por inmunoabsorción ligado a enzimas)

MODELO DE DOLOR ARTRÓSICO. Los efectos en los niveles de factor de necrosis tumoral-α (TNF-α) en la médula espinal del dolor artrósico de larga duración se estudiaron los días 22 y 50 después de la artrosis de rodilla inducida por MIA. No se observaron diferencias estadísticamente significativas en la sección lumbar de las médulas espinales comparado con animales sanos normales. Tampoco se observaron diferencias estadísticamente significativas en el grupo tratado durante 5-días con TLR4-A1 (10 $mg \cdot kg^{-1} \cdot day^{-1}$). Sin embargo, el grupo tratado con MIA mostraba los niveles de TNF-α más bajos de entre lost res grupos analizados.

MODELO DE DOLOR POSTOPERATORIO. Los efectos del dolor agudo postoperatorio que surgen de un procedimiento quirúrgico se analizaron para los niveles del factor de necrosis tumoral (TNF-α) y de las citoquinas proinflamatorias de expresión temprana interleucina-6 (IL-6) e interleucina-1β (IL-1β) en un estadío más temprano (día 4 y 10). Todos los grupos experimentales presentaron niveles similares para cada proteína proinflamatoria para el día 4.

En el día 10, solo los niveles de IL-6 mostraban diferencias estadísticamente significativas en todos los grupos cuando se comparaba con el control sano (intacto). Además, los niveles de IL-6 de los grupos tratados con TLR4-A1 y con morfina eran significativamente mayores que aquellos del grupo con incisión. Dicho esto, todos los grupos excepto el control intacto mostraban mayores niveles de IL-6 el día 10 que el día 4.

Por otra parte, aunque no de manera estadísticamente significativa, los niveles de IL-1b también eran mayores para el día 10. Aunque no se observaba ninguna diferencia clara entre los grupos experimentales.

Con respecto al TNF-α, los niveles permanecieron estables para todos los grupos el día 4. Sin embargo, todos los grupos con incisión experimentaron un descenso para el día 10, especialmente visible en los grupos tratados (morfina, TLR4-A1 y TLR4-A1 + morfina). Las barras de error deben seguramente haber dificultado la existencia de niveles de significancia entre ambos días analizados.

5. DISCUSIÓN

Discusión general.

Durante la pasada década, diversos estudios han puesto de manifiesto la enorme contribución al desarrollo y mantenimiento del dolor crónico por parte de las células gliales en la médula espinal y, a tal efecto, los receptores TLR4 se han postulado como elementos con un papel fundamental en este asunto (Bettoni *et al.*, 2008; Milligan y Watkins, 2009). La unión de ligandos endógenos a los receptores TLR4 activa la célula, la cual comienza a producir y liberar una serie de sustancias (prostaglandinas, aminoácidos excitadores, factores de crecimiento y citoquinas proinflamatorias) que potencian el dolor incrementando la excitabilidad de las neuronas vecinas (Tanga *et al*., 2005; Sauer *et al*., 2014). A este respecto, nos propusimos estudiar y comparar los cambios fisiológicos que pudieran ocurrir a nivel tanto periférico como espinal en dos modelos de dolor en animales de experimentación: uno capaz de generar dolor mixto (neuropático y nociceptivo) y otro en principio solo nociceptivo. A pesar de la existencia de una evidente relación, los resultados de este trabajo se discutirán por separado en dos bloques diferentes, de acuerdo al mecanismo de nocicepción subyacente en cada modelo.

En primer lugar, se eligió por su gran reproducibilidad un modelo clásico de dolor mixto, consistente en la generación de un estado artrósico en rata. Se llevó a cabo un estudio comparativo entre la analgesia resultante de la administración de un bloqueante sintético del receptor TLR4 (TLR4-A1) y la morfina. Seguidamente, con objeto de evaluar la fiabilidad de esta molécula TLR4-A1 en desenmascarar presuntas vías de señalización nociceptiva mediadas por el receptor TLR4, tres diferentes protocolos farmacológicos fueron llevados a cabo: (1) administración intraperitoneal o (2) intratecal, durante los primeros cinco días inmediatamente después de inducir la patología; y (3) de administración intraperitoneal, después de que la patología se hubiera desarrollado completamente. Esta parte representa una continuación de trabajos previos desarrollados en nuestro laboratorio sobre la acción analgésica de dos diferentes bloqueantes del receptor TLR4 (TAK-242 o CLI-095 y TLR4-A1) en un modelo de dolor neuropático inducido por un agente quimioterapéutico (Goicoechea *et al*., 2011; Pascual *et al*., 2011; Rincón Carvajal *et al*., 2011). Como se ha descrito anteriormente, los receptores TLR4 podrían no solo estar participando en el desarrollo de un comportamiento de hipesensibilidad en un modelo de dolor artrósico inducido por iodoacetato, sino también estar tomando parte en las características histopatológicas de la enfermedad. Dado que las células gliales en la médula espinal contribuyen a este comportamiento de dolor crónico (Sagar *et al*.,

2011), nuestro propósito consistió primero en determinar el grado de implicación del receptor TLR4 en esta hipersensibilidad, y segundo en distinguir la nocicepción mediada por receptores TLR4 periféricos de receptores centrales, a través de un estudio integrativo de los muchos cambios fisiológicos e histológicos que ocurren en diferentes localizaciones (nervio periférico y médula espinal).

El segundo bloque, analiza la implicación de los receptores TLR4 en la nocicepción de carácter transitorio que tiene lugar tras el postoperatorio en un modelo típico de dolor nociceptivo en rata y que cursa con alodinia e hiperalgesia durante menos de una semana. En este caso, además del efecto analgésico agudo del compuesto TLR4-A1, se evaluó también el tiempo de recuperación tras repetidas administraciones del fármaco. El objetivo estaba básicamente dirigido a determinar la contribución de los receptores TLR4 en la nocicepción a corto plazo. De manera sinérgica, el efecto de la morfina administrada de manera repetida durante días sobre el tiempo de recuperación después de la cirugía y el fenómeno de tolerancia e hipersensibilidad inducida por opioides fueron también estudiados. Se ha descrito que la administración repetida de morfina potencia la duración de la alodinia en modelos de dolor periférico e inflamatorio y activa las células gliales en la médula espinal (Loram *et al*., 2012), y a este respecto nos propusimos comprobar qué pasaba en un modelo de dolor postquirúrgico. Los cambios fisiológicos e histológicos que ocurrían en diferentes localizaciones fueron evaluados de la misma forma y manera que en el bloque previo.

5.1. Modelo de dolor artrósico de rodilla inducido químicamente con monosodio iodoacetato

a) Comprensión del estado de dolor crónico y sus mecanismos en el modelo de artrosis en rata.

Durante el proceso de crecimiento, la epífisis, en los mamíferos, produce e incorpora nueva matriz cartilaginosa al extremo de los huesos largos, mientras que se reabsorbe y osifica en la zona más cercana a la diáfisis del hueso. Es decir, la osificación y eliminación de cartílago en huesos como tibia o fémur avanza desde la diáfisis (o centro) hacia sus epífisis (o extremos). Una vez que las epífisis han sustituido toda la matriz cartilaginosa por hueso, el crecimiento se detiene (Geneser, 2000). En humanos, dicho proceso de crecimiento comienza en el segundo trimestre de la gestación y finaliza alcanzado el estado adulto, hacia los veinte años de edad (García Poblete *et al.*, 2006). Sin embargo,

a esta misma edad equivalente en ratas, todavía existe potencial de crecimiento del hueso largo (Poole *et al.*, 2010). De hecho, las placas de crecimiento en roedores adultos permanecen abiertas a pesar de haber alcanzado la edad de madurez sexual (Aigner *et al*., 2010). Esta es probablemente la razón por la que después de inducir la artrosis en el modelo aquí empleado, observemos al analizar los comportamientos nociceptivos de los animales, una tendencia al alza que acaba por estabilizarse sin alcanzar los umbrales basales. Sospechamos por tanto, que podría estar dándose un proceso de remodelación de la articulación de la rodilla debido posiblemente al afloramiento de los condrocitos desde las columnas dispuestas de manera perpendicular y ordenada en la zona de mineralización. De hecho, los análisis de las secciones histológicas de las rodillas recogidas 22 días después de la inyección de MIA mostraban una remodelación de la unidad hueso-cartílago con síntesis ocasional de cartílago junto a la superficie articular (Fig.16). Por consiguiente, a pesar de la buena aproximación a la enfermedad artrósica en humanos que el modelo inducido por MIA pueda representar, un modelo de roedores ideal para la artrosis en humanos parece ser, como se ha sugerido desde hace tiempo, imposible de alcanzar.

Dicho esto, la inyección intra-articular de MIA en la rodilla origina un modelo agudo para el estudio de la degradación del cartílago y del dolor articular y, a este respecto, debemos ser críticos respecto a lo que el modelo nos cuenta. Dado que la artrosis es un proceso activo que resulta en la ruptura del equilibrio entre la formación y destrucción de cartílago, tomar como ejemplo las placas de crecimiento de los roedores puede ser de gran utilidad para entender cómo combatir el desequilibrio metabólico originado en el cartílago articular en la enfermedad artrósica en humanos. En este sentido, las medidas histomorfométricas de los cambios estructurales en la unidad hueso-cartílago en este trabajo han sido, en la medida de lo posible, evaluadas y valoradas de acuerdo a los procedimientos establecidos por la OARSI, para así poder alcanzar una mejor estandarización del análisis de dichos cambios.

Como se ha descrito con anterioridad (Ferreira-Gomes *et al.*, 2008; Procházková *et al*., 2009), la inyección intraarticular de 2 mg de iodoacetato sódico (MIA) en la cavidad articular de la rodilla resulta en la reducción de los umbrales de nocicepción tras estimular, de manera aguda, la articulación de la rodilla mecánicamente (knee-bend

test) o la planta de la pata de manera táctil o térmica (tests de von Frey test y de Hargreaves respectivamente). Sin embargo, esta reducción era más pronunciada (mayor grado de nocicepción; mayores diferencias estadísticamente significativas) para el knee-bend y von Frey tests que para el test de retirada de la pata (test de Hargreaves). En realidad, se considera un hecho establecido que tras una lesión periférica, se produce un aumento en la intensidad de la respuesta frente a un estímulo mecánico, normal e inocuo en el tejido intacto situado alrededor del lugar de la lesión, pero no así un cambio en el umbral nociceptivo frente a estímulos térmicos (Cousins *et al*., 2008; Kam y Power, 2008). Además de esto, también se hizo evidente una mayor distribución del peso corporal sobre la pata no tratada con MIA (Catwalk test), evidenciando la existencia de nocicepción espontánea. Se cree que estos cambios son el resultado de procesos que tienen lugar en el asta dorsal de la médula espinal tras una lesión, y constituyen el santo y seña de la sensibilización central.

Seguidamente, se llevó a cabo un análisis del aspecto macroscópico de la superficie del cartílago articular con objeto de correlacionar el dolor articular inducido por MIA con alteraciones estructurales en los componentes de la articulación de la rodilla. Dicha evaluación mostró un extenso deterioro de las superficies del cartílago en tibia y fémur, con abundante fibrosis, lo que en efecto parecía correlacionarse con lo observado en los tests de comportamiento. Dado que cuando se estudia una única parte de una sección no suele representar exactamente la sección entera, y dado que un análisis general del conjunto pierde mucho detalle, la meseta tibial fue sometida a análisis histológicos bajo el microscopio y examinada de manera más precisa en tres zonas. Una vez más, como se ha descrito anteriormente (Ferreira-Gomes *et al.*, 2008), la histología de la rodilla casaba con los tests de comportamiento, mostrando una amplia degeneración y una pérdida completa de la matriz cartilaginosa a lo largo de toda la superficie articular (desde la parte lateral más externa hasta parte medial más interna).

La sensibilización periférica está caracterizada por la interacción entre los nociceptores periféricos y la inflamación, y puede iniciar el típico dolor de articulación artrósica vía sensibilización central. La correlación del análisis del comportamiento animal junto con parámetros neurofisiológicos periféricos numéricamente cuantificables puede proporcionar información objetiva sobre los procesos fisiopatológicos de la génesis de dolor. Existe un número muy reducido de estudios sobre los cambios en la composición

morfológica de los nervios periféricos en ratas, quizás debido a la relativa facilidad de los estudios electrofisiológicos comparados con los histológicos. Como se ha descrito previamente en la literatura, el nervio safeno, conocido por inervar la estructura de la rodilla, es un nervio puramente sesitivo (Porr *et al*., 2013; Tassone y Raghavendra, 2015). La pregunta acerca de si las fibras A o C, o si las fibras dañadas o intactas son más importantes para la producción de dolor espontáneo permanece aún sin respuesta. En este estudio, las fribras nerviosas gruesamente mielinadas (táctiles de bajo umbral y propioceptivas) y las finamente mielinadas (termorreceptivas) fueron evaluadas. Las fibras amielínicas C permanecieron sin estudiarse. Los axones periféricos no son estructuras quiescentes. Su morfología (y también sus funciones fisiológicas) está sujeta a las células de Schwann mielinizantes que las enrollan. Parece ser que las células de Schwann determinan la densidad de empaquetado de los neurofilamentos axónicos y de ahí, el calibre del axón. La mielinización aumenta localmente el calibre del axón, mientras que la hipomielinización de los axones resulta en la reducción del diámetro axonal. De manera adicional, una elevada densidad de neurofilamentos (bajo calibre axonal) se ha visto en ciertos casos de neuropatía (Cole *et al*., 1994). Teniendo esto en cuenta, bajo condiciones normales el nervio consiste en un simple haz (fascículo) de fibras nerviosas aferentes. Dentro de este fascículo, cada fibra nerviosa (mielínica o no) está envuelta por un laxo tejido conjuntivo de sostén llamado endoneuro. A su vez, el fascículo está rodeado de una capa de colágeno cubierta de células epiteliales, esto es, el perineuro. En las secciones de nervio correspondientes a las rodillas inyectadas con MIA, el porcentaje del área de endoneuro parecía no tener diferencias en comparación con su contralateral, sin embargo se apreciaba claramente un amplio edema en el espacio subperineural y un aumento de la presencia de mastocitos. La explicación más factible es que las condiciones inflamatorias confieren una alteración del perineuro y/o de las berreras capilares en el endoneuro (Antonijevic *et al*., 1995), lo que perimitiría a las células inmunes patrullar el endoneuro con asiduidad. Los diámetros de las fibras nerviosas mielinizadas y el grosor de la banda de mielina se había visto reducido, mientras que los diámetros de los áxones estaba aumentado en comparación con el nervio control contralateral. La proporción del diámetro del axón respecto al diámetro total de la fibra (G ratio) fue también calculada y mostró valores incrementados. Esto significa que el tamaño de la fibra nerviosa en su conjunto estaba reducido

(hipomielinazado), cursando con engrosamiento axoplásmico que resultaba en un medio inflamado – como se deduce de los numerosos mastocitos observados–.

La determinación de células microgliales o astrocitos peroxidasa positivas fue determinada por medio de histoquímica con DAB e inmunodetección contra el marcador específico de microglía Iba-1 o contra el marcador específico de astrocitos GFAP como corresponda. Se observó un aumento del marcaje para Iba-1 en las ratas tratadas con MIA para el día 22, lo que indica activación glial. El marcaje para Iba-1 estaba aumentado de manera significativa en las láminas superficiales y profundas del asta dorsal ipsilateral en la sección lumbar L3 y en las láminas superficiales del asta ipsilateral en la sección lumbar L4 de ratas tratadas con MIA, comparado con elasta dorsal contralateral. El marcaje positivo para GFAP en astrocitos también se vió significativamente aumentado en las láminas superficiales y medias del asta dorsal ipsilateral en la sección lumbar L3 de ratas tratadas con MIA, en comparación con el asta dorsal contralateral. Se piensa que las láminas superficiales en el asta dorsal reciben la llegada de fibras finamente mielinadas (Aδ) y amielínicas (C) de termorreceptores y nociceptores (nociceptores mecanosensitivos), mientras que las láminas más profundas reciben la llegada de fibras gruesamente mielinadas (A) conocidas como aferencias mecanosensitivas de bajo umbral (receptores táctiles que señalizan vibración, tacto y presión) (Lu, 2008;Watson *et al*., 2012). Por consiguiente, el incremento del marcaje para Iba-1 y GFAP de las láminas superficiales es consistente con el comportamiento nociceptivo visto para el test de retirada de la pata (paw-flick), mientras que el incremento del marcaje para Iba-1 en las láminas profundas es consistente con el comportamiento nociceptivo más marcado visto para los tests de von Frey y knee-bend. La activación microglial se considera el primer estadío de la inflamación del Sistema Nervioso Central (SNC). La ausencia de elevado marcaje para GFAP en láminas más profundas puede atender a la activación más temprana de Iba-1. La activación en la sección lumbar L5 permaneció inalterada para ambos tipos de células gliales, al comparar con la médula contralateral y con la médula ipsilateral de ratas tratadas con salino. Esto debe ser debido al hecho de que el nervio femoral, que recibe la rama articular del nervio safeno de la articulación de la rodilla, contacta con las secciones espinales L3 y L4, pero no con L5, la cual es dominio exclusivo del nervio

ciático. Por consiguiente, hasta aquí, consideramos probada la reproducibilidad del modelo en nuestras instalaciones.

b) *Estudio sobre el papel de los receptores TLR4 en un modelo de artrosis en rata.*

El efecto analgésico de la administración aguda de TLR4-A1 ocurría a los 30 minutos, con un efecto máximo entre los 30 minutos y 1 hora de duración hasta 1 hora–1 hora 30 minutos, como se deduce de los tests de estimulación aguda. Sin embargo, los efectos parecía continuarse cuando ningún estímulo era aplicado (Catwalk test). Este puede explicarse de la siguiente manera. El dolor neuropático está caracterizado por dolor espontáneo, alodinia e hiperalgesia, con un papel determinante de los mediadores inflamatorios en la sensibilización aferente (Djouhri *et al*., 2006). La estructura química del compuesto TLR4-A1, que presenta un catión amonio cuaternario, presumiblemente le dificulta atravesar la barrera hematoencefálica. Sin embargo, una pequeña cantidad debe conseguir cruzar desde la periferia al sistema nervioso central; por consiguiente, los primeros efectos en desaparecer corresponden a aquellos que se oponen al estímulo aplicado en un lugar remoto de la fuente de daño (von Frey test). La gran mayoría de moléculas de TLR4-A1 deben permanecer en la periferia; por lo tanto los siguientes efectos en desaparecer concuerdan con aquellos que se oponen a estímulos aplicados en el sitio preciso de la lesión (knee-bend test). La deleción del dolor espontáneo es el último efecto en desaparecer. Este tiene especial sentido por dos razones: primero, la ausencia de un estímulo externo; y segundo, siendo TLR4-A1 un compuesto anfifílico, es dado a agregar, existiendo por consiguiente la probabilidad de un pequeño efecto residual con forme los agregados se disuelven.

La administración repetida de TLR4-A1 no resultaba en tolerancia, como demuestran los resultados obtenidos de los tests de estimulación aguda: el efecto agudo, evaluado diariamente 1 hora después de la administración intraperitoneal durante el curso de quince días, mostraba una analgesia similar para cada día testado. Sin embargo, con la excepción del primer día, TLR4-A1 parecía no tener efecto alguno sobre la nocicepción espontánea ningún día.

La administración intraperitoneal del compuesto TLR4-A1 durante 5 días comenzando poco después de la inyección intra-articular de MIA demostró un perfil analgésico doble. Durante una primera fase (primeras dos semanas) la alodinia estaba completamente contrarrestada; sin embargo, durante una segunda fase (siguientes dos semanas) había

una tendencia a imitar los resultados obtenidos para los animales tratados con MIA sin tratamiento farmacológico. Esto podría explicarse de la siguiente manera: durante las primeras dos semanas, TLR4-A1 administrado de manera repetida durante casi una semana bloquea el efecto llamada de las células inmunes que habría causado una rápida sensibilización de las fibras nerviosas aferentes. Sin embargo, el daño (muerte de condrocitos) es evidente. Cuando la presencia de TLR4-A1 cesa, la reparación del tejido se reanuda progresivamente, sensibilizando el nervio periférico. No se observaron diferencias comparadas con la pata contralateral control cuando se estimulaba con una fuente de calor. Como se ha mencionado anteriormente, la existencia de una respuesta aumentada a un estímulo mecánico (táctil) no nocivo pero ausencia de respuesta a un estímulo térmico en una zona remota al sitio de la lesión indica la existencia de sensibilización central. Dado que solo la hiperalgesia térmica ha sido completamente bloqueada, este tratamiento con TLR4-A1 parece estar bloqueando el componente nociceptivo pero no neuropático del dolor. Este es consistente con la hipótesis mencionada anteriormente que sugería la predominancia de un papel periférico cuando es administrado de manera sistémica. El efecto de TLR4-A1 también se mantenía durante los 15 días de tratamiento cuando ambas articulaciones de la rodilla y un área remota eran estimuladas, aunque la analgesia era más marcada para el primero. Por otra parte, este protocolo farmacológico no parecía tener efecto sobre la nocicepción espontánea. La presencia de nocicepción espontánea junto con los escasos efectos anti-alodínicos cuando un lugar remoto a la lesión era estimulado subrayaron el efecto periférico (pero no central) que la administración sistémica tenía. Este fue corroborado más adelante con los resultados obtenidos en la administración intratecal: una administración intratecal durante 5 días del compuesto TLR4-A1, empezando poco después de la inyección intra-articular de MIA, confinaba el compuesto al sistema nervioso central. El compuesto no podía hacer frente al masivo efecto llamada inflamatorio generado en la periferia, por consiguiente, durante la primera semana la alodinia se vio incrementada. Sin embargo, con forme pasaba el tiempo, no se observaba sensibilización central alguna, como sugiere la ausencia de alodinia distal tras la primera semana. Por el contrario, la nocicepción era evidente a lo largo de tres semanas como se deduce de la hiperalgesia térmica. En este caso, el componente neuropático del dolor pero no el nociceptivo parecía estar bloqueado.

El examen macroscópico de las articulaciones de las rodillas mostraba que TLR4-A1 protegía de alguna manera del extenso daño. Aunque las estructuras de las patas ipsilaterales y sus contralaterales eran notablemente diferentes a primera vista, el estado no parecía ser tan malo como se apreciaba con las ratas a las que no se le dio TLR4-A1. La escasa presencia de osteocitos en los cóndilos femorales y la apariencia blanco opaca de las mesetas tibiales nos hizo pensar que el MIA estaba ejerciendo su acción inductora de apotosis, pero no se producía una respuesta inflamatoria masiva reclutada al tejido dañado ya que no se apreciaba ningún grado de fibrosis. De hecho, al examinar las secciones teñidas de las rodillas al microscopio, se veía la erosión del cartílago junto con las nuevas células que rellenaban y proliferaban en las fisuras de la matriz cartilaginosa, sin embargo no se apreciaba un crecimiento incontrolado de pannus más allá del límite de la superficie articular (sinovitis). Esta proliferación más organizada de células en las ratas tratadas con TLR4-A1 puede ser explicada por su acción periférica durante los cinco tempranos días en que se administró sistemáticamente.

De manera similar a las secciones de nervio correspondientes a las rodillas inyectadas con MIA de animales tratados con salino, el porcentaje del área de endoneuro en animales tratados durante 5 días con TLR4-A1 no mostraron diferencias aparentes en comparación con su nervio contralateral, y un edema era también evidente en el espacio subperineural. Sin embargo, no se observaba la presencia aumentada de mastocitos. Los diámetros de las fibras nerviosas, sus correspondientes axones y el grosor de las bandas de mielina permanecieron invariables en comparación con los nervios contralaterales. Lo mismo ocurría para la razón G (G ratio). Esto es, la administración temprana de TLR4-A1 protegía de alguna manera de alteraciones en el grosor de la banda de mielina o en el calibre del axón. Además se correlacionaba particularmente con la ausencia de activación glial en el asta dorsal ipsilateral (con la única excepción del marcaje contra GFAP en las láminas profundas del segmento L3). Esto también se correlacionaba con lo observado en los tests de comportamiento: falta de hiperalgesia térmica y solo alodinia táctil en estados tardíos cuando un sitio remoto a la articulación de la rodilla era estimulado.

Como apreciación final, los niveles de TNF-α en las secciones de médula espinal correspondientes a un fragmento aproximadamente L2-L6 también fueron examinados,

observándose diferencias significativas en la expresión proteica de esta citoquina de expresión temprana en ninguno de los grupos en los días analizados (22 y 50).

5.2. Modelo de dolor postoperatorio inducido quirúrgicamente por incisión en la planta de la pata.

El modelo de dolor postoperatorio utilizado en este trabajo fue desarrollado por primera vez hace dos décadas por Brennan y cols. El modelo ha sido usado de manera repetida durante años por diferentes grupos variándolo con ligeras modificaciones.

La estimulación táctil en de un punto distante situado a 1 cm de la herida (área de hiperalgesia secundaria) daba lugar a diferencias (comparado con el grupo control) que se extendían hasta el día 9 para el test de von Frey y hasta el día 3-4 para el test de retirada de la pata (paw-flick). Esta presunta sensibilización periférica puede contribuir a la hipersensibilidad al dolor y a la inflamación. Sin embargo, los análisis de las fibras nerviosas periféricas rara vez mostraban algún macrófago patrullando el endoneuro en ambas patas contralateral e ipsilateral. Dado que la apariencia macroscópica de los nervios puede conducirnos a conclusiones erróneas, una serie de parámetros fueron analizados con la intención de ser más objetivos. El diámetro de las fibras nerviosas y el de sus correspondientes axones, el grosor de la banda de mielina y la razón G no variaban demasiado entre los diferentes grupos. Esto es, después de 10 días, no se apreciaban cambios a nivel nervioso inducidos por la incisión en la planta de la pata trasera.

De acuerdo con los análisis en busca de marcador microglial (Iba-1) en las astas dorsales de la médula espinal, se apreció un aumento del marcaje para Iba-1 a día 10 en las láminas superficiales del asta dorsal ipsilateral en secciones lumbares L3 y en láminas superficiales y medias del asta dorsal ipsilateral en la sección lumbar L4 de ratas con incisión, en comparación con el asta dorsal contralateral. Por el contrario, no se observaron cambios significativos para el marcaje contra la proteína GFAP. Los astrocitos contribuyen a mantener el dolor crónico y la ausencia de activación a día 10 respaldaría la condición aguda de este modelo de dolor. El aumento sustancial de la activación de la microgía solo en las láminas superficiales sugiere la existencia de dolor nociceptivo. Esto guarda consistencia con los descubrimientos realizados por un grupo

diferente (Romero-Sandoval *et al*., 2008), que afirmaban que la expresión aumentada del marcador de microglia Iba1 y del marcador de astrocitos GFAP en el asta dorsal de la región lumbar de la médula espinal está asociado con comportamientos alodínicos después de una incisión quirúrgica. Sin embargo, como ellos mismos mencionaban, después de remitir el comportamiento hipersensitivo, la expresión de Iba1 y GFAP volvía a niveles de expresión basales, de tal manera que el aumento significativo de la expresión de éstos podría ser evidente en todo el asta dorsal, o solo en las láminas superficiales y profundas dependiendo de cuánto tiempo hubiera pasado desde la incisión quirúrgica.

El nivel de IL-6 en un homogeneizado de secciones L2-L6 de médulas espinales estaba marcadamente incrementado a día postoperatorio 10 comparado con el día postoperatorio 4 y con el grupo sano control. Cualquier otra citoquina (TNF-α o IL-1β) mostraba niveles similares a los del grupo control, aunque ligeramente reducidos en el día postoperatorio 10 para TNF-α. Se han descrito altos niveles de IL-6 en algunas condiciones inflamatorias crónicas, especialmente relacionadas al proceso inflamatorio que sigue a una lesión nerviosa, y al inicio y mantenimiento del dolor neuropático (Starkweather, 2010). Una elevada actividad de IL-6 ha sido igualmente asociada a elevadas producciones de NGF en astrocitos, como también se ha encontrado en algunas neuropatías (Vargas *et al*., 2004).

a) *Estudio del papel de los receptores TLR4 en el modelo postoperatorio en rata.*

Siguiendo el mismo sistema de planteamiento de tests en el sitio medio de la planta de la pata trasera mencionado antes, el efecto del tratamiento crónico con TLR4-A1 administrado de manera sistémica causaba la disipación de cualquier signo de alodinia táctil significativa desde el día cinco en adelante, cinco días antes de lo que lo hacía sin tratamiento (grupo con vehículo). Además, la hiperalgesia térmica desaparecía después de la primera administración, dos o tres días antes de lo que lo hacía en el grupo no tratado. Por otro lado, el efecto agudo de TLR4-A1, es decir, las respuestas evaluadas poco después de la administración sistémica diaria, mostró ser analgésica. Solo dos días (4 y 5) mostraban de manera significativa un descenso de los umbrales de retirada comparado con el nivel basal, mientras que el resto de los días prácticamente solapaban los datos obtenidos para la pata sin incisión. Para el paw-flick test se veía un efecto

antihiperalgésico para la mayoría de los días. Esto podría sugerir un efecto antiinflamatorio para TLR4-A1 en la periferia, ya que los modelos de dolor inflamatorio están caracterizados por un descenso de los umbrales de latencia (Ren y Dubner, 1999; Huang *et al*., 2006). Sin embargo, el otro componente, la estimulación táctil estaba solo bloqueada parcialmente, lo que sugería que el dolor quirúrgico es diferente del dolor inflamatorio estricto, pero también del dolor neuropático.

Los nervios periféricos no parecían muy diferentes a los del grupo no tratado. Los diámetros de las fibras nerviosas y sus axones, el grosor de la banda de mielina y la razón G permanecieron prácticamente invariables comparados con los nervios contralaterales. Esto es, TLR4-A1 parecía tener un efecto protector.

En relación al marcaje inmunohistoquímico para la activación glial, no se observaron diferencias estadísticamente significativas en el asta dorsal ipsilateral de las ratas con incisión, en comparación con los astas dorsales contralaterales. El perfil de citoquinas fue similar al de los animales no tratados que sufrieron una incisión en sus patas traseras.

b) *Comprensión de los mecanismos subyacentes a la transición desde un estado de dolor agudo a subcrónico después de administraciones sistémicas repetidas de morfina.*

Se piensa que los opioides son capaces de activar sistemas de dolor tanto inhibitorio como facilitatorio, y la predominancia de uno sobre otro conducía a mecanismos anti o pronociceptivos (Freye, 2010). Existe un gran interés en desarrollar aproximaciones conducidas a usar administraciones concomitantes de fármacos con opioides (ej.: antagonistas de NMDA, NSAID, agonistas α-2) o rotaciones de opioides, de tal manera que el paciente puede disfrutar de los efectos beneficiosos (analgésicos) de los opioides evitando la hipersensibilidad inducida por opioides (OIH) (Herrera *et al*., 2009). Sin embargo no hay estrategias completamente efectivas para evitar la OIH a fecha de hoy (Horvath RJ, Romero-Sandoval EA, De Leo JA., 2010). El uso de protocolos minuciosamente detallados de hiperalgesia inducida por opioides (de acuerdo con la exposición aguda o crónica, a altas o bajas dosis, tipo de opioide y ruta de administración) son esenciales para obtener respuestas observables y medibles ya que incluso cuando se emplean modelos animales, la OIH puede parecen tolerancia o ser

confundida con el efecto de retirada. Y más importante, diferentes mecanismos pueden subyacer al fenómeno en cada circunstancia específica (Low *et al*., 2012).

Normalmente se refiere a la hiperalgesia inducida por opioides (OIH) como altas dosis de opiáceos, sin embargo se habla poco sobre dosis bajas. Por consiguiente, utilizamos como referencia la dosis dada en (Loram *et al.*, 2012). Consideramos 5 $mg \cdot kg^{-1}$ como la dosis limitante para producer analgesia sin sedación, y por tanto el límite entre dosis altas y bajas de morfina, y la administramos de manera intraperitoneal dos veces al día durante nueve días consecutivos a las 12h y a las 18h ((Horvath *et al.*, 2010), el equivalente a dos inyecciones diarias de 10 $mg \cdot kg^{-1}$ durante el curso de 24 h, pero reducida la dosis a la mitad). Además, contamos con el conocimiento de que los ratones que recibían tratamiento de morfina crónica (10 $mg \cdot kg^{-1}$, sc dos veces al día durante 4 días) no desarrollaban tolerancia en un modelo de dolor inflamatorio (Zollner *et al*., 2008).

Como se ha afirmado antes para los otros dos grupos, el umbral de retirada por estimulación con filamentos de von Frey y el umbral de latencia ante un estímulo calorífico fueron medidos antes de la cirugía y después dos veces diarias a lo largo de 9 días. El efecto crónico de la morfina en respuesta a estímulos táctiles aplicados en un sitio situado a 1 cm de la incisión mostraba la ausencia de recuperación de los umbrales basales y estaba incluso lejos de los resultados obtenidos para la pata con incisión en animales sin tratamiento. Lo mismo ocurría con las latencias de retirada ante un estímulo calorífico, que pueden dividirse particularmente en dos fases: una fase temprana con latencias que se solapan con aquellas de animales sin tratamiento, y una segunda fase donde todos los grupos dejan a los animales tratados con morfina atrás, los cuales no se recuperan. Exactamente del mismo modo al ya descrito, no se apreciaba recuperación cuando los estímulos se aplicaban inmediatamente adyacentes a la incisión. La administración repetida de morfina visiblemente enlentecía el tiempo normal de recuperación.

Por otra parte, el efecto agudo de la morfina estaba preservado. Efectos antialodínicos sostenidos fueron observados durante todos los nueve días, solapando con los umbrales del grupo control sano a lo largo de todo el curso del experimento. La analgesia (esto es, latencias superiores a la línea basal) eran también evidentes y manternidas en todos los

tiempos. Podemos concluir por tanto que no se desarrolló tolerancia a la administración de morfina. Y el impedimento de la recuperación debe corresponderse a dependencia física o a la hipersensibilidad inducida por opioides.

El análisis de las secciones de los nervios periféricos mostraba valores similares para el diámetro de las fibras y sus axones correspondientes, así como para el grosor de la banda de mielina y la razón G. Es decir, la morfina no afectaba de una manera visible a la pata. De acuerdo con un estudio anterior (Horvath *et al.*, 2010), no se observan cambios en la expresión de Iba1 y GFAP en el asta dorsal entre grupos cuando la morfina es administrada de manera crónica. Del mismo modo, nosotros no observamos diferencias estadísticamente significativas en el asta dorsal ipsilateral de ratas con incisión, comparadas con el asta contralateral. Una vez más, el perfil de las citoquinas fue similar al de los animales sin tratamiento que sufrieron una incisión en sus patas traseras.

c) *Estudio del tiempo de recuperación cuando la morfina se administra de manera repetida junto con TLR4-A1 como coadyuvante.*

Iniciamos la discusión de esta sección teniendo en cuenta la idea de que la modulación de la glía podría atenuar los síntomas del dolor neuropático y aumentar la efectividad de la morfina (Mika, 2008). De acuerdo con Due y cols. (Due *et al.*, 2012), la activación del complejo TLR4/MD2 por el metabolito M3G de la morfina parace ser responsible de la inducción del comportamiento nociceptivo táctil pero no térmico. Por consiguiente, utilizamos una molécula bloqueadora del receptor TLR4 como coadyuvante de la administración de morfina para comparar lo que veíamos con el grupo tratado con morfina previamente descrito. Cuando la molécula bloqueante del receptor TLR4 precedía la administración de morfina, el efecto crónico sobre los tiempos de recuperación se asemejaba estrechamente a aquél de los animales con incisión del grupo sin tratamiento. Esto es, ninguno de los compuestos administrados parecía tener ningún efecto sobre el tiempo de recuperación normal de las ratas con cirugías en las patas traseras. Sin embargo, cuando se examinó el efecto agudo diario, se produjo un efecto agudo antialodínico resultante de la sinergia entre los patrones de los umbrales para ratas tratadas con TLR4-A1 y con morfina. La analgesia aguda en respuesta a la estimulación térmica también parecía bastante evidente y consistente con el efecto

sinérgico de estos dos agentes. Por consiguiente, la combinación del compuesto bloqueante TLR4-A1 con morfina resultaba en los efectos beneficiosos (analgésicos) de la morfina sin empeorar o impedir el tiempo de recuperación medio que se producía a corto plazo. Es decir, se confirmaba que ninguno de los compuestos administrados parecía tener efecto alguno en el tiempo normal de recuperación de las ratas con cirugías en las patas traseras cuando se daba una combinación de ambos y, lo que es más, en clara oposición a Due y cols., la activación de los receptores TLR4 mediada por morfina parecía ser responsable tanto del comportamiento nociceptivo táctil como térmico.

Las secciones de los nervios también mostraron diámetros invariables para las fibras y nerviosas y sus axones, en comparación con el nervio contralateral. El grosor de la banda de mielina y la razón G también permanecieron inalterados. En relación al marcaje glial, no apreciamos diferencias estadísticamente significativas en el asta dorsal ipsilateral de ratas con incisión, en comparación el asta contralateral. Como ya se ha descrito para los otros dos grupos tratados, el perfil de las citoquinas era similar al de los animales no tratados con incisión en las patas traseras.

Podemos por tanto concluir que la incisión alteraba los niveles de IL-6 de un modo similar en todos los grupos con independencia del tratamiento dado.

6. CONCLUSIONES

En base a los resultados obtenidos a partir del **modelo de dolor artrósico de rodilla inducido con yodoacetato monosódico**, podemos afirmar que:

1. El bloqueo de los receptores TLR4 puede prevenir el desarrollo de la sensibilización inducida por la artrosis, ya que TLR4-A1 disminuye la hiperalgesia térmica (al calor) cuando es administrado intraperitonealmente y la alodinia táctil cuando es administrado de manera intratecal.

2. En línea con los resultados obtenidos de los ensayos de conducta, bloquear los receptores TLR4 también previene las alteraciones histológicas e inmunohistoquímicas relacionadas con la artrosis.

De los resultados obtenidos en el **modelo de dolor postoperatorio quirúrgico inducido por una incisión en la planta de la pata**, podemos confirmar que:

1. El bloqueo periférico de los receptores TLR4 disminuye las alteraciones del comportamiento relacionadas con la sensibilización periférica y central.

2. La administración de morfina induce analgesia pero no reduce el tiempo de recuperación.

3. Dado que la coadministración de TLR4-A1 y morfina no induce ningún efecto aditivo en la conducta nociceptiva, los receptores TLR4 y opioide no parecen compartir mecasnimos de acción comunes.

En conjunto, los resultos de ambos modelos indican que el receptor TLR4 puede ser una diana interesante para desarrollar nuevos fármacos analgésicos centrados en evitar la sensibilización periférica y central.

REFERENCES

Abdollahi-Roodsaz, S., Joosten, L.A., Roelofs, M.F., Radstake, T.R., Matera, G., Popa, C., van der Meer, Jos WM, Netea, M.G., van den Berg, Wim B. Inhibition of toll-like receptor 4 breaks the inflammatory loop in autoimmune destructive arthritis. Arthritis & Rheumatism 2007; 56:2957-2967.

Aigner, T., Cook, J., Gerwin, N., Glasson, S., Laverty, S., Little, C., McIlwraith, W., Kraus, V. Histopathology atlas of animal model systems–overview of guiding principles. Osteoarthritis and Cartilage 2010; 18:S2-S6.

Alegre De Miquel, C., Rodríguez de la Serna, A, Huguet Codina, R., Rosselló Taberna, I. Datos epidemiológicos de la artrosis cervical en consultas de reumatología. Dolor. Investigación Clínica & Terapéutica 2011; 26:20-28.

Aley, K.O., Levine, J.D. Multiple receptors involved in peripheral alpha 2, mu, and A1 antinociception, tolerance, and withdrawal. J. Neurosci. 1997; 17:735-744.

Angst, M.S., Clark, J.D. Opioid-induced hyperalgesia: a qualitative systematic review. Anesthesiology 2006; 104:570-587.

Antonijevic, I., Mousa, S.A., Schafer, M., Stein, C. Perineurial defect and peripheral opioid analgesia in inflammation. J. Neurosci. 1995; 15:165-172.

Arendt-Nielsen, L., Nie, H., Laursen, M.B., Laursen, B.S., Madeleine, P., Simonsen, O.H., Graven-Nielsen, T. Sensitization in patients with painful knee osteoarthritis. Pain 2010; 149:573-581.

Arrich, J., Piribauer, F., Mad, P., Schmid, D., Klaushofer, K., Mullner, M. Intra-articular hyaluronic acid for the treatment of osteoarthritis of the knee: systematic review and meta-analysis. CMAJ 2005; 172:1039-1043.

Arroyo-Espliguero, R., Avanzas, P., Jeffery, S., Kaski, J.C. CD14 and toll-like receptor 4: a link between infection and acute coronary events? Heart 2004; 90:983-988.

Ashraf, S., Walsh, D.A. Angiogenesis in osteoarthritis. Curr. Opin. Rheumatol. 2008; 20:573-580.

Austin, P.J., Moalem-Taylor, G. The neuro-immune balance in neuropathic pain: involvement of inflammatory immune cells, immune-like glial cells and cytokines. J. Neuroimmunol. 2010; 229:26-50.

Avila-Martin, G., Galan-Arriero, I., Gómez-Soriano, J., Taylor, J. Treatment of rat spinal cord injury with the neurotrophic factor albumin-oleic acid: translational application for paralysis, spasticity and pain. PloS one 2011; 6: e26107.

Ayala, A.H.P., Fernández-López, J.C. Prevalencia y factores de riesgo de la osteoartritis. Reumatología clínica 2007; 3:S6-S12.

Banik, R.K., Brennan, T.J. Spontaneous discharge and increased heat sensitivity of rat C-fiber nociceptors are present in vitro after plantar incision. Pain 2004; 112:204-213.

Bao, L., Wang, H.F., Cai, H., Tong, Y., Jin, S., Lu, Y., Grant, G., HoÈkfelt, T., Zhang, X. Peripheral axotomy induces only very limited sprouting of coarse myelinated afferents into inner lamina II of rat spinal cord. Eur. J. Neurosci. 2002; 16:175-185.

Barron, M.C., Rubin, B.R. Managing osteoarthritic knee pain. J. Am. Osteopath. Assoc. 2007; 107:21-27.

Benito, P., Calvet, J., Lisbona, P., Martínez, J., Moller, I., Monfort, J. Guía de Buena Práctica Clínica en Geriatría: Artrosis. Sociedad Española de Geriatría y Gerontología, Sociedad Española de Reumatología, 2008.

Bennett, G.J., Hargreaves, K.M. Reply to Hirata and his colleagues. Pain 1990; 42:255.

Bettoni, I., Comelli, F., Rossini, C., Granucci, F., Giagnoni, G., Peri, F., Costa, B. Glial TLR4 receptor as new target to treat neuropathic pain: efficacy of a new receptor antagonist in a model of peripheral nerve injury in mice. Glia 2008; 56:1312-1319.

Beyreuther, B., Callizot, N., Stohr, T. Antinociceptive efficacy of lacosamide in the monosodium iodoacetate rat model for osteoarthritis pain. Arthritis Research and Therapy 2007; 9:R14.

Bilak, H., Tauszig-Delamasure, S., Imler, J. Toll and Toll-like receptors in Drosophila. Biochem. Soc. Trans. 2003; 31:648-651.

Blanco, F., de la Sociedad, Panel de Expertos. Primer documento de consenso de la Sociedad Española de Reumatología sobre el tratamiento farmacológico de la artrosis de rodilla. Reumatología Clínica 2005; 1:38-48.

BOE, 2005. Anexo III, Tabla 1 del REAL DECRETO 1201/2005, de 10 de octubre, sobre protección de los animales utilizados para experimentación y otros fines científicos, relativa a la Directiva 2003/65/CE del Parlamento Europeo y el Consejo, de 22 de julio de 2003, por la que se modificó la Directiva 86/609/CEE del Consejo, de 24 de noviembre de 1986, para garantizar la coherencia de los anexos de dicha Directiva con la evolución científica y técnica más reciente. (BOE-A-2005-17344; 252: 34367-34391).

Bora, F.W.,Jr, Miller, G. Joint physiology, cartilage metabolism, and the etiology of osteoarthritis. Hand Clin. 1987; 3: 325-336.

Bove, S., Calcaterra, S., Brooker, R., Huber, C., Guzman, R., Juneau, P., Schrier, D., Kilgore, K. Weight bearing as a measure of disease progression and efficacy of anti-inflammatory compounds in a model of monosodium iodoacetate-induced osteoarthritis. Osteoarthritis and cartilage 2003; 11:821-830.

Brandt, K. Paracetamol in the treatment of osteoarthritis pain. Drugs 2003: 63(2):23-41.

Brennan, T.J., Vandermeulen, E.P., Gebhart, G.F. Characterization of a rat model of incisional pain. Pain 1996; 64:493-501.

Brodal, P. The Central Nervous System: Structure and Function (2.Glia: Insulation and Protection of Axons)., 4th ed. Oxford University Press, New York, 2010a.

Brodal, P. The Central Nervous System: Structure and Function (13.Peripheral Parts of the Somatosensory System). 4th ed. Oxford University Press, New York, 2010b.

Brown, A.G. REVIEW ARTICLE THE DORSAL HORN OF THE SPINAL CORD. Quarterly Journal of Experimental Physiology 1982; 67:193-212.

Brunn, G.J., Bungum, M.K., Johnson, G.B., Platt, J.L. Conditional signaling by Toll-like receptor 4. FASEB J. 2005; 19:872-874.

Butt, R.H., Pfeifer, T.A., Delaney, A., Grigliatti, T.A., Tetzlaff, W.G., Coorssen, J.R. Enabling coupled quantitative genomics and proteomics analyses from rat spinal cord samples. Mol. Cell. Proteomics 2007; 6:1574-1588.

Caldwell, J.R., Hale, M.E., Boyd, R.E., Hague, J.M., Iwan, T., Shi, M., Lacouture, P.G. Treatment of osteoarthritis pain with controlled release oxycodone or fixed combination oxycodone plus acetaminophen added to nonsteroidal antiinflammatory drugs: a double blind, randomized, multicenter, placebo controlled trial. J. Rheumatol. 1999; 26:862-869.

Cano Montoro, J.G., Cases Gómez, I. Guía de Actuación Clínica en AP 2002.

Cao, L., Tanga, F.Y., DeLeo, J.A. The contributing role of CD14 in toll-like receptor 4 dependent neuropathic pain. Neuroscience 2009; 158: 896-903.

Capdevila, S., Giral, M., Ruiz de la Torre, J.L., Russell, R.J., Kramer, K. Acclimatization of rats after ground transportation to a new animal facility. Lab. Anim. 2007; 41:255-261.

Carlson, J.D., Maire, J.J., Martenson, M.E., Heinricher, M.M. Sensitization of pain-modulating neurons in the rostral ventromedial medulla after peripheral nerve injury. J. Neurosci. 2007; 27:13222-13231.

Carmona, L. Proyecto EPISER 2000: Prevalencia de enfermedades reumáticas en la población española. Metodología, resultados del reclutamiento y características de la población. Revista española de Reumatología 2001; 28:18-25.

Cervero, F., Laird, J. Mechanisms of touch-evoked pain (allodynia): a new model. Pain 1996; 68:13-23.

Chang, G., Chen, L., Mao, J. Opioid tolerance and hyperalgesia. Med. Clin. North Am. 2007; 91:199-211.

Chapman, C.R., Nakamura, Y. A passion of the soul: an introduction to pain for consciousness researchers. Conscious. Cogn. 1999; 8:391-422.

Chen, G., Tanabe, K., Yanagidate, F., Kawasaki, Y., Zhang, L., Dohi, S., Iida, H. Intrathecal endothelin-1 has antinociceptive effects in rat model of postoperative pain. Eur. J. Pharmacol. 2012; 697:40-46.

Cherry, J.D., Olschowka, J.A., O'Banion, M.K. Neuroinflammation and M2 microglia: the good, the bad, and the inflamed. J Neuroinflammation 2014; 11:98.

Chu, L.F., Clark, D.J., Angst, M.S. Opioid tolerance and hyperalgesia in chronic pain patients after one month of oral morphine therapy: a preliminary prospective study. The Journal of Pain 2006; 7:43-48.

Cialdai, C., Giuliani, S., Valenti, C., Tramontana, M., Maggi, C.A. Effect of Intra-articular 4-(S)-amino-5-(4-{4-[2,4-dichloro-3-(2,4-dimethyl-8-quinolyloxymethyl)phenylsulfonamido]-tetrahydro-2H-4-pyranylcarbonyl}piperazino)-5-oxopentyl](trimethyl)ammonium chloride hydrochloride (MEN16132), a kinin B2 receptor antagonist, on nociceptive response in monosodium iodoacetate-induced experimental osteoarthritis in rats. J. Pharmacol. Exp. Ther. 2009; 331:1025-1032.

Cifuentes, D., Rocha, L., Silva, L., Brito, A., Rueff-Barroso, C., Porto, L., Pinho, R. Decrease in oxidative stress and histological changes induced by physical exercise calibrated in rats with osteoarthritis induced by monosodium iodoacetate. Osteoarthritis and Cartilage 2010; 18:1088-1095.

Clark, J.D., Shi, X., Li, X., Qiao, Y., Liang, D., Angst, M.S., Yeomans, D.C. Morphine reduces local cytokine expression and neutrophil infiltration after incision. Mol Pain 2007; 3:28.

Clark, J.D. Chronic pain prevalence and analgesic prescribing in a general medical population. J. Pain Symptom Manage. 2002; 23:131-137.

Clegg, D.O., Reda, D.J., Harris, C.L., Klein, M.A., O'Dell, J.R., Hooper, M.M., Bradley, J.D., Bingham III, C.O., Weisman, M.H., Jackson, C.G. Glucosamine, chondroitin sulfate, and the two in combination for painful knee osteoarthritis. N. Engl. J. Med. 2006; 354:795-808.

Clements, K., Ball, A., Jones, H., Brinckmann, S., Read, S., Murray, F. Cellular and histopathological changes in the infrapatellar fat pad in the monoiodoacetate model of osteoarthritis pain. Osteoarthritis and Cartilage 2009; 17:805-812.

Coggeshall, CJ Woolf P Shortland RE. Peripheral nerve injury triggers central sprouting of myelinated afferents. Nature 1992; 355:75-78.

Cole, J.S., Messing, A., Trojanowski, J.Q., Lee, V.M. Modulation of axon diameter and neurofilaments by hypomyelinating Schwann cells in transgenic mice. J. Neurosci. 1994; 14, 6956-6966.

Comas, M., Sala, M., Román, R., Hoffmeister, L., Castells, X. Variaciones en la estimación de la prevalencia de artrosis de rodilla según los criterios diagnósticos utilizados en los estudios poblacionales. Gaceta sanitaria 2010; 24, 28-32.

Combe, R., Bramwell, S., Field, M.J. The monosodium iodoacetate model of osteoarthritis: a model of chronic nociceptive pain in rats? Neurosci. Lett. 2004; 370:236-240.

Costa, B., Trovato, A.E., Colleoni, M., Giagnoni, G., Zarini, E., Croci, T. Effect of the cannabinoid CB1 receptor antagonist, SR141716, on nociceptive response and nerve demyelination in rodents with chronic constriction injury of the sciatic nerve. Pain 2005; 116:52-61.

Courtney, C.A., O'Hearn, M.A., Hornby, T.G. Neuromuscular function in painful knee osteoarthritis. Curr. Pain Headache Rep. 2012; 16:518-524.

Cousins, M.J., Bridenbaugh, P.O., Carr, D.B., Horlocker, T.T. Cousins and Bridenbaugh's Neural Blockade in Clinical Anesthesia and Pain Medicine. Part IV: Neuronal Blockade and the Management of Pain. Chapter 31 - Introduction to Pain Mechanisms: Implications for Neural Blockade (Siddall, Philip J.; Cousins, Michael J.) (p.670), 4th ed. Lippincott, Williams & Wilkins, China, 2008.

Creamer, P., Hunt, M., Dieppe, P. Pain mechanisms in osteoarthritis of the knee: effect of intraarticular anesthetic. J. Rheumatol. 1996; 23:1031-1036.

Cui, J., Fu, E. Do Nociceptors and Nociception Solely Imply Noxious Stimuli? J Anesth Crit Care Open Access 1, 2014.

Cui, Y., Chen, Y., Zhi, J., Guo, R., Feng, J., Chen, P. Activation of p38 mitogen-activated protein kinase in spinal microglia mediates morphine antinociceptive tolerance. Brain Res. 2006; 1069:235-243.

de Conno, F., Caraceni, A., Martini, C., Spoldi, E., Salvetti, M., Ventafridda, V. Hyperalgesia and myoclonus with intrathecal infusion of high-dose morphine. Pain 1991; 47:337-339.

Deumens, R., Steyaert, A., Forget, P., Schubert, M., Lavand'homme, P., Hermans, E., De Kock, M. Prevention of chronic postoperative pain: cellular, molecular, and clinical insights for mechanism-based treatment approaches. Prog. Neurobiol. 2013; 104:1-37.

Djouhri, L., Koutsikou, S., Fang, X., McMullan, S., Lawson, S.N. Spontaneous pain, both neuropathic and inflammatory, is related to frequency of spontaneous firing in intact C-fiber nociceptors. J. Neurosci. 2006; 26:1281-1292.

Doubell, T., Mannion, R., Woolf, C. Intact sciatic myelinated primary afferent terminals collaterally sprout in the adult rat dorsal horn following section of a neighbouring peripheral nerve. J. Comp. Neurol. 1997; 380:95-104.

Dubovy, P., Klusakova, I., Hradilova Svizenska, I. Inflammatory profiling of Schwann cells in contact with growing axons distal to nerve injury. Biomed. Res. Int. 2014, 691041.

Dubuc, B., Robert, P., Paquet, D., Daigen, A. The BRAIN FROM TOP TO BOTTOM: Ascending Pain Pathways, 2013.

Due, M.R., Piekarz, A.D., Wilson, N., Feldman, P., Ripsch, M.S., Chavez, S., Yin, H., Khanna, R., White, F.A. Neuroexcitatory effects of morphine-3-glucuronide are dependent on Toll-like receptor 4 signaling. J Neuroinflammation 2012; 9:200.

DuPen, A., Shen, D., Ersek, M. Mechanisms of opioid-induced tolerance and hyperalgesia. Pain Management Nursing 2007; 8:113-121.

Echeverry, S., Zhang, J., Lee, S., Lim, T. Contribution of Inflammation to Chronic Pain Triggered by Nerve Injury. INTECH Open Access Publisher, 2012.

Edenfeld, G., Stork, T., Klämbt, C. Neuron-glia interaction in the insect nervous system. Curr. Opin. Neurobiol. 2005; 15:34-39.

Eker, H., Cok, O.Y., Aribogan, A., Arslan, G. Intra-Articular Lidocaine Injection in Chronic Knee Pain Due to Osteoarthritis: Preliminary Clinical Experience in 18 Patients: 461. Reg. Anesth. Pain Med. 2008; 33:e217.

Eliav, E., Benoliel, R., Tal, M. Inflammation with no axonal damage of the rat saphenous nerve trunk induces ectopic discharge and mechanosensitivity in myelinated axons. Neurosci. Lett. 2001; 311:49-52.

Eroglu, C., Barres, B.A. Regulation of synaptic connectivity by glia. Nature 2010; 468:223-231.

Erridge, C. Endogenous ligands of TLR2 and TLR4: agonists or assistants? J. Leukoc. Biol. 2010; 87:989-999.

Ertürk, C., Altay, M.A., Altay, N., Kalender, A.M., Öztürk, İ.A. Will a single periarticular lidocaine–corticosteroid injection improve the clinical efficacy of intraarticular hyaluronic acid treatment of symptomatic knee osteoarthritis? Knee Surgery, Sports Traumatology, Arthroscopy 2014; 1-8.

Fernihough, J., Gentry, C., Malcangio, M., Fox, A., Rediske, J., Pellas, T., Kidd, B., Bevan, S., Winter, J. Pain related behaviour in two models of osteoarthritis in the rat knee. Pain 2004; 112:83-93.

Ferreira-Gomes, J., Adães, S., Mendonça, M., Castro-Lopes, J.M. Analgesic effects of lidocaine, morphine and diclofenac on movement-induced nociception, as assessed by the Knee-Bend and CatWalk tests in a rat model of osteoarthritis. Pharmacology Biochemistry and Behavior 2012; 101:617-624.

Ferreira-Gomes, J., Adães, S., Castro-Lopes, J.M. Assessment of movement-evoked pain in osteoarthritis by the knee-bend and CatWalk tests: a clinically relevant study. The Journal of Pain 2008; 9:945-954.

Fields, H.L., Malick, A., Burstein, R. Dorsal horn projection targets of ON and OFF cells in the rostral ventromedial medulla. J. Neurophysiol. 1995; 74:1742-1759.

Finan, P.H., Buenaver, L.F., Bounds, S.C., Hussain, S., Park, R.J., Haque, U.J., Campbell, C.M., Haythornthwaite, J.A., Edwards, R.R., Smith, M.T. Discordance between pain and radiographic severity in knee osteoarthritis: findings from quantitative sensory testing of central sensitization. Arthritis & Rheumatism 2013; 65:363-372.

Freye, E. Kapitel 29. Toleranzentwicklung und Hyperalgesie unter chronischer Opioideinnahme. Analgetischer versus hyperalgetischer Effekt der Opioide (p.331). 8 ed. Springer Medizin Verlag, Heidelberg, 2010.

Fukagawa, H., Koyama, T., Kakuyama, M., Fukuda, K. Microglial activation involved in morphine tolerance is not mediated by toll-like receptor 4. Journal of anesthesia 2013; 27:93-97.

Gangloff, M. Different dimerisation mode for TLR4 upon endosomal acidification? Trends Biochem. Sci. 2012; 37:92-98.

García Poblete, E., Fernández García, H., Moro Rodríguez, J.E., Uranga Ocio, J.A., Nieto Bona, M.P., García Gómez de las Heras, Mª Soledad, Sánchez Mora, N. Histología Humana Práctica: Enfermería. Capítulo 8. Tejido Óseo. Editorial Universitaria Ramón Areces, Madrid, 2006.

Garriga, X.M. Definición, etiopatogenia, clasificación y formas de presentación. Atención Primaria 2014; 46:3-10.

Gebhart, G. Descending modulation of pain. Neuroscience & Biobehavioral Reviews 2004; 27:729-737.

Geneser, F. Histología, Sobre Bases Biomoleculares. Capítulo 12. Tejido Esquelético, 3ª ed. Médica Panamericana, Madrid, 2000.

Gil-Dones, F., Alonso-Orgaz, S., Avila, G., Martin-Rojas, T., Moral-Darde, V., Barroso, G., Vivanco, F., Scott-Taylor, J., Barderas, M. An optimal protocol to analyze the rat spinal cord proteome. Biomarker insights 2008; 4:135-164.

Gilerovich, E., Moshonkina, T., Fedorova, E., Shishko, T., Pavlova, N., Gerasimenko, Y.P., Otellin, V. Morphofunctional characteristics of the lumbar enlargement of the spinal cord in rats. Neurosci. Behav. Physiol. 2008; 38:855-860.

Goicoechea, C., Rincón, A., Pascual, D., Martín, M.I. Papel de los receptores TLR-4 en la hiperalgesia y alodinia producida por paclitaxel en rata, 2011.

Gómez, R., Villalvilla, A., Largo, R., Gualillo, O., Herrero-Beaumont, G. TLR4 signalling in osteoarthritis - finding targets for candidate DMOADs. Nature Reviews Rheumatology 2014; 11(3):159-70.

Gondokaryono, S.P., Ushio, H., Niyonsaba, F., Hara, M., Takenaka, H., Jayawardana, S.T., Ikeda, S., Okumura, K., Ogawa, H. The extra domain A of fibronectin stimulates murine mast cells via Toll-like receptor 4. J. Leukoc. Biol. 2007; 82:657-665.

Guadagno, J., Xu, X., Karajgikar, M., Brown, A., Cregan, S. Microglia-derived TNFα induces apoptosis in neural precursor cells via transcriptional activation of the Bcl-2 family member Puma. Cell death & disease 2013; 4:e538.

Gupta, A., Mulder, J., Gomes, I., Rozenfeld, R., Bushlin, I., Ong, E., Lim, M., Maillet, E., Junek, M., Cahill, C.M., Harkany, T., Devi, L.A. Increased abundance of opioid receptor heteromers after chronic morphine administration. Sci. Signal. 2010; 3(131):ra54.

Hagiwara, Y., Ando, A., Chimoto, E., Saijo, Y., Ohmori-Matsuda, K., Itoi, E. Changes of articular cartilage after immobilization in a rat knee contracture model. Journal of Orthopaedic Research 2009; 27: 236-242.

Harden, R.N., Wallach, G., Gagnon, C.M., Zereshki, A., Mukai, A., Saracoglu, M., Kuroda, M.M., Graciosa, J.R., Bruehl, S. The osteoarthritis knee model: psychophysical characteristics and putative outcomes. The Journal of Pain 2013; 14:281-289.

Henrotin, Y., Kurz, B., Aigner, T. Oxygen and reactive oxygen species in cartilage degradation: friends or foes? Osteoarthritis and Cartilage 2005; 13:643-654.

Herrera, C., Linares, R., Restrepo, M., RODRÍGUEZ, C.H. Hiperalgesia inducida por opioides en el manejo del dolor en pacientes con cáncer. Libro dolor y cáncer. Bogota: ACED , 2009; 151-169.

Hertz, L. Advances in Molecular and Cell Biology. Non-Neuronal Cells of the Nervous System: Function and Disfunction (42. the Role of Astrocytes and Microglia in Persistent Pain). Elsevier, Amsterdam (The Netherlands), 2004.

Hochman, J.R., French, M.R., Bermingham, S.L., Hawker, G.A. The nerve of osteoarthritis pain. Arthritis care & research 2010; 62:1019-1023.

Horvath RJ, Romero-Sandoval EA, De Leo JA. Glial modulation in pain states. Translation into humans., in: Kruger L, L.A. (Ed.). Boca Raton, FL: CRC Press, 2010.

Horvath, R.J., Landry, R.P., Romero-Sandoval, E.A., DeLeo, J.A. Morphine tolerance attenuates the resolution of postoperative pain and enhances spinal microglial p38 and extracellular receptor kinase phosphorylation. Neuroscience 2010; 169:843-854.

Hoshino, K., Takeuchi, O., Kawai, T., Sanjo, H., Ogawa, T., Takeda, Y., Takeda, K., Akira, S. Cutting edge: Toll-like receptor 4 (TLR4)-deficient mice are hyporesponsive to lipopolysaccharide: evidence for TLR4 as the Lps gene product. J. Immunol. 1999; 162:3749-3752.

Huang, Q., Ma, Y., Adebayo, A., Pope, R.M. Increased macrophage activation mediated through toll-like receptors in rheumatoid arthritis. Arthritis & Rheumatism 2007; 56:2192-2201.

Huang, J., Zhang, X., McNaughton, P.A. Inflammatory pain: the cellular basis of heat hyperalgesia. Curr. Neuropharmacol. 2006; 4:197-206.

Hunter, D.J., McDougall, J.J., Keefe, F.J. The symptoms of osteoarthritis and the genesis of pain. Med. Clin. North Am. 2009; 93:83-100.

Hutchinson, M.R., Zhang, Y., Shridhar, M., Evans, J.H., Buchanan, M.M., Zhao, T.X., Slivka, P.F., Coats, B.D., Rezvani, N., Wieseler, J. Evidence that opioids may have toll-like receptor 4 and MD-2 effects. Brain Behav. Immun. 2010a; 24:83-95.

Hutchinson, M.R., Lewis, S.S., Coats, B.D., Rezvani, N., Zhang, Y., Wieseler, J.L., Somogyi, A.A., Yin, H., Maier, S.F., Rice, K.C. Possible involvement of toll-like receptor 4/myeloid differentiation factor-2 activity of opioid inactive isomers causes spinal proinflammation and related behavioral consequences. Neuroscience 2010b; 167:880-893.

Hutchinson, M.R., Ramos, K.M., Loram, L.C., Wieseler, J., Sholar, P.W., Kearney, J.J., Lewis, M.T., Crysdale, N.Y., Zhang, Y., Harrison, J.A. Evidence for a role of heat shock protein-90 in toll like receptor 4 mediated pain enhancement in rats. Neuroscience 2009; 164:1821-1832.

Hutchinson, M.R., Northcutt, A.L., Hiranita, T., Wang, X., Lewis, S.S., Thomas, J., van Steeg, K., Kopajtic, T.A., Loram, L.C., Sfregola, C., Galer, E., Miles, N.E., Bland, S.T., Amat, J., Rozeske, R.R., Maslanik, T., Chapman, T.R., Strand, K.A., Fleshner, M., Bachtell, R.K., Somogyi, A.A., Yin, H., Katz, J.L., Rice, K.C., Maier, S.F., Watkins, L.R. Opioid activation of toll-like receptor 4 contributes to drug reinforcement. J. Neurosci. 2012; 32:11187-11200.

IASP. The International Association for the Study of Pain: Global year against musculoskeletal pain: Osteoarthritis-related pain, 2009.

IASP Scientific Program Committee, 2014. Pain 2010: an updated review Refresher Course Syllabus.

Ikeda, H., Kiritoshi, T., Murase, K. Synaptic plasticity in the spinal dorsal horn. Neurosci. Res. 2009; 64, 133-136.

Im, H., Kim, J., Li, X., Kotwal, N., Sumner, D.R., van Wijnen, A.J., Davis, F.J., Yan, D., Levine, B., Henry, J.L. Alteration of sensory neurons and spinal response to an experimental osteoarthritis pain model. Arthritis & Rheumatism 2010; 62:2995-3005.

Ito, N., Obata, H., Saito, S. Spinal microglial expression and mechanical hypersensitivity in a postoperative pain model: comparison with a neuropathic pain model. Anesthesiology 2009; 111:640-648.

Jordan, K.M., Arden, N.K., Doherty, M., Bannwarth, B., Bijlsma, J.W., Dieppe, P., Gunther, K., Hauselmann, H., Herrero-Beaumont, G., Kaklamanis, P., Lohmander, S., Leeb, B., Lequesne, M., Mazieres, B., Martin-Mola, E., Pavelka, K., Pendleton, A., Punzi, L., Serni, U., Swoboda, B., Verbruggen, G., Zimmerman-Gorska, I., Dougados, M., Standing Committee for International Clinical Studies Including Therapeutic Trials ESCISIT. EULAR Recommendations 2003: an evidence based approach to the management of knee osteoarthritis: Report of a Task Force of the Standing Committee for International Clinical Studies Including Therapeutic Trials (ESCISIT). Ann. Rheum. Dis. 2003; 62:1145-1155.

Jorgensen, T.S., Graven-Nielsen, T., Ellegaard, K., Danneskiold-Samsoe, B., Bliddal, H., Henriksen, M. Intra-Articular Analgesia and Steroid Reduce Pain Sensitivity in Knee OA Patients: An Interventional Cohort Study. Pain Res. Treat. 2014; 710490.

Juni, A., Klein, G., Pintar, J., Kest, B. Nociception increases during opioid infusion in opioid receptor triple knock-out mice. Neuroscience 2007; 147:439-444.

Kalff, K., El Mouedden, M., van Egmond, J., Veening, J., Joosten, L., Scheffer, G.J., Meert, T., Vissers, K. Pre-treatment with capsaicin in a rat osteoarthritis model reduces the symptoms of pain and bone damage induced by monosodium iodoacetate. Eur. J. Pharmacol. 2010; 641:108-113.

Kam, P., Power, I. Principles of Physiology for the Anaesthetist. Chapter 13 - Physiology of Pain (p.391), 2nd ed. Oxford University Press Inc., New York, 2008.

Kapoor, M., Martel-Pelletier, J., Lajeunesse, D., Pelletier, J., Fahmi, H. Role of proinflammatory cytokines in the pathophysiology of osteoarthritis. Nature Reviews Rheumatology 2010; 7:33-42.

Kawai, T., Akira, S. TLR signaling. Cell Death & Differentiation 2006; 13:816-825.

Kelly, S., Dobson, K., Harris, J. Spinal nociceptive reflexes are sensitized in the monosodium iodoacetate model of osteoarthritis pain in the rat. Osteoarthritis and Cartilage 2013; 21:1327-1335.

Kidd, B.L. Problems with pain-is the messenger to blame? Ann. Rheum. Dis. 1996; 55:275.

Kissin, I., Gelman, S. Chronic postsurgical pain: still a neglected topic? J. Pain Res. 2012; 5:473-489.

Kitahata, L.M. Pain pathways and transmission. Yale J. Biol. Med. 1993; 66:437-442.

Kohno, T., Moore, K.A., Baba, H., Woolf, C.J. Peripheral nerve injury alters excitatory synaptic transmission in lamina II of the rat dorsal horn. J. Physiol. (Lond.) 2003; 548:131-138.

Komatsu, T., Sakurada, S., Kohno, K., Shiohira, H., Katsuyama, S., Sakurada, C., Tsuzuki, M., Sakurada, T. Spinal ERK activation via NO–cGMP pathway contributes to nociceptive behavior induced by morphine-3-glucuronide. Biochem. Pharmacol. 2009; 78:1026-1034.

Koppert, W. Opioid-induzierte Hyperalgesie: Pathophysiologie und Klinik. Anaesthesist 2004; 53:455-466.

Koppert, W., Schmelz, M. The impact of opioid-induced hyperalgesia for postoperative pain. Best Practice & Research Clinical Anaesthesiology 2007; 21:65-83.

Kosuwon, W., Sirichatiwapee, W., Wisanuyotin, T., Jeeravipoolvarn, P., Laupattarakasem, W. Efficacy of symptomatic control of knee osteoarthritis with 0.0125% of capsaicin versus placebo. Medical journal of the Medical Association of Thailand 2010; 93:1188.

Lan, L.S., Ping, Y.J., Na, W.L., Miao, J., Cheng, Q.Q., Ni, M.Z., Lei, L., Fang, L.C., Guang, R.C., Jin, Z. Down-regulation of Toll-like receptor 4 gene expression by short interfering RNA attenuates bone cancer pain in a rat model. Mol Pain 2010; 6:1-13.

Lasarte, J.J., Casares, N., Gorraiz, M., Hervas-Stubbs, S., Arribillaga, L., Mansilla, C., Durantez, M., Llopiz, D., Sarobe, P., Borras-Cuesta, F., Prieto, J., Leclerc, C. The extra domain A from fibronectin targets antigens to TLR4-expressing cells and induces cytotoxic T cell responses in vivo. J. Immunol. 2007; 178:748-756.

Laslett, L.L., Jones, G. Capsaicin for osteoarthritis pain. Springer, 2014; 277-291.

Latremoliere, A., Woolf, C.J. Central sensitization: a generator of pain hypersensitivity by central neural plasticity. The Journal of Pain 2009; 10:895-926.

Latz, E., Verma, A., Visintin, A., Gong, M., Sirois, C.M., Klein, D.C., Monks, B.G., McKnight, C.J., Lamphier, M.S., Duprex, W.P. Ligand-induced conformational changes allosterically activate Toll-like receptor 9. Nat. Immunol. 2007; 8:772-779.

Lefebvre, J.S., Lévesque, T., Picard, S., Paré, G., Gravel, A., Flamand, L., Borgeat, P. Extra domain A of fibronectin primes leukotriene biosynthesis and stimulates neutrophil migration through activation of Toll-like receptor 4. Arthritis & Rheumatism 2011; 63:1527-1533.

Leon, C.G., Tory, R., Jia, J., Sivak, O., Wasan, K.M. Discovery and development of toll-like receptor 4 (TLR4) antagonists: a new paradigm for treating sepsis and other diseases. Pharm. Res. 2008; 25:1751-1761.

Lewis, S.S., Hutchinson, M.R., Rezvani, N., Loram, L.C., Zhang, Y., Maier, S.F., Rice, K.C., Watkins, L.R. Evidence that intrathecal morphine-3-glucuronide may cause pain enhancement via toll-like receptor 4/MD-2 and interleukin-1β. Neuroscience 2010; 165:569-583.

Li, J., Csakai, A., Jin, J., Zhang, F., Yin, H. Therapeutic Developments Targeting Toll-like Receptor-4-Mediated Neuroinflammation. ChemMedChem 2015; 11(2):154-65.

Li, Q. Antagonists of toll like receptor 4 maybe a new strategy to counteract opioid-induced hyperalgesia and opioid tolerance. Med. Hypotheses 2012; 79(6):754-6.

Li, X., Angst, M.S., Clark, J.D. A murine model of opioid-induced hyperalgesia. Mol. Brain Res. 2001; 86:56-62.

Liang, D., Shi, X., Qiao, Y., Angst, M.S., Yeomans, D.C., Clark, J.D. Chronic morphine administration enhances nociceptive sensitivity and local cytokine production after incision. Mol. Pain 2008; 4:7.

Liu, P., Okun, A., Ren, J., Guo, R., Ossipov, M.H., Xie, J., King, T., Porreca, F. Ongoing pain in the MIA model of osteoarthritis. Neurosci. Lett. 2011; 493:72-75.

Lo, G.H., LaValley, M., McAlindon, T., Felson, D.T. Intra-articular hyaluronic acid in treatment of knee osteoarthritis: a meta-analysis. JAMA 2003; 290:3115-3121.

Loram, L.C., Grace, P.M., Strand, K.A., Taylor, F.R., Ellis, A., Berkelhammer, D., Bowlin, M., Skarda, B., Maier, S.F., Watkins, L.R. Prior exposure to repeated morphine potentiates mechanical allodynia induced by peripheral inflammation and neuropathy. Brain Behav. Immun. 2012; 26:1256-1264.

Low, Y., Clarke, C.F., Huh, B.K. Opioid-induced hyperalgesia: a review of epidemiology, mechanisms and management. Singapore Med. J. 2012; 53:357-360.

Lu, Y. Synaptic wiring in the deep dorsal horn. Focus on "Local circuit connections between hamster laminae III and IV dorsal horn neurons". J. Neurophysiol. 2008; 99:1051-1052.

Ma, Q., Tian, L. A-fibres sprouting from lamina I into lamina II of spinal dorsal horn after peripheral nerve injury in rats. Brain Res. 2001; 904:137-140.

Ma, Q., Tian, L., Woolf, C.J. Resection of sciatic nerve re-triggers central sprouting of A-fibre primary afferents in the rat. Neurosci. Lett. 2000; 288:215-218.

Mach, D., Rogers, S., Sabino, M., Luger, N., Schwei, M., Pomonis, J., Keyser, C., Clohisy, D., Adams, D., O'leary, P.,. Origins of skeletal pain: sensory and sympathetic innervation of the mouse femur. Neuroscience 2002; 113:155-166.

Magerl, W., Klein, T. Handbook of Clinical Neurology. Pain (Cervero, F.; Jensen, T.S.). Chapter 33. Experimental Human Models of Neuropathic Pain. Elsevier B.V., Amsterdam (The Netherlands) ,2006.

Mao, J. Opioid-induced abnormal pain sensitivity. Curr. Pain Headache Rep. 2006; 10:67-70.

Mapp, P. Innervation of the synovium. Ann. Rheum. Dis. 1995; 54:398-403.

Marchand, F., Perretti, M., McMahon, S.B. Role of the immune system in chronic pain. Nature Reviews Neuroscience 2005; 6:521-532.

Marion Lee, M., Sanford Silverman, M., Hans Hansen, M., Vikram Patel, M. A comprehensive review of opioid-induced hyperalgesia. Pain physician 2011; 14:145-161.

Matsunaga, A., Kawamoto, M., Shiraishi, S., Yasuda, T., Kajiyama, S., Kurita, S., Yuge, O. Intrathecally administered COX-2 but not COX-1 or COX-3 inhibitors attenuate streptozotocin-induced mechanical hyperalgesia in rats. Eur. J. Pharmacol. 2007; 554:12-17.

McCormack, W.J., Parker, A.E., O'Neill, L.A. Toll-like receptors and NOD-like receptors in rheumatic diseases. Arthritis Res Ther 2009; 11:243.

McDougall, J.J. Arthritis and pain Neurogenic origin of joint pain. Arthritis Research and Therapy 2006; 8: 220.

McDougall, J.J., Bray, R.C., Sharkey, K.A. Morphological and immunohistochemical examination of nerves in normal and injured collateral ligaments of rat, rabbit, and human knee joints. Anat. Rec. 1997; 248:29-39.

McLachlan, E.M., Hu, P. Inflammation in dorsal root ganglia after peripheral nerve injury: Effects of the sympathetic innervation. Autonomic Neuroscience 2014; 182:108-117.

Melzack, R., Katz, J. The McGill Pain Questionnaire: appraisal and current status, 2001.

Memon, I., Khan, K.M., Siddiqui, S., Perveen, S., Ishaq, M. Temporal expression of calcium/calmodulin-dependent adenylyl cyclase isoforms in rat articular chondrocytes: RT-PCR and immunohistochemical localization. J. Anat. 2010; 217:574-587.

Meng, L., Zhu, W., Jiang, C., He, X., Hou, W., Zheng, F., Holmdahl, R., Lu, S. Research article Toll-like receptor 3 upregulation in macrophages participates in the initiation and maintenance of pristane-induced arthritis in rats. Arthritis Res Ther. 2010;12(3):R103.

Merskey, H.E. Classification of chronic pain: descriptions of chronic pain syndromes and definitions of pain terms. Pain 1986; Suppl. 3:S1-226.

Mifflin, K.A., Kerr, B.J. The transition from acute to chronic pain: understanding how different biological systems interact. Canadian Journal of Anesthesia/Journal canadien d'anesthésie 2014; 61:112-122.

Mika, J. Modulation of microglia can attenuate neuropathic pain symptoms and enhance morphine effectiveness. Pharmacol. Rep. 2008; 60:297-307.

Milligan, E.D., Watkins, L.R. Pathological and protective roles of glia in chronic pain. Nature Reviews Neuroscience 2009; 10:23-36.

MINISTERIO DE SANIDAD, SERVICIOS SOCIALES E IGUALDAD, 2013. Estrategia en enfermedades reumáticas y musculoesqueléticas del Sistema Nacional de Salud. Estrategia aprobada por el Pleno del Consejo Interterritorial del Sistema Nacional de Salud el 20 de diciembre de 2012.

Mulak, A., Larauche, M., Taché, Y. Modulation of Visceral Pain by Stress: Implications in Irritable Bowel Syndrome. INTECH Open Access Publisher, 2012.

Nagakura, Y., Jones, T.L., Malkmus, S.A., Sorkin, L., Yaksh, T.L. The sensitization of a broad spectrum of sensory nerve fibers in a rat model of acute postoperative pain and its response to intrathecal pharmacotherapy. Pain 2008; 139:569-577.

Nakagawa, T., Kaneko, S. Spinal astrocytes as therapeutic targets for pathological pain. Journal of pharmacological sciences 2010; 114:347-353.

Nguyen, M.D., Julien, J., Rivest, S. Innate immunity: the missing link in neuroprotection and neurodegeneration? Nature Reviews Neuroscience 2002; 3:216-227.

Norimoto, M., Sakuma, Y., Suzuki, M., Orita, S., Yamauchi, K., Inoue, G., Aoki, Y., Ishikawa, T., Miyagi, M., Kamoda, H. Up-Regulation of Pain Behavior and Glial Activity in the Spinal Cord after Compression and Application of Nucleus Pulposus onto the Sciatic Nerve in Rats. Asian spine journal 2014; 8:549-556.

Obata, H., Eisenach, J.C., Hussain, H., Bynum, T., Vincler, M. Spinal glial activation contributes to postoperative mechanical hypersensitivity in the rat. The Journal of Pain 2006; 7:816-822.

Ocasio, F.M., Jiang, Y., House, S.D., Chang, S.L. Chronic morphine accelerates the progression of lipopolysaccharide-induced sepsis to septic shock. J. Neuroimmunol. 2004; 149:90-100.

Oda, K., Kitano, H. A comprehensive map of the toll-like receptor signaling network. Mol. Syst. Biol. 2006; 2, 2006.0015.

Ohara, K., Shimizu, K., Matsuura, S., Ogiso, B., Omagari, D., Asano, M., Tsuboi, Y., Shinoda, M., Iwata, K. Toll-like receptor 4 signaling in trigeminal ganglion neurons contributes tongue-referred pain associated with tooth pulp inflammation. J. Neuroinflammation 2013; 10:139.

Okamura, Y., Watari, M., Jerud, E.S., Young, D.W., Ishizaka, S.T., Rose, J., Chow, J.C., Strauss, J.F. The extra domain A of fibronectin activates Toll-like receptor 4. J. Biol. Chem. 2001; 276:10229-10233.

Olson, J.K., Miller, S.D. Microglia initiate central nervous system innate and adaptive immune responses through multiple TLRs. J. Immunol. 2004; 173:3916-3924.

Ospelt, C., Brentano, F., Rengel, Y., Stanczyk, J., Kolling, C., Tak, P.P., Gay, R.E., Gay, S., Kyburz, D. Overexpression of toll-like receptors 3 and 4 in synovial tissue from patients with early rheumatoid arthritis: toll-like receptor expression in early and longstanding arthritis. Arthritis & Rheumatism 2008; 58:3684-3692.

Oteo, A., Ruíz-Ibán, M.Á., Miguens, X., Villoria, J., Sánchez-Magro, I. Características neuropáticas del dolor por artrosis de rodilla en España. Estudio ENDARE, 2013.

Owen M, S., Eva Marie Y., M., B., B. Mutagenetix Phenotypic Mutation 'lps3', 2015. https://mutagenetix.utsouthwestern.edu/phenotypic/phenotypic_rec.cfm?pk=233.

Pal, A., Das, S. Chronic morphine exposure and its abstinence alters dendritic spine morphology and upregulates Shank1. Neurochem. Int. 2013; 62:956-964.

Panter, G., Jerala, R. The ectodomain of the Toll-like receptor 4 prevents constitutive receptor activation. J. Biol. Chem. 2011; 286:23334-23344.

Pascual, D., Rincón, A., Martín, M.I., Goicoechea, C. ¿Pueden ser los receptores TLR-4 una diana interesante para el tratamiento del dolor neuropático? Resultados preliminares en un modelo de neuropatía por paclitaxel en rata. Comunicación oral. Congreso: XX Reunión de Farmacólogos de la Comunidad de Madrid–XX FARMADRID 2011. Libro de Resúmenes p 5.

Patro, N., Nagayach, A., Patro, I.K. Iba1 expressing microglia in the dorsal root ganglia become activated following peripheral nerve injury in rats. Indian J Exp Biol. 2010; 48(2):110-6.

Peri, F., Calabrese, V. Toll-like Receptor 4 (TLR4) Modulation by Synthetic and Natural Compounds: An Update: Miniperspective. J. Med. Chem. 2013; 57:3612-3622.

Peri, F., Piazza, M. Therapeutic targeting of innate immunity with Toll-like receptor 4 (TLR4) antagonists. Biotechnol. Adv. 2012; 30:251-260.

Piazza, M., Rossini, C., Della Fiorentina, S., Pozzi, C., Comelli, F., Bettoni, I., Fusi, P., Costa, B., Peri, F.,. Glycolipids and benzylammonium lipids as novel antisepsis agents: synthesis and biological characterization. J. Med. Chem. 2009; 52:1209-1213.

Pogatzki, E.M., Vandermeulen, E.P., Brennan, T.J. Effect of plantar local anesthetic injection on dorsal horn neuron activity and pain behaviors caused by incision. Pain 2002; 97:151-161.

Pomonis, J.D., Boulet, J.M., Gottshall, S.L., Phillips, S., Sellers, R., Bunton, T., Walker, K. Development and pharmacological characterization of a rat model of osteoarthritis pain. Pain 2005; 114:339-346.

Poole, R., Blake, S., Buschmann, M., Goldring, S., Laverty, S., Lockwood, S., Matyas, J., McDougall, J., Pritzker, K., Rudolphi, K. Recommendations for the use of preclinical models in the study and treatment of osteoarthritis. Osteoarthritis and Cartilage 2010; 18:S10-S16.

Porr, J., Chrobak, K., Muir, B. Entrapment of the saphenous nerve at the adductor canal affecting the infrapatellar branch–a report on two cases. The Journal of the Canadian Chiropractic Association 2013; 57: 341.

Porreca, F., Ossipov, M.H., Gebhart, G. Chronic pain and medullary descending facilitation. Trends Neurosci. 2002; 25:319-325.

Pritzker, K., Gay, S., Jimenez, S., Ostergaard, K., Pelletier, J., Revell, P., Salter, D.v.d., Van den Berg, W. Osteoarthritis cartilage histopathology: grading and staging. Osteoarthritis and cartilage 2006; 14:13-29.

Procházková, M., Zanvit, P., Dolezal, T., Prokesova, L., Krsiak, M. Increased gene expression and production of spinal cyclooxygenase 1 and 2 during experimental osteoarthritis pain. Physiological research 2009; 58:419.

Raffa, R.B., Pergolizzi, J.V. Opioid-induced hyperalgesia: is it clinically relevant for the treatment of pain patients? Pain Management Nursing 2013; 14:e67-e83.

Raghavendra, V., DeLeo, J.A. The role of astrocytes and microglia in persistent pain. Advances in Molecular and Cell Biology 2003; 31:951-966.

Ren, K., Dubner, R. Interactions between the immune and nervous systems in pain. Nat. Med. 2010; 16: 1267-1276.

Ren, K., Dubner, R. Inflammatory Models of Pain and Hyperalgesia. ILAR J. 1999; 40:111-118.

Rexed, B. The cytoarchitectonic organization of the spinal cord in the cat. J. Comp. Neurol. 1952; 96:415-495.

Rey, R., Cadden, J., Wallace, L.E. Histoire De La Douleur. Harvard University Press, 1998.

Rincón Carvajal, A., Pascual, D., Martín Fontelles, M.I., Quesada, E., Goicoechea García, C. TLR4 receptor signalling inhibitor TLR4-A1, blocks the development of hyperalgesia and allodynia induced by paclitaxel in rats, 2011.

Rinner, U., Hudlicky, T. Synthesis of morphine alkaloids and derivatives, in: Anonymous . Springer, 2012; 33-66.

Romero-Sandoval, A., Chai, N., Nutile-McMenemy, N., DeLeo, J.A. A comparison of spinal Iba1 and GFAP expression in rodent models of acute and chronic pain. Brain Res. 2008a; 1219:116-126.

Romero-Sandoval, E.A., Horvath, R.J., DeLeo, J.A. Neuroimmune interactions and pain: focus on glial-modulating targets. Curr. Opin. Investig Drugs 2008b; 9:726-734.

Sagar, D.R., Burston, J.J., Hathway, G.J., Woodhams, S.G., Pearson, R.G., Bennett, A.J., Kendall, D.A., Scammell, B.E., Chapman, V. The contribution of spinal glial cells to chronic pain behaviour in the monosodium iodoacetate model of osteoarthritic pain. Mol Pain 2011; 7: 88.

Saito, O., Svensson, C., Buczynski, M., Wegner, K., Hua, X., Codeluppi, S., Schaloske, R., Deems, R., Dennis, E., Yaksh, T. Spinal glial TLR4-mediated nociception and production of prostaglandin E2 and TNF. Br. J. Pharmacol. 2010; 160:1754-1764.

Salter, M.W. Deepening understanding of the neural substrates of chronic pain. Brain 2014; 137:651-653.

Sauer, R., Hackel, D., Morschel, L., Sahlbach, H., Wang, Y., Mousa, S.A., Roewer, N., Brack, A., Rittner, H.L. Toll like receptor (TLR)-4 as a regulator of peripheral endogenous opioid-mediated analgesia in inflammation. Mol Pain 2014; 10:10.

Schaible, H.,. Peripheral and central mechanisms of pain generation, in: Anonymous . Springer 2006; 3-28.

Scholz, J., Woolf, C.J. The neuropathic pain triad: neurons, immune cells and glia. Nat. Neurosci. 2007; 10:1361-1368.

Schuelert, N., Zhang, C., Mogg, A., Broad, L., Hepburn, D., Nisenbaum, E., Johnson, M., McDougall, J. Paradoxical effects of the cannabinoid CB2 receptor agonist GW405833 on rat osteoarthritic knee joint pain. Osteoarthritis and Cartilage 2010; 18:1536-1543.

Schuelert, N., McDougall, J.J. Cannabinoid-mediated antinociception is enhanced in rat osteoarthritic knees. Arthritis & Rheumatism 2008; 58:145-153.

Schug, S.A., Pogatzki-Zahn, E.M. Chronic pain after surgery or injury. Pain Clinical Updates 2011; 19:1-4.

Sghirlanzoni, A., Pareyson, D., Lauria, G. Sensory neuron diseases. The Lancet Neurology 2005; 4:349-361.

Shehab, S., Spike, R., Todd, A. Evidence against cholera toxin B subunit as a reliable tracer for sprouting of primary afferents following peripheral nerve injury. Brain Res. 2003; 964:218-227.

Shortland, P., Molander, C. The time-course of Aβ-evoked c-fos expression in neurons of the dorsal horn and gracile nucleus after peripheral nerve injury. Brain Res. 1998; 810:288-293.

Sinatra, R.S., Ford, D.H. The effects of acute and chronic morphine treatment on the process of facial nerve regeneration. Brain Res. 1979; 175:315-325.

Sjøgren, P., Jonsson, T., Jensen, N., Drenck, N., Jensen, T.S. Hyperalgesia and myoclonus in terminal cancer patients treated with continuous intravenous morphine. Pain 1993; 55:93-97.

Skou, S.T., Graven-Nielsen, T., Lengsoe, L., Simonsen, O., Laursen, M.B., Arendt-Nielsen, L. Relating clinical measures of pain with experimentally assessed pain mechanisms in patients with knee osteoarthritis. Scandinavian Journal of Pain 2013; 4:111-117.

Smith, H.S. Opioid metabolism. 2009; 84:613-624.

Smith, H.S. Activated microglia in nociception. Pain Physician. 2010; 13:295-304.

Sohn, D.H., Sokolove, J., Sharpe, O., Erhart, J.C., Chandra, P.E., Lahey, L.J., Lindstrom, T.M., Hwang, I., Boyer, K.A., Andriacchi, T.P. Plasma proteins present in osteoarthritic synovial fluid can stimulate cytokine production via Toll-like receptor 4. Arthritis Res Ther 2012; 14:R7.

Solís, J.R., Martínez, V.M.P., Blanco, S.B., Calvo, M.H. Tratado de Geriatría para residentes 2007. Capítulo 67 - Osteoartritis, 689.

Solomon, R.L., Corbit, J.D. An opponent-process theory of motivation: I. Temporal dynamics of affect. Psychol. Rev. 1974; 81:119.

Song, P., Zhao, Z. The involvement of glial cells in the development of morphine tolerance. Neurosci. Res. 2001; 39:281-286.

Sorge, R.E., LaCroix-Fralish, M.L., Tuttle, A.H., Sotocinal, S.G., Austin, J.S., Ritchie, J., Chanda, M.L., Graham, A.C., Topham, L., Beggs, S., Salter, M.W., Mogil, J.S. Spinal cord Toll-like receptor 4 mediates inflammatory and neuropathic hypersensitivity in male but not female mice. J. Neurosci. 2011; 31:15450-15454.

Starkweather, A. Increased interleukin-6 activity associated with painful chemotherapy-induced peripheral neuropathy in women after breast cancer treatment. Nurs. Res. Pract. 2010; 281531.

Sweitzer, S., Martin, D., DeLeo, J. Intrathecal interleukin-1 receptor antagonist in combination with soluble tumor necrosis factor receptor exhibits an anti-allodynic action in a rat model of neuropathic pain. Neuroscience 2001; 103:529-539.

Sweitzer, S.M., DeLeo, J.A.,. The active metabolite of leflunomide, an immunosuppressive agent, reduces mechanical sensitivity in a rat mononeuropathy model. The Journal of Pain 2002; 3:360-368.

Takagi, M. Toll-like receptor-a potent driving force behind rheumatoid arthritis. Journal of Clinical and Experimental Hematopathology 2011; 51:77-92.

Takashima, K., Matsunaga, N., Yoshimatsu, M., Hazeki, K., Kaisho, T., Uekata, M., Hazeki, O., Akira, S., Iizawa, Y., Ii, M. Analysis of binding site for the novel small-molecule TLR4 signal transduction inhibitor TAK-242 and its therapeutic effect on mouse sepsis model. Br. J. Pharmacol. 2009; 157:1250-1262.

Takeshita, N., Yoshimi, E., Hatori, C., Kumakura, F., Seki, N., Shimizu, Y. Alleviating effects of AS1892802, a Rho kinase inhibitor, on osteoarthritic disorders in rodents. Journal of pharmacological sciences 2011; 115: 481-489.

Tanga, F.Y., Nutile-McMenemy, N., DeLeo, J.A. The CNS role of Toll-like receptor 4 in innate neuroimmunity and painful neuropathy. Proc. Natl. Acad. Sci. U. S. A. 2005; 102:5856-5861.

Tanimura, N., Saitoh, S., Matsumoto, F., Akashi-Takamura, S., Miyake, K. Roles for LPS-dependent interaction and relocation of TLR4 and TRAM in TRIF-signaling. Biochem. Biophys. Res. Commun. 2008; 368:94-99.

Tassone, H., Raghavendra, M. Saphenous nerve block, 2015.

Teghanemt, A., Widstrom, R.L., Gioannini, T.L., Weiss, J.P. Isolation of monomeric and dimeric secreted MD-2. Endotoxin.sCD14 and Toll-like receptor 4 ectodomain selectively react with the monomeric form of secreted MD-2. J. Biol. Chem. 2008; 283:21881-21889.

Tong, Y., Wang, H.F., Ju, G., Grant, G., Hökfelt, T., Zhang, X. Increased uptake and transport of cholera toxin B-subunit in dorsal root ganglion neurons after peripheral axotomy: Possible implications for sensory sprouting. J. Comp. Neurol. 1999; 404:143-158.

Vallejo, R., Tilley, D.M., Vogel, L., Benyamin, R. The role of glia and the immune system in the development and maintenance of neuropathic pain. Pain Practice 2010; 10:167-184.

van Laar, M., Pergolizzi Jr, J.V., Mellinghoff, H., Merchante, I.M., Nalamachu, S., O'Brien, J., Perrot, S., Raffa, R.B. Pain treatment in arthritis-related pain: beyond NSAIDs. The open rheumatology journal 2012; 6:320.

Vargas, M.R., Pehar, M., Cassina, P., Estevez, A.G., Beckman, J.S., Barbeito, L. Stimulation of nerve growth factor expression in astrocytes by peroxynitrite. In Vivo 2004; 18:269-274.

Voscopoulos, C., Lema, M. When does acute pain become chronic? Br. J. Anaesth. 2010; 105 Suppl 1:i69-85.

Wadachi, R., Hargreaves, K.M. Trigeminal nociceptors express TLR-4 and CD14: a mechanism for pain due to infection. J. Dent. Res. 2006; 85:49-53.

Wall, P.D., Melzack, R., Bonica, J.J. Textbook of pain, 1994.

Wang, H., Dai, Y., Fukuoka, T., Yamanaka, H., Obata, K., Tokunaga, A., Noguchi, K. Enhancement of stimulation-induced ERK activation in the spinal dorsal horn and gracile nucleus neurons in rats with peripheral nerve injury. Eur. J. Neurosci. 2004; 19:884-890.

Watkins, L.R., Hutchinson, M.R., Rice, K.C., Maier, S.F. The “toll” of opioid-induced glial activation: improving the clinical efficacy of opioids by targeting glia. Trends Pharmacol. Sci. 2009; 30:581-591.

Watkins, L.R., Hutchinson, M.R., Johnston, I.N., Maier, S.F. Glia: novel counter-regulators of opioid analgesia. Trends Neurosci. 2005; 28:661-669.

Watkins, L.R., Maier, S.F. Glia: a novel drug discovery target for clinical pain. Nature Reviews Drug Discovery 2003; 2:973-985.

Watkins, L.R., Hutchinson, M.R., Ledeboer, A., Wieseler-Frank, J., Milligan, E.D., Maier, S.F. Glia as the "bad guys": Implications for improving clinical pain control and the clinical utility of opioids. Brain Behavior and Immunity 2007a; 21:131-146.

Watkins, L.R., Hutchinson, M.R., Milligan, E.D., Maier, S.F. "Listening" and "talking" to neurons: Implications of immune activation for pain control and increasing the efficacy of opioids. Brain Res. Rev. 2007b; 56:148-169.

Watson, C., Paxinos, G., Puelles, L. The Mouse Nervous System. Chapter 23 - Pain (G. Brett and R. Callister). Elsevier Inc. China, 2012.

Wenham, C.Y., Conaghan, P.G. Imaging the painful osteoarthritic knee joint: what have we learned? Nature clinical practice Rheumatology 2009; 5:149-158.

West, J.P., Lysle, D.T., Dykstra, L.A. Tolerance development to morphine-induced alterations of immune status. Drug Alcohol Depend. 1997; 46:147-157.

White, F.A., Kocsis, J.D. A-fiber sprouting in spinal cord dorsal horn is attenuated by proximal nerve stump encapsulation. Exp. Neurol. 2002; 177: 385-395.

Whiteside, G.T., Harrison, J., Boulet, J., Mark, L., Pearson, M., Gottshall, S., Walker, K. Pharmacological characterisation of a rat model of incisional pain. Br. J. Pharmacol. 2004; 141:85-91.

Williams, J.M., Brandt, K.D. Temporary immobilisation facilitates repair of chemically induced articular cartilage injury. J. Anat. 1984; 138 (Pt 3):435-446.

Winnall, W.R., Muir, J.A., Hedger, M.P. Differential responses of epithelial Sertoli cells of the rat testis to Toll-like receptor 2 and 4 ligands: implications for studies of testicular inflammation using bacterial lipopolysaccharides. Innate Immun. 2011; 17:123-136.

Wittich, C.M., Ficalora, R.D., Mason, T.G., Beckman, T.J. Musculoskeletal injection. 2009; 84:831-837.

Woolf, C.J., Jones, I., Tam, P., Atkinson, D. PAIN. Pain hypersensitivity, 2012.

Woolf, C.J. Central sensitization: implications for the diagnosis and treatment of pain. Pain 2011; 152:S2-S15.

Wu, C.L., Raja, S.N. Treatment of acute postoperative pain. The Lancet 2011; 377:2215-2225.

Ydens, E., Lornet, G., Smits, V., Goethals, S., Timmerman, V., Janssens, S. The neuroinflammatory role of Schwann cells in disease. Neurobiol. Dis. 2013; 55:95-103.

Zahn, P.K., Pogatzki, E.M., Brennan, T.J. Mechanisms for pain caused by incisions. Reg. Anesth. Pain Med. 2002; 27:514-516.

Zahn, P.K., Brennan, T.J. Primary and secondary hyperalgesia in a rat model for human postoperative pain. Anesthesiology 1999; 90:863-872.

Zanoni, I., Ostuni, R., Marek, L.R., Barresi, S., Barbalat, R., Barton, G.M., Granucci, F., Kagan, J.C. CD14 controls the LPS-induced endocytosis of Toll-like receptor 4. Cell 2011; 147:868-880.

Zimmermann, M. Ethical guidelines for investigations of experimental pain in conscious animals. Pain 1983; 16:109-110.

Zollner, C., Mousa, S.A., Fischer, O., Rittner, H.L., Shaqura, M., Brack, A., Shakibaei, M., Binder, W., Urban, F., Stein, C., Schafer, M. Chronic morphine use does not induce peripheral tolerance in a rat model of inflammatory pain. J. Clin. Invest. 2008; 118:1065-1073.